UNIVERSITY OF LONDON THESIS

Degree PhD Year 2007 Name of Author THOMAS EDWARD HOLDEN

Modulation of excitatory synaptic transmission to hippocampal interneurons by metabotropic glutamate receptors

Thomas Edward Holden

Thesis submitted for the degree of Doctor of Philosophy to the University of London

Institute of Neurology, University College London

Submitted September, 2006

Department of Clinical and Experimental Epilepsy
Institute of Neurology
University College London
Queen Square
London, WC1N 3BG

ProQuest LLC
789 East Eisenhower Parkway
P.O. Box 1346
Ann Arbor, MI 48106-1346

Abstract

The hippocampus is a medial temporal lobe structure implicated both in consolidation of experience into long-term memory and generation of epileptiform discharges. Information processing in the hippocampus occurs through interactions between glutamatergic granule cells and pyramidal neurons, and a smaller number of GABAergic inhibitory interneurons. Excitatory connections onto interneurons are a relatively poorly characterised class of synapse, yet they have a central role in mediating the recruitment of inhibitory drive within the hippocampus.

This thesis describes investigation of modulation of excitatory synaptic transmission to interneurons in area CA1 of the hippocampus by metabotropic glutamate receptors (mGluRs). mGluRs are G protein-coupled heptahelical transmembrane receptors, which exert powerful modulatory effects upon synaptic transmission and neuronal excitability. Use of patch clamp electrophysiology in acute brain slices allowed synaptic responses elicited by stimulation of afferent inputs to be recorded in single neurons within a functionally intact network.

The selective group I mGluR agonist (S)-3,5-dihydroxyphenylglycine (DHPG) was found to acutely depress glutamatergic transmission to stratum radiatum interneurons in the rat hippocampal CA1 subfield. Both mGluR1 and mGluR5 subtypes contributed to this phenomenon. DHPG-evoked depression was consistently accompanied by an elevation in paired-pulse ratio, implying a presynaptic mechanism of expression. However, it was also attenuated by blocking G protein and Ca^{2+} signalling within the postsynaptic neuron, arguing for a postsynaptic site of induction. The DHPG-evoked depression was unaffected by antagonists of $GABA_B$ and CB1 endocannabinoid receptors but was occluded when presynaptic P/Q-type Ca^{2+} channels were blocked. A heterosynaptic depression was observed in a test pathway when a high-frequency tetanus was delivered to an independent conditioning pathway. This depression was reversible and abolished by group I mGluR antagonists. Group I mGluRs thus provide a mechanism for population activity in glutamatergic synapses to influence synaptic excitation of cortical interneurons.

Contributions

All of the experimental data described in thesis are my own. All brain slice preparation, electrophysiological recording, confocal imaging, epifluorescence imaging and other experimental work was carried out by myself.

Project ideas and experimental designs were developed with the assistance of Dimitri Kullmann.

Data analysis was carried out by myself, in part using custom software programs written by Dimitri Kullmann in the LabView development environment (National Instruments, USA).

All figures, tables and written work are my own.

- Ph.D. supervisor – Professor Dimitri M. Kullmann *(Department of Clinical and Experimental Epilepsy, Institute of Neurology, University College London)*.
- Secondary Ph.D. supervisor – Professor Angus R. Silver *(Department of Physiology, University College London)*.
- Wellcome Trust Four Year Ph.D. in Neuroscience Programme Co-ordinator – Professor David I. Attwell *(Department of Physiology, University College London)*.
- University College London internal viva examiner – Professor John Garthwaite *(Wolfson Institute of Biomedical Research, University College London)*.
- External Viva examiner – Dr Marco Capogna *(MRC Anatomical Neuropharmacology Unit, University of Oxford)*.

To my mother

Acknowledgements

"Pain is temporary. It may last a minute, or an hour, or a day, or a year, but eventually it will subside and be replaced by something else. Quitting lasts forever."
Lance Armstrong

I would like to thank Dimitri Kullmann for all of his help and support throughout my Ph.D. He has been an outstanding supervisor in every respect, and I have always felt extremely proud to be part of his research group. I have learned so much during my time in the lab, and Dimitri ensured that I was never without guidance, encouragement and the equipment necessary to carry out my research. Finally, I would like to thank him for his kindness and understanding during some extremely difficult times in my personal life.

I am grateful to the past and present members of the research group for their assistance, and for taking the time to train me in experimental techniques and data analysis. Two people deserve my particular gratitude. Firstly, Annalisa Scimemi, for dedicating a great deal of her time to training me, and for being an excellent teacher. Secondly, Karri Lamsa, for being a great friend, providing constant entertainment and laughter, and somehow always managing to turn the darkest, most difficult days into happy ones.

My thanks go to the Wellcome Trust Four Year Ph.D. in Neuroscience committee. In particular, David Attwell and Alasdair Gibb for their guidance, support and inspiration. I am extremely grateful to the Wellcome Trust for their generous funding of my Ph.D. I would like to thank Angus Silver for being my secondary supervisor.

On a personal level, I wish to thank my friends and family for their support. I would like to offer my deepest thanks to my mother, to whom this work is dedicated. Her endless love and support has always been unwavering, even through the very darkest times. Her inner strength and refusal to ever give up hope has been inspirational, and I will never forget the many ways in which she helped me in this achievement.

Table of contents

Chapter 1. General Introduction

Section 1. Anatomy of the hippocampus

1.1.1 The role of the hippocampus in the living brain

The hippocampus is one of the most thoroughly-studied areas of the mammalian central nervous system. This structure plays a fundamental role in some forms of learning and memory. The precise roles of the hippocampus are not yet fully understood, but it is widely agreed to be of critical importance in the generation of new memories regarding experienced events, i.e. episodic memory formation. Furthermore, *in vivo* electrophysiological studies in rodents have demonstrated the existence of so-called 'place cells', which are activated when the animal travels through specific areas of its environment, and appear to play a central role in spatial mapping, forming a so-called 'cognitive map' of the environment (O' Keefe, 1978). A second major reason for the extensive experimental investigation of the hippocampus is that it has been implicated in a number of neurological and psychiatric disorders. These include epilepsy, Alzheimer's disease and schizophrenia. The hippocampus has the lowest seizure threshold of any brain region. The majority of patients suffering from epilepsy have seizures that involve the hippocampus, and these seizures are often the most difficult to control medically. This brain region, together with the neighbouring entorhinal cortex, also shows high susceptibility to the cellular pathology associated with Alzheimer's disease. In addition, the hippocampus is highly vulnerable to the cytotoxic effects of ischaemia and hypoxia.

1.1.2 Location of the hippocampus within the brain

The hippocampus is part of a brain region known as the limbic system, located within the medial temporal lobe. This horseshoe-shaped rim of grey matter surrounding the junction between the diencephalon and each cerebral hemisphere

was first described by Broca in 1878. There is some debate as to precisely which structures comprise the limbic system. Most authors include the hippocampal formation, amygdala, cingulate and parahippocampal gyri, septal nuclei, hypothalamus, parts of the midbrain reticular formation and certain olfactory areas. Some authors also suggest that certain regions of the thalamus, fornix and the mammillary bodies are included.

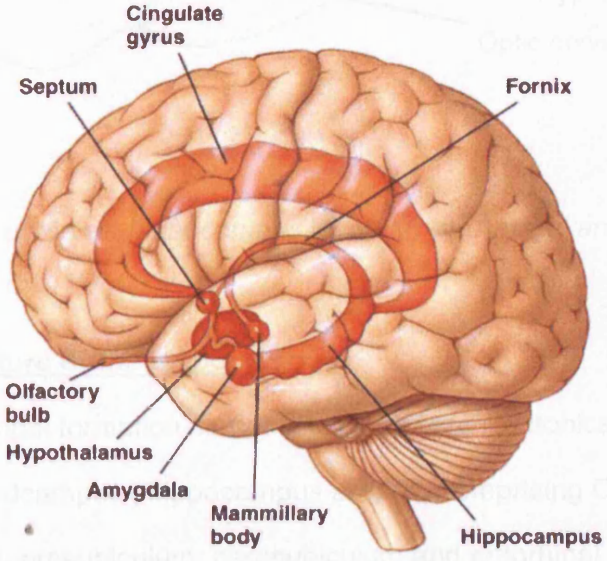

Figure 1.1. *Location of major structures of the limbic system in the human brain (from Neuropsychology web resource, www.driesen.com).*

In the rat, the hippocampus occupies a large portion of the forebrain. It is an elongated structure, with its long axis extending in a C-shaped manner rostrodorsally from the septal nuclei of the basal forebrain, over and behind the diencephalon, and caudoventrally to the temporal lobe (O'Keefe, 1978). The long axis of the hippocampal formation is referred to as the septotemporal axis, with the septal pole located rostrally. The orthogonal axis is known as the transverse axis.

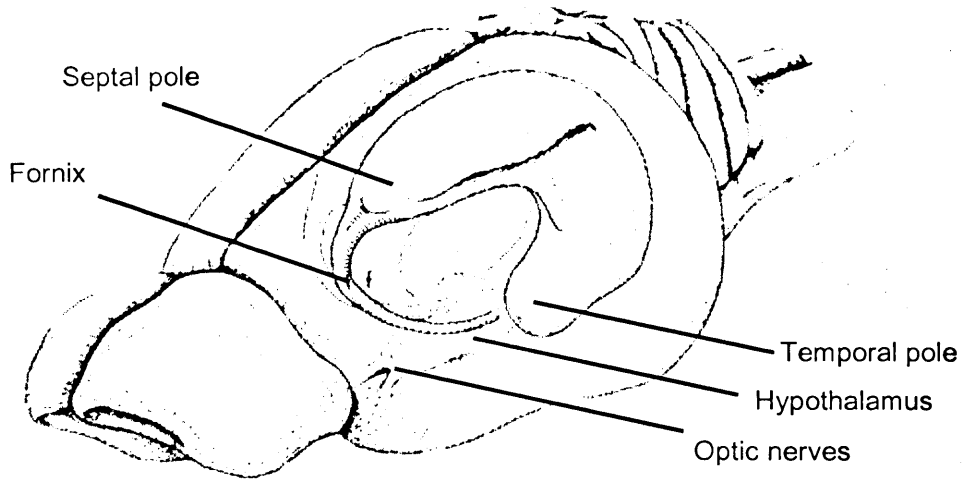

Figure 1.2. *Position of the rat hippocampus* in situ *(from Amaral and Witter, 1995)*

1.1.3 Internal structure of the hippocampus

The hippocampal formation comprises six cytoarchitectonically distinct regions – dentate gyrus, hippocampus ('hippocampus proper', comprising CA3, CA2 and CA1 subfields), subiculum, presubiculum, parasubiculum and entorhinal cortex. The subiculum, presubiculum and parasubiculum may be grouped together as the subicular complex (Amaral and Witter, 1995). The six regions of the hippocampal formation are grouped together because they are sequentially linked by unique and primarily unidirectional connections. It should be noted, however, that the precise composition of the hippocampal formation remains a matter of debate among authors, depending upon the criteria applied. The hippocampus proper is a curved sheet of cortex folded into the medial surface of the temporal lobe. The subiculum is a transitional zone continuous with the hippocampus proper at one of its edges and the cortex of the parahippocampal gyrus at the other edge. The alveus is a thin layer of white matter which separates the hippocampus from the lateral ventricle. It consists of axons originating from CA1 pyramidal cells, which are directed either towards subcortical termination sites or the contralateral hippocampus.

The hippocampus itself is divided into two major U-shaped interlocking sectors, the dentate gyrus and the hippocampus proper containing the CA1-CA3 subfields. These subfields are so called because the hippocampus proper is also known as *cornu ammonis*, or the horn of Ammon, after an Egyptian deity with the head of a ram. Initially, Ramon y Cajal (1911) divided the hippocampus proper into the large-celled regio inferior proximal to the dentate gyrus, and the small-celled regio superior located distally from the dentate gyrus. On the basis of differences in cell morphology and fibre projections, Lorente de No (1934) further divided the hippocampus proper into the four CA subfields. CA3 and CA2 correspond to regio inferior, while CA1 is equivalent to regio superior. The distinction between CA2 and CA3 is subtle, and often these two subfields are simply referred to as CA3. CA4 refers to the scattered cells inside the hilus of the dentate gyrus, though the boundaries of this region are somewhat more vague than the precise divisions of CA1 and CA2/3. Thus the major, clearly defined subfields of the hippocampus proper are CA1 and CA3.

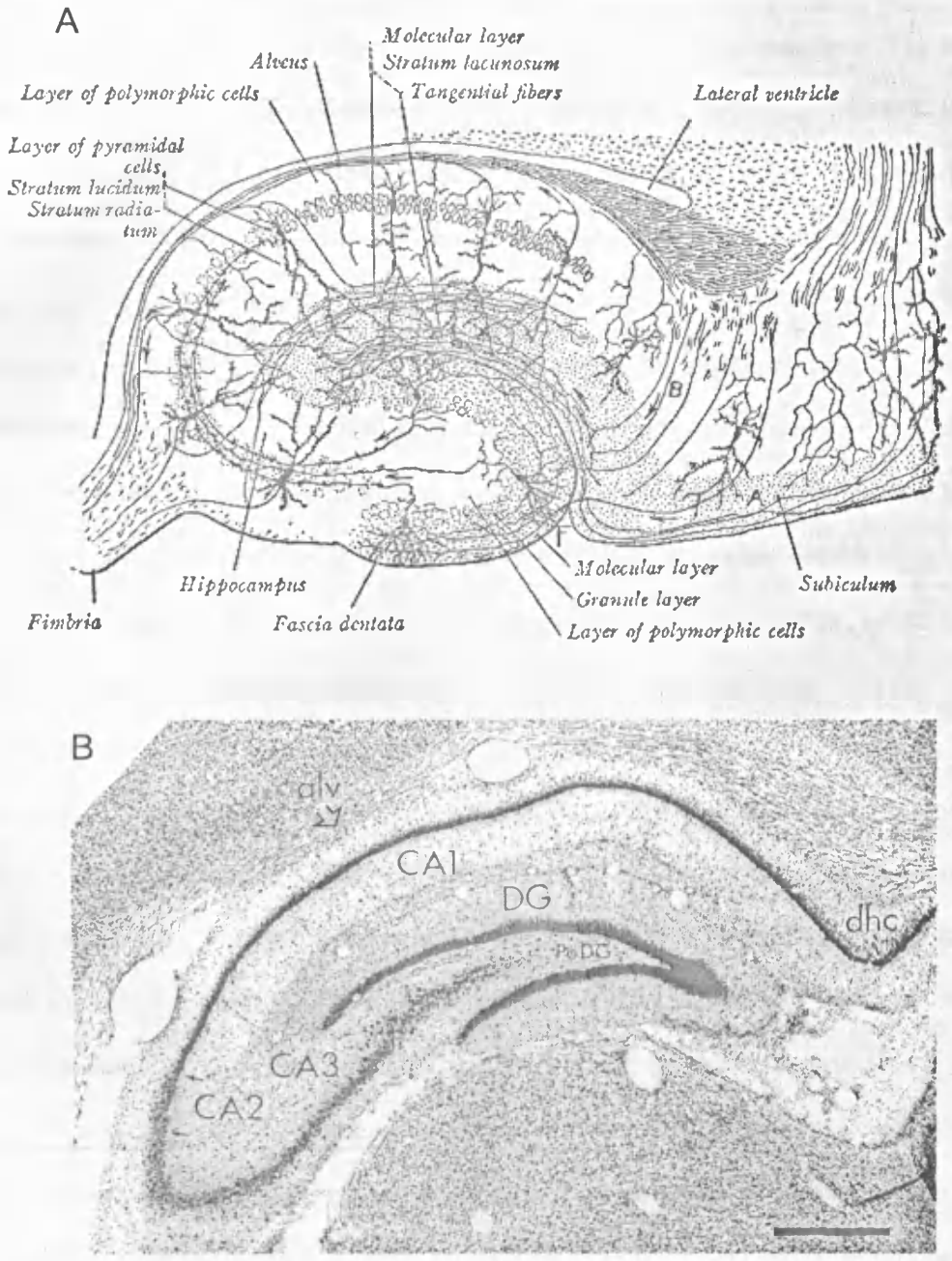

Figure 1.3. *Transverse sections through the rat hippocampus.* ***A****, diagram showing major projections of the hippocampus proper (from Ramon y Cajal, 1911).* ***B****, Nissl-stained transverse section of adult rat hippocampus, clearly showing different subfields and interlocking cornu ammonis and dentate gyrus sectors. Scale bar 500μm (from Amaral and Witter, 1995).*

The cerebral cortex classically has a six-layered structure, but this differs in the hippocampus. The six-layered entorhinal cortex becomes four-layered at the subiculum and then three-layered at the hippocampus proper. These three layers are

molecular, pyramidal and polymorphic, and may be further subdivided into six strata. Starting from the ventricular surface these are as follows: 1. The alveus, containing axons of CA1 pyramidal cells directed towards the fimbria or subiculum; 2. stratum oriens, containing basal dendrites of pyramidal cells, somata and dendrites of basket cells, and afferents from the septum; 3. stratum pyramidale, a compact layer of densely-packed pyramidal cell somata; 4. stratum radiatum, containing apical dendrites of pyramidal neurons, CA3-CA3 associational connections, and CA3-CA1 Schaffer collateral axons; 5. stratum lacunosum; 6. stratum moleculare. These last two layers are often grouped together, and contain mainly perforant path axons from entorhinal cortex. The CA3 subfield contains an additional layer between s.pyramidale and s.radiatum, called *stratum lucidum*. This layer contains mossy fibres, which are axons of dentate granule cells (Blackstad et al., 1970). Interneurons are present within all layers of the hippocampus. The dentate gyrus also has a trilaminar structure, comprising: 1. molecular layer, containing apical dendrites of granule cells; 2. granule cell layer, with densely packed granule cell bodies; 3. polymorphic cell layer, which is located in the hilus of the dentate gyrus and merges with the CA4 subfield. this layer contains the initial segments of granule cell axons as they gather together to form the mossy fibre bundle (Blackstad et al., 1970). The basic organisational principal is the same in all areas of the hippocampus – an ordered sheet of principal cells with their somata densely packed in a compact layer, and their dendrites all running in the same direction, often extending for hundreds of microns. Inputs to each area generally traverse the dendrites at roughly 90°, making en passant synapses within a restricted region of the dendritic fields of many neurons.

Information processing in the hippocampus occurs through interactions between a large number of glutamatergic principal neurons and a smaller number of inhibitory interneurons that release the neurotransmitter γ-aminobutyric acid (GABA). The principal neurons of the hippocampus are the giant CA3 pyramidal cells, the smaller CA1 pyramidal cells, and the granule cells of the dentate gyrus. Pyramidal cells have both apical and basal dendrites, while granule cells have only apical

dendrites and are thus monopolar neurons. Principal neurons within a given subfield are relatively homogeneous in terms of morphology, connectivity and functional properties. In contrast, hippocampal interneurons are a highly heterogeneous population of neurons fulfilling a variety of complex functions. Interneurons are discussed in detail in Section 1.3.

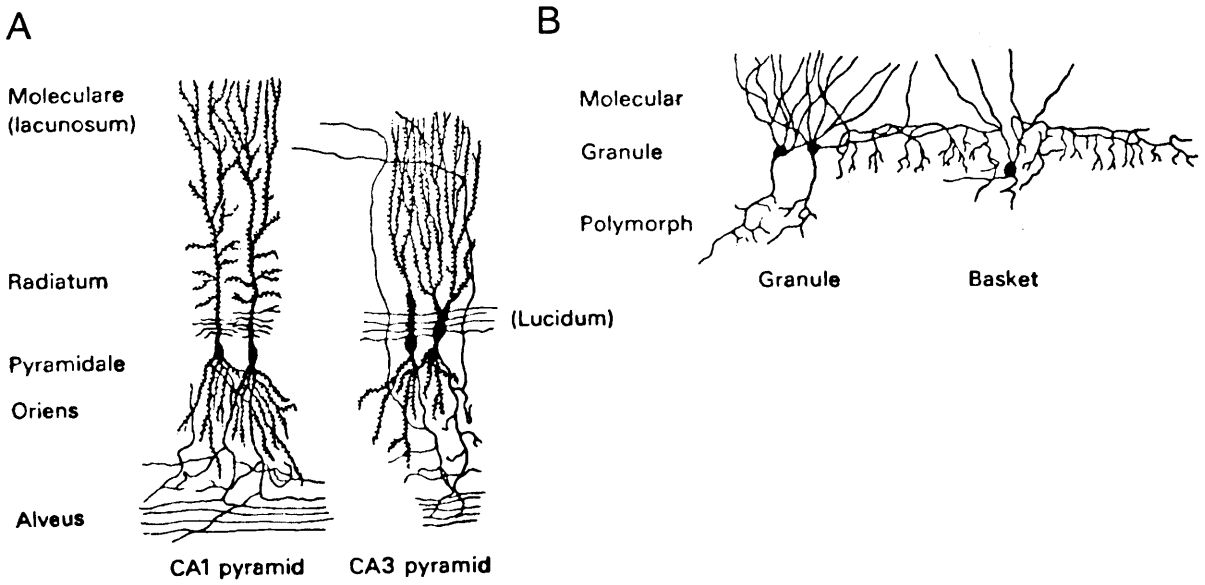

Figure 1.4. ***A****, examples of CA1 and CA3 pyramidal cells.* ***B****, examples of a dentate granule cell and a basket cell (from Lorente de No, 1934).*

1.1.4 Basic circuitry of the hippocampus

The hippocampal formation contains an incredibly complex array of major projections and local microcircuits, involving numerous neurotransmitter systems and distinct classes of synapse. A detailed review of the entire hippocampal circuitry is clearly beyond the scope of this discussion. Instead, I focus on the elements comprising the basic hippocampal circuitry, and later consider in more detail certain local microcircuits (see Section 1.3). The aim here is to place the experiments described in this thesis within the context of the relevant anatomical and physiological properties of the hippocampus.

Information passes through the hippocampus in a unidirectional series of excitatory pathways. This was first emphasised by Anderson et al. (1971), who used the term trisynaptic circuit to describe the series of three excitatory pathways within the hippocampus itself. The major input to the hippocampus is the perforant path, a projection from neurons in layer II of the entorhinal cortex which passes through the subiculum and terminates in both the dentate gyrus and CA3 (Steward and Scoville, 1976; Ruth et al., 1982; 1988). The layer II entorhinal cortex-dentate granule cell synapse is the first in the trisynaptic circuit. Each dentate granule cell gives rise to a single unmyelinated mossy fibre axon, which extends around seven thinner collaterals within the polymorphic layer before entering the CA3 subfield and terminating on the proximal apical dendrites of CA3 pyramidal cells in stratum lucidum (Anderson et al., 1971; Claiborne et al., 1986). This is the second synapse in the trisynaptic circuit. The mossy fibre-CA3 synapse is highly specialised and has many unique properties (reviewed by Henze et al., 2000). Within stratum lucidum, mossy fibre axons have large presynaptic varicosities (3-10 μm in diameter) distributed at intervals of approximately 140 μm along their length (Claiborne et al., 1986). These large presynaptic boutons form highly morphologically complex contacts with thorny excrescences on the apical dendrites of CA3 pyramidal cells. Thorny excrescences are densely lobed dendritic spine protrusions with up to 16 branches. A mossy fibre bouton can make as many as 37 synaptic contacts with a single CA3 pyramidal cell dendrite (Chicurel and Harris, 1992). Granule cells also synapse onto cells of the polymorphic layer, providing associational connections to other layers of the dentate gyrus. In addition, mossy fibre axons have fine collaterals which contact local inhibitory interneurons. Ascady et al. (1998) performed a detailed *in vivo* intracellular labelling study of granule cells in rats, combined with immunocytochemistry and electron microscopy. *In vivo* electrophysiology was also employed, with the objective of quantitatively identifying the postsynaptic targets of individual granule cell axons. Single granule cells formed large, complex "mossy" synapses on 11-15 CA3 pyramidal cells and 7-12 hilar mossy cells. In contrast, GABAergic interneurons,

identified with immunostaining for the substance P-receptor, parvalbumin, and mGluR1a-receptor, were selectively innervated by very thin filopodial extensions of the mossy terminals, and by small en passant boutons in both the hilar and CA3 regions. These terminals formed single, often perforated, asymmetric synapses on the cell bodies, dendrites, and spines of GABAergic interneurons. The number of filopodial extensions and small terminals was approximately 10 times larger than the number of mossy terminals. These findings show that, in contrast to cortical pyramidal neurons, (i) granule cell axons develop distinct types of terminals to activate interneurons and pyramidal cells; and (ii) they innervate more inhibitory than excitatory cells. These findings may explain the physiological observations that increased activity of granule cells suppresses the overall excitability of the CA3 recurrent system, and may form the structural basis of the target-dependent regulation of glutamate release in the mossy fibre system.

CA3 pyramidal cells project both to CA1 and other levels of CA3, with the projections to CA1 termed Schaffer collaterals, the final connection in the trisynaptic circuit. CA1 pyramidal cells project via the alveus to both the subiculum and the deep layers of the entorhinal cortex, predominantly layer V (Swanson and Cowan, 1977). They also have small, fine local collaterals which extend into stratum oriens (Knowles and Schwartzkroin, 1981) and terminate on basal dendrites of other CA1 pyramidal cells (Deuchars and Thomson, 1996). However, the level of connectivity is low (Deuchars and Thomson, 1996), and CA1 pyramidal cells clearly lack the extensive network of associational connections present among CA3 pyramidal cells. Completing the overall circuit, projections arise from the deep layers of the entorhinal cortex back to many of the cortical areas which originally projected to layer II of the entorhinal cortex. Information may thus be processed by the hippocampal circuitry and returned to the cortical area from which it originated. This processing is clearly important in consolidation of experience into long-term memory.

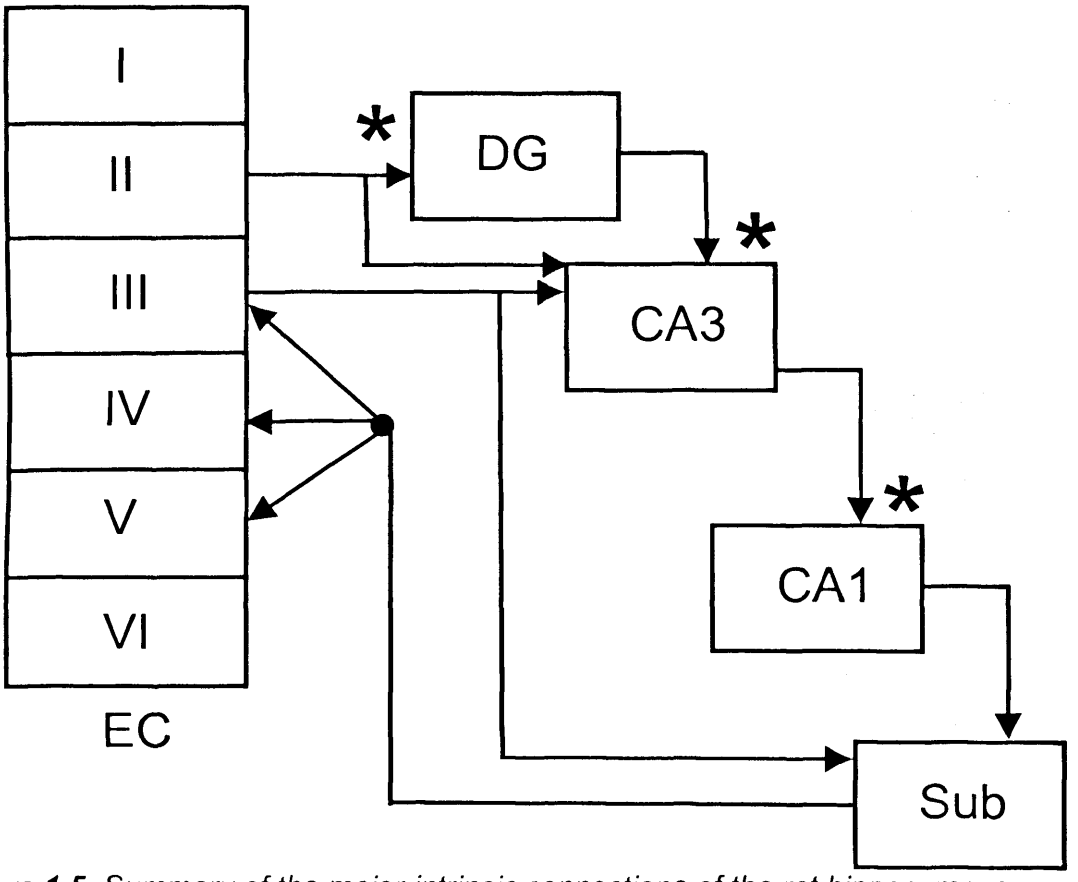

Figure 1.5. *Summary of the major intrinsic connections of the rat hippocampus. Synapses of the trisynaptic circuit are marked with an asterisk. DG, dentate gyrus; EC, entorhinal cortex; Sub, subiculum.*

1.1.5 Properties of the CA3-CA1 connection

Modulation and functional properties of synaptic connections from CA3 pyramidal cells to CA1 interneurons are the main subjects of this thesis. I therefore consider in greater detail the anatomical properties of CA3-CA1 connections. It should be noted that virtually all studies to date have investigated connections to CA1 pyramidal cells, illustrating that excitatory synaptic connections onto interneurons are a relatively poorly characterised class of synapse (discussed in Section 1.4). Nevertheless, it is important to consider all of the available literature in order to build as complete a picture as possible of the CA3-CA1 connection.

CA3 pyramidal cell axons exhibit a highly ordered and spatially distributed pattern of projections, in terms of both associational connections within CA3 to other CA3 pyramidal cells, and from CA3 to CA1. In a detailed intracellular labelling study, Ishizuka et al. (1990) showed that CA3 projections are organised in several distinct

gradients. For example, CA3 pyramidal cells located near the dentate gyrus project more heavily to levels of CA1 located septal to their position. In contrast, CA3 pyramidal cells closer to CA1 project more heavily to levels of CA1 located temporally. This study demonstrated that the older notion of Schaffer collaterals extending linearly through CA1 with equal contact probability throughout the subfield is incorrect. Similar gradient rules were also shown to apply to associational CA3-CA3 projections. CA2 pyramidal cells project to CA1, but the projection is sparse and diffuse, and does not follow the ordered gradient system of the CA3-CA1 projection (Ishizuka et al., 1990). It should be noted that, in addition to the projections within the ipsilateral hippocampus, CA3 pyramidal cells also project to the same areas in the contralateral hippocampus. These are known as commissural projections.

Schaffer collaterals contact both apical dendrites of CA1 pyramidal cells in stratum radiatum, and basal dendrites in stratum oriens. It has been estimated that a single CA1 pyramidal cell may be innervated by over 5,000 CA3 pyramidal cells (Amaral et al., 1990). Each CA3 pyramidal cell forms excitatory synaptic contacts with many CA1 pyramidal cells. Single CA3 pyramidal cells give rise to highly arborised axonal plexuses that distribute to as much as 75% of the septotemporal extent of the CA1 subfield (Tamamaki et al., 1984), indicating that Schaffer collateral projections are divergently distributed along the septotemporal axis. Intracellular labelling demonstrated that the axonal plexus from a single CA3 pyramidal cell may be up to 150-300 mm in length, and is estimated to form as many as 30,000 to 60,000 synaptic contacts within area CA1 (Li et al., 1994).

At the light microscope (LM) level, individual CA3-CA1 projections are thin unmyelinated axons with numerous en passant boutons (Ishizuka et al., 1990; Sorra and Harris, 1993). Using serial electron microscopy (EM), Sorra and Harris (1993) demonstrated that Schaffer collaterals have numerous multiple-synapse boutons, and determined that individual Schaffer collateral axons can form multiple synapses onto a single CA1 pyramidal cell. Schaffer collaterals terminate as asymmetrical axospinous synapses on CA1 pyramidal cell dendrites, with considerable variation in synaptic

morphology possibly reflecting differences in physiological efficacy of the synapses (Harris and Stevens, 1989). Serial EM was used to demonstrate that varicosities vary greatly in length, volume, mitochondrial content and number of synapses formed (inferred by number of postsynaptic densities), indicating extensive anatomical heterogeneity in CA3-CA1 connections (Shepherd and Harris, 1998).

Much less data are available on the patterns of connectivity and ultrastructure of Schaffer collateral connections onto CA1 interneurons. By combining LM, serial EM and immunohistochemistry, Gulyas et al. (1999) were able to quantify the total number of excitatory and inhibitory synaptic inputs to three neurochemically-defined populations of CA1 interneurons. This study is discussed further below, in section 1.3.1.4. The interneurons studied were immunopositive for one of the three neurochemical markers parvalbumin, calretinin or calbindin. Excitatory inputs were identified on the basis that they were GABA-immunonegative and were asymmetrical, which are defining features of excitatory synapses. However, this means of identification is not conclusive, highlighting the need for more detailed ultrastructural studies to increase understanding of the anatomical properties of Schaffer collateral inputs onto CA1 interneurons. Each cell type appeared to be associated with a distinct pattern of excitatory inputs. Both parvalbumin- and calretinin-positive interneurons received excitatory synapses within all layers of CA1. While much of this afferent drive would be provided by Schaffer collaterals, in strata radiatum and oriens, there would also be some activation from local feedback CA1 axon collaterals. In contrast, calbindin-positive cells received inputs almost exclusively from Schaffer collaterals in stratum radiatum. This suggests that calbindin-positive interneurons are involved explicitly in feedforward inhibition, whereas parvalbumin- and calretinin-positive cells are innervated less specifically in both a feedforward and feedback manner. The density of excitatory inputs to both calbindin- and calretinin-immunopositive interneurons was approximately similar. Parvalbumin-positive interneurons received a number of excitatory inputs several times greater than the other two subtypes. These observations clearly have implications for the role of these interneuron subtypes in

hippocampal network function, but it is impossible to speculate on this further from these data alone, and is not relevant to the present section. At the ultrastructural level, excitatory synapses formed asymmetrical synapses onto interneurons, with extensive variation in the size of presynaptic terminals and synaptic active zones.

A detailed study was carried out to characterise the ultrastructural aspects of glutamatergic connections onto hippocampal interneurons (Gulyas et al., 1993b). However, this examined the connection between presynaptic CA3 pyramidal cells and parvalbumin-positive postsynaptic CA3 interneurons, as opposed to CA1 interneurons. Nonetheless, there may be many similarities between these types of connection, and in any case, heterogeneity may exist in the ultrastructural aspects of excitatory synaptic connections onto different interneuron subtypes. High-resolution electron microscopy was used to show that CA3 pyramidal cells form single axonal contacts with one active zone onto postsynaptic interneurons.

Section 2. Metabotropic glutamate receptors in the hippocampus

Metabotropic glutamate receptors (mGluRs) are heptahelical transmembrane receptors with a variety of roles in the modulation of neuronal excitability and synaptic transmission. Eight mGluR subtypes have currently been identified. They have precisely-defined functional roles and are expressed in highly specific patterns in the hippocampus and other cortical networks.

1.2.1 Cloned mGluRs

The starting point for cloning of the first mGluR was the discovery that injection of rat brain mRNA into *Xenopus* oocytes could be used to express and measure G protein-dependent responses to exogenous glutamate, such as phosphoinositide hydrolysis to generate inositol-1,4,5-trisphosphate (IP_3) and the resulting mobilisation of intracellular Ca^{2+} (Sugiyama et al., 1987). The first mGluR cDNA was cloned by two

independent groups, both using a rat cerebellar library, and was termed mGlu1a (Houamed et al., 1991; Masu et al., 1991). Cloning of other mGluR subtypes quickly followed, using homology screening by cross-hybridisation of a rat brain cDNA library with the mGlu1a cDNA (Tanabe et al., 1992). The current system for mGluR classification was originally proposed by Nakanishi (1992), who suggested that mGluRs could be classified into three groups, based upon sequence homology (there is ~70% homology within a group, and ~40% homology between groups), signal transduction mechanism and pharmacological profile. Eight mGluRs have currently been cloned. Group I comprises mGluR1 and mGluR5, Group II comprises mGluR2 and mGluR3, and group III comprises mGluR4, mGluR6, mGluR7 and mGluR8. Splice variants have been identified for mGluR 1, 4, 5, 7 and 8 (for review see Pin and Duvoisin, 1995; Conn and Pin, 1997).

Receptor	Group	Transduction mechanism	Selective agonist	Selective antagonist
mGluR1	I	+ PLC	3,5-DHPG	CPCCOEt
mGluR5				
mGluR2	II	- AC	LY354740	LY341495
mGluR3				
mGluR4	III	- AC	L-AP4	LY341495 or MSOP
mGluR6				
mGluR7				
mGluR8				

Table 1.1. *The eight currently identified mGluRs are divided into three groups according to sequence homology, signal transduction mechanism and pharmacological profile. LY341495 is an extremely potent antagonist of group II mGluRs at nanomolar concentrations. At higher concentrations, it is also highly selective for group III mGluRs (+PLC, upregulation of phospholipase C activity; -AC, downregulation of adenylate cyclase activity).*

1.2.2 Structural properties of mGluRs

The most commonly-studied G protein-coupled receptors (GPCRs) are the rhodopsin, β-adrenergic (βAR) and muscarinic acetylcholine (mAchR) receptors. They have a high degree of homology with other types of GPCR, and the rhodopsin receptor in particular has been used as a framework for developing a generalised model for GPCR structures (e.g. Palczewski et al., 2000). mGluRs are family 3 GPCRs. This family also includes Ca^{2+}-sensing (CaS) and $GABA_B$ receptors, together with some putative olfactory, pheromone and taste receptors. Family 3 GPCRs are heptahelical transmembrane receptors. The seven transmembrane spanning structure is highly conserved among GPCRs, with an extracellular N-terminus and intracellular C-terminus. Each transmembrane domain consists of approximately 24 hydrophobic amino acids, with intracellular and extracellular loops of varying sizes between each domain. The seven domains associate to form an oblong ring structure within the plasma membrane.

In contrast to most classical GPCRs, mGluRs are thought to exist within the membrane as functional homodimers. mGluR dimerisation was first demonstrated by co-immunoprecipitation of two distinct epitope-tagged forms of mGluR5 (Romano et al., 1996). Further evidence was provided by studies expressing in cell culture systems the N-terminal extracellular portion of mGluR1, which was shown to exist as a soluble disulphide-bonded homodimer, with the N-terminal cysteine rich extracellular domain of particular importance in formation of disulphide bonds (Okamoto et al., 1998; Robbins et al., 1999). Mutagenesis studies combined with co-immunoprecipitation and SDS-PAGE (sodium dodecyl sulphate polyacrylamide gel electrophoresis; used to determine molecular weight of proteins) identified the critical cysteine residues involved in dimerisation of mGluR1 (Tsuji et al., 2000) and mGluR5 (Romano et al., 2001). Despite clear evidence for formation of homodimeric receptors, mGluRs have not been shown to form heterodimers. For example, despite their high degree of sequence homology, mGluR1 and mGluR5 do not form heterodimers (Romano et al., 1996). The functional importance of dimerisation remains

incompletely understood. The available evidence suggests that mGluR dimerisation may not be directly involved in the proper folding of the receptor, in order to permit agonist binding and functional activation. Dimerisation has been shown to occur in the endoplasmic reticulum (ER), and one possible reason for this phenomenon is that trafficking of the receptor could be affected by its oligomerisation status (see Hermans and Challiss, 2001).

The mGluR family is heterogeneous in size, ranging from 854 to 1179 amino acid residues. Although similar in general structure to other GPCRs, mGluRs share little sequence homology and are considered sufficiently divergent to have originated from a separate evolutionary derived receptor family (Tanabe et al., 1992; Hollmann and Heinemann, 1994). All eight mGluR subtypes share a common structural organisation. Analysis of the primary sequence of cloned mGluR1a revealed two characteristic features which differentiate mGluRs from classical GPCRs. Firstly, a large extracellular domain of approximately 600 amino acids, which includes the ligand binding site; and secondly, a lack of sequence homology with classical GPCRs within the transmembrane region. mGluRs contain 19 conserved cysteine residues within the extracellular sequence, indicating that this area is likely to be stabilised by disulphide bridges (Houamed et al., 1991; Masu et al., 1991).

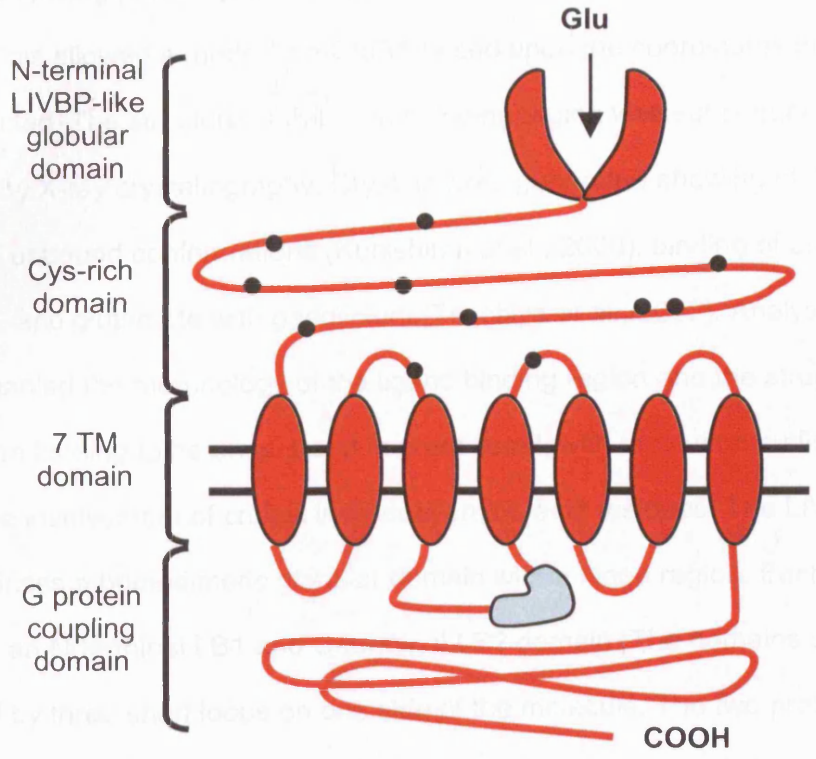

Figure 1.6. *Generalised mGluR structure (Cys, cysteine; TM, transmembrane; LIV-BP, leucine isoleucine valine binding protein).*

The large extracellular region points towards differences in the ligand binding region between mGluRs and classical GPCRs. The neurotransmitter binding site is located within the hydrophobic core of the receptor in a pocket formed in the centre of the seven transmembrane domains in many classical GPCRs, for example the βAR (Kobilka, 1992). In contrast, the mGluR ligand binding site is located within the large extracellular N-terminal domain. This was demonstrated by expression in a cell culture system of the entire extracellular region of mGluR1 (Okamoto et al., 1998), and subsequently a shorter region spanning from the N terminus to a trypsin-sensitive site immediately before the cysteine-rich region (Tsuji et al., 2000). In both cases, the expressed fragment retained ligand binding capacity and selectivity comparable to the full-length receptor. O'Hara et al. (1993) demonstrated that the mGluR N-terminal

domain possesses extensive amino acid sequence homology with the bacterial periplasmic binding protein (PBP) leucine-, isoleucine- and valine- binding protein (LIV-BP). This allowed a model of mGluR1 based upon the coordinates of LIV-BP to be constructed. The structure of the ligand binding region was subsequently confirmed by X-ray crystallography. Crystals were generated showing glutamate-bound and unbound conformations (Kunishima et al., 2000), binding of an antagonist (S-MCPG), and glutamate with gadolinium (Tsuchiya et al., 2002). Analysis of these crystals enabled the morphology of the ligand binding region and the structural basis of glutamate binding to be understood in great detail, with resolution sufficient to pinpoint the involvement of critical individual amino acid residues. The LIV-BP-like area comprises a homodimeric globular domain with a hinge region. Each protomer comprises an N-terminal LB1 and C-terminal LB2 domain. The domains are connected by three short loops on one side of the molecule. The two protomers are linked by a disulphide bond at Cys140. Glutamate binding occurs between the two protomers, in the crevice between the LB1 and LB2 domains. A conformational change occurs upon glutamate binding, with the two protomers closing together like a clamshell, shortening their separation by over 20 Å. Glutamate binding thus stabilises the active conformation of the ligand binding region. This mechanism is very similar to the mode of action of PBPs. High-resolution X-ray crystallography has allowed identification of the amino acid residues critically involved in glutamate binding, and detailed modelling schemes for ligand binding and resultant conformational changes have been published (Kunishima et al., 2000; Tsuchiya et al., 2002). The mechanism via which glutamate binding leads to activation of G proteins and other intracellular signal transduction cascades is not yet understood. One possibility is a shift in the orientation of one or more of the transmembrane α-helices, transmitted from the ligand binding region via the cysteine-rich domain (Hermans and Challiss, 2001).

1.2.3 Group I mGluR-activated intracellular signal transduction cascades

I now review the downstream intracellular signal transduction cascades which are triggered following mGluR activation by binding of glutamate to the receptor. This section provides an overview of intracellular signalling mechanisms, since this aspect of mGluR functionality was not investigated in detail in the projects described in this thesis. I review mainly group I mGluR-associated signalling cascades, since investigation of modulation of synaptic transmission by this group of receptors is the primary focus of this thesis.

Following activation by ligand binding, group I mGluRs mediate downstream effects via G protein-dependent and independent intracellular signalling pathways. G proteins are composed of α, β and γ subunits. Activation via ligand binding results in a conformational change in GPCRs, causing them to catalyse exchange of GDP for GTP in their associated G proteins. This results in dissociation of the heteromeric G protein, generating α-GTP and βγ subunits, both of which then interact with their downstream targets. The GTPase activity of the G protein α subunit mediates hydrolysis of GTP to GDP, with concomitant conversion of the G protein back to the inactive state. Group I mGluRs couple preferentially to the activation of phosphoinositide-specific phospholipase C (PLC) through coupling to $G_{q/11}$ proteins (reviewed by Hermans and Challiss, 2001). The phosphatidyl inositide signal transduction cascade is extremely prominent in neuronal signalling. In contrast to the group I mGluRs, the group II and III receptors exert effects downstream of G protein activation via downregulation of the adenylyl cyclase (AC)/cyclic adenosine monophosphate (cAMP)/protein kinase A (PKA) transduction cascade, the other highly prominent pathway in neuronal signalling. The phosphatidyl inositide signalling cascade operates as follows. Following activation via G protein coupling, the enzyme PLC hydrolyses its substrate phosphatidylinositol 4,5-bisphosphate (PIP_2) to yield inositol 1,4,5-trisphosphate (IP_3) and diacylglycerol (DAG). These two products then activate separate branches of the signalling cascade. DAG, a hydrophobic molecule which remains within the cytosolic face of the cell membrane, activates the enzyme

protein kinase C (PKC), which subsequently exerts a variety of downstream effects. The DAG signal is rapidly terminated by conversion into phosphatidic acid and subsequent recycling into phospholipids. IP_3 is water-soluble, and diffuses within the cytoplasm to trigger release of Ca^{2+} from intracellular stores. IP_3 acts on specific receptors on the endoplasmic reticulum, the major IP_3-sensitive intracellular Ca^{2+} store. The IP_3 receptor is a macromolecular complex that functions both as an IP_3 sensor and Ca^{2+} channel. Ca^{2+} is concentrated in the ER through the action of a Ca^{2+}-ATPase within the ER membrane, and subsequent binding to low-affinity Ca^{2+} binding proteins. Ca^{2+} therefore rapidly enters the cytoplasm along a steep concentration gradient via the ion channel of the activated IP_3 receptor. The IP_3 signal is rapidly terminated by dephosphorylation of the molecule to inositol and subsequent recycling. The Ca^{2+} release from intracellular stores acts as a second messenger to modulate the activity of many mediators. G protein-mediated activation of the phosphatidyl inositide signalling cascade thus has a wide variety of downstream effects, mediated initially by activation of PKC and release of intracellular Ca^{2+}.

Many studies investigating group I mGluR-mediated intracellular signalling have been carried out using molecular cloning and heterologous expression of mGluRs in systems such as *Xenopus* oocytes and transfected mammalian cells. While activation of the PLC/IP_3/Ca^{2+} pathway is always detected following group I mGluR activation, coupling to other signalling cascades has also been detected. The type of cascade involved appears to some extent to be dependent upon the expression system in which the mGluR is characterised. Alternative coupling of GPCRs may result from receptor overexpression in recombinant systems (Hermans and Challiss, 2001). However, in some cases coupling of group I mGluRs to multiple downstream transduction cascades is physiologically relevant, and may contribute to the complexity of neuronal responses to glutamate. There is evidence from a number of studies carried out in heterologous expression systems for coupling of group I mGluRs to the AC/cAMP/PKA pathway, which has been shown to be both inhibited via group I mGluR coupling to pertussis toxin (PTx)-sensitive $G_{i/o}$ proteins, and up-

regulated via coupling to G_S proteins. In addition, PKC has been shown to be involved in modulation of a number of ion channels, and activation of the following downstream effectors: (i) phospholipase A (PLA); (ii) phospholipase D (PLD); mitogen-activated protein kinase (MAPK) (reviewed by Hermans and Challiss, 2001). Group I mGluRs thus appear to modulate the activity of multiple intracellular signalling pathways through functional coupling to a variety of G proteins. In addition, there is evidence for group I mGluR intracellular signalling mediated via G protein-independent mechanisms. This type of interaction occurs in a more limited manner, and it is important to realise that the majority of downstream signalling events are dependent upon G protein activation. A number of G protein-independent signalling mechanisms have been characterised in detail in other types of GPCR, such as the β_2-adrenergic receptor (reviewed by Hall et al., 1999), but remain to be fully explored in the mGluR family. An important mechanism for activation of downstream effectors that does not require G proteins instead depends upon G protein-coupled receptor kinases (GRKs). Activated GPCRs are phosphorylated by GRKs. This event is followed by binding to the GPCR of another family of proteins, known as arrestins. The regions arrestins bind to, generally the third intracellular loop and the portion of the C-terminal tail closest to the membrane, are also primary determinants for G protein signalling. Binding of arrestins thus inhibits G protein signalling. Arrestins also act as adaptor proteins for recruitment of other effector molecules, for example Src-family protein tyrosine kinases. For some GPCRs this Src-dependent pathway leads to MAPK activation (reviewed by Hall et al., 1999) Heuss et al. (1999) described a dual signalling mechanism mediated by group I mGluRs, in which signal transduction involved activation of either G proteins or tyrosine kinases. Synaptic activation of group I mGluRs via mossy fibre stimulation evoked a G protein-independent excitatory postsynaptic response in CA3 pyramidal cells, while inhibiting an afterhyperpolarisation current through a G protein-dependent mechanism. The G protein-independent transduction mechanism instead required a Src-family protein tyrosine kinase. This study is significant because it provides the first functional

evidence for G protein-independent mGluR signalling, as opposed to biochemical and molecular studies carried out in recombinant expression systems. Evidence for PLC-independent modulation of ion channel functionality was provided by Ireland and Abraham (2002), who demonstrated that group I mGluR activation using the selective agonist DHPG caused depolarisation and increased spiking in CA1 pyramidal cells through inhibition of slow- and medium-duration AHP (after-hyperpolarisation) K^+ currents, with a differential contribution from both mGluR1 and mGluR5. This was mediated by a mechanism insensitive to selective blockade of PLC (using U-73122), PKC (using chelerythrine) and IP_3-triggered release of Ca^{2+} from intracellular stores (using cyclopiazonic acid). This study indicates that group I mGluRs inhibit AHP K^+ currents through a PLC-, PKC- and IP_3-independent signalling pathway. Inhibition of G protein activity using the endogenous G protein regulatory protein RGS4 has suggested that DHPG-induced suppression of the AHP current in CA1 is G protein dependent (Saugstad et al., 1998). However, contradictory evidence was provided by Gee and Lacaille (2004). Their results confirmed that DHPG-induced depolarisation is mediated by a PLC-independent pathway. However, using a non-hydrolysable GTP analogue (GDPβS) and N-ethylmaleimide (NEM) to inhibit G protein signalling suggested that DHPG-induced depolarisation is G protein independent. One possible explanation may be differences in the mechanism between interneurons, which were studied by Gee and Lacaille (2004), and CA1 pyramidal cells, which were investigated by Ireland and Abraham (2002). It may be proposed that the PLC-independent DHPG-induced depolarisation is initiated either (i) at the level of the group I mGluR, which is capable of coupling to multiple types of G protein, or activating G protein-independent signalling pathways (reviewed by Hermans and Challiss, 2001); (ii) at the level of G_q, which may couple to multiple signal transduction pathways; (iii) via direct interaction between a G protein subunit and the K^+ channels that mediate the AHP current. Further research is therefore necessary in order to determine the level at which DHPG-induced modulation of AHP K^+ currents is initiated.

1.2.4 Modulation of neuronal ion channel function by group I mGluRs

Here I review the role of group I mGluRs in modulation of neuronal ion channel function. The projects carried out within this thesis are focused upon modulation of glutamatergic synaptic transmission to GABAergic interneurons by group I mGluRs. However, in addition to modulating synaptic transmission, these receptors also directly exert powerful effects upon neuronal excitability via interaction with ion channels. Such effects have been observed in both pyramidal cells and interneurons in the hippocampus. In both pyramidal cells and interneurons, the principal direct effects of selective group I mGluR activation are depolarisation and increased firing of action potentials (e.g. Mannaioni et al., 2001). The underlying mechanisms have been characterised in detail in pyramidal cells. Much less information is available regarding group I mGluR-mediated modulation of ion channels in GABAergic interneurons. In pyramidal cells, group I mGluRs increase neuronal excitability through the following mechanisms. Firstly, inhibition of at least four distinct K^+ currents – the AHP current (Charpak et al., 1990; Desai and Conn, 1991; Ireland and Abraham, 2002), the M current (Charpak et al., 1990), a leak current (Guerineau et al., 1994) and a voltage-dependent slow-inactivating current (Luthi et al., 1996). Secondly, activation of Ca^{2+}-activated and Ca^{2+}-independent non-selective cationic conductances (Crepel et al., 1994; Guerineau et al., 1995; Congar et al., 1997; Heuss et al., 1999; Chuang et al., 2000; 2002; Gee et al., 2003). Group I mGluR activation results in an inward current, which depolarises the neuron. There is evidence that this is at least partially mediated by the transient receptor potential (TRP) family of non-selective cation channels in CA3 pyramidal cells (Gee et al., 2003). In cerebellar Purkinje cells, group I mGluR-mediated inward currents have been shown to be mediated by the TRPC1 channel (Kim et al., 2003).

While it may reasonably be proposed that many of these mechanisms are common to both pyramidal cells and interneurons, there are likely to be significant differences, indicating that detailed investigation of group I mGluR-mediated modulation of ion channels in GABAergic interneurons represents an important area

of future research. The complexity of group I mGluR-mediated effects is likely to be increased by the heterogeneity of the hippocampal interneuron population. Previous studies have already demonstrated that in the CA1 subfield, activation of group I and II mGluRs increases intracellular Ca^{2+} and depolarises interneurons in stratum oriens/alveus, but has little effect upon interneurons in strata radiatum and lacunosum-moleculare (Carmant et al., 1997; Woodhall et al., 1999). There is extensive variation in response to group I mGluR activation even among interneurons within a limited area. Within CA1 stratum oriens, inward current response to group I mGluR activation varied dramatically between four defined classes of interneuron (van Hooft et al., 2000). Indeed, there are distinct differences in response to group I mGluR activation even between CA3 and CA1 pyramidal cells. Activation of group I mGluRs using the selective agonist DHPG evokes a voltage-dependent inward current response in CA3, but not CA1 pyramidal cells. Investigation of mGluR1-knockout mice suggested that this may be because the voltage-dependent inward current is mediated by the mGluR1 subtype (Chuang et al., 2002). This is consistent with the finding from high-resolution immunohistochemical studies that CA3 pyramidal cells express both mGluR1 and mGluR5, while CA1 pyramidal cells express only mGluR5 (Lujan et al., 1996).

1.2.5 mGluR pharmacology

mGluR pharmacology is highly complex, with numerous compounds available which act with varying efficacy at different mGluR subtypes. In designing experiments to investigate mGluR function, it is important to be aware that many commonly used agonists and antagonists may affect several distinct mGluR subtypes or groups, depending upon the concentration used. An increasing degree of subtype specificity is apparent in the newer mGluR pharmacological agents; however, selective agonists and antagonists are not yet available for every mGluR subtype. The selective agonists

most commonly used to differentiate between the three groups of mGluRs are listed in Table 1.1. For detailed review of mGluR pharmacology, see Schoepp et al. (1999).

1.2.6 Group I mGluR expression patterns in the hippocampus

The present section describes expression patterns of metabotropic glutamate receptors in the hippocampus. The majority of projects described in this thesis involve investigation of modulation of excitatory synaptic transmission to CA1 interneurons by group I mGluRs (Chapters 5 to 9). From this point onwards in the present chapter, I therefore focus primarily on the group I receptors.

mGluRs are widely expressed throughout the hippocampus, and exhibit highly specific patterns of expression. There is both anatomical and functional evidence for target-dependent expression of the group III receptor mGluR7. Expression of the receptor at presynaptic terminals originating from the same axon is dependent upon the identity of the postsynaptic target neuron. Anatomical evidence indicates that at both glutamatergic (Shigemoto et al., 1996; 1997) and GABAergic (Somogyi et al., 2003) synapses, mGluR7 is strongly enriched in the presynaptic active zone of terminals contacting interneurons, but not terminals contacting pyramidal cells. This apparent target-dependent expression is supported by electrophysiological evidence. Use of sequential paired recordings demonstrated that activation of group III mGluRs depressed glutamate release at Schaffer collateral terminals originating from the same axon at connections onto CA1 interneurons but not pyramidal cells (Scanziani et al., 1998). This illustrates the high degree of precision in mGluR expression patterns. In understanding the role of mGluRs in modulation of synaptic transmission, it is essential to determine whether each subtype is pre- and/or postsynaptically situated, the brain areas in which it is localised, whether expression is confined to specific cell types and whether the receptor exhibits target-dependent expression. Furthermore, it is important to realise that mGluR expression may be developmentally-regulated. This has been shown for group I mGluRs, for example, by

Lopez-Bendito et al. (2002). mGluR1α and mGluR5 were shown to exhibit differential changes in expression in specific neuronal subtypes in the neocortex and hippocampus throughout the first three weeks of postnatal development.

The currently available anatomical evidence suggests that the group I mGluRs are expressed postsynaptically, while the group II and III receptors are presynaptically expressed. Evidence for postsynaptic group I mGluR expression came from high-resolution immunohistochemical studies, in which immunogold labelling of receptors using highly specific subtype-selective antibodies was combined with serial transverse electron microscopy. This allowed receptor distribution to be investigated in detail at the level of single synapses. The first direct anatomical evidence for postsynaptic group I mGluR expression was presented by Martin et al. (1992), who demonstrated that mGluR1α is enriched in the CA1 subfield and is postsynaptically expressed. mGluR5 was also shown to be exclusively postsynaptically expressed in the hippocampus (Shigemoto et al., 1993). These findings were supported by Baude et al. (1993), who showed that immunoreactivity for mGluR1α in the hippocampus was present in somatostatin-positive GABAergic interneurons. Immunogold labelling combined with electron microscopy revealed that mGluR1α is expressed postsynaptically, mainly at the periphery of the postsynaptic density (PSD) of type 1 synapses. mGluR1α was also present extrasynaptically, in somatic and dendritic membranes at sites where no synapses were located. This demonstration of perisynaptic localisation of group I mGluRs at postsynaptic sites was supported by subsequent studies. mGluR1 and mGluR5 are present in the CA1 subfield in both pyramidal cells and interneurons. Pyramidal cells are strongly enriched for mGluR5 (Lujan et al., 1996), whereas interneurons are enriched for mGluR1α (Baude et al., 1993; Petralia et al., 1997). Group I mGluRs are concentrated on dendritic spines at type 1 synapses in a perisynaptic annulus surrounding the ionotropic glutamate receptors (defined as within 60 nm of the edge of the synapse), followed by an extrasynaptic wider band of receptors decreasing in density (60 – 900 nm) (Lujan et al., 1996; 1997; Petralia et al., 1997; Lopez-Bendito et al., 2002). Co-

immunolocalisation studies using both a polyclonal mGluR1α antibody and a monoclonal antibody to the AMPA receptor GluR2/3/4c indicated that mGluRs and AMPA receptors are differentially localised at cerebellar synapses. AMPA receptors were concentrated in the postsynaptic membrane directly opposing the release site, whereas mGluR1α was located at the periphery of the same synapse (Nusser et al., 1994). AMPA receptors may thus be physically segregated from postsynaptic group I mGluRs. How does this pattern of receptor expression correspond to the functional role of group I mGluRs in modulation of synaptic transmission? Baude et al. (1993) originally put forward the idea that the perisynaptic location of group I mGluRs may serve as the structural basis for their role in activity-dependent processes, with activation occurring only during high-frequency presynaptic activity. This suggestion is supported by electrophysiological evidence demonstrating that mGluR-activated currents are preferentially evoked by high-frequency presynaptic stimulation (Batchelor et al., 1994; Batchelor and Garthwaite, 1997).

In contrast to the numerous studies demonstrating exclusively postsynaptic localisation of group I mGluRs, there is very little evidence to suggest any significant presynaptic expression of these receptors in the hippocampus. A single study by Romano et al. (1995) using an mGluR5-selective antibody confirmed that the receptor is concentrated on dendritic spines and shafts. However, significant mGluR5 immunoreactivity was also detected in presynaptic axon terminals. Although the existence of presynaptic group I mGluRs in the hippocampus cannot be ruled out, this finding must be interpreted with caution, given the wealth of contradictory evidence. One possible explanation may be the method of immunostaining used (Lujan et al., 1997).

Of particular relevance to the projects described in this thesis are expression patterns of group I mGluRs in hippocampal interneurons. Given the extensive heterogeneity of the interneuron population and existence of numerous distinct subtypes (see Section 1.3.1), it may be expected that expression of mGluRs would vary according to interneuron subtype. This issue has so far been addressed in detail

by two studies. Ferraguti et al. (2004) investigated which classes of CA1 interneuron express mGluR1α using double and triple immunofluorescence labelling. The mGluR1α antibody was co-applied with antibodies for neurochemical markers for distinct interneuron subtypes. These markers were the neuropeptides somatostatin (SS), cholecystokinin (CCK) and vasoactive intestinal polypeptide (VIP); and the Ca^{2+} binding proteins calretinin and parvalbumin (PV). Previous studies have demonstrated that mGluR1α is characteristically expressed only in non-principal cells, and is particularly enriched in somatostatin-positive interneurons in CA1 stratum oriens (Baude et al., 1993). mGluR1α-immunopositive interneurons have also been reported at lower density in strata pyramidale, radiatum and lacunosum moleculare (Martin et al., 1992; Baude et al., 1993; Lujan et al., 1996; Shigemoto et al., 1997). Ferraguti et al. (2004) identified several distinct types of interneuron immunopositive for both mGluR1α and somatostatin, which target different domains of CA1 pyramidal cells. These interneurons were characterised by the presence of specific neurochemical markers. These included (i) O-LM ('oriens-lacunosum moleculare') interneurons expressing PV (see Freund and Buzsaki, 1996); (ii) interneurons expressing VIP and/or calretinin, which selectively target other interneurons; (iii) CCK-immunopositive interneurons targeting dendrites of pyramidal cells; (iv) interneurons which could not be positively identified which may correspond to oriens-bistratified cells, immunopositive for SS and immunonegative for PV. Furthermore, no mGluR1α immunoreactivity was detected in interneurons co-expressing CCK and VIP, or in interneurons immunolabelled very intensely for PV. By specifically characterising the interneuron subtypes expressing mGluR1α and identifying their postsynaptic targets, this important study provides insight regarding the role of mGluR1α in modulation of synaptic transmission in the hippocampus. The second study investigating group I mGluR expression patterns in hippocampal interneurons was carried out by van Hooft et al. (2000). This study focused on detailed investigation of CA1 oriens-alveus interneurons. Group I mGluR expression was quantitatively analysed in individual neurons using single cell RT-PCR (reverse transcriptase polymerase chain reaction).

Immunohistochemical detection of neurochemical markers (PV, SS, calretinin and calbindin) was carried out. Neuronal morphology was analysed by filling cells with biocytin during electrophysiological recording and subsequent staining using fluophore-conjugated streptavidin. Interneurons were classified according to (i) action potential firing pattern; (ii) inward current response to the mGluR agonist ACPD. Four distinct interneuron subtypes were identified. Type I interneurons expressed both mGluR1 and mGluR5, responded to ACPD with a large inward current, and were SS immunopositive. Somata were located at the oriens-alveus border and axons projected vertically towards stratum lacunosum moleculare. These interneurons appeared to be O-LM ('oriens-lacunosum moleculare') cells (see Freund and Buzsaki, 1996). Type III interneurons expressed predominantly mGluR5, responded to ACPD with a moderate inward current and were immunopositive for PV. Dendritic trees were vertically-orientated, and axons terminated exclusively in stratum pyramidale. The authors suggested that these interneurons may be basket cells (see Freund and Buzsaki, 1996). Type II and IV interneurons represent a heterogeneous population in terms of morphology, with considerable variation in orientation of dendritic trees and zones of axonal arborisation. Type II interneurons expressed exclusively mGluR1 and were immunopositive for calbindin, while type IV interneurons expressed both mGluR1 and mGluR5 and were immunopositive for calbindin and calretinin. The study of van Hooft et al. (2000) demonstrates that even within a relatively limited area of the hippocampus, in this case the single layer of stratum oriens in the CA1 subfield, there is extensive variation in expression of group I mGluRs among interneurons. Group I mGluR expression patterns appear to correlate with both physiological properties of interneurons and patterns of dendritic and axonal projection, suggesting that mGluR1 and mGluR5 are selectively expressed by interneuron subtypes with specific functional roles within the hippocampal network. Interestingly, van Hooft et al. (2000) showed that activation of group I mGluRs under current-clamp conditions increased spike frequency and resulted in rhythmic firing activity in type I and II, but not in type III and IV interneurons. This would suggest that the mGluR1 subtype is responsible for

mediating this effect. Synchronous action potential firing may allow GABAergic interneurons to act as "pacemakers" controlling the excitability of pyramidal cells. These findings suggest that induction of rhythmic action potential firing in CA1 interneurons may be group I mGluR-induced, pointing to a key role for these receptors in the regulation of hippocampal network function. This topic is addressed further in the General Discussion (Chapter 10).

Section 3. Inhibitory interneurons in the hippocampus

A detailed review of the anatomical and physiological properties of every known type of hippocampal interneuron is beyond the scope of this discussion. The aim of this section is to emphasise the heterogeneity of the interneuron population, describe the functional properties of this cell type, and discuss their physiological roles within the hippocampus.

1.3.1 Heterogeneity of hippocampal interneurons

Hippocampal interneurons are a highly heterogeneous population, in terms of morphology, connectivity, firing patterns, neurochemical content and physiological roles. This reflects the fact that specific interneuron subtypes have distinct functional roles, and this specialisation is essential in synchronising pyramidal cell firing in order to induce and maintain oscillatory activity. This highly complex aspect of brain function is achieved largely by precisely-controlled spatio-temporal release of GABA onto specific domains of pyramidal cell membrane by distinct interneuron subtypes (Klausberger et al., 2005; Somogyi and Klausberger, 2005; Baude et al., 2006).

Interneurons may be classified according to an extensive variety of parameters. No overall unified classification system currently exists (see e.g. Maccaferri and Lacaille, 2003 for review). Nonetheless, the importance of accurate identification of GABAergic interneuron subtypes from which electrophysiological recordings and other types of data are obtained is becoming increasingly apparent at

the time of writing. It is clear that meaningful insights into cortical network function are considerably less likely to be gained if GABAergic interneurons are treated as a homogeneous population. There is extensive variation in numerous aspects of cortical interneuron morphology and physiology. This must be taken into account by attempting to identify in as much detail as possible the cell from which data are obtained.

The most common individual criteria used for interneuron classification are described below. However, there is increasing evidence from recent studies that GABAergic interneurons cannot be accurately identified according to a single criterion, since this approach is overly simplistic and there may be overlap of certain characteristics between very different sub-groups of interneurons. Indeed, even when accurate high-resolution immunohistochemical analysis is employed, classification according to a single neurochemical marker (generally a neuropeptide or Ca^{2+}-binding protein; see below for further detail) alone is often insufficient to delineate between distinct interneuron subtypes with specific input patterns and spatio-temporal outputs. For example, parvalbumin is expressed by at least four distinct classes of interneuron (Somogyi and Klausberger, 2005). Instead, it seems that this cell type may be definitively classified into subtypes with specific functional roles only if several criteria are examined together in the same neuron, e.g. somatodendritic pattern to identify location of inputs and outputs, combined with high-resolution immunohistochemistry to determine expression of at least one and preferably multiple neurochemical marker proteins and neurotransmitter receptors. Further information may be gained by examining the temporal structure of spiking *in vivo* (Somogyi and Klausberger, 2005).

1.3.1.1 Neuronal morphology

The morphology of a neuron can provide much information regarding its functional role within a neuronal circuit. Most importantly, the pattern of axonal projections will identify the postsynaptic targets, while the somatodendritic location allows the location, and thus usually the type, of afferent inputs to be determined.

High-resolution visualisation of the entire axonal and dendritic processes of single neurons is now routinely possible using intracellular labelling techniques combined with confocal microscopy.

Hippocampal interneurons display extensive morphological diversity. At present there is no universally accepted anatomical nomenclature for interneurons. Cells may be identified according to classical definitions which are based upon appearance (e.g. basket cells). Alternatively, terms may be used which emphasise the postsynaptic target (e.g. axo-axonic cells), orientation of the dendritic tree (e.g. vertical and horizontal cells in stratum oriens), or for long-projection cells the origin and target brain regions (e.g. hippocampo-septal interneurons). Finally, interneurons may be defined by the two specific layers containing the soma and axonal processes (e.g. oriens-lacunosum moleculare 'O-LM cells', pyramidale-lacunosum moleculare 'P-LM cells', radiatum-lacunosum moleculare 'R-LM cells', and oriens-oriens and radiatum 'O-bistratified cells') (reviewed by Freund and Buzsaki, 1996; Somogyi and Klausberger, 2005). The number of anatomically distinct types of hippocampal interneuron remains unclear. Parra et al. (1998) identified 16 morphologically distinct types of CA1 interneuron. However, interneurons with similar morphology displayed widespread variation in firing pattern and pharmacological properties, indicating the existence of a neuronal population with highly variable properties which cannot be classified into a small number of clearly-defined groups. More recently, a review by Somogyi and Klausberger (2005) identified a different group of at least 16 distinct interneuron subtypes in area CA1, 12 types of which innervated mainly specific domains of pyramidal cells, while four types innervated primarily other interneurons. Cells were classified according to dendritic pattern, axonal outputs, and presence of at least one, and often multiple, neurochemical markers. The authors point out that these classifications are not entirely definitive, and more subtypes may be identified as further information regarding expression of neurochemical markers etc. is gained. Nonetheless, this discussion highlights that identification according to multiple criteria

may allow CA1 interneurons to be classified to some extent into distinct sub-groups, rather than existing as an entirely heterogeneous population.

1.3.1.2 Neurochemical content

A variety of immunohistochemical techniques have been used to identify numerous specific neurochemical markers for interneurons. Inhibitory interneurons may be identified by the presence of GABA and enzymes in the GABA biosynthetic pathway such as GAD65 (glutamic acid decarboxylase, Mr 65 kDa) and GAD67 (Ribak, 1978; Storm-Mathisen et al., 1983). Different populations of interneurons may be distinguished by the presence of various peptides, including somatostatin, cholecystokinin (CCK), vasoactive intestinal peptide (VIP), neuropeptide Y and substance P; or by Ca^{2+} binding proteins such as calbindin, parvalbumin and calretinin (reviewed by Freund and Buzsaki, 1996). It may be expected that grouping of interneurons according to neurochemical markers could begin to reveal correlations with anatomical and physiological properties. However, within a single neurochemically-defined subgroup exist numerous different types of morphologically- and physiologically-defined interneurons (Freund and Buzsaki, 1996; Parra et al., 1998; Maccaferri and Lacaille, 2003). For example, somatostatin-positive interneurons have been anatomically classified as O-LM, O-bistratified, P-LM and R-LM cells (Freund and Buzsaki, 1996; Katona et al., 1999a; Oliva, Jr. et al., 2000; Maccaferri et al., 2000; Losonczy et al., 2002). Similarly, parvalbumin-positive interneurons include basket cells, axo-axonic cells, O-LM cells and bistratified cells (Freund and Buzsaki, 1996; Maccaferri et al., 2000; Klausberger et al., 2003; Ferraguti et al., 2004; Klausberger et al., 2004; Klausberger et al., 2005; Somogyi and Klausberger, 2005).

1.3.1.3 Physiological properties

Patch clamp recording may be combined with intracellular labelling techniques in order to provide information on both the physiological properties and morphology of the same neuron. Action potential firing pattern is one classical criterion which may be

used to distinguish different subgroups of interneurons. Early classifications divided hippocampal interneurons into fast- and regular-spiking cells (Kawaguchi and Hama, 1988). Parra et al. (1998) identified three groups of CA1 interneurons according to spike discharge patterns, which were regular, irregular or clustered into groups. As noted previously, identification according to firing pattern did not correlate with morphological or pharmacological classifications. It is important to realise that action potential generation results from a complex interaction between numerous temporally-overlapping voltage-gated conductances. These are mediated by many distinct ion channels, all of which may display unique expression patterns among different subtypes of interneuron. Action potential firing pattern must therefore be considered an imprecise means of classification, which does not accurately describe the complex underlying patterns of voltage-gated ion channel expression.

Interneurons display extensive heterogeneity in neurotransmitter receptor expression, which affects the physiological properties of the cell. Subsets of CA1 interneurons are differentially sensitive to agonists of mGluR, noradrenaline, muscarine and serotonin receptors (Parra et al., 1998). Immunohistochemistry has been used to provide evidence for variations between different subtypes of interneurons in expression of AMPA receptors, mGluRs, $GABA_A$ receptor subunits, 5HT-2 and 5HT-3 serotonin receptors, opioid receptors, and muscarinic and nicotinic acetylcholine receptors (reviewed by Freund and Buzsaki, 1996). Svoboda et al. (1999) demonstrated that opioid receptor subtype expression correlates with axonal projection patterns in CA1 interneurons. Stratum oriens interneurons innervating the pyramidal cell perisomatic region were more likely to express μ-opioid receptors, whereas interneurons projecting to pyramidal cell dendritic layers more frequently expressed δ-opioid receptors. There is extensive evidence that expression of ionotropic glutamate receptors varies between populations of interneurons. Heterogeneity in AMPA receptor subunit composition among different groups of interneurons has been determined both by immunohistochemistry (see Freund and Buzsaki, 1996) and the electrophysiological properties of the receptor (McBain and

Dingledine, 1993; Isa et al., 1996). Quantitative immunogold labelling combined with serial EM was used to demonstrate variability in NMDA receptor density between different types of excitatory synapse onto subsets of CA1 interneurons (Nyiri et al., 2003). Cell type-specific differences in short-term plasticity of excitatory inputs have been reported in subgroups of hippocampal interneurons identified by molecular markers and patterns of axonal arborisation (Losonczy et al., 2002). Furthermore, Maccaferri and Dingledine (2002) identified two populations of CA1 interneurons with markedly different EPSP kinetics ('fast' and 'slow'). These differences are apparently associated with variations in NMDA receptor expression, and determine the functional role of the interneuron in mediating feedforward dendritic inhibition of CA1 pyramidal cells. It is clear that ionotropic glutamate receptor expression may vary in different ways among subgroups of hippocampal interneurons. Heterogeneity in ionotropic glutamate receptor expression affects the physiological properties of the neuron, since these receptors are involved in mediating somatic and dendritic integration of synaptic inputs and EPSP-spike coupling. Differences in integrative properties affect both the probability and timing of GABA release in response to a given pattern of presynaptic input.

1.3.1.4 Network connectivity

As described previously, interneurons may be classified morphologically according to the two specific layers containing the soma and axonal processes (e.g. O-LM cells). However, in some cases it is also possible to distinguish different subtypes of interneuron according to the type and pattern of afferent inputs. For example, CA1 interneurons may receive inputs from specific CA1 pyramidal cell recurrent collaterals, or from general CA1 pyramidal cell afferent projections (Freund and Buzsaki, 1996). Distinguishing interneurons according to such criteria obviously provides valuable information regarding the role of the cell within local neuronal circuits. This is illustrated by the example of CA1 somatostatin-positive O-LM cells, which are synaptically activated by local CA1 pyramidal cell recurrent collaterals and

are fundamentally involved in feedback inhibitory circuits (Blasco-Ibanez and Freund, 1995). In an impressive study combining LM, serial EM and immunohistochemistry, Gulyas et al. (1999) were able to quantify the total number of excitatory and inhibitory synaptic inputs to three neurochemically-defined populations of CA1 interneurons. In contrast to previous studies (Parra et al., 1998; see also Section 2.1.2 above), some correlation was found between molecular markers and anatomical properties. Parvalbumin-positive interneurons had the most extensive dendritic trees and the thickest dendrites, and received the densest synaptic innervation. This cell type received the lowest ratio of GABAergic inputs. Calretinin-positive cells had the smallest dendritic trees and received the highest ratio of GABAergic inputs. The third cell type, calbindin-positive interneurons, lay between the other two in terms of dendritic tree size, number of synaptic inputs and ratio of GABAergic inputs. Each cell type also appeared to be associated with a distinct pattern of excitatory inputs. Both parvalbumin- and calretinin-positive interneurons received excitatory synapses within all layers of CA1. In contrast, calbindin-positive cells received inputs primarily from Schaffer collaterals in stratum radiatum. This suggests that calbindin-positive interneurons are involved explicitly in feedforward inhibition, whereas parvalbumin- and calretinin-positive cells are innervated less specifically in both a feedforward and feedback manner. More recent work employing similar techniques demonstrated that in CA1, cholecystokinin-positive basket cells receive considerably less synaptic input than parvalbumin-positive basket cells. However, the ratio of inhibitory synapses is higher on cholecystokinin-positive cells, and this cell type appears to be under a more diverse and complex control (Matyas et al., 2004). These differences in connectivity seem to correlate with distinct functional roles for these interneuron subtypes (Freund, 2003), which are discussed in Section 2.3.2.

It is clear that network connectivity represents an important criterion for classification of interneurons, and can provide valuable insights regarding their function. Some recent studies have demonstrated that in certain cases at least partial

correlations exist between connectivity of afferent inputs, molecular markers and anatomical properties (Gulyas et al., 1999; Matyas et al., 2004).

1.3.2 Physiological properties of hippocampal interneurons

Here I focus on the physiological properties of inhibitory interneurons which give this cell type its distinctive characteristics. Excitatory synaptic connections onto interneurons, including the pre- and postsynaptic neurotransmitter receptors involved, are considered separately in Section 1.4.

1.3.2.1 The role of GABA in synaptic transmission

The dendrites, soma and axon initial segment of principal cells are innervated by inhibitory interneurons, which release the neurotransmitter GABA, together with certain neuromodulatory peptides, onto their postsynaptic targets. Interneurons also form GABAergic synaptic connections with other interneurons. Activation of the ionotropic $GABA_A$ receptor leads to opening of the receptor ion channel, which is selective for anions, particularly Cl^-. In most neurons the chloride reversal potential (E_{Cl}, approximately -89 mV) is negative to the resting membrane potential, resulting in a driving force which causes Cl^- ions to enter and hyperpolarise the cell. This causes the membrane potential to move away from the threshold for action potential firing. Such events are known as inhibitory postsynaptic potentials (IPSPs) or inhibitory postsynaptic currents (IPSCs), depending upon whether the change in membrane potential or the transmembrane flow of ionic current is being considered. IPSPs are biphasic, with the early phase mediated by Cl^- entry through $GABA_A$ receptor ion channels, and the late phase mediated by outward K^+ flux through channels coupled by G proteins to metabotropic $GABA_B$ receptors. Opening of $GABA_A$ receptor ion channels decreases the input resistance of the neuron and shunts excitatory currents, and can thus reduce the effectiveness of concomitant excitatory inputs. The action of GABAergic interneurons thus controls and limits the flow of excitatory transmission

through the hippocampus and other neuronal networks. It should be noted that in some circumstances, release of GABA may elicit a depolarising response in the postsynaptic target cell, depending upon factors such as developmental stage of the animal, patterns of presynaptic activity, and the postsynaptic target domain (reviewed by Stein and Nicoll, 2003). Recent research has shown that cortical pyramidal cell axons display a depolarising response to GABA released from GABAergic axo-axonic cells, which are the cell type almost exclusively responsible for innervating the axon initial segment. This occurs due to a depolarised reversal potential (E_{GABA}) for axonal relative to perisomatic GABAergic inputs (Szabadics et al., 2006). Axo-axonic cells are thus strategically-placed inhibitory neurons which act to control neuronal output.

Ionotropic receptors for glutamate, the major excitatory neurotransmitter of the CNS, gate cation-permeable ion channels. Fast excitatory neurotransmission in the CNS is mediated primarily by influx of Na^+ through the ion channel of the AMPA-class glutamate receptor. The rapid influx of cations causes depolarisation of the cell, pushing the membrane potential closer to the threshold for action potential firing and thereby propagating the signal between neurons.

1.3.2.2 Differential expression of intrinsic voltage-gated ion channels

Interneurons express populations of intrinsic voltage-gated ion channels which in some cases are distinct from those expressed by principal cells. This was initially demonstrated through analysis of action potential waveforms, which showed differences in action potential duration, afterhyperpolarisation and interspike interval (Lacaille et al., 1987; Kawaguchi and Hama, 1988). As may be expected, there exists considerable heterogeneity among different subgroups of hippocampal interneurons in terms of action potential kinetics, and only a few types have been characterised in detail (Lacaille et al., 1987; Kawaguchi and Hama, 1988; Freund and Buzsaki, 1996). In general, interneurons display action potentials of lower amplitude and considerably shorter duration than pyramidal cells, with a high spontaneous firing frequency (5-80Hz) and lower threshold for action potential generation in response to afferent

stimulation (Lacaille et al., 1987; Kawaguchi and Hama, 1988; Martina and Jonas, 1997). Principal cells are either regularly spiking or intrinsically bursting ('complex spiking'), and exhibit changes in action potential frequency during sustained spiking or depolarising current injection (reviewed by Connors and Gutnick, 1990). This is known as spike frequency adaptation. In contrast, a classical property of most types of inhibitory interneuron is fast spiking, with generation of trains of high frequency action potentials with no spike frequency adaptation. These properties are of fundamental importance in influencing overall network behaviour, and result from differences in expression of subpopulations of voltage-gated ion channels between the two cell types.

Numerous distinct potassium conductances contribute in complex and often subtle ways towards shaping the action potential. For example, I_K activates rapidly upon membrane depolarisation and does not inactivate. This conductance acts to repolarise the neuron during an action potential, since there is a driving force causing K^+ to leave the cell, as the potassium reversal potential (E_K, approximately -90 mV) is virtually always negative to the membrane potential of the cell. Differences in K^+ channel expression between interneurons and pyramidal cells, and between interneuronal subtypes, may therefore profoundly affect action potential kinetics. A detailed review of the properties of all known K^+ channels and their expression in specific cell types is beyond the scope of this discussion. The important concepts are that K^+ channels are of fundamental importance in shaping action potentials, and that differential K^+ channel expression is partly responsible for the specialised spiking properties of interneurons, namely fast spiking with no spike frequency adaptation. Martina et al. (1998) used patch clamp recording combined with single cell RT-PCR analysis of K^+ channel mRNA to investigate differences in K^+ channel function and expression between CA1 pyramidal cells and dentate basket cell interneurons. Kv3 (Kv3.1b and Kv3.2) subunit transcripts were found in almost all basket cells but very few pyramidal cells. In contrast, Kv4 (Kv4.2 and Kv4.3) transcripts were found in almost all pyramidal cells but only around 50% of basket cells. Other studies have

demonstrated that Kv3.1b and Kv3.2 are expressed in around 80-100% of parvalbumin-positive interneurons, and Kv3.2 is present in around 40% of somatostatin positive interneurons (Du et al., 1996; Chow et al., 1999; Atzori et al., 2000). Both of these interneuron subpopulations exhibit fast spiking characteristics (Freund and Buzsaki, 1996). Kv3 channels are thus present in many interneurons and absent in most pyramidal cells. Kv3 channel activity contributes towards generation of short-duration action potentials. These channels activate at membrane potentials close to the action potential peak, facilitate rapid repolarisation and limit afterhyperpolarisation. Kv3 channels can facilitate recovery of both Na^+ channels and transient A-type K^+ channels from inactivation. Taken together, these effects contribute towards high frequency spiking (Erisir et al., 1999; Lien and Jonas, 2003). It is important to realise that many other K^+ channels are involved in determining the specialised spiking properties of interneurons, and considerable further research is required before the underlying mechanisms and heterogeneity between interneurons and pyramidal cells are fully understood.

Differences in expression and function of voltage-gated Na^+ channels between principal cells and interneurons are not well characterised. Na^+ channels show less molecular and functional diversity than other types of voltage-gated ion channel (reviewed by Hille, 2001). Opening of Na^+ channels is responsible for the initial depolarisation in the action potential. There is a rapid influx of Na^+ ions, since the sodium reversal potential (E_{Na}, approximately +40 mV) is considerably more positive than the resting membrane potential. There are a number of differences in Na^+ channel inactivation kinetics in dentate basket cell interneurons in comparison to CA1 pyramidal cells. The steady-state inactivation curve is steeper and shifted towards more positive potentials in interneurons, and inactivation kinetics show a slower onset and faster recovery (Martina and Jonas, 1997). The dynamics of recovery from inactivation regulate the fraction of available Na^+ channels during a train of action potentials. Rapid recovery of Na^+ channels in interneurons supports fast, sustained

spiking, whereas slower recovery in pyramidal cells results in spike frequency adaptation.

Heterogeneity in Ca^{2+} channel expression between hippocampal interneurons and pyramidal cells and between different interneuronal subtypes exists but has not yet been extensively investigated. Low threshold-activated Ca^{2+} channels have been shown to facilitate burst firing in stratum lacunosum-moleculare interneurons, demonstrating that interneurons express Ca^{2+} channels with properties distinct from those of pyramidal cells (Fraser and MacVicar, 1991). Using paired recordings, Poncer et al. (1997; 2000) demonstrated that Ca^{2+} channel subtypes involved in mediating vesicular release of GABA from presynaptic terminals differ between subtypes of CA3 interneuron. N-type Ca^{2+} channels are necessary for generation of IPSCs from stratum radiatum interneurons onto CA3 pyramidal cells, whereas P-type channels are necessary in stratum oriens and stratum lucidum interneurons.

Spatial distribution of ion channels is a further important determinant of interneuron function. The density of dendritic Na^+ and sustained K^+ currents are higher in somatostatin-positive CA1 interneurons than in pyramidal cells (Martina et al., 2000). Action potentials may thus be initiated throughout the dendritic tree and propagated rapidly to the soma even during high frequency firing, ensuring fast and stable sustained signalling.

1.3.3 Physiological roles of hippocampal interneurons

GABAergic interneurons fulfil a variety of essential functions within the hippocampus and other cortical networks. I begin by considering their roles within local inhibitory microcircuits, and then discuss the role of such circuits in large-scale network activities. Many of the mechanisms discussed in this section also operate within the neocortex and elsewhere within the CNS.

1.3.3.1 Feedforward and feedback inhibitory circuits

At the local circuit level, GABAergic interneurons mediate feedforward and feedback inhibition of principal cells. In addition, interneurons form synapses onto other interneurons, giving rise to a network of inhibitory cells connected by GABAergic synaptic contacts. Feedforward and feedback inhibition act to modulate and stabilise the activity of the principal cell population. By causing hyperpolarisation and shunting excitatory inputs through increases in membrane Cl^- conductance, GABAergic synaptic connections onto dendritic and perisomatic regions of principal cells reduce the efficacy of excitatory afferents. Interneurons thus inhibit glutamatergic excitation between pyramidal cells.

In feedforward inhibitory circuits, afferent excitatory inputs activate the interneuron, which forms inhibitory synapses onto a separate group of principal cells. This disynaptic circuit reduces the probability of principal cell firing by limiting the window for temporal EPSP summation. Feedforward inhibition thus increases the temporal precision of principal cell output in response to excitatory input. In feedback inhibitory circuits, the first event is activation of principal cells by excitatory afferents. The output of the principal cells is fed back to the interneuron via recurrent excitatory axon collaterals. The interneuron fires action potentials and releases GABA, acting to inhibit a group of pyramidal cells including those which initially activated the interneurons. Thus feedforward inhibition is regulated by the level of excitatory input, while feedback inhibition is proportional to the rate of output (Buzsaki, 1984). It is clear that excitatory synaptic connections onto interneurons are of fundamental importance in activation of both types of inhibitory microcircuit.

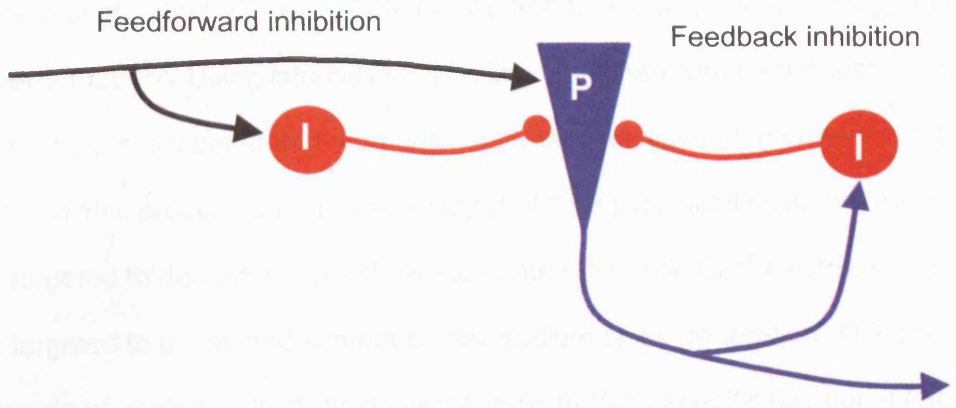

Figure 1.7. *Schematic representation of feedforward and feedback inhibition. In the feedforward circuit, excitatory afferents (black) activate an interneuron (red), which in turn forms an inhibitory connection onto a principal cell (blue). The principal cell is also directly activated by the excitatory afferents. In the feedback circuit, recurrent excitatory collaterals (blue) feed back the output of the principal cell via an inhibitory interneuron. Excitatory and inhibitory synapses are represented by arrows and circles, respectively.*

Hippocampal interneurons may be activated by local and distal feedforward and feedback projections originating from dentate granule cells and pyramidal cells, and by extrahippocampal afferents. Certain interneuron subtypes are innervated exclusively by extrahippocampal afferents, and thus mediate feedforward inhibition only. Most interneurons of this type have somata located in stratum lacunosum-moleculare and the dentate molecular layer (Buzsaki, 1984; Freund and Buzsaki, 1996). In contrast, most interneurons with somata located in stratum pyramidale, stratum oriens and the hilus are innervated by both local and distal excitatory inputs; and by extrahippocampal afferents, and are thus involved in mediating both feedforward and feedback inhibition (Buzsaki, 1984; Lacaille et al., 1987). Examples of interneuron subtypes which are strongly involved in feedback inhibition are basket cells, O-LM cells and trilaminar interneurons (Blasco-Ibanez and Freund, 1995; Freund and Buzsaki, 1996).

Anatomical and physiological studies have shown that axons of different classes of interneuron target precise and different zones of pyramidal cell membrane (Gulyas et al., 1993a; Buhl et al., 1994; Freund and Buzsaki, 1996; Miles et al., 1996;

Maccaferri et al., 2000; Freund, 2003; Pouille and Scanziani, 2004; Somogyi and Klausberger, 2005). Using intracellular labelling combined with paired recording, Miles et al. (1996) demonstrated that morphologically distinct types of interneuron act to control dendritic properties and axonal output of CA3 pyramidal cells. Interneuron axons targeted to dendrites were shown to control dendritic Ca^{2+} electrogenesis, while axons targeted to axons and somata control sodium spike generation. This provides an example of anatomically distinct interneurons fulfilling specific functional roles within the hippocampal network. Furthermore, simultaneous somatic and dendritic recordings from CA1 pyramidal cells have shown that feedforward inhibition activates interneurons which primarily target the perisomatic region (Pouille and Scanziani, 2001). Subcellular partitioning of feedforward inhibition facilitates precise coincidence detection of excitatory inputs converging on the soma, while giving a broader temporal integration window within the dendritic compartment.

Both feedforward and feedback inhibition can exert powerful effects upon the activity of the pyramidal cell population. For example, basket cells mediating feedback inhibition are bidirectionally connected to principal cells (Lacaille et al., 1987; Buhl et al., 1994). The time required for the onset of recurrent inhibition in CA3 pyramidal cells is shorter than the latency of the action potential-induced depolarising afterpotential. Single IPSPs from feedback inhibitory basket cells contacting perisomatic regions could suppress repetitive spiking of pyramidal cells, thereby strongly influencing the activity of the pyramidal cell population (Miles et al., 1996).

At the level of local circuits, information processing in the hippocampus and elsewhere in the brain is regulated by the spatial and temporal activation of excitatory and inhibitory synaptic connections, and the integrative properties of the postsynaptic neurons. Recent studies have shown that specific patterns of presynaptic activity may activate distinct inhibitory circuits within the hippocampus. Using paired recordings combined with immunocytochemistry and light and electron microscopy, Maccaferri et al. (2000) demonstrated that morphologically and neurochemically-defined subtypes of CA1 stratum oriens interneuron innervate specific domains of postsynaptic

pyramidal cells. The kinetic properties of somatically recorded unitary IPSCs, the degree of paired pulse depression, and the postsynaptic response to a train of presynaptic action potentials strongly correlated with the innervated cell surface domain. These findings suggest that CA1 pyramidal cells are subject to multiple forms of feedback inhibition, mediated by distinct subtypes of stratum oriens interneurons. More recent work has demonstrated the existence of two populations of CA1 stratum radiatum feedforward interneurons which are activated via EPSPs with distinct kinetics ('fast' or 'slow') (Maccaferri and Dingledine, 2002). These differences in functional properties are NMDA receptor-dependent, and affect EPSP integration and spike timing. Action potentials generated in the different interneuron subtypes were temporally segregated to distinct phases of EPSPs recorded in CA1 pyramidal cells, suggesting specific roles for these two types of feedforward inhibitory cells in controlling pyramidal cell activity. Pouille and Scanziani (2004) made simultaneous somatic and dendritic recordings from CA1 pyramidal cells using combinations of voltage- and current-clamp, while activating recurrent feedback inhibition by stimulating CA1 pyramidal cell axons in the alveus. With a single stimulus, IPSCs were larger in the soma, indicating more prominent somatic inhibition in response to single action potentials. However, during a train of action potentials recurrent inhibition rapidly shifted from the somatic to the dendritic compartment. Recordings from stratum oriens interneurons revealed that this frequency-dependent inhibition results from two separate inhibitory microcircuits formed by distinct interneuron subtypes, which target specific postsynaptic domains and exhibit distinct EPSC kinetics and passive membrane properties. In the first circuit, so-called 'onset-transient' interneurons, which fire a single action potential at the beginning of a stimulus train, act to mediate transient somatic inhibition in response to low frequency stimulation. In the second circuit, 'late-persistent' interneurons (identified as O-LM cells), which have a greater firing probability later in the train, mediate prolonged inhibition of the dendritic compartment. These two inhibitory loops thus extract distinct temporal features of a spike train and route them as independent signals to specific

postsynaptic target domains of CA1 pyramidal cells. The onset of a spike train activates perisomatic inhibitory conductances via 'onset-transient' interneurons, acting as a form of coincidence detection to synchronise CA1 pyramidal cell activity with the onset of an incoming spike series. The frequency of the spike train determines activation of 'late-persistent' interneurons and thus controls dendritic inhibition. Distinct patterns of afferent activity can thus be interpreted and encoded by local inhibitory microcircuits, which in turn synchronise and modulate population activity of principal cells. This study therefore demonstrates the high degree of precision in control and function of local inhibitory microcircuits, and the importance of such circuits in controlling and shaping pyramidal cell activity.

1.3.3.2 Interneurons in oscillations

Extracellular field potential recordings in the hippocampus and neocortex have demonstrated large-scale network oscillations, which represent the synchronous discharge of populations of principal neurons. Oscillations fall into distinct frequency bands, the most common being theta (4-7 Hz), gamma (30-80 Hz) and ultra-fast (200 Hz "ripples"). There is considerable evidence that oscillations are of central importance in complex neural functions such as information processing, exploratory behaviour and spatial navigation, sensory representation, learning and memory, and sleep states. To give one example, gamma-frequency oscillations are thought to mediate 'binding' of various aspects of a specific visual stimulus. Properties such as texture, shape and colour are encoded by transient groupings of neurons through assembly coding. Synchronous discharge ('binding') of distributed groupings of neurons comprising an assembly relating to a specific object is achieved through the influence of distinct gamma frequency oscillatory patterns upon their membrane potential (reviewed by Singer, 1993; 1999).

Interconnected networks of GABAergic interneurons are of fundamental importance in the generation and maintenance of pyramidal cell oscillations. Cobb et al. (1995) demonstrated that single inhibitory interneurons can phase spontaneous

firing and subthreshold oscillations at theta frequencies in hippocampal pyramidal cells. This is due to the interaction of hyperpolarising $GABA_A$ receptor-mediated synaptic events with intrinsic oscillatory mechanisms mediated by voltage-gated ion channels. Due to the divergence of interneuron axonal projections, the authors estimate that over a thousand pyramidal cells may share a common temporal reference established by a single interneuron. Transient gamma frequency oscillations and fast rhythmic IPSPs in simultaneously recorded pyramidal cells have been observed in hippocampal slices during blockade of ionotropic glutamate receptors. Oscillations are prolonged by mGluR agonists and blockade of $GABA_B$ receptors. These findings suggest that the critical mechanism for induction of gamma frequency oscillations is mutual $GABA_A$ receptor-mediated inhibition among interconnected interneurons within a network (Whittington et al., 1995; 1997). IPSPs generated through feedback inhibition have been shown to both spatially and temporally limit action potential generation in populations of interconnected hippocampal pyramidal cells (Fisahn et al., 1998). This narrowing of the action potential window supports coincidence detection in the postsynaptic neuronal population and maintains a short temporal integration window, allowing generation of numerous distinct neuronal assemblies.

Excitatory synaptic connections onto interneurons are essential for generation of network oscillations. Experimental techniques and computer simulations have been employed to develop models of networks containing interneurons and pyramidal cells. Such studies have demonstrated that excitation of interneuron networks by synchronous EPSPs entrains rhythmic firing of interneurons in a distinct frequency band due to their mutual interconnectivity. Within the gamma frequency range, oscillation frequency accelerates with increasing excitatory drive onto interneurons, thereby shortening IPSC decay. The output of the interneuron network arrives as rhythmic IPSPs which entrain the firing patterns of pyramidal cell populations (reviewed by Singer, 1993; 1999; McBain and Fisahn, 2001).

Recent evidence has demonstrated that neurochemically-defined hippocampal interneurons may have distinct roles in generation and maintenance of oscillations and modification of network behaviour according to emotional and physiological states. Freund (2003) makes a detailed comparison of various features of cholecystokinin- and parvalbumin-positive interneurons innervating the perisomatic region of pyramidal cells. These features include patterns of local and subcortical afferent inputs, postsynaptic actions, and expression of presynaptic modulatory receptors. The numerous distinguishing features suggest that a locally-driven network of parvalbumin-positive basket cells acts as a non-plastic system to entrain pyramidal cell firing at theta and gamma frequencies. In contrast, cholecystokinin-positive interneurons are subject to a more complex and diverse modulatory control, and their output is likely to be affected by the emotional, motivational and general physiological state of the animal. This interneuron subpopulation may therefore be involved in making subtle mood-dependent alterations to pyramidal cell activity. This hypothesis was further supported by subsequent experimental work, in which intracellular labelling combined with LM and serial EM was used to reconstruct the entire dendritic tree of these two interneuron subtypes (Matyas et al., 2004). Parvalbumin-positive cells formed a strongly interconnected inhibitory network and were subject to extensive excitatory innervation from pyramidal cells, consistent with a role in generation and maintenance of oscillations. Cholecystokinin-positive cells showed a much lower level of mutual interconnectivity, and were subject to a greater level of local and extrinsic inhibitory input. Taken together with the greater expression of presynaptic modulatory receptors, this suggests a less critical involvement in network oscillations for this interneuron subtype.

Section 4. Glutamatergic synapses onto hippocampal interneurons

In the previous section, I have shown the fundamental involvement of GABAergic interneurons in feedforward and feedback inhibitory microcircuits. I have also discussed the central importance of this cell type in shaping and modulating pyramidal cell activity, thereby mediating a wide variety of complex neural functions. I now review the functional mechanisms underlying glutamatergic excitation of hippocampal interneurons, and how this class of synapse is modulated. The central topic of this thesis is modulation of excitatory connections onto interneurons by metabotropic glutamate receptors (mGluRs).

Although both excitatory synapses between principal cells and GABAergic inhibitory connections have been extensively characterised, relatively less is known about excitatory connections onto interneurons. From the earliest electrophysiological investigations of the brain, considerable effort has been devoted to studying excitatory connections between principal cells, since these represent the pathways via which information travels within and between brain areas. In addition to modern techniques such as patch clamp recording, the activity of the principal cell population may also be studied using the simpler technique of field potential recording. Interneuron activity cannot be monitored in this way. This goes some way towards explaining why historically there is a much greater wealth of information on the properties of synaptic connections onto principal cells. Current experimental techniques facilitate high-resolution electrophysiological recording from morphologically- and/or neurochemically-identified neurons of any type within the functionally intact network of an acute or organotypic brain slice preparation. With such advances comes the potential to make a detailed investigation of each class of synapse within the CNS. Although GABAergic interneurons represent only around 10% of the neuronal population within the hippocampus (Amaral et al., 1990), I have shown their critical involvement in mediating a wide variety of network functions. It is therefore important to understand the mechanisms by which interneurons are excited and the ways in which they sense the activity of the principal cell population. Achieving a detailed

characterisation of the functional properties and modulation of glutamatergic synapses onto interneurons is thus essential in reaching a complete understanding of the hippocampus and other cortical networks.

1.4.1 Sources of afferent input to interneurons in the CA1 subfield

Interneurons mediating feedforward and feedback inhibition in area CA1 receive glutamatergic input from the axons of CA3 and CA1 pyramidal cells. The layers in which the dendritic tree is located, and the source of the excitatory input, determine the functional role of the interneuron within the hippocampal circuitry.

Interneurons within the CA1 subfield are activated by two classes of glutamatergic afferent input. Firstly, CA3 pyramidal cell axons (Schaffer collaterals). Up to eight primary collaterals originate from the principal axon of CA3 pyramidal cells, which bifurcate further and extend through stratum radiatum and stratum oriens of the CA1 subfield (Ishizuka et al., 1990). These axons innervate the apical (in stratum radiatum) and basal (in stratum oriens) dendrites of CA1 pyramidal cells. They also form feed-forward inhibitory circuits by innervating GABAergic interneurons in CA1 stratum radiatum and stratum oriens, which in turn inhibit CA1 pyramidal cells by releasing GABA at synapses formed onto their apical and basal dendrites. The second class of input are CA1 pyramidal cell axons, which form local feed-back inhibitory circuits by innervating interneurons within the CA1 subfield. CA1 pyramidal cell axons emanate from the soma, and pass through stratum oriens to the alveus. Local axon collaterals are extended into stratum oriens and stratum pyramidale to contact inhibitory interneurons (Knowles and Schwartzkroin, 1981). Anatomical evidence thus indicates that inhibitory interneurons in the CA1 subfield may be innervated by CA3 pyramidal cell axons in stratum radiatum, and by both CA3 and CA1 pyramidal cell axons in stratum oriens and stratum pyramidale.

1.4.2 Postsynaptic ionotropic glutamate receptor expression

Both ionotropic and metabotropic glutamate receptors are of central importance in mediating synaptic transmission from principal cells to interneurons. Glutamatergic Schaffer collateral afferents target the dendritic spines of pyramidal cells and the dendritic shafts of the various subtypes of interneuron in strata radiatum and oriens in area CA1. Metabotropic glutamate receptors have a variety of roles in modulating transmission (see section 1.4.5.1). Ionotropic glutamate receptors directly mediate fast excitatory synaptic transmission, and are divided into three classes. α-amino-3-hydroxy-5-methyl-4-isoxazole propionic acid receptors (AMPARs), kainate receptors (KARs) and N-methyl-D-aspartate receptors (NMDARs). All three classes consist of multimeric ligand-gated ion channels which are assembled from various combinations of subunits, some of which confer specific properties onto the receptor (reviewed by Dingledine et al., 1999). Electrophysiological studies have shown that subthreshold EPSPs in interneurons are mediated predominantly by AMPARs, though there is also evidence for limited involvement of kainate receptors (Jonas et al., 1994; Geiger et al., 1997; Thomson, 1997; Cossart et al., 1998; Frerking et al., 1998; Cossart et al., 2002).

These findings have been confirmed by high-resolution immunohistochemical studies. Dendritic spine synapses on CA1 pyramidal cells exhibit an unequal distribution of level of synaptic AMPAR content, with large synapses having dense AMPAR labelling, and some small synapses having disproportionately less or lacking immunolabelling altogether (Baude et al., 1995; Nusser et al., 1998; Takumi et al., 1999). In contrast, synapses onto interneuron dendrites show on average a higher level of AMPAR immunolabelling, and a Gaussian distribution of AMPAR content (Baude et al., 1995; Nusser et al., 1998). Immunogold labelling has demonstrated the presence of synaptic NMDARs on interneuron dendrites (He et al., 1998; Takumi et al., 1999; Racca et al., 2000), with more recent work showing heterogeneity in synaptic NMDAR content between neurochemically-identified interneuron subtypes (Nyiri et al., 2003). Both pre- and postsynaptic expression of kainate receptor KA1 and

KA2 subunits has been demonstrated at mossy fibre synapses onto CA3 pyramidal cells (Darstein et al., 2003). However, no specific immunohistochemical data are currently available on KAR expression in hippocampal interneurons.

1.4.3 Excitation of hippocampal interneurons by ionotropic glutamate receptors

1.4.3.1 Fast excitation mediated by AMPA receptors

A distinctive property of principal cell-interneuron synapses is that glutamatergic EPSPs exhibit substantially more rapid kinetics and have relatively larger amplitudes than EPSPs at synapses between principal cells within the same network. The half-duration of somatically-recorded EPSPs in hippocampal interneurons is between 3.7 and 9.8 ms at physiological temperatures, with peak amplitudes of 0.9-3.4 mV (Miles, 1990; Geiger et al., 1997; Ali and Thomson, 1998; Ali et al., 1998). The half-duration of EPSPs at connections between pyramidal cells is considerably longer, at between 17 and 27 ms, with peak amplitudes of 0.7-1.4 mV (Miles and Wong, 1986; Deuchars and Thomson, 1996). Single EPSPs in some interneuron subtypes are sufficiently large to evoke action potentials with high reliability (Miles, 1990). Individual hippocampal pyramidal cells have been shown to elicit spiking in postsynaptic interneurons with relatively high reliability and temporal precision *in vivo*, with the probability of spike transmission varying according to the behavioural state of the animal (Csicsvari et al., 1998).

AMPAR subunit composition has been identified as an important determinant of rapid EPSP kinetics in interneurons. AMPARs are multimeric assemblies of GluR1-4 subunits, each existing in two alternatively spliced versions termed flip and flop (reviewed by Hollmann and Heinemann, 1994; Dingledine et al., 1999). Receptors lacking the GluR2 subunit are permeable to Ca^{2+} ions and display inwardly-rectifying I-V relationships (Hollmann et al., 1991; Mishina et al., 1991; Jonas and Burnashev, 1995; Koh et al., 1995aa; Washburn et al., 1997). Hippocampal principal cells have been shown to express high levels of GluR2 edited at the Q-R site. In contrast,

various subtypes of interneuron possess AMPARs with inwardly-rectifying I-V relationships and significant Ca^{2+} permeability, indicating low edited GluR2 expression (McBain and Dingledine, 1993; Jonas et al., 1994; Geiger et al., 1995; 1997; Toth and McBain, 1998; Toth et al., 2000). Recent work has demonstrated targeting of AMPARs of distinct subunit composition to specific postsynaptic sites depending upon the type of presynaptic input. In stratum lucidum interneurons, Ca^{2+}-permeable AMPARs are found exclusively at sites postsynaptic to mossy fibre inputs, whereas synaptic responses elicited by CA3 pyramidal cell stimulation are mediated by Ca^{2+}-impermeable AMPARs. Both types of synapse have been shown to co-exist within the same individual interneuron. In contrast, only Ca^{2+}-impermeable AMPARs are expressed in CA3 pyramidal cells (Toth and McBain, 1998; Toth et al., 2000). Input-dependent targeting of AMPARs allows distinct mechanisms of both short- and long-term plasticity to be expressed at specific synapses within the same interneuron (Toth et al., 2000). Subsequent work demonstrated that mossy fibre-interneuron synapses express a continuum of AMPAR subtypes, ranging from Ca^{2+} permeable to Ca^{2+}-impermeable, and that specific AMPAR subtypes are co-localised with specific NMDAR subtypes (Lei and McBain, 2002).

In a detailed electrophysiological and computational investigation of glutamatergic transmission from granule cells to dentate basket cells, Geiger et al. (1997) conclude that the factors which determine EPSP time course and amplitude include (i) the electrotonic (passive membrane) properties of the postsynaptic neuron; (ii) the location and number of synaptic contacts; and (iii) the time course and amplitude of the postsynaptic conductance change. EPSPs with rapid kinetics are generated in interneurons because (i) the membrane time constant (T_m) of the postsynaptic neuron is fast due to low specific membrane resistance (R_m); (ii) most glutamatergic synapses are located close to the soma; and (iii) the postsynaptic conductance change is brief. The rapid postsynaptic conductance change is due to (i) the precise timing of quantal transmitter release from the presynaptic terminal; (ii) fast deactivation of AMPARs, resulting in rapid decay of the quantal EPSC; and (iii)

relatively low affinity of basket cell AMPARs for glutamate. Electron microscopic analysis has shown that excitatory connections onto interneurons are small and comprise a single active zone for vesicle release (Gulyas et al., 1993b; Acsady et al., 1998). This may minimise intersite variability in the timing of transmitter release, thereby achieving a higher degree of synchrony (Geiger et al., 1997). In addition, Monte Carlo-based computer simulations have been performed using empirical data for synaptic morphology and AMPAR density, distribution, gating properties and EPSC kinetics. These simulations demonstrated that precise timing of quantal transmission is further enhanced by rapid clearance of glutamate from the synaptic cleft at principal cell-interneuron synapses, due to rapid diffusion and transmitter buffering (Geiger et al., 1999). AMPAR deactivation kinetics and glutamate binding affinity are largely determined by the subunit composition of interneuron AMPARs, namely the low $GluR2_{flip}$ and high GluR4 content, as revealed by *in situ* hybridisation, single cell RT-PCR and immunocytochemical analysis (Geiger et al., 1995; 1997; Baude et al., 1995; Koh et al., 1995b; Angulo et al., 1997). The findings of Geiger et al. (1997) provide a comprehensive demonstration of the mechanisms underlying rapid EPSP kinetics at one type of excitatory synapse onto interneurons. It is important to realise, however, that this represents only a single class of synapse, namely mossy fibre connections onto dentate basket cells. Given the wide diversity of anatomical and physiological properties of different classes of synapse, it is clear that considerable further research is necessary before the mechanisms underlying glutamatergic excitation of interneurons are fully understood at all types of connection within the hippocampus.

Rapid EPSP kinetics in inhibitory interneurons have two major implications for this function of the cell type within a network. Firstly, rapid EPSPs may enable detection of synchronous pyramidal cell activity, thereby allowing interneurons to act as coincidence detectors. Secondly, rapid EPSPs minimise latency in feedforward and feedback inhibitory systems, enhancing temporal precision in controlling population activity of pyramidal cells (Geiger et al., 1997). EPSP kinetics are an important

determinant of the probability of a given temporal and spatial pattern of inputs causing sufficient depolarisation for the threshold for action potential generation to be reached. This is known as EPSP-spike coupling. Other important factors include the resting and threshold potential of the postsynaptic neuron, and the effect of intrinsic subthreshold voltage-gated conductances upon membrane potential. Expression of distinct subpopulations of voltage-gated ion channels by interneurons and pyramidal cells (see Section 1.3.2.2) gives rise to differences in the biophysical properties of intrinsic membrane conductances, which in turn affects EPSP-spike coupling. In interneurons, voltage-gated outward conductances curtail EPSP amplification by voltage-gated Na^+ currents, acting to provide a narrow window for spike generation (Fricker and Miles, 2000). It is thus clear that precise and rapid signalling in interneurons is due to a complex and extensive variety of underlying mechanisms.

1.4.3.2 Excitation mediated by kainate receptors

Glutamatergic excitation of hippocampal interneurons is mediated predominantly by fast AMPAR EPSPs. There is a limited contribution from excitation mediated by KARs and NMDARs. KARs are multimeric assemblies formed from subunits encoded by five genes - GluR 5,6,7, and KA-1 and -2. These subunits possess significant structural homology to AMPAR subunits, but they do not appear to co-assemble (reviewed by Hollmann and Heinemann, 1994; Dingledine et al., 1999). Experiments with GluR6-deficient transgenic mice demonstrated that GluR6-containing KARs are expressed primarily in the pyramidal cell population, whereas interneurons predominantly express GluR5-containing KARs (Bureau et al., 1999). These results should be interpreted with caution, as subsequent research has demonstrated compensatory expression of other KAR subunits in knockout mice (Christensen et al., 2004). However, the findings were confirmed by double *in situ* hybridisation in hippocampal slices. However, a significant population of GABAergic interneurons were found to co-express GluR5 and GluR6, and functional heteromeric receptors were generated in HEK293 cells (Paternain et al., 2000).

Electrophysiological studies suggest that there is some evidence for expression of postsynaptic KARs with different subunit compositions in distinct subtypes of CA1 interneurons. KARs expressed in oriens/alveus-lacunosum moleculare (OALM) cells are putative GluR5-containing receptors, as they are selectively activated by ATPA and selectively antagonised by LY293558. KARs in stratum radiatum interneurons are less sensitive to these drugs, suggesting that they do not contain the GluR5 subunit (Cossart et al., 1998; Frerking et al., 1998). These findings are consistent with sparse expression of KA-2 mRNA in cells within stratum oriens and the alveus (Bahn et al., 1994).

Postsynaptic KARs have been shown to contribute to EPSPs in various subtypes of CA1 interneuron. Two early studies demonstrated that the KAR component may be isolated using the selective AMPAR antagonist GYKI53655 and NMDAR antagonist D-APV while recording from a single neuron and activating afferent inputs using extracellular stimulation. The KAR synaptic current is similar to the AMPAR current in its I-V relationship, coefficient of variation and response to short stimulus trains. However, the KAR current has a considerably slower rise (~5 ms rise time at 22°C) and decay (~100ms decay time constant). The peak current amplitude is much smaller than that of the AMPAR current, indicating that the contribution of KARs to the EPSC is minor. Despite their small amplitude, KAR EPSCs elicited interneuron activation and burst firing, suggesting an important role in excitation of interneurons (Cossart et al., 1998; Frerking et al., 1998). In contrast to the findings of these studies regarding KAR EPSC kinetics, currents mediated by recombinant and native KARs expressed in heterologous expression systems exhibit rapid rise and decay when activated by brief glutamate pulses or glutamate steps (Swanson and Heinemann, 1998; Cui and Mayer, 1999). Huettner (1990) showed that this is also the case in dissociated rat dorsal root ganglion (DRG) cells. Subsequent work by Cossart et al. (2002) demonstrated KAR, AMPAR and mixed AMPAR/KAR EPSCs in CA1 interneurons and CA1 and CA3 pyramidal cells. KAR EPSCs were of small amplitude but exhibited fast kinetics comparable with those recorded in heterologous expression

systems, in contrast to the slow kinetics observed in previous studies (Cossart et al., 1998; Frerking et al., 1998). Furthermore, KARs were shown to provide a substantial contribution to EPSCs recorded in CA1 interneurons and from mossy fibre inputs to CA3 pyramidal cells.

There is extensive evidence that presynaptic KARs act to depress release of glutamate and GABA in the hippocampus. Furthermore, axonal KARs have been shown to elicit ectopic action potentials in interneurons (Semyanov and Kullmann, 2001). The majority of studies to date have investigated modulation of GABA release, or have focused on glutamatergic connections onto principal cells. However, it is likely that presynaptic KARs have a role in modulating release of glutamate onto interneurons. The situation is complicated by the fact that different mechanisms operate at distinct types of hippocampal synapse. For detailed review, see Kullmann (2001). It is clear that both pre- and postsynaptic KARs play a variety of important roles in glutamatergic synaptic transmission to hippocampal interneurons, and that further investigation is required in order to fully characterise these mechanisms.

1.4.3.3 Excitation mediated by NMDA receptors

NMDARs are heteromultimers assembled from NR1 and NR2A, NR2B, NR2C or NR2D subunits (reviewed by Hollmann and Heinemann, 1994; Dingledine et al., 1999). Postsynaptic NMDARs are activated by synaptically released glutamate at excitatory connections onto interneurons. Under normal physiological conditions, the NMDAR contribution to subthreshold EPSPs is minor, since the channel pore is blocked by Mg^{2+} ions at the resting potential, and local dendritic voltage changes mediated by AMPAR or KAR activation are too short and/or too small to relieve the block. At depolarised membrane potentials or in the absence of extracellular Mg^{2+}, the NMDAR component of EPSPs is relatively large (McBain and Dingledine, 1993; Perouansky and Yaari, 1993; Isa et al., 1996; Geiger et al., 1997). NMDAR-mediated synaptic currents have a characteristically slow time course throughout the CNS, and generally have similar rise and decay times in both hippocampal pyramidal cells and

interneurons (McBain and Dingledine, 1993; Perouansky and Yaari, 1993; Isa et al., 1996; Geiger et al., 1997). It should be noted that NMDAR currents with an exceptionally low rise time were recorded in stratum oriens-alveus interneurons (Perouansky and Yaari, 1993). This may point to heterogeneity in NMDAR kinetics among other subsets of hippocampal interneurons, but this possibility has not yet been systematically investigated. In CA3 stratum lucidum interneurons, NMDARs with distinct subunit compositions and kinetics are specifically co-localised with Ca^{2+}-permeable and -impermeable AMPARs, depending upon the type of presynaptic input. This selective targeting of NMDARs affects both mechanisms of interneuron excitation and long-term synaptic plasticity (Lei and McBain, 2002). Slow excitation mediated by NMDARs and possibly also KARs may act to integrate synaptic activity during temporal EPSP summation, and adjust the membrane potential close to the threshold for action potential initiation.

1.4.4 Synaptic plasticity at excitatory connections onto interneurons

1.4.4.1 Short-term synaptic plasticity

The most common experimental strategy for investigation of short-term modifications of synaptic strength is application of a pair of pulses to the presynaptic input. A frequency of 20 Hz, giving an interpulse interval of 50 ms, is often used when carrying out extracellular stimulation of afferent fibres in the hippocampus. Changes in the paired-pulse ratio (PPR) are observed either as paired-pulse facilitation (PPF) or paired-pulse depression (PPD). PPF is thought to be suggestive of a change in probability of neurotransmitter release due to transient elevation in $[Ca^{2+}]$ within the presynaptic terminal. PPD is generally attributed to depletion of the pool of readily releasable vesicles. Other mechanisms can also be involved, such as feedback inhibition of presynaptic receptors, and postsynaptic mechanisms such as receptor desensitisation (for review, see Zucker and Regehr, 2002).

Principal cell-interneuron synapses exhibit considerable short-term plasticity. Experimental evidence suggests that there is some correlation between the type of interneuron and whether PPF or PPD is displayed. Paired recordings have demonstrated strong PPF at pyramidal cell synapses onto horizontal oriens-alveus interneurons in area CA1 (Ali and Thomson, 1998). In contrast, CA1 pyramidal cell synapses onto basket and bistratified interneurons show pronounced PPD (Ali et al., 1998). PPD also occurs at granule cell-dentate basket cell synapses (Geiger et al., 1997). The type of short-term plasticity exhibited at pyramidal cell connections onto interneurons has also been shown to be target cell-dependent in the neocortex. PPF occurs in bitufted somatostatin-positive interneurons. In contrast, PPD is expressed in parvalbumin-positive multipolar interneurons (Reyes et al., 1998; Watanabe et al., 2005). Geiger et al. (1999) argue that PPF occurs predominantly at principal cell synapses onto interneurons innervating mainly the distal dendritic compartment of their postsynaptic targets, whereas PPD occurs at connections onto interneurons innervating perisomatic regions. While this assertion is generally supported by the limited experimental evidence available, it is likely to be proven overly rigid and simplistic as the short-term dynamics of further classes of principal cell-interneuron synapse are characterised. Given the huge diversity of the interneuron population and the incredible complexity of neuronal circuits within the hippocampus and elsewhere in the brain, there are likely to be many exceptions to this general rule.

Expression of specific short-term synaptic dynamics by distinct interneuron subtypes has important implications for network function. PPD combined with fast EPSPs could enable interneurons to selectively detect coincident single-spike activity in several presynaptic principal cells. PPF in combination with fast EPSPs may facilitate detection of high-frequency bursting in single principal cells (Geiger et al., 1997; 1999).

1.4.4.2 Long-term synaptic plasticity in hippocampal interneurons

Glutamatergic synaptic connections onto interneurons exhibit both long-term depression (LTD) and long-term potentiation (LTP). Currently, information regarding these effects in interneurons is limited, particularly in comparison to the wealth of literature regarding LTD and LTP in principal cells. The situation is further complicated by the extensive heterogeneity of the hippocampal interneuron population. It is important to realise that characterising mechanisms of long-term plasticity is important in fully understanding the processes underlying excitation of GABAergic interneurons. However, the subject is too large and complex for a detailed review to be attempted in this discussion. LTD and LTP have not been directly investigated in this thesis, and so this discussion has instead focused upon the topics which are more directly relevant to the projects involved. Here I review briefly the fundamental points relating to LTD and LTP in CA1 interneurons. It should be noted that a specific form of LTD induced by group I mGluR activation exists in CA1 pyramidal cells (e.g. Palmer et al., 1997; Oliet et al., 1997; Faas et al., 2002; Huang and Hsu, 2005). This particular form of LTD is discussed separately in the section dealing with modulation of excitatory synaptic transmission to CA1 interneurons by mGluRs (Section 1.4.5.3).

Until recently, it was widely believed that, in direct contrast to principal cells, GABAergic interneurons in the hippocampus did not display conventional forms of LTP or LTD. It was suggested that this lack of conventional mechanisms of long-term plasticity at excitatory connections onto inhibitory interneurons allowed these neurons to act as stable and accurate oscillators, mediating synchronisation of pyramidal cell firing and thereby facilitating generation of large-scale network oscillations (reviewed by McBain et al., 1999). However, more recent work has demonstrated that some forms of long-term plasticity exist in certain classes of hippocampal interneuron. Little information is currently available regarding LTD in interneurons. High frequency stimulation of mossy fibres evokes LTP in postsynaptic CA3 pyramidal cells, but LTD in interneurons in CA3 stratum lucidum. Two forms of LTD exist – an NMDA receptor-dependent LTD associated with synapses containing Ca^{2+}-impermeable AMPA

receptors; and an NMDA receptor-independent LTD associated with synapses containing Ca^{2+}-permeable AMPA receptors (Toth et al., 2000; Lei and McBain, 2004). At present no studies have been performed to systematically investigate LTD in interneurons in the CA1 subfield, nor has group I mGluR-associated LTD in interneurons been extensively studied. A form of LTP evoked by pairing theta-burst stimulation with postsynaptic depolarisation occurs in stratum oriens interneurons, which are innervated by axon collaterals of local pyramidal cells. However, this form of LTP does not occur in CA1 stratum radiatum interneurons, many of which receive Schaffer collateral excitation and project to local pyramidal cells. This LTP is NMDA receptor-independent, but the group I mGluR subtype mGluR1α is required for its induction (Perez et al., 2001; Lapointe et al., 2004). Using perforated patch recording in order to preserve neuronal integrity, Lamsa et al. (2005) demonstrated NMDA receptor-dependent LTP with Hebbian characteristics (pathway-specific and evoked by pairing of pre- and postsynaptic activity) in approximately 50% of CA1 stratum radiatum feed-forward inhibitory interneurons. These findings are relevant to the projects described in this thesis, since the majority involve investigation of excitatory transmission to CA1 interneurons in the stratum radiatum layer. However, LTP induction protocols were not used in the experiments described in this thesis, and the objectives did not directly involve investigation of long-term synaptic plasticity. The recent findings described above indicate that both NMDA receptor-dependent and group I mGluR-dependent forms of LTP occur at excitatory connections onto specific classes of interneuron in the CA1 subfield. This represents an important aspect of understanding mechanisms of interneuron activation.

1.4.5 Modulation of excitatory synaptic transmission to hippocampal interneurons

Both excitatory and inhibitory synapses are subject to a complex and extensive array of modulatory effects, mediated by a diverse range of neurotransmitter systems. Such modulatory mechanisms provide numerous layers of subtle control over network function. Modulation of glutamatergic transmission to hippocampal interneurons has not yet been extensively characterised, but nonetheless represents an important area of research. The importance of GABAergic interneurons in the hippocampal circuitry has been discussed in detail in Section 1.3. In order to understand the ways in which inhibitory systems become activated in the hippocampus, it is necessary to characterise not only the functional properties of excitatory connections onto GABAergic interneurons, as discussed above, but also the diverse range of modulatory mechanisms to which they are subject. I now review modulation of excitatory transmission at principal cell-interneuron synapses in the CA1 subfield of the hippocampus. Particular emphasis is placed upon the involvement of metabotropic glutamate receptors, since modulation of glutamatergic synaptic transmission to CA1 interneurons by mGluRs is the subject of this thesis.

1.4.5.1 Modulation of excitatory synaptic transmission in the CA1 subfield by metabotropic glutamate receptors

Metabotropic glutamate receptors (mGluRs) are heptahelical transmembrane receptors which exert diverse and powerful modulatory effects upon neuronal excitability and synaptic transmission. Eight mGluR subtypes have currently been identified. They have precise functional roles and are expressed in highly specific patterns in the hippocampus and other cortical networks. Metabotropic glutamate receptors are reviewed in detail in Section 1.2. Here I specifically discuss their role in modulation of glutamatergic synaptic transmission to interneurons. The majority of projects described in this thesis involve investigation of modulation of excitatory synaptic transmission to CA1 interneurons by group I mGluRs. This discussion

therefore focuses primarily upon the group I receptors, with an overview of the roles of the group II and III mGluRs.

Early studies demonstrated that application of the nonselective mGluR agonist ACPD in hippocampal slices exerted different effects upon excitatory synaptic transmission to distinct interneuron subtypes. In two morphologically-defined subsets of CA1 stratum oriens interneurons, ACPD caused a large enhancement of spontaneous and evoked EPSCs. Miniature EPSCs recorded in the presence of tetrodotoxin were unaffected, consistent with activation of presynaptic mGluRs (McBain et al., 1994). In contrast, ACPD caused a depression of evoked EPSCs in interneurons in CA1 stratum radiatum (Desai et al., 1994) and the dentate gyrus (Doherty and Dingledine, 1997). An increase in the rate of EPSC failures suggested that the effect was presynaptically mediated. ACPD is a nonselective mGluR agonist (Schoepp et al., 1999). The same concentration was used in hippocampal slices in all of these studies. Given the enormous heterogeneity of mGluR subtype expression at different classes of synapse (see Section 1.2.6), the effects observed in these early studies could result from activation of various combinations of mGluRs at synapses onto the distinct types of interneuron involved. Detailed pharmacological dissection of mGluR activity using newer subtype-selective compounds became necessary in order to identify the receptor subtypes involved, and hence understand the underlying mechanisms.

Group III mGluRs comprise the mGluR 4, 6, 7 and 8 subtypes. High-resolution immunohistochemistry combined with electron microscopy has demonstrated that mGluR7 is expressed at high levels in both glutamatergic (Shigemoto et al., 1996; 1997) and GABAergic (Somogyi et al., 2003) presynaptic terminals. Anatomical evidence suggests that mGluR7 is expressed exclusively presynaptically, and is the most widely-expressed of the group III mGluRs (Shigemoto et al., 1996; 1997; Somogyi et al., 2003) A number of studies carried out in hippocampal slices have shown that activation of group III mGluRs using selective agonists such as L-AP4 leads to a depression of excitatory synaptic transmission to CA1 pyramidal cells (e.g.

Baskys and Malenka, 1991; Gereau and Conn, 1995; Capogna, 2004). However, the majority of studies to date have been carried out in pyramidal cells rather than interneurons. The limited data available demonstrate that group III mGluR activation inhibits release of both glutamate (Scanziani et al., 1998; Price et al., 2005) and GABA (Semyanov and Kullmann, 2000; Kogo et al., 2004) onto CA1 interneurons. Scanziani et al. (1998) performed an impressive study in organotypic hippocampal slice cultures using sequential paired recordings from three connected neurons – a presynaptic CA3 pyramidal cell, and postsynaptic CA1 pyramidal cell and CA1 oriens-alveus interneuron. In an elegant demonstration of target-dependent synaptic transmission, presynaptic terminals on the same individual axon were shown to exhibit distinct modulatory mechanisms depending upon the type of postsynaptic target cell. Activation of group III mGluRs using the selective agonist L-AP4 caused a depression of evoked EPSCs in CA1 interneurons but not CA1 pyramidal cells. Changes in PPR, together with other experimental factors, suggested that the effect is presynaptically-mediated. Doherty and Dingledine (1998) demonstrated that In dentate-hilar border interneurons, excitatory inputs from both granule cells and CA3 pyramidal cells were depressed by selective agonists of group I and group III mGluRs. However, the selective group II mGluR agonist DCG-IV depressed transmission only at granule cell inputs, with CA3 pyramidal cell inputs remaining unaffected . There is thus physiological evidence for target-dependent mGluR expression, which is supported by extensive immunohistochemical data (see Section 1.2.6 for discussion of mGluR expression patterns).

Less is known regarding the role of group II mGluRs in modulation of excitatory transmission in the CA1 subfield. Group II mGluRs comprise the mGluR 2 and 3 subtypes. Selective activation of group II mGluRs leads to a presynaptically-mediated depression of glutamatergic transmission at the perforant path input to CA1 pyramidal cells (Kew et al., 2001; Capogna, 2004). Limited data are available regarding modulation of excitatory synaptic transmission to CA1 GABAergic interneurons by group II mGluRs. Activation of group II mGluRs causes an inhibition

of excitatory input from mossy fibres to hilar interneurons. This effect is developmentally regulated, and acts to modulate feedback inhibition in the dentate gyrus (Doherty et al., 2004). A recent study by Price et al. (2005) demonstrated that selective activation of group II mGluRs leads to a presynaptically-mediated depression of excitatory synaptic transmission from the perforant path input to CA1 stratum lacunosum moleculare interneurons. The experimental evidence obtained thus far clearly indicate that group II mGluRs play an important role in modulating glutamatergic inputs onto hippocampal interneurons. The receptors act to inhibit excitatory synaptic transmission via presynaptically-mediated mechanisms.

Presynaptic mGluRs which depress excitatory transmission by inhibiting vesicular glutamate release may act as a homeostatic negative feedback system, monitoring glutamate levels and reducing further release when the ambient extracellular concentration is high. An important question is whether mGluRs at excitatory connections onto interneurons are tonically activated by the ambient glutamate concentration under normal physiological conditions. Application in hippocampal slices of LY341495, which at relatively high concentrations acts as a broad-spectrum mGluR antagonist (Schoepp et al., 1999), caused an enhancement of EPSC amplitude in O-LM cells and basket cells in around 50% of neurons tested. Use of subtype-selective mGluR antagonists demonstrated that mGluR 2,3 and 8 were the main subtypes involved (Losonczy et al., 2003). The findings of this study thus suggest that certain mGluR subtypes are tonically active and mediate a depression of glutamatergic synaptic transmission onto some interneurons. How are presynaptic mGluRs activated? The classical view of autoreceptor activation is that presynaptic receptors are activated by transmitter released from the same synapse. However, this mechanism has not been unequivocally proven experimentally, and recent studies have provided a wealth of evidence for spillover transmission, whereby glutamate diffuses to neighbouring synapses and activates receptors. For detailed discussion of this phenomenon, see Rusakov et al. (1999) and Kullmann (2000).

I now review in detail the role of group I mGluRs in modulation of glutamatergic synaptic transmission in the CA1 subfield, since the group I receptors are the primary focus of the investigations carried out in this thesis. As with the group II mGluRs, limited information is available regarding the role of these receptors in modulation of glutamatergic synaptic transmission in area CA1, and virtually all data have been obtained in pyramidal cells rather than GABAergic interneurons. Furthermore, most studies to date have been performed in the dentate gyrus/CA3 area. Extensive research is thus necessary in order to characterise the role of group I mGluRs in modulating glutamatergic inputs to CA1 inhibitory cells. Early studies carried out in hippocampal slices using group I mGluR-selective agonists and antagonists demonstrated that group I mGluRs act to reversibly inhibit excitatory inputs at the Schaffer collateral-CA1 pyramidal cell connection. Analysis of PPR and miniature EPSCs indicated that the mechanism involves a presynaptic action (Gereau and Conn, 1995; Manzoni and Bockaert, 1995; Rodriguez-Moreno et al., 1998). Subsequent work confirmed the existence of this modulatory mechanism, and the availability of new subtype-selective group I mGluR antagonists (LY367385 blocks mGluR1, while MPEP blocks mGluR5) revealed that the presynaptic depression of EPSCs in CA1 pyramidal cells is mediated entirely by the mGluR1 subtype, with no contribution from mGluR5 (Mannaioni et al., 2001). The involvement of a presynaptic mechanism was further confirmed by Rodriguez-Moreno et al. (1998), in a study performed using both synaptosomes and hippocampal slices. Synaptosomes are isolated intact nerve terminals, prepared by homogenisation of specific brain areas followed sequential centrifugation steps. They are commonly used to study synaptic transmission because they contain the molecular machinery necessary for the uptake, storage, and release of neurotransmitters. Synaptosomes were prepared from the entire hippocampus. Glutamate release was monitored using online fluorimetry, and evoked by depolarisation of synaptosomes using the K^+ channel blocker 4-AP, which results in opening of voltage-gated Ca^{2+} channels and subsequent vesicle release. Application of the selective group I mGluR agonist DHPG to a synaptosome

preparation strongly facilitated release of glutamate. Importantly, this observation demonstrates that functional group I mGluRs are present in isolated nerve terminals, and are therefore presumably expressed presynaptically in at least some areas of the hippocampus.

What are the mechanisms underlying group I mGluR-mediated acute depression of synaptic transmission? It is interesting to note that electrophysiological evidence (changes in PPR and analysis of miniature EPSCs and the statistic $1/CV^2$) suggests that group I mGluR-mediated depression of glutamatergic transmission is presynaptically-mediated (Gereau and Conn, 1995; Manzoni and Bockaert, 1995; Rodriguez-Moreno et al., 1998; Mannaioni et al., 2001), while anatomical data from high-resolution immunohistochemical studies have demonstrated that mGluR1 and mGluR5 are expressed predominantly postsynaptically in the hippocampus (Baude et al., 1993; Lujan et al., 1996; Shigemoto et al., 1997; Lujan et al., 1997; Petralia et al., 1997; Lopez-Bendito et al., 2002; see Section 1.2.6). Depression of glutamatergic and GABAergic synaptic transmission in the hippocampus by group II and III mGluRs is mediated by presynaptically-expressed receptors. Three main mechanisms via which neurotransmitter release is inhibited downstream of G protein-dependent and independent signal transduction cascades triggered by presynaptic mGluR activation have been identified: (i) suppression of N-type and P/Q-type Ca^{2+} channels; (ii) activation of presynaptic K^+ channels; (iii) direct action on proteins involved in the vesicle release machinery (reviewed by Anwyl, 1999). However, given that presynaptic group I mGluRs do not appear to be widely expressed in the hippocampus, an alternative explanation must be invoked for the physiological mechanism underlying group I mGluR-mediated acute depression of synaptic transmission which electrophysiological evidence suggests involves a presynaptic action (Gereau and Conn, 1995; Manzoni and Bockaert, 1995; Rodriguez-Moreno et al., 1998; Mannaioni et al., 2001). This issue is directly relevant to the findings reported in this thesis, and is addressed in detail in the General Discussion (Chapter 10).

1.4.5.2 Modulation of excitatory synaptic transmission by endocannabinoids

Endocannabinoids are a class of endogenous lipid molecules which exert powerful effects upon intercellular signalling via binding at specific heptahelical G protein-coupled receptors. At present, two endocannabinoid receptors have been cloned. CB1 receptors are widely expressed throughout the CNS, where high-resolution immunohistochemistry has indicated that expression appears to be exclusively presynaptic; and elsewhere in the body including the lungs, liver, kidneys and intestines. CB2 receptor expression appears to be limited to the immune system and peripheral nervous system. There are currently no anatomical data to support CB2 expression in the CNS, and this receptor will not be considered further in this discussion. There is evidence for another, as yet unidentified, endocannabinoid receptor, though this remains controversial (Hajos et al., 2001; Hoffman et al., 2005; discussed below; see also Begg et al., 2005). Endogenous CB1 receptor agonists share two common structural motifs – a polyunsaturated fatty acid moiety (e.g. arachidonic acid (ADA)), and a polar head group consisting of either ethanolamine or glycerol. The two best characterised endocannabinoids are anandamide (arachidonylethanolamide) and 2-AG (2-arachidonoylglycerol). Others include virodhamine (*O*-arachidonoyl ethanolamine) and noladin ether (2-arachidonoyl glyceryl ether). Biosynthetic pathways of endocannabinoids are not yet fully understood, and represent an important area of current research. Biosynthesis begins with cleavage by enzymes with phospholipase activity of phospholipid precursors present in the membranes of neurons, glia, and other cell types. Subsequent enzymatic reactions result in the generation of the active endocannabinoid. For detailed discussion of possible pathways of anandamide and 2-AG biosynthesis, see Freund et al. (2003); De Petrocellis et al. (2004). Unlike classical or peptide neurotransmitters, endocannabinoids are hydrophobic molecules, raising the question of how they are able to move within an aqueous environment to reach receptors on nearby cells. Anandamide and 2-AG precursors have been detected at high levels on the surface of neurons, suggesting that at least some endocannabinoid biosynthesis

occurs within the cell membrane, thereby allowing direct access to the external medium. The mechanism underlying the actual release step is not understood, but may involve simple diffusion or facilitation by lipid-binding proteins such as the lipocalins. Endocannabinoid signalling is terminated by uptake of the molecule via specific active transporters, followed by degradation by intracellular enzymes (reviewed by Freund et al., 2003; De Petrocellis et al., 2004).

I now focus on the roles of endocannabinoids in regulation of synaptic transmission. Recent studies have shown that endocannabinoids act as powerful retrograde messengers at many classes of synapse in the CNS. Activation of specific phospholipases in the postsynaptic neuron, either by Ca^{2+}-mediated or receptor-mediated signalling, leads to the formation and release of endocannabinoids. These diffuse to nearby presynaptic terminals and activate CB1 receptors, resulting in inhibition of neurotransmitter release which can persist for tens of seconds. Endocannabinoids mediate a phenomenon associated with GABAergic synaptic transmission known as depolarisation-induced suppression of inhibition (DSI), which has been studied in both the cerebellum and hippocampus. The first study to characterise DSI showed that depolarisation of cerebellar Purkinje cells suppresses spontaneous IPSCs for tens of seconds. The frequency, but not amplitude, of miniature IPSCs was altered, suggesting that the suppression is presynaptically-mediated. Dialysis of Purkinje cells with Ca^{2+} chelators prevented DSI. These findings imply that DSI is caused by inhibition of GABA release, induced by a retrograde messenger released in response to depolarisation-associated entry of Ca^{2+} into the postsynaptic Purkinje cell (Llano et al., 1991). DSI was also demonstrated in the hippocampus. The first studies showed that DSI can be induced by high-frequency firing or by depolarisation of CA1 pyramidal cells, is sensitive to postsynaptic dialysis of Ca^{2+} chelators, and requires presynaptic G protein signalling (Pitler and Alger, 1992; 1994). A phenomenon with very similar characteristics to DSI was discovered at glutamatergic synapses in the cerebellum formed by both parallel fibre and climbing fibre inputs to postsynaptic Purkinje cells, and was termed depolarisation-induced

suppression of excitation (DSE) (Kreitzer and Regehr, 2001b). There is evidence for a DSE-like phenomenon at glutamatergic synapses in the hippocampus. However, while cerebellar DSE could be induced using the same protocol as for DSI (50 -1000 ms depolarisation of postsynaptic Purkinje cells to evoke a depression of IPSCs or EPSCs lasting tens of seconds; Kreitzer and Regehr, 2001), a much longer depolarisation of 5-10 seconds was required to induce suppression of EPSCs at Schaffer collateral inputs to CA1 pyramidal cells (Ohno-Shosaku et al., 2002). Depolarised hippocampal neurons release endocannabinoids, including anandamide and 2-AG, in a Ca^{2+}-dependent manner (Di Marzo et al., 1994; Stella et al., 1997; reviewed by Freund et al., 2003). The link between DSI/DSE and endocannabinoid signalling was identified in 2001. Endocannabinoids acting upon presynaptic CB1 receptors and released in a Ca^{2+}-dependent manner in response to postsynaptic depolarisation were identified as the retrograde signal responsible for DSI and DSE induction in both the hippocampus (Wilson and Nicoll, 2001; Ohno-Shosaku et al., 2001) and cerebellum (Kreitzer and Regehr, 2001a; 2001b). The key experimental finding in these studies was that DSI and DSE were blocked by CB1 receptor antagonists (e.g. AM251; SR141717) and occluded by CB1 receptor agonists (e.g. WIN 55,212-2). Further support for central involvement of endocannabinoids in DSI was provided by the finding that DSI in the hippocampus is absent in CB1 receptor knockout mice (Varma et al., 2001; Wilson et al., 2001). How do presynaptic CB1 receptors act to inhibit release of GABA and glutamate? Activation of CB1 GPCRs leads to a number of downstream effects, which are initiated by the βγ subunit of $G_{i/o}$ proteins: (i) Inhibition of both N-type and P/Q-type Ca^{2+} channels, which mediate the Ca^{2+} influx into the presynaptic terminal which triggers vesicular neurotransmitter release; (ii) activation of G protein-coupled inward-rectifier K^+ (GIRK) channels; (iii) inhibition of adenylyl cyclase, resulting in reduction of cAMP and down-regulation of PKA, and subsequent downstream effects; (iv) stimulation of MAPK signalling; (v) activation of PLCγ, and subsequent generation of IP_3 and release of Ca^{2+} from intracellular stores, together with DAG/PKA stimulation (reviewed by De Petrocellis et

al., 2004). G protein-mediated inhibition of presynaptic N-type and P/Q-type Ca^{2+} channels is likely to be the effect primarily responsible for suppression of transmitter release. This has been demonstrated at a glutamatergic climbing fibre input to a Purkinje cell during DSE by imaging action potential-associated presynaptic Ca^{2+} influxes. Purkinje cell depolarisation decreased Ca^{2+} entry with a time course similar to DSE-associated EPSC suppression. This effect was blocked by CB1 receptor antagonists (Kreitzer and Regehr, 2001b). However, it is clear that CB1 receptor activation leads to a wide range of downstream effects within the neuron, and the possibility of contribution by additional mechanisms to inhibition of GABA and glutamate release cannot be ruled out. The physiological significance of mechanisms of synaptic plasticity such as DSI and DSE in network behaviour is at present poorly understood, but clearly represents an essential area of research. This issue is addressed in detail in the General Discussion (Chapter 10).

The suggestion that endocannabinoids may be involved in retrograde signalling in group I mGluR-induced depression of EPSCs in CA1 interneurons was prompted by evidence that group I mGluRs are coupled to endocannabinoid synthesis in the hippocampus (Varma et al., 2001). Anatomical studies involving high-resolution immunohistochemistry combined with electron microscopy have shown that CB1 receptors in the hippocampus are expressed primarily in clusters on the axon terminals of GABAergic interneurons. Glutamatergic Schaffer collateral terminals were not thought to express CB1 receptors (Tsou et al., 1999; Katona et al., 1999b; Hajos et al., 2000; Nyiri et al., 2005). Nevertheless, evidence from previous electrophysiological studies demonstrated some actions of exogenous or endogenous cannabinoid agonists on glutamatergic signalling in the hippocampus (Misner and Sullivan, 1999; Ohno-Shosaku et al., 2002). These findings have been interpreted as implying the presence of non-CB1 receptors of unknown molecular identity (Hajos et al., 2001; Hoffman et al., 2005). In keeping with this proposal, CB1 receptor antagonists have been shown to attenuate the acute, although not the persistent, action of DHPG on EPSCs recorded in pyramidal cells (Rouach and Nicoll, 2003). A

very recent paper by Katona et al. (2006) reports expression of CB1 receptors at glutamatergic Schaffer collateral axon terminals. Immunogold labelling using highly sensitive antibodies, combined with electron microscopy, was used to demonstrate in the CA1 subfield the presence of the CB1 receptor in glutamatergic axon terminals. Furthermore, the enzyme diacylglycerol lipase α (DGL-α), required for synthesis of the endocannabinoid 2-arachidonoyl-glycerol (2-AG), was concentrated in dendritic spine heads opposing CB1-positive glutamatergic axon terminals. Very similar anatomical findings were reported by Kawamura et al. (2006). These recent studies confirm the presence of presynaptic CB1 receptors at glutamatergic CA1 Schaffer collateral terminals, together with postsynaptic expression of enzymes required for endocannabinoid synthesis. It appears that the receptors had not been detected at these sites by previous immunohistochemical studies (Tsou et al., 1999; Katona et al., 1999b; Hajos et al., 2000; Nyiri et al., 2005) because expression levels of CB1 are much lower at glutamatergic terminals than GABAergic terminals (Katona et al., 2006; Kawamura et al., 2006). Quantitative silver-enhanced immunogold microscopy revealed that CB1 levels were ~20 times lower at glutamatergic than GABAergic terminals (Kawamura et al., 2006).

Furthermore, very recent electrophysiological data confirm that functional CB1 receptors are expressed at glutamatergic CA3 pyramidal cell axon terminals. The selective CB1 receptor antagonist WIN55,212-2 was shown to inhibit glutamatergic synaptic transmission from Schaffer collaterals to CA1 pyramidal cells, accompanied by a robust elevation in PPR. This effect was clearly demonstrated both in individual CA1 pyramidal cells using whole-cell patch clamp recording, with the depression of EPSCs reversed by the selective CB1 agonist AM251 (Kawamura et al., 2006); and in local populations of CA1 pyramidal cells using field potential recording (Takahashi and Castillo, 2006). Both studies included experiments to eliminate the question of potential species- and strain-dependent variations in CB1 expression raised by Hoffman et al. (2005). Two lines of evidence in a recent study by Monory et al. (2006) provide further support for the presence of functional CB1 receptors at glutamatergic

terminals in the hippocampus. Firstly, immunohistochemistry combined with confocal microscopy revealed CB1 receptors co-localised with vesicular glutamate transporter 1 (VGLUT1) at glutamatergic terminals in the hippocampus. Secondly, excessive activation of glutamatergic transmission is a key pathogenic event leading to epileptiform seizures. Glutamatergic circuits in the hippocampal formation are particularly susceptible to excessive pathological activity, and abnormally high activation of kainate-class ionotropic glutamate receptors using exogenous agonists is a widely used animal model of epilepsy (the so-called 'KA model') (Ben-Ari and Cossart, 2000). Monory et al. (2006) generated knockout mice with conditional deletion of the *CB1* gene in cortical glutamatergic neurons or forebrain GABAergic neurons, as well as virally-induced deletion of the *CB1* gene in the hippocampus. These manipulations indicated that the presence of CB1 receptors in glutamatergic hippocampal neurons is both necessary and sufficient to provide a significant degree of endogenous protection against kainate-induced seizures. The study of Monory et al. (2006) therefore provides further evidence for a critical functional role of CB1 endocannabinoid receptors in glutamatergic principal cells in the hippocampus.

Thus both anatomical (Katona et al., 2006; Kawamura et al., 2006; Monory et al., 2006), electrophysiological (Misner and Sullivan, 1999; Ohno-Shosaku et al., 2002; Kawamura et al., 2006; Takahashi and Castillo, 2006) and functional *in vivo* pathophysiological studies (Monory et al., 2006) have confirmed the presence of functional CB1 endocannabinoid receptors at glutamatergic CA1 Schaffer collateral terminals, which act to inhibit excitatory synaptic transmission from CA3 to CA1 pyramidal cells. Whether CB1 receptors are located at Schaffer collateral terminals presynaptic to CA1 stratum radiatum GABAergic interneurons is currently unknown. However, the research discussed above makes these receptors strong potential candidates for mediating retrograde signalling in group I mGluR-mediated inhibition of glutamatergic synaptic transmission to CA1 interneurons.

1.4.5.3 Group I mGluR-mediated long-term depression in CA1 interneurons

In addition to short-term modulation of glutamatergic synaptic transmission, group I mGluRs are responsible for mediating a specific type of LTD in the CA1 subfield. It should be noted that virtually all studies to date have been carried out in CA1 pyramidal cells, and group I mGluR-mediated LTD in hippocampal GABAergic interneurons is at present poorly understood. In considering LTD, it is important to distinguish between depotentiation (reversal of previously-established LTP induced by specific stimulus protocols), and LTD of naive inputs. There are at least two forms of mechanistically-distinct LTD, which can coexist at the same synapses. One form is triggered by activation of NMDA receptors, and the other by activation of group I mGluRs. LTD mediated by group I mGluRs was first described definitively by Palmer et al. (1997). Application of DHPG to hippocampal slices caused an acute depression of EPSPs followed by a small LTD at the Schaffer collateral-CA1 pyramidal cell connection. LTD was greatly enhanced under conditions of hyperexcitability, generated by omitting Mg^{2+} from the perfusate and/or blockade of $GABA_A$ receptors. LTD was not induced by selective agonists for group II and III mGluRs. DHPG-induced LTD did not cross-saturate with NMDA receptor-dependent LTD induced by low-frequency stimulation, demonstrating that both forms of LTD can coexist at the same class of synapse. Interestingly, group I mGluR LTD was reversed by mGluR antagonists. This effect is not attributable to the presence of residual agonist in the slice, since this reversal was observed hours after washout of DHPG, and LTD was re-established upon washout of the mGluR antagonist. Extremely similar findings were obtained by Oliet et al. (1997), who also demonstrated that group I mGluR LTD, but not NMDA receptor LTD, required activation of protein kinase C and involved T-type Ca^{2+} channels.

Which group I mGluR subtypes are responsible for induction of LTD? This question is complicated by the fact that, while subtype-selective antagonists are available for both mGluR1 (LY367385) and mGluR5 (MPEP), a subtype-selective agonist is available only for mGluR5 (CHPG). Nonetheless, evidence from a number

of studies suggests that the mGluR5 subtype is exclusively responsible for induction and expression of group I mGluR LTD (Palmer et al., 1997; Oliet et al., 1997; Huber et al., 2001; Faas et al., 2002; Huang and Hsu, 2005). Interestingly, the larger initial acute depression has been shown to depend entirely upon the mGluR1 subtype (Mannaioni et al., 2001). The biochemical cascades leading from group I mGluR activation to acute and persistent synaptic depression remain incompletely understood. Although both receptors are abundant postsynaptically (Lujan et al., 1996; Lopez-Bendito et al., 2002), at least part of the depression of excitatory transmission appears to be expressed presynaptically (Fitzjohn et al., 2001; Faas et al., 2002; Watabe et al., 2002; Rammes et al., 2003; Tan et al., 2003). It involves postsynaptic phosphoinositide 3-kinase, protein synthesis and dephosphorylation and removal of AMPA receptors from synapses (Huber et al., 2000; Snyder et al., 2001; Xiao et al., 2001; Huang et al., 2004). A retrograde action of endocannabinoids on non-CB1 receptors has been proposed to contribute to the acute, although not the long-lasting, DHPG-evoked depression (Rouach and Nicoll, 2003). The acute presynaptic depression is mediated at least partly by a decrease in Ca^{2+} influx into presynaptic terminals (Faas et al., 2002). Distinct mechanisms underlie modulation of synapses formed on different cell types (for review see Toth and McBain, 2000), even those supplied by the same axon (Scanziani et al., 1998; Rusakov et al., 2004). Thus, it is not possible to extrapolate the above findings, which were almost exclusively obtained in hippocampal pyramidal cells, to GABAergic interneurons. Instead, further research is necessary in order to achieve characterisation of both mGluR-dependent and independent forms of long-term plasticity in specific populations of hippocampal interneurons.

1.4.5.4 Modulation of excitatory synaptic transmission to CA1 interneurons by other neurotransmitter systems

Other types of neurotransmitter receptor are involved in mediating modulatory effects at excitatory connections onto hippocampal GABAergic interneurons. Many of

the mechanisms and receptor subtypes involved have not yet been characterised in detail. Blockade of A_1 adenosine receptors using the selective antagonists 8-cyclopentyl-1,3-dipropylxanthine and *N*-cyclopentyl-9-methyladenine enhances excitatory input to dentate interneurons by increasing synaptic reliability of glutamatergic inputs. The effect of the selective antagonists suggests that the ambient adenosine concentration is sufficient to activate presynaptic A_1 receptors. Conversely, application of exogenous adenosine decreased synaptic reliability and reduced spontaneous EPSC frequency (Doherty and Dingledine, 1997). These findings suggest that A_1 receptors have an inhibitory role in modulating glutamatergic transmission to hippocampal interneurons, with the effect upon spontaneous EPSC frequency consistent with a presynaptic action. ATP-gated presynaptic P2X2 purinergic channels act to facilitate excitatory transmission from CA3 pyramidal cells to CA1 stratum radiatum interneurons, but not to CA1 pyramidal cells (Khakh et al., 2003). This study provides further evidence for target-dependent expression of distinct modulatory mechanisms which differ between excitatory connections onto principal cells and interneurons.

Section 5. Summary of introduction and Ph.D. objectives

The aim of the General Introduction was to place the experimental work described in this thesis into context by reviewing the relevant background information; and to emphasise the significance of the research by highlighting the importance of subjects which at present are not well understood, namely the functional properties of excitatory connections onto GABAergic interneurons and their modulation by neurotransmitter receptors such as mGluRs. The following topics have been reviewed in this chapter.

1. The anatomy of the hippocampus, with particular emphasis upon properties of the CA3-CA1 connection.
2. Metabotropic glutamate receptors: structure; intracellular signal transduction mechanisms; expression patterns in the hippocampus; and roles in modulation of neuronal excitability.
3. GABAergic interneurons in the hippocampus: heterogeneity and criteria for classification; physiological properties; and roles in neuronal circuits, including feed-forward and feed-back inhibition and generation of network oscillations.
4. Functional properties of excitatory synaptic connections onto hippocampal interneurons.
5. Modulation of glutamatergic synaptic transmission to GABAergic interneurons in the hippocampus by various neurotransmitter systems. The main focus was mGluRs, with emphasis on the group I receptors.

The overall objective of the Ph.D. was to investigate the functional properties and modulation by metabotropic glutamate receptors of glutamatergic synaptic connections onto inhibitory interneurons in the CA1 subfield of the hippocampus. The General Introduction highlights the critical roles played by GABAergic interneurons in hippocampal neuronal circuits and network function. It is of central importance to understand the functional properties of glutamatergic synapses responsible for

activating interneurons and thereby recruiting inhibitory drive within the hippocampal network, and the complex and subtle array of modulatory influences to which they are subject.

The results chapters are ordered as follows. Chapter 3 describes a preliminary electrophysiological project carried out at the start of the Ph.D., with the objective of using a two-pathway stimulation experimental design combined with whole-cell patch clamp recording in acute hippocampal slices to quantitatively compare two distinct classes of glutamatergic input to the same CA1 interneuron for modulation by group III mGluRs. A number of experimental difficulties were encountered, which appeared to result from low connectivity of certain classes of afferent input to CA1 interneurons. An epifluorescence Ca^{2+} imaging technique designed to facilitate detection of excitatory connections among populations of neurons in a hippocampal slice was explored, with the aim of overcoming the experimental challenges associated with low connectivity. This is described in detail in chapter 4. Although both these projects provided scope for further investigations, the experimental work was subsequently focused upon electrophysiological investigation of modulation of excitatory synaptic transmission to CA1 interneurons by group I mGluRs, using whole-cell patch clamp recording in acute hippocampal slices. This work represents the main part of the results section of this thesis, and is described in chapters 5 to 9. Group I mGluR activation was found to powerfully modulate glutamatergic connections onto stratum radiatum interneurons by mediating an acute depression of synaptic transmission. This effect had not been previously demonstrated. The aim of the subsequent experiments was to achieve a detailed characterisation of this effect. This included identifying the mGluR subtypes involved and their relative contribution to the depression; characterising the underlying mechanism in detail; and determining whether the effects of selective group I mGluR activation using an exogenous agonist could be reproduced under more physiological conditions, by evoking heterosynaptic depression using synaptically-released glutamate. In addition, morphological analysis

of interneurons from which electrophysiological recordings were obtained was carried out using confocal fluorescence imaging.

Chapter 2. Methods and materials

2.1 Overview of patch clamping in brain slices

Patch clamp recording in acute brain slices was first described by Edwards et al. (1989), and has since become an extremely widely-used experimental technique in the investigation of synaptic physiology. It has been successfully applied to acute tissue slices prepared from virtually all areas of the CNS, and from animals of defined ages for developmental studies. The principal advantages of the patch clamp technique are the ability to use a high-resolution electrophysiological recording technique on visually identified neurons with their structure and the majority of their synaptic contacts preserved within a functionally intact network. Synaptic responses may thus be elicited by precise stimulation of afferent inputs, and responses mediated by specific ionotropic receptor subtypes (e.g. AMPA-class glutamate receptors, $GABA_A$ receptors) may be isolated using pharmacology. In the whole-cell patch clamp configuration, the contents of the cell are gradually washed out by the contents of the pipette during the first few minutes of recording. Thus a variety of intracellular solutions may be used, depending upon the type of synaptic response being recorded. Furthermore, other agents may be added to the intracellular solution, including fluorescent indicators, drugs acting at the intracellular face of transmembrane ion channels (e.g. QX314, an intracellular Na^+ channel blocker), and molecules which affect signal transduction systems. Patch clamp recording can be combined with other methods, e.g. fluorometric measurement of intracellular ions, confocal microscopy and single cell RT-PCR (reverse transcriptase polymerase chain reaction). In combination with electrophysiological recording, numerous other physiological and anatomical properties of individual neurons may be investigated at extremely high resolution.

2.2 Specific methods for hippocampal slice preparation

2.2.1 Animals

All experiments were performed using tissue obtained from male P21-28 (3-4 week old) Sprague-Dawley rats. Animals were kept under a 12 hour light-dark cycle with free access to water and a normal laboratory diet (SDS R and M number 1 expanded, Scientific Dietary Services, UK). All procedures were performed in accordance with the UK Home Office Animals (Scientific Procedures) Act, 1986.

2.2.2 Hippocampal slice preparation

Animals were decapitated under deep terminal pentobarbital anaesthesia (140 mg/kg, administered intraperitoneally). An incision was made along the length of the head, the skull was opened and the brain removed in < 30 seconds and placed immediately into ice-cold sucrose-based artificial cerebrospinal fluid (ACSF) slicing solution, containing (mM) sucrose 70, NaCl 80, KCl 2.5, NaH_2PO_4 1.25, $NaHCO_3$ 25, $MgCl_2$ 7, $CaCl_2$ 0.5, glucose 25; pH 7.2, 297 mOsm, bubbled continuously with 95% O_2 / 5% CO_2. Increased neuronal survival was achieved by using this sucrose-based slicing solution, as the sodium and calcium content is considerably lower than in standard ACSF, resulting in a lower level of network excitability and reduction in pathological effects resulting from the slicing procedure.

The hippocampi were dissected out rapidly (< 1 min) in order to cool the tissue as quickly as possible and thereby minimise any pathological effects resulting from hypoxia-ischaemia. The entire brain was submerged in ice-cold sucrose slicing solution during dissection. Using custom-built plastic spatulas, the midbrain was removed and the hippocampi were gently pulled away from the surrounding temporal cortex. They were then placed into an agar block with two grooves slightly wider than the hippocampi. Each end of the block was trimmed off, and the side with rostral pole of the hippocampi glued face downwards to a plastic base using ultra fast-drying cyanoacrylate adhesive (RS Components, UK). This assembly was then placed into the slicing chamber, which was filled with ice-cold sucrose slicing solution. Transverse

350 µm thick slices were cut with a vibratome (Leica, VT1000S). Slices were left in ice-cold sucrose slicing solution for 1 min after cutting, and transferred to an interface chamber for storage. The chamber was gassed continuously with 95% O_2/ 5% CO_2, and slices were stored on moist filter paper on top of a reservoir of restoration ACSF, containing (mM) NaCl 117, KCl 5.3, $NaHCO_3$ 26, NaH_2PO_4 1.0, glucose 15, $MgCl_2$ 2.0, $CaCl_2$ 2.0; pH 7.2, 297 mOsm. Slices were incubated for at least one hour prior to recording. Whole-cell patch clamp recordings could be obtained for up to approximately 6-8 hours after slicing. Slices were transported to the recording chamber in a small volume of restoration ACSF in a glass pipette.

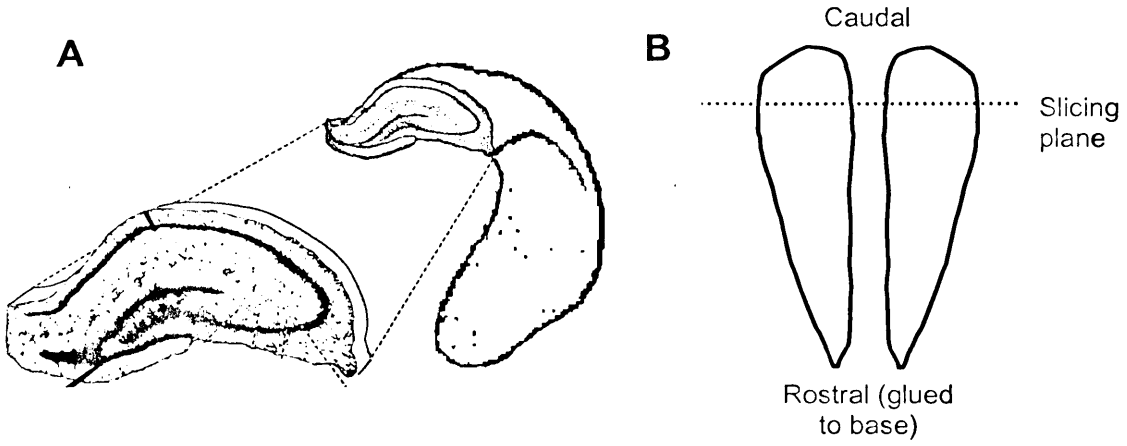

Figure 2.1 *A, Schematic representation of preparation of transverse slices from the left hippocampus.* ***B****, orientation of left and right hippocampi for transverse slicing when placed in horizontal grooves in agar block.*

2.3 Theoretical explanation of patch clamp electrophysiological recording

Patch clamp recording is an immensely powerful and versatile experimental technique, which may be used in a variety of configurations to make electrophysiological recordings from cultured neurons, tissue slices and even *in vivo*. It allows both high-resolution observation of currents through single ion channels, and whole-cell recording from individual cells. One reason for the popularity of patch clamping is the extremely high resolution it provides in measuring membrane currents

– it is possible to measure ionic currents of < 1 pA (10^{-12} A). This is possible because a seal of extremely high resistance (in the order of gigaohms, i.e. > 10^9 Ω; a so-called 'gigaseal') is formed between the end of a glass recording pipette and the cell membrane. This high-resistance seal is the primary reason for extremely low electrical noise, and thus high resolution, in patch clamp recordings. An in-depth review of the numerous configurations and potential applications of patch clamp recording, together with detailed consideration of the associated biophysics is beyond the scope of this discussion. Excellent references are Sakmann and Neher (1995) and Sherman-Gold et al. (1993). It should be noted that single-channel recording is an extremely important and widely-used application of the patch clamp technique, which has provided a wealth of valuable information on ion channel function. The perforated-patch configuration of the whole-cell patch clamp method is also an important experimental technique, since it prevents dialysis of the cell contents by the pipette filling solution, thereby leaving intact signalling cascades involving diffusible second messengers. These applications are not discussed here. Instead, I focus upon reviewing the basic concepts underlying the most widely-used application of the patch clamp technique in this thesis – whole-cell voltage clamp recording.

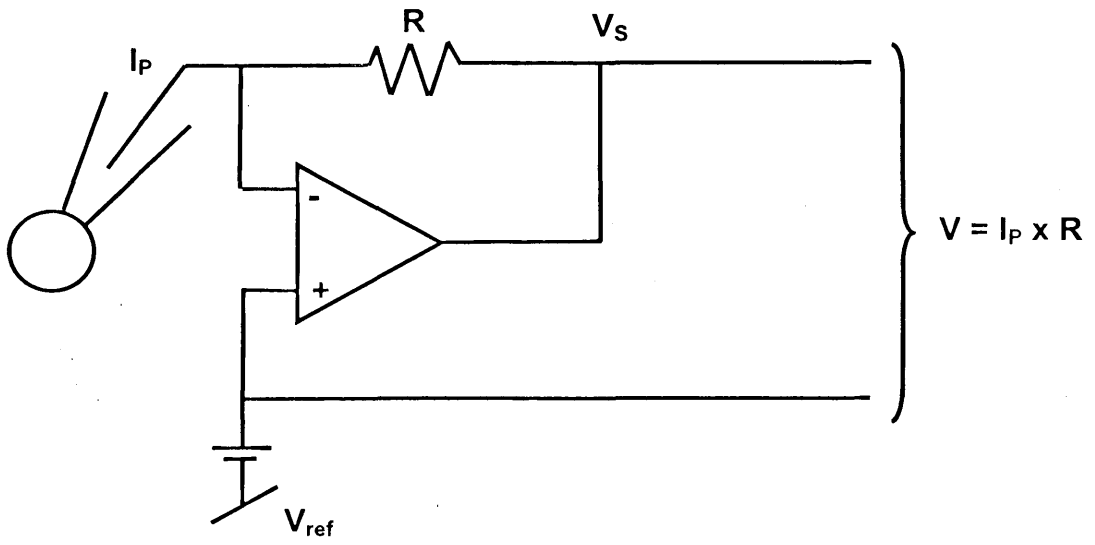

Figure 2.2 *Schematic representation of a current-to-voltage converter, located in the headstage of the patch clamp amplifier. This system allows the cell membrane potential (V_m) to be clamped at a fixed value, whilst the transmembrane flow of ionic current is measured. Current flow through the electrode (I_P) across a high-impedance resistor (R) causes a voltage drop that is proportional to I_P. The operational amplifier acts as a feedback sensor, continuously adjusting the voltage source (V_S) to maintain the pipette at the selected reference potential (V_{ref}).*

Under voltage clamp conditions, the cell membrane potential (V_m) is 'clamped' at a fixed potential, and the transmembrane flow of ionic current in response to various experimental manipulations is recorded. The first step of patch clamp recording is common to all configurations, both single-channel and whole-cell – a gigaseal must be established between the patch pipette and the cell membrane. The patch pipette is a glass capillary, with the end pulled into the desired shape in a multi-stage process using a specialised puller device (e.g. Flaming-Brown). Relatively blunt, low-resistance (3-5 MΩ) electrodes are used for whole cell recording, in comparison to sharp electrode recording, which uses much higher resistance electrodes (≥ 50 MΩ). Whole-cell recording provides complete control over the chemical composition of the cell interior. A variety of pipette filling solutions may be used, to which may be added fluorescent indicators, and/or pharmacological agents which exert their effects intracellularly, e.g. highly selective antagonists of signal transduction cascades. Movement of the patch pipette is controlled by micromanipulators. Formation of the

gigaseal is monitored electrically by continuously measuring electrode resistance by observing the magnitude of the current pulse evoked by repeated application of a test voltage pulse ('t-pulse'), e.g. 5 mV of 5 ms duration at 50 Hz. The formation of a gigaseal is achieved by applying positive hydraulic pressure to the patch pipette, and releasing the pressure as the tip touches the cell surface. If successful, the membrane forms a seal with the pipette tip which has a resistance in the order of gigaohms, and the current pulse evoked by the t-pulse is virtually abolished due to the huge increase in resistance (I = V/R; Ohm's law). The pipette capacitance transients (C_p), produced by the pipette capacitance charging and discharging in response to each t-pulse, are cancelled using 'fast' compensation adjustment at the amplifier. A negative voltage is then applied to the pipette (e.g. -60 mV). At this stage, a single-channel recording may be established in one of three configurations – cell-attached, inside-out or outside-out. Alternatively, the whole-cell configuration may be established. By applying a sharp suction pulse, the patch of membrane within the pipette may be ruptured, allowing low-resistance access to the cell interior. Large, slow capacitance transients then appear, caused by charging and discharging of the cell membrane capacitance (C_m). These are cancelled using the 'slow' compensation circuitry at the amplifier. Dialysis of the cell by the patch pipette filling solution occurs within ≤ 10-15 min. Diffusion rates depend upon the molecular weight and charge of the diffusion particle.

The whole-cell patch clamp electrode acts continuously as both a voltage sensor and current source (Fig 2.2). The current-to-voltage converter of the patch clamp amplifier is contained within the headstage, which also contains the holder for the patch pipette. A chlorided sliver wire inside the patch pipette forms a Ag/AgCl electrode, allowing ionic currents (e.g. carried by Na^+ or Cl^- ions) flowing in the pipette solution to be detected as electrical currents by the headstage. A second Ag/AgCl pellet in the recording bath is connected to the headstage ground point to complete the circuit. Current flow through the electrode (I_p) across a resistor of high impedance (R) causes a voltage drop that is proportional to the measured pipette current. An operational amplifier acts as a feedback sensor, injecting the correct amount of

current to maintain V_m at the selected potential, known as the reference potential (V_{ref}). Due to the extremely high resistance of the gigaseal between the patch pipette and the cell membrane, all current flow through the electrode is assumed to flow exclusively across the cell membrane, and is therefore proportional to the membrane conductance. The disadvantage of using a single electrode both as a voltage sensor and current source is that the recording arrangement contains an unknown and potentially varying series resistance (R_s) in the form of the electrode and its access to the cell interior. In order to achieve accurate electrophysiological recording, it is essential that the series resistance be small relative to the cell membrane resistance. This is achieved through a number of measures, including (i) use of low-resistance electrodes; (ii) recording from small cells with high impedance; (iii) electronic compensation of series resistance.

The most widely-used application of the patch clamp technique in the projects described in this thesis is whole-cell voltage-clamp recording of pharmacologically-isolated, synaptically-evoked excitatory postsynaptic currents (EPSCs). EPSC amplitude correlates with the transmembrane flux of ionic current through postsynaptic ionotropic glutamate receptors during the transient ligand-induced opening of the receptor channel pore. EPSCs are mediated via AMPA/kainate receptors, with any contribution from NMDA receptors removed by the use of the selective antagonist DL-APV. EPSCs were evoked via extracellular stimulation of glutamatergic afferent inputs.

It should be noted that the recording temperature used was sub-optimal – all experiments were carried out at room temperature (~20 °C). *In vivo* conditions are more accurately simulated in brain slice preparations by making electrophysiological recordings at more physiological temperatures (~33 °C is widely-used). However, recording at higher temperatures leads to three main difficulties. (i) Increased difficulty of patch clamp recording; (ii) Fewer healthy neurons from which to record, and more rapid degradation of acute brain slices, due to more rapid occurrence of pathological processes induced by the slicing procedure; (iii) Increased technical complexity of

maintaining storage and perfusion ACSF at a constant temperature. Experiments described in this thesis were carried out at room temperature because all effects could be clearly detected, and many of the experiments were pilot studies designed to establish which aspects of the project were important to subsequently investigate in greater detail. Clearly, in order to enhance accuracy of the results, certain experiments would have been repeated at physiological temperature if more time had been available.

2.4 Specific methods for whole-cell patch clamp electrophysiological recording

2.4.1 Whole-cell patch clamp recording in hippocampal slices

Experiments were carried out at room temperature (20 °C) unless otherwise stated. Slices were submerged in the recording chamber of an upright microscope (Olympus BX50WI), and held in position by a C-shaped platinum frame crossed with fine nylon lines. The recording chamber was perfused continuously at 3 ml per min with ACSF ('Ringer' solution), containing (mM) NaCl 119, KCl 2.5, $MgSO_4$ 1.3, $MgCl_2$ 2.7, NaH_2PO_4 1.0, $NaHCO_3$ 26.2, glucose 11, $CaCl_2$ 2.5; pH 7.2, 297 mOsm, bubbled continuously with 95% O_2 / 5% CO_2. Drugs were added to the ACSF in order to apply them to the slice. Several perfusion reservoirs were available with different batches of ACSF containing various combinations of drugs to be washed into the slice.

Neurons were patch clamped under visual guidance using infra-red differential interference contrast (IR-DIC) microscopy. DIC uses polarised light to give a three-dimensional image. Infrared microscopy uses long wavelength light (~700 nm), which penetrates further into the slice, facilitating visualisation of neurons deeper in the tissue. One advantage of IR-DIC microscopy is that thicker slices with a more intact neuronal network may be used. Electrophysiological recordings were made using an Axopatch 1D patch clamp amplifier (Axon Instruments, USA). Data acquisition and analysis were carried out using custom programs written in Labview development environment (National Instruments, USA). Patch clamp electrodes were prepared

from borosilicate glass (0.86 mm internal diameter, GC150F-7.5, Harvard Instruments, USA) using a Flaming-Brown electrode puller (Sutter Instrument Company, USA). Pipette resistance (R_P) was 4-6 MΩ. Unless otherwise stated, a caesium gluconate-based pipette filling solution was used for recordings in whole-cell configuration, containing (mM) Cs gluconate 117.5, CsCl 17.5, CsOH HEPES 10, CsOH EGTA 0.2, NaCl 8, Mg ATP 2, Na_3GTP 0.3, QX314Br 5; pH 7.2, 290 mOsm. A caesium gluconate-based pipette filling solution was selected in order to optimise the space clamp. Cs^+ ions have low permeability through K^+ channels. Once the cell interior had been dialysed with the pipette solution after achieving whole-cell access (assumed to occur in ≤ 15 min), the high concentration of Cs^+ ions resulted in an intracellular blockade of K^+ channels. This improved the space clamp by preventing K^+ leak conductances, which result from the strong concentration gradient driving K^+ out of the cell at the resting membrane potential. K^+ leak conductances are mediated by a number of different K^+ channel subtypes, not all of which have yet been definitively identified. One important class of K^+ channel are non-voltage-gated channels with four transmembrane helices (termed 4TM architecture) and two intracellular P loops (Goldstein et al., 2001). An important issue when using a caesium-based pipette filling solution is that action potential firing is inhibited due to K^+ channel blockade. In order to avoid contamination by action currents when recording pharmacologically-isolated EPSCs, action potential firing was further suppressed via intracellular blockade of voltage-gated Na^+ channels by inclusion of QX314-Br in the pipette filling solution. These two factors facilitated an accurate space clamp and prevented EPSC contamination by action currents, but precluded analysis of spiking patterns. This may be important, for example, when attempting to classify interneuron subtypes by physiological criteria, or determine possible roles in network function. Potassium-based pipette filling solutions would be used in order to investigate action potential firing. This subject is discussed further in Chapter 10. For loading of single neurons with Ca^{2+}-sensitive fluorescent indicators via the patch pipette, a potassium methylsulphonate-based filling solution was used, containing (mM) K-

methylsulphonate 117.5, KOH 17.5, K HEPES 10, Na-phosphocreatine 10, $MgCl_2$ 4, Na-ATP 4, Na-GTP 0.4, Fluo4 200μM; pH 7.2, 290 mOsm. The non-esterified polar form of Fluo4 was used, as the indicator did not diffuse across a membrane to enter the cell.

Experiments were performed in whole-cell voltage clamp mode unless otherwise stated. Thus the membrane potential was clamped at a fixed value and transmembrane ionic currents were recorded. The majority of recordings were made from GABAergic interneurons in the CA1 subfield of the hippocampus. This cell type displays extensive heterogeneity in a variety of characteristics (see Chapter 1, Section 1.3), including physiological features such as resting membrane potential (V_m), spiking patterns etc. Among hippocampal interneurons, V_m ranges from approximately -50 to -70 mV (Lacaille et al., 1987; Parra et al., 1998). There is less variation among CA1 pyramidal cells, which have a V_m of approximately -60 mV (e.g. Lacaille et al., 1987). Neurons were therefore voltage-clamped at -60 mV unless otherwise stated. Series resistance (R_S) was monitored with a voltage step in each recording cycle, and was < 40 MΩ. Holding current (I_{hold}) was < 200 pA. Cells were rejected if R_S or I_{hold} varied by > 20% over the course of the experiment. Records were filtered at 5 kHz and digitised at 10 kHz to avoid aliasing noise.

2.4.2 Extracellular stimulation of presynaptic afferent inputs

Synaptic responses may be elicited from various pathways in the hippocampus by extracellular stimulation of the appropriate axons in the slice. As current flows from one pole of a bipolar stimulus electrode to the other, axons are depolarised and fire action potentials, causing release of neurotransmitter from presynaptic terminals. Monopolar stimulus electrodes were tested initially, but cleaner monosynaptic EPSCs could be elicited with greater reliability by using bipolar electrodes. Bipolar stimulus electrodes were custom prepared from sharp stainless steel electrodes (Frederick Haer & Co, USA). A pair of electrodes were placed inside a glass capillary and the ends sealed with cyancacrylate adhesive. Tip separation was

adjusted as necessary. Constant current isolated stimulator devices (Digitimer, UK) under the control of the data acquisition software were used to deliver stimuli of 50 μs duration, with intensities generally ranging from 10-500 μA. Stimulus intensity was adjusted to give an EPSC amplitude of 100-300 pA. Stimulus intensities were not adjusted during the recording once an appropriate value was selected prior to the start of the actual experiment. The variation in stimulus intensities between recordings was due to factors such as distance of the stimulus electrode from the recorded neuron, and the number of afferent fibres activated by each stimulus. The goal in selecting an appropriate stimulus intensity was to evoke EPSCs in the 100-300 pA range. This is the optimum EPSC amplitude range for recording from interneurons for the types of experiment carried out in this thesis (D. Kullmann, personal communication). Lower EPSC amplitudes result in greater trial-to-trial variability, due to quantal fluctuations in neurotransmitter release from stochastic events. Higher EPSC amplitudes result in non-linearity, voltage escape and shunting. Selecting an appropriate range of EPSC amplitudes, and thus stimulus intensity, is a trade-off between avoiding quantal fluctuations and from low-amplitude EPSCs, and non-linearity and voltage escape from high-amplitude EPSCs. Therefore EPSC amplitudes which are too low or too high generate experimental complications which obscure accurate data analysis.

Activation of excitatory inputs to CA1 pyramidal cells and interneurons through stimulation of CA3 pyramidal cell axons (Schaffer collaterals) is a commonly used experimental technique in this thesis (Fig 2.3). Schaffer collaterals extend into CA1 from the cell bodies of CA3 pyramidal cells in stratum pyramidale, forming glutamatergic synaptic contacts onto both pyramidal cells and interneurons (Ishizuka et al., 1990). A cut was made in the slice between CA3 and CA1 to prevent stimulus-induced and spontaneous epileptiform discharges in the network of recurrent excitatory collaterals in CA3 from spreading to CA1 and contaminating the synaptic response. In general, clearer AMPA EPSCs were recorded if the recording electrode was positioned distally from the stimulus electrode within stratum radiatum. If

necessary the stimulus electrode could be carefully re-positioned after a whole-cell recording had been established in order to obtain a clearer synaptic response.

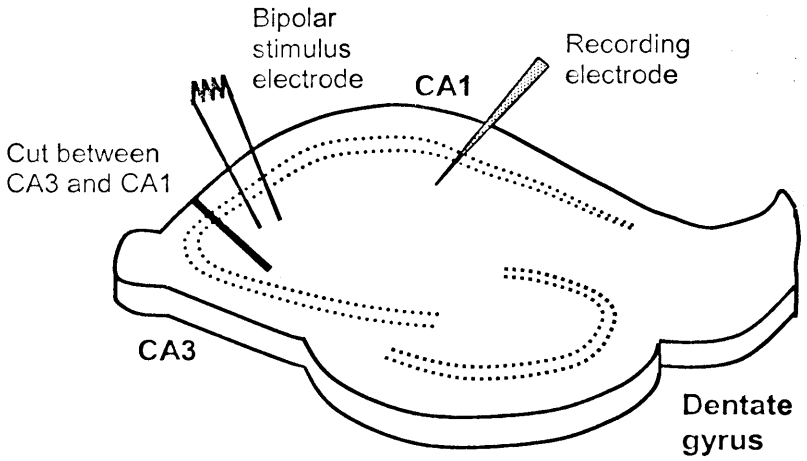

Figure 2.3 *Configuration of stimulus and recording electrodes for recording AMPA EPSCs elicited by extracellular stimulation of Schaffer collaterals in CA1 stratum radiatum interneurons.*

2.4.3 Whole-cell voltage clamp recording of pharmacologically-isolated AMPA EPSCs

Recordings were made in whole-cell voltage-clamp configuration. The membrane potential of the neuron was maintained at a fixed value, which was selected to simulate the hyperpolarised physiological resting potential of hippocampal interneurons. Use of whole-cell voltage-clamp in this manner allowed stimulus-evoked EPSCs to be recorded. Paired pulses were delivered in each recording cycle at a frequency of 20 Hz, giving a 50 ms interpulse interval. The ratio of the amplitude of the second EPSC to the first EPSC is known as the paired pulse ratio (PPR). Changes in PPR generally result from alterations in neurotransmitter release, due Ca^{2+} accumulation in the presynaptic terminal (reviewed by Zucker and Regehr, 2002). PPR analysis may thus be used as a criterion to determine whether a given mechanism involves a presynaptic action. PPR was calculated by measuring amplitude of EPSC traces averaged across 20 cycles (10 min) in each stage of the

experiment (e.g. baseline; activation of a specific receptor subtype via drug application; washout). The peak amplitude of the second pulse was then normalised by that of the first to determine PPR. Constant current isolated stimulator devices (Digitimer) under the control of the data acquisition software were used to deliver stimuli of 50 μs duration, with intensities generally ranging from 10-500 μA. Numerous configurations of recording cycle were used in the experiments described in this thesis. These are described in detail in the methods section at the start of each chapter. The standard recording cycle consisted of: (i) single stimulus to CA1 stratum radiatum, to activate Schaffer collateral afferent inputs. (ii) Pair of stimuli at 20 Hz, giving an interpulse interval of 50 ms. This facilitated investigation of presynaptic effects via calculation of PPR. (iii) Voltage step to monitor series resistance. The interval between each stimulus was 10 s, giving a 30 s duty cycle for recording of EPSCs. The following drugs were always present in the perfusion ACSF once the whole-cell recording configuration had been successfully established. Picrotoxin (100 μM) to block $GABA_A$ receptors, and DL-2-amino-5-phosphonovalerate (DL-APV, 50 μM) to block NMDA receptors. Upon completion of the experiment, the AMPA/kainate receptor antagonist 2,3-dioxyo-6-nitro-1,2,3,4-tetrahydrobenzo[f]quinoxaiine-7-sulphonamide (NBQX, 10 μM) was bath applied to confirm that EPSCs were mediated by AMPA/kainate receptors.

2.5 Morphological analysis of individual neurons using immunohistochemistry and confocal microscopy

2.5.1 Immunohistochemical staining of individual recorded neurons using Alexa488

Biocytin was routinely added to the patch pipette filling solution at a concentration of (0.4% w/v; i.e. 4 mg per ml). The biocytin dialysed into the neuron during the course of the recording. The majority of experiments had a duration of at least 50 min, allowing sufficient time for biocytin to reach far into dendritic and axonal processes. Upon completion of the experiment, the slice was immediately transferred

from the recording chamber to a 1.5 ml plastic Eppendorf tube, filled with 1 ml phosphate-buffered saline (PBS; Sigma, UK), containing (mM) NaCl 137, KCl 2.7, phosphate buffer 10; pH 7.4, together with 4% paraformaldehyde (PFA) to fix the slice tissue. PFA acts to cross-link proteins. The Eppendorf tube was stored overnight in a fridge at 4° C to allow fixation to take place. PFA was then washed out of the slice using 3 × 20 min washes in 1 ml PBS, with gentle shaking. Permeabilisation of cell membranes was achieved using a 2 hour incubation with gentle shaking in 1 ml PBS containing 0.5% w/v Triton X-100, a non-ionic surfactant related to the Pluronic range of detergents. This solution was then aspirated, and replaced with 1 ml PBS containing 0.1% w/v streptavidin conjugated to the fluorophore Alexa488. Streptavidin is a tetrameric protein purified from *Streptomyces avidinii* that binds extremely tightly to biocytin with a K_d of ~10^{-14} mol/L. This is one of the strongest known biochemical interactions, and is thus widely used in immunohistochemical techniques. Staining of the slice with the fluorescent streptavidin-Alexa488 conjugate was achieved using a 2 hour incubation with gentle shaking. The conjugate was able to cross neuronal membranes and bind strongly to biocytin due to the preceding permeabilisation step using triton X-100. Following the 2 hour incubation, the streptavidin-Alexa488 conjugate was washed out of the slice using 3 × 20 min washes in 1 ml PBS, with gentle shaking. Slices were then mounted individually on microscope slides with coverslips, using DABCO mounting medium (Sigma, UK).

2.5.2 Confocal image acquisition

Imagining of immunohistochemically-stained slices was carried using a Zeiss LSM 510 confocal laser scanning microscope. A three-dimensional fluorescence image was obtained of the immunopositive neuron from which the patch clamp recording had been made, together with a DIC image of the surrounding area of the hippocampal slice. The primary objective was to accurately assess the position of the soma within CA1 stratum radiatum, and image the pattern of dendritic projections within the subfield. This was facilitated by superimposing the fluorescent image of the

individual immunopositive neuron over the background DIC image. In order to achieve this aim, relatively low magnification was used in the majority of image acquisition (Plan-Apochromat ×10 non-immersion lens). To achieve more detailed visualisation of particular areas, e.g. projections arising from the soma or complex areas of dendritic branching, higher magnification was used (Plan-Apochromat ×20 non-immersion lens). In some cases axonal projections could also be visualised. This issue is of central importance, and is discussed further in Chapter 9, Sections 9.3 and 9.4.

Fluorescence images were acquired using an argon laser set to 488 nm for excitation; and a 505 nm long-pass emission filter. Upper and lower limits of the immunopositive neuron within the slice were identified, and the thickness of the imaging plane set accordingly. Images were acquired every 3 μm within this area, and a three-dimensional confocal projection of the cell subsequently constructed from the individual frames.

2.6 Summary of pharmacological agents used in all projects

Full name of drug	Abbreviated name	Conc (μM)	Pharmacological effect
DL-2-amino-5-phosphonovalerate	DL-APV	50	NMDA receptor antagonist
2,3-dioxyo-6-nitro-1,2,3,4-tetrahydrobenzo[f]quinoxaiine-7-sulphonamide	NBQX	25	AMPA/kainate receptor antagonist
n/a	Picrotoxin	100	$GABA_A$ receptor antagonist
3-(3,4-Dichlorophenyl)methyl]amino] propyl]diethoxymethyl)phosphinic acid	CGP52432	5	$GABA_B$ receptor antagonist
N-(2,6-Dimethylphenylcarbamoyl-methyl-triethylammonium bromide	QX314-Br	5	Intracellular Na^+ channel blocker
DL-*threo*-β-Benzyloxyaspartic acid	TBOA	50	Glutamate uptake transporter blocker, selective for EAAT1 and EAAT2 subtypes

L(+)-amino-4-phosphonobutyric acid	L-AP4	50	Selective group III mGluR agonist
(S)-3,5-dihydroxyphenylglycine	(S)-3,5-DHPG	30	Selective group I mGluR agonist
(1*S*,3*R*)-1-Aminocyclopentane-1,3-dicarboxylic acid	(1*S*,3*R*)-ACPD	50	Broad-spectrum mGluR agonist, with greater selectivity for group I and II at 50 μM concentration
(2S)-2-Amino-2-[(1S,2S)-2-carboxycycloprop-1-yl]-3-(xanth-9-yl) propanoic acid	LY341495	Variable	Selective group II mGluR antagonist at nanomolar concentrations, selective for group III receptors at higher concentrations.
S-2-methyl-4-carboxy-phenylglycine	LY367385	100	Selective mGluR1 antagonist
2-Methyl-6-(phenylethynyl)-pyridine	MPEP	10	Selective mGluR5 antagonist
(RS)-a-methyl-4-carboxyphenylglycine	MCPG	500	Broad-spectrum mGluR antagonist
α-methylserine-O-phosphate	MSOP	100	Selective group III mGluR antagonist
N-(Piperidin-1-yl)-5-(4-iodophenyl)-1-(2,4-dichlorophenyl)-4-methyl-1*H*-pyrazole-3-carboxamide	AM251	2	Selective CB1 endocannabinoid receptor antagonist
(*R*)-(+)-[2,3-Dihydro-5-methyl-3-(4-morpholinylmethyl)pyrrolo[1,2,3-de]-1,4-benzoxazin-6-yl]-1-naphthalenylmethanone mesylate	WIN 55,212-2	0.80	Selective CB1 endocannabinoid receptor agonist
8-Cyclopentyl-1,3-dipropylxanthine	DPCPX	0.20	Selective A_1 adenosine receptor antagonist
ω-conotoxin GVIA	CgTx	0.25	Highly selective peptide blocker of N-type Ca^{2+} channels
ω-agatoxin IVA	AgTx	0.10	Highly selective peptide blocker of P/Q-type Ca^{2+} channels
Guanosine 5'-[β-thio]diphosphate trilithium salt	GDPβS	1000	Non-hydrolysable GTP analogue; potent inhibitor of G protein signalling

Table 2.1 *Summary of pharmacological agents used in all projects described within this thesis. Concentrations shown are those used in experiments described within this thesis to achieve maximal pharmacological effect in the hippocampal slice preparation.*

Chapter 3: Quantitative comparison of two distinct classes of glutamatergic afferent input to CA1 interneurons for modulation by group III mGluRs

3.1 Introduction

Activation of GABAergic interneurons is subject to a wide variety of modulatory influences with numerous levels of subtle control. An important questions is whether all classes of excitatory input to a given interneuron are subject to the same modulatory mechanisms, and whether there may be quantitative differences in the strength of modulatory effects, and susceptibility to activation by glutamate spillover, at different classes of input. This would provide additional levels of control in activation of the GABAergic system within the hippocampal network. The aim of this project was to investigate modulation of excitatory synaptic transmission by presynaptic group III metabotropic glutamate receptors at two distinct classes of glutamatergic input to interneurons in area CA1 of the hippocampus. A two-pathway experimental design was used, in order to facilitate comparison of two distinct classes of glutamatergic afferent inputs onto individual CA1 interneurons for modulatory effects by group III mGluRs. CA3 and CA1 pyramidal cell axons were activated using two stainless steel bipolar stimulus electrodes, with current delivered by separate isolated stimulator devices under the control of the data acquisition software. Placement of stimulus electrodes at appropriate locations within the hippocampal slice was of central importance if activation of two distinct input classes were to be successfully achieved. Interneurons within the CA1 subfield are activated by two classes of glutamatergic afferent input. Firstly, CA3 pyramidal cell axons (Schaffer collaterals). Up to eight primary collaterals originate from the principal axon of CA3 pyramidal cells, which bifurcate further and extend through stratum radiatum and stratum oriens of the CA1 subfield (Ishizuka et al., 1990). These axons innervate the apical (in stratum radiatum) and basal (in stratum oriens) dendrites of CA1 pyramidal cells. In addition, CA3 pyramidal cell axons form feed-forward inhibitory circuits by innervating GABAergic

interneurons in CA1 stratum radiatum and stratum oriens, which in turn inhibit CA1 pyramidal cells by releasing GABA at synapses formed onto their apical and basal dendrites. The second class of input are CA1 pyramidal cell axons, which form local feed-back inhibitory circuits by innervating interneurons within the CA1 subfield. CA1 pyramidal cell axons pass through stratum oriens to the alveus. Local axon collaterals are extended into stratum oriens and stratum pyramidale. Axons bifurcate in the alveus, with the major branch projecting caudally toward the subiculum and the second, thinner branch projecting rostrally to the fimbria. Further bifurcation occurs within the alveus, to produce several axon branches following parallel paths (Knowles and Schwartzkroin, 1981). Anatomical evidence thus indicates that inhibitory interneurons in the CA1 subfield may be innervated by CA3 pyramidal cell axons in stratum radiatum, and by both CA3 and CA1 pyramidal cell axons in stratum oriens and stratum pyramidale.

There is extensive evidence for widespread variation in functional and modulatory properties at different classes of synapse. Glutamatergic afferent inputs to CA1 interneurons from CA3 and CA1 pyramidal cell axons represent two distinct classes of excitatory synapse. The aim of the experiments described in the present chapter was to determine whether both classes of input to the same CA1 interneuron are subject to modulation by inhibition of glutamate release by presynaptic group III mGluRs. Quantitative comparison of the degree of group III mGluR modulation between the two classes of input was carried out, in order to investigate whether the relative influence of a specific modulatory mechanism differs at distinct classes of input to the same inhibitory interneuron. This may be important in furthering understanding of mechanisms of feed-forward and feed-back inhibition, and of target-dependent synaptic transmission.

3.2 Methods

Whole-cell patch clamp recordings were made from CA1 pyramidal cells and stratum radiatum interneurons in 350 µm thick transverse hippocampal slices prepared from P21-28 Sprague-Dawley rats. Slices were continuously perfused with ACSF at a rate of 3 ml per minute. A cut was made in the slice between CA3 and CA1 to prevent the spread of stimulus-induced epileptiform discharges due to the network of recurrent excitatory collaterals in CA3. Patch clamp recording was visually guided by infra-red DIC microscopy. Neurons were voltage-clamped at -60 mV using a caesium gluconate-based intracellular solution containing QX314-Br (5 mM) to prevent spiking. In order to test for presynaptic effects, paired pulse stimulation was delivered in each recording cycle. Paired pulses were delivered at a frequency of 20 Hz, giving an inter-pulse interval of 50 ms. The recording duty cycle consisted of a single pulse followed in a separate trial by paired pulses, firstly to the CA3 input and then to the CA1 input. Finally, a calibration pulse was applied to monitor the integrity of the whole-cell recording by measuring I_{hold}, R_S and R_A. The inter-trial interval was 5 s, giving a 25 s duty cycle. CA3 and CA1 pyramidal cell axons were activated using two stainless steel bipolar stimulus electrodes, with current delivered by separate isolated stimulator devices under the control of the data acquisition software. Unless otherwise stated, stimulus intensity was 10-500 µA, with a duration of 50 µs. To record pharmacologically-isolated AMPA EPSCs, the following drugs were always present in the perfusion ACSF: DL-APV (50 µM) to block NMDA receptors, and picrotoxin (100 µM) to block $GABA_A$ receptors. Upon completion of the experiment, NBQX (10 µM) was bath applied to verify that EPSCs were mediated by AMPA/kainate receptors. Group III mGluRs were activated using the selective agonist L-AP4 (50 µM), and blocked using the selective antagonist MSOP (100 µM). These drugs were applied via the ACSF perfusion system. To quantitatively compare group III mGluR modulation of excitatory transmission at both distinct classes of input, a 10 min baseline was recorded, followed by a 20 min exposure to L-AP4 (50 µM) to selectively activate group III mGluRs, and 20 min washout. If either input were subject

to modulation by these receptors, a depression of EPSC amplitude would be expected, since presynaptic group III mGluRs have been shown to depress synaptic transmission by inhibiting release of glutamate (e.g. Gereau and Conn, 1995; Capogna, 2004; Price et al., 2005) and GABA (Semyanov and Kullmann, 2000; Kogo et al., 2004). The magnitude of depression of EPSCs evoked by each input, together with any changes in PPR, could then be quantitatively compared.

3.3 Results

3.3.1 Excitation of interneurons in CA1 stratum oriens

Whole-cell recordings were initially made from interneurons in CA1 stratum oriens. At all times two extracellular stimulus electrodes were positioned in the slice. The initial objective was to find a configuration of recording and stimulating electrodes that would reliably allow EPSCs elicited from both pathways to be recorded in the same interneuron. Once an optimal configuration had been established, experiments would be carried out in which L-AP4 was applied to selectively activate group III mGluRs. The magnitude of depression of EPSCs evoked by each input would then be quantitatively compared.

Numerous electrode configurations were tested when recording interneurons in CA1 stratum oriens. Stimulating electrodes were positioned at all points along the transverse axis of the hippocampal slice in stratum oriens and alveus. The recording electrode was positioned at varying points along the transverse and dorso-ventral axes, effectively covering the whole of CA1 stratum oriens. Recordings were rejected if EPSCs evoked via stimulation of either input were polysynaptic, of low amplitude (≤ 30 pA), or displayed unusual kinetics. Monosynaptic AMPA EPSCs with large amplitude and fast kinetics could be elicited via Schaffer collateral stimulation by positioning the stimulus electrode in CA1 stratum radiatum close to CA3, just beyond the cut made to prevent the spread of stimulus-induced epileptiform discharges; and the recording electrode distally in CA1 stratum oriens, towards the subiculum.

Improved success in eliciting monosynaptic EPSCs was achieved if the recording electrode was located more dorsally (i.e. closer to stratum pyramidale). From a total of 101 whole-cell recordings, monosynaptic AMPA EPSCs were evoked in 32 stratum oriens interneurons via Schaffer collateral stimulation (32% success rate, n = 101; Table 3.1) Despite positioning the second stimulus electrode at various points along the entire length of the alveus, eliciting AMPA EPSCs in CA1 stratum oriens interneurons through activation of CA1 pyramidal cell axons via alveus stimulation proved extremely problematic. In most cases, no EPSCs were elicited even by high intensity stimulation of the alveus (up to 1-2 mA). When alveus stimulation generated AMPA EPSCs, they generally had significantly slower kinetics than those elicited by Schaffer collateral stimulation, were of lower amplitude (maximum ~100 pA), and were often polysynaptic. Monosynaptic AMPA EPSCs were evoked via alveus stimulation in 8 stratum oriens interneurons (8% success rate, n = 101; Table 3.1). The position of the stimulus electrode within the alveus did not appear to affect the probability of eliciting an AMPA EPSC. From a total of 101 whole-cell recordings, monosynaptic AMPA EPSCs were evoked in the same stratum oriens interneuron via stimulation of two distinct classes of input in only 2 cells (2% success rate, n = 101; Table 3.1).

Total number of whole-cell recordings from CA1 s.oriens interneurons	Recordings with AMPA EPSCs elicited from SC pathway	Recordings with AMPA EPSCs elicited from alveus pathway	Recordings with AMPA EPSCs elicited from both pathways
101	32	8	2

Table 3.1 *Whole-cell recordings in which monosynaptic AMPA EPSCs were evoked in CA1 stratum oriens interneurons by stimulation of the Schaffer collateral (SC), alveus, or both pathways.*

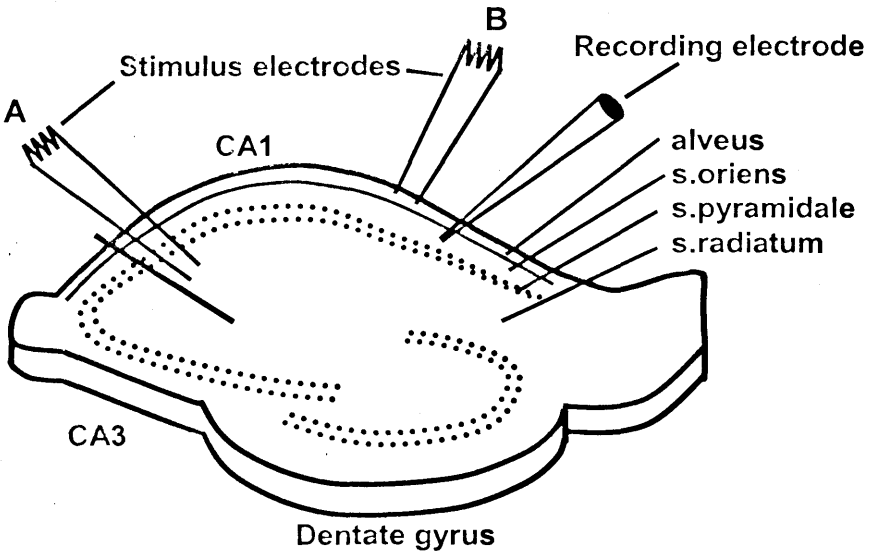

Figure 3.1 *Configuration of stimulus and recording electrodes in hippocampal slice. The experimental objective was to determine optimal electrode configuration for recording of AMPA EPSCs in CA1 stratum oriens interneurons evoked by stimulation of two distinct classes of glutamatergic afferent input. CA3 and CA1 pyramidal cell axons were activated by extracellular stimulation of Schaffer collateral (A) and alveus (B) pathways respectively.*

3.3.2 Excitation of putative basket cell interneurons in CA1 stratum pyramidale

A specific subtype of GABAergic interneuron known as basket cells have soma located in stratum pyramidale or a short distance below this layer in dorsal CA1 stratum radiatum. Basket cells are known to be innervated by Schaffer collaterals (Freund and Buzsaki, 1996). As CA1 pyramidal cell axons pass through stratum oriens to the alveus, local axon collaterals are extended into stratum oriens and stratum pyramidale (Knowles and Schwartzkroin, 1981). It is therefore possible that basket cells may also be reliably activated via stimulation of the alveus pathway. This interneuron subtype therefore represents a particularly suitable candidate for achieving a high success rate in evoking monosynaptic AMPA EPSCs via stimulation of excitatory inputs originating from both CA3 and CA1 pyramidal cells. The objective of this series of experiments was to make whole-cell recordings exclusively from CA1 basket cells, in order to determine whether a greater success rate in eliciting

monosynaptic AMPA EPSCs via stimulation of both pathways could be achieved in this cell type than in CA1 stratum oriens interneurons.

Visual identification of basket cells under DIC microscopy was problematic. Basket cell somata were difficult to identify within the densely packed layer of pyramidal cell soma in stratum pyramidale. Interneurons with somata located just below stratum pyramidale in stratum radiatum could be identified more readily. However, such cells were present infrequently, and it was impossible to confirm that they were basket cells, as opposed to other interneuron subtypes or pyramidal cells with abnormally-shaped soma located just outside stratum pyramidale. Post-hoc immunohistochemistry combined with confocal microscopy to achieve morphological and neurochemical analysis of recorded interneurons was not carried out in this study. The recorded neurons could therefore not be definitively identified as basket cells. However, this was a pilot study, with the objective of determining whether monosynaptic AMPA EPSCs could be reliably elicited in basket cells via stimulation of two distinct classes of input. If the pilot study proved successful, robust means of identifying neurons, such as post-hoc immunohistochemistry and analysis of somatodendritic and axonal projection patterns, would be used in subsequent experiments.

Recordings were made from putative basket cells with somata located in CA1 stratum pyramidale or a short distance below this layer in dorsal CA1 stratum radiatum. As in previous experiments (Section 3.3.1), numerous positions of recording and stimulus electrodes were tested in order to determine the optimum configuration for evoking monosynaptic AMPA EPSCs in the same interneuron via stimulation of both afferent input pathways. The recording electrode was placed at a number of different locations along the transverse axis of the hippocampal slice, and multiple re-positioning of both stimulus electrodes was carried out within each recording. From a total of 10 recordings, monosynaptic EPSCs were evoked in 6 cells via stimulation of the Schaffer collateral pathway (60% success rate, n = 10; Table 3.2); 3 cells via

stimulation of the alveus pathway (30% success rate); and in no cells via stimulation of both pathways (no successful experiments).

Total number of whole-cell recordings from putative CA1 basket cells	Recordings with AMPA EPSCs elicited from SC pathway	Recordings with AMPA EPSCs elicited from alveus pathway	Recordings with AMPA EPSCs elicited from both pathways
10	6	3	0

Table 3.2 *Whole-cell recordings in which monosynaptic AMPA EPSCs were evoked in putative CA1 basket cells by stimulation of the Schaffer collateral (SC), alveus, or both pathways.*

3.4 Discussion

The present study demonstrated a low success rate in evoking monosynaptic AMPA EPSCs in the same CA1 interneuron via stimulation of two distinct classes of glutamatergic afferent input. EPSCs were evoked with a reasonable success rate via activation of CA3 pyramidal cell axons by extracellular stimulation of the Schaffer collateral pathway in both CA1 stratum oriens interneurons (32% success rate, n = 101; Table 3.1) and putative CA1 basket cells (60% success rate, n = 10; Table 3.2). This indicates strong connectivity between CA3 pyramidal cell axons and interneurons with soma located in stratum oriens and stratum pyramidale in the CA1 subfield. This class of input could therefore readily be tested for modulation by group III mGluRs by selectively activating the receptors via L-AP4 application and monitoring changes in EPSC amplitude. Using monosynaptic paired recordings in organotypic hippocampal slice cultures, Scanziani et al. (1998) demonstrated that Schaffer collateral inputs to CA1 stratum oriens interneurons, but not CA1 pyramidal cells, are subject to modulation via presynaptic group III mGluRs. The receptors act to inhibit excitatory synaptic transmission by reducing glutamate release from the presynaptic terminal. Thus activation of feed-forward inhibitory interneurons in CA1 stratum oriens appears to be modulated by group III mGluRs. These receptors have been shown to be

activated by spillover of glutamate from nearby synapses (Semyanov and Kullmann, 2000), adding additional levels of subtle control over this inhibitory system. However, different classes of synapse vary widely in functional properties and expression of pre- and postsynaptic neurotransmitter receptors, and it is currently unknown whether excitatory synapses from CA1 pyramidal cell axons which activate local feed-back inhibitory circuits are subject to group III mGluR modulation. Furthermore, quantitative comparisons have not yet been carried out in order to determine whether there are differences in the relative influence of the group III mGluR modulatory mechanism between these two classes of input. Investigating these issues was the objective of the present study. A major experimental difficulty was encountered, however, in evoking monosynaptic AMPA EPSCs in CA1 interneurons by activation of CA1 pyramidal cell axons via extracellular stimulation of the alveus. Despite testing numerous configurations of recording and stimulus electrodes, and multiple re-positioning of stimulus electrodes during whole-cell recording, evoking EPSCs in both CA1 stratum oriens interneurons and putative CA1 basket cells via extracellular stimulation of the alveus pathway had a low success rate.

It should be noted that there is a low level of connectivity between local CA1 axon collaterals and stratum oriens interneurons. Anatomical work using intracellular dye injection into single CA1 pyramidal cells in hippocampal slices has shown that these local axon collaterals are very thin relative to the parent branch, display few varicosities, and rarely extend more than 100 μm into stratum oriens (Knowles and Schwartzkroin, 1981). It is therefore possible that a low level of connectivity between interneurons and the small local CA1 pyramidal cell axon collaterals in stratum oriens may have been a factor in the poor probability of activating CA1 interneurons via extracellular stimulation of the alveus pathway. Nonetheless, a small number of recent studies have described successfully evoking monosynaptic EPSCs in interneurons with somata in stratum oriens via extracellular stimulation of the alveus pathway (Wierenga and Wadman, 2003; Pouille and Scanziani, 2004). Indeed, one study succeeded in evoking EPSCs in interneurons with somata in stratum oriens via

extracellular stimulation of both feedforward (Schaffer collateral) and feedback (local CA1 axon collaterals arising from the alveus) afferent inputs (Wierenga and Wadman, 2003), the very objective of the present investigation. The two inputs exhibited clearly-defined variations in synaptic dynamics, suggesting that other differences may exist at distinct input classes to the same interneuron, potentially including modulation of synaptic transmission by mGluRs. The experiments described in the present chapter were performed in late 2002, before these papers were published. Had more time been available, the authors mentioned above would have been contacted in the later stages of the Ph.D., in order to discuss in detail methods for successfully evoking EPSCs generated by local CA1 pyramidal cell axon collaterals in interneurons with somata in stratum oriens via extracellular stimulation of the alveus pathway.

Alternative means of stimulation may have yielded a higher success rate when evoking monosynaptic AMPA EPSCs in the same CA1 interneuron via stimulation of two distinct classes of glutamatergic afferent input. A device which may have proven useful in the present study was used by Royer et al. (1999). This consisted of a horizontal array of 28 tungsten stimulus electrodes, which was used to activate afferent inputs in amygdala slices. Each electrode was subject to independent control. A similar device could be placed horizontally in a hippocampal slice, within and parallel with the alveus, and individual or multiple electrodes activated in order to improve the probability of eliciting EPSCs in interneurons with soma located in stratum oriens. This would provide wider coverage of the alveus than a single bipolar electrode, thereby enhancing the probability of activating afferent fibres originating from CA1 pyramidal cells which were monosynaptically-connected to the interneuron being recorded. FHC (Canada) markets a matrix of extracellular stimulus electrodes, comprising 24 elements each subject to individual control (catalogue number MX12345 (iin)), which may prove a useful tool in the present study (M. Capogna, personal communication).

An alternative means of activating CA1 pyramidal cell inputs to interneurons with somata in stratum oriens is by making paired recordings between

monosynaptically-connected cell pairs. This has been achieved by making paired recordings between CA1 pyramidal cells and horizontal oriens-alveus interneurons (Ali and Thomson, 1998) and basket cell and bistratified interneurons in area CA1 (Ali et al., 1998). Paired whole-cell patch clamp recording is a powerful experimental technique for high-resolution study of synaptic transmission, simultaneously providing extensive control over both pre- and postsynaptic neurons, and providing much greater information regarding the presynaptic input in comparison to extracellular stimulation of afferent fibre bundles (for review see Miles and Poncer, 1996). However, in the present study, using this technique would require establishing simultaneous paired recordings between an interneuron with its soma located in stratum oriens, and both monosynaptically connected CA1 and CA3 pyramidal cells, so that the two classes of input could be quantitatively compared for modulation by group III mGluRs. This type of three-way paired recording represents an extremely challenging experimental approach. Sequential paired recordings have been successfully employed in previous studies (e.g. Scanziani et al., 1998), but simultaneous three-way paired recordings would be required in the present study, so that two distinct input classes to the same CA1 interneuron could be compared for modulation by group III mGluRs. This approach would provide additional advantages. Firstly, greatly increased precision in the control of the presynaptic inputs to the interneuron being investigated. Secondly, data would be obtained at much higher resolution, since mGluR modulation would be studied at connections between individual neurons, as opposed to the presynaptic input being provided by an unknown number of incoming axons activated by extracellular stimulation. This highlights the limitation of extracellular stimulation versus paired recordings between individual monosynaptically-connected cell pairs.

Chapter 4. Optical probing of glutamatergic synaptic connections in hippocampal slices using Ca^{2+} epifluorescence imaging

4.1 Introduction

A major experimental difficulty in the investigation of neuronal circuits in cortical networks is the identification of postsynaptic targets of a given neuron. This problem is compounded when patch clamping in brain slices, since the slicing process inevitably results in severing of some longer axons, making identification of functional pathways highly problematic in certain brain areas. Recent studies have employed a technique based upon calcium imaging that facilitates rapid identification of postsynaptic targets (Smetters et al., 1999; Peterlin et al., 2000; Kozloski et al., 2001; Billups et al., 2002). This system relies on imaging intracellular Ca^{2+} fluorescence simultaneously in populations of neurons in a neocortical or hippocampal slice. Slices are first incubated with a membrane permeant Ca^{2+}-sensitive fluorescent indicator, such as fura2-AM or fluo4-AM. This facilitates bulk-loading of the indicator into a large proportion of neurons within the slice. The acetoxymethylester group is then cleaved by intracellular esterases, converting the indicator to the membrane-impermeant form, thereby ensuring that the indicator molecules remain within the neuron. Following action potentials in a presynaptic cell, postsynaptic neurons coupled by excitatory synapses show Ca^{2+} transients due to depolarisation-induced opening of voltage-gated Ca^{2+} channels (see Helmchen et al., 1996; Johnston et al., 1996). Using Ca^{2+} imaging techniques, it is possible to detect (i) sub-threshold EPSCs, which can produce Ca^{2+} influxes localised to a single dendritic spine; (ii) Na^{+} action potentials, which elicit generalised Ca^{2+} accumulations throughout the cell due to back-propagation of the spike; and (iii) Ca^{2+} spikes via voltage-gated Ca^{2+} channels, which are generated in dendritic regions and have a longer duration than those produced by Na^{+} spikes (Smetters et al., 1999). Ca^{2+} channels inactivate slowly in comparison to Na^{+} channels, allowing for a longer duration voltage change. The presynaptic neuron is activated experimentally via a whole-cell patch clamp recording electrode, or an

extracellular stimulus electrode. Excitatory synaptic connections may be identified by imaging somatic Ca^{2+} transients which are time-locked to action potentials generated by stimulation of presynaptic neurons (Smetters et al., 1999; Peterlin et al., 2000; Kozloski et al., 2001; Billups et al., 2002). This technique may be used in a number of ways. Once a target cell is localised, a simultaneous paired recording of both the presynaptic neuron and one of its monosynaptically-connected postsynaptic targets can be obtained by using a second patch clamp recording electrode. Without this type of imaging technique to identify postsynaptic targets, paired recordings are difficult and time-consuming to establish, with a relatively high experimental failure rate. This imaging method thus facilitates the high-resolution study of individual connections of pyramidal cell axons. The imaging technique may also be used to investigate patterns of connectivity within neuronal networks, by identifying the numerous postsynaptic targets of a specific presynaptic input (Peterlin et al., 2000; Kozloski et al., 2001).

The objective of the electrophysiological project described in Chapter 3 was to compare two distinct inputs to the same individual CA1 interneuron for modulation by presynaptic group III metabotropic glutamate receptors. These inputs were local CA1 pyramidal cell axon collaterals (activated by stimulation of the alveus in CA1), and incoming CA3 pyramidal cell axons (Schaffer collaterals; activated by stimulation in CA1 stratum radiatum). The study gave rise to a poor success rate in eliciting synaptic responses from both pathways independently within the same CA1 interneuron (2 of 101 whole-cell recordings in CA1 stratum oriens; 0 of 10 whole-cell recordings in putative CA1 basket cells; see Chapter 3). One possible explanation is that there is a low level of connectivity between most CA1 interneurons and inputs from both CA1 and CA3 pyramidal cells. The first objective of the present study was to investigate whether Ca^{2+} epifluorescence imaging combined with bulk-loading of Ca^{2+}-sensitive fluorescent indicators in populations of neurons within a hippocampal slice could be used for rapid detection of CA1 interneurons postsynaptically connected to local CA1 pyramidal cell axon collaterals and incoming CA3 pyramidal cell axons. It was necessary to adapt the optical probing technique first described by Smetters et al.

(1999). The original studies involved stimulating individual presynaptic neurons, and establishing paired recordings with postsynaptic cells functionally identified as displaying stimulus-induced Ca^{2+} signals using epifluorescence imaging (Smetters et al., 1999; Peterlin et al., 2000; Kozloski et al., 2001; Billups et al., 2002). The initial aim of the present study was to adapt the technique to facilitate detection of postsynaptic targets of axon bundles in defined pathways, activated by extracellular stimulation. This would represent a powerful means of rapidly and reliably detecting excitatory connections in areas with low connectivity. Once established, the technique could then be extended to make paired recordings from individual monosynaptically-connected cell pairs. Paired whole-cell patch clamp recording is a powerful experimental technique for high-resolution study of synaptic transmission, simultaneously providing extensive control over both pre- and postsynaptic neurons (for review see Miles and Poncer, 1996). The objectives of the experiments described in this chapter were as follows. Firstly, to establish optimum conditions for bulk-loading of hippocampal slices with Ca^{2+}-sensitive fluorescent indicators. Secondly, to determine optimum imaging conditions and stimulus parameters for epifluorescence-guided detection of postsynaptic Ca^{2+} transients evoked in CA1 interneurons by extracellular stimulation of specific afferent input pathways. Thirdly, to reliably make whole-cell voltage-clamp recordings from target cells identified using the epifluorescence technique. Once these objectives had been achieved, the technique would initially be used to facilitate the experiments to investigate group III mGluR modulation of two distinct classes of excitatory inputs to the same CA1 interneuron, as described in Chapter 3. Epifluorescence imaging could also be used to facilitate high-resolution investigation of modulation of glutamatergic synapses onto CA1 interneurons by facilitating establishing of paired recordings between individual monosynaptically connected cell pairs.

4.2 Methods

4.2.1 Electrophysiological recording

Experiments were carried out using 350 µm thick transverse hippocampal slices unless otherwise stated. Extracellular field potential recordings were made using a borosilicate glass electrode filled with ACSF. A caesium gluconate-based pipette filling solution was used for whole-cell patch clamp recordings, containing (mM) Cs-gluconate 117.5, CsCl 17.5, CsOH HEPES 10, CsOH EGTA 0.2, NaCl 8, Mg ATP 2, Na_3 GTP 0.3, QX314Br 5, pH 7.2, 290 mOsm. For loading of single neurons with Ca^{2+}-sensitive fluorescent indicator via the patch pipette, a potassium methylsulphonate-based filling solution was used, containing (mM) K-methylsulphonate 117.5, KOH 17.5, K HEPES 10, Na phosphocreatine 10, $MgCl_2$ 4, Na-ATP 4, Na-GTP 0.4, Fluo4 200µM, pH 7.2, 290 mOsm. The non-esterified polar form of the indicator (usually Fluo4) was used, as diffusion across a membrane was not necessary for the indicator to enter the cell if applied via the patch pipette. The concentration of fluorescent indicator in the pipette solution was 50 µM. Neurons were voltage-clamped at -60 mV. EPSCs were evoked using stainless steel extracellular stimulus electrodes, controlled by isolated stimulator devices. Stimulus intensities ranged from 10 - 500 µA, though were usually < 200 µA, with a duration of 50 µs. If necessary, the bipolar stimulus electrodes were repositioned in order to optimally evoke monosynaptic EPSCs. To record pharmacologically-isolated AMPA EPSCs, the following drugs were always present in the perfusion ACSF: DL-APV (50 µM) to block NMDA receptors, and picrotoxin (100 µM) to block $GABA_A$ receptors. Upon completion of the experiment, NBQX (10 µM) was bath applied to confirm that EPSCs were mediated exclusively by AMPA receptors. The recording duty cycle consisted of a single pulse, paired pulse, and calibration pulse to monitor the integrity of the whole-cell recording by measuring I_{hold}, R_S and R_A. The inter-trial interval was 10 s, giving a 30 s duty cycle.

4.2.2 Loading of fluorescent Ca^{2+} indicators – bulk-loading of entire slice

Following a recovery period of at least one hour after slicing, slices were transferred to a custom-designed chamber for bulk-loading of the membrane-permeant Ca^{2+}-sensitive fluorescent indicator (Fig 4.1). All incubations were carried out in the dark to prevent photobleaching of the indicator. Hippocampal slices were submerged on nylon mesh in 2.5 ml oxygenated ACSF containing (mM) NaCl 119, KCl 2.5, $MgSO_4$ 1.3, $MgCl_2$ 2.7, NaH_2PO_4 1.0, $NaHCO_3$ 26.2, glucose 11, $CaCl_2$ 2.5, pH 7.2, 297 mOsm. A small magnetic stir-bar beneath the nylon mesh ensured continuous circulation of the indicator solution within the chamber. A small port allowed the solution to be continuously bubbled with 95% O_2 / 5% CO_2. Two Ca^{2+}-sensitive fluorescent indicators were initially tested - Fura2-AM and Fluo4-AM. The non-polar hydrophobic acetoxymethylester (AM) forms of the indicators were used to ensure diffusion of the indicator across the cell membrane. Following uptake into the neuron, the acetoxymethylester form was cleaved to the membrane-impermeant form by intracellular esterases. Varying concentrations of indicator were tested in order to optimise the bulk-loading procedure. Concentrated indicator solutions containing 50 µg Fura2-AM or Fluo4-AM were prepared in 100% dimethylsulphoxide (DMSO) together with 5% pluronic F-127. Final concentrations of fluorescent indicator between 1 and 10 mM were tested in order to determine the concentration required to achieve optimum staining. A concentration of 2 mM appeared to provide optimum staining, and was used in the experiments described in this chapter. Solutions were sonicated for 2 min to ensure that the indicator was fully dissolved. Pluronic F-127 is a nonionic surfactant polyol (Mr 12.5 kD), which has been found to facilitate the solubilisation of hydrophobic dyes in physiological media, and has been widely used in previous studies to facilitate fluorescent indicator loading in hippocampal neurons (e.g. Regehr and Tank, 1991; Faas et al., 2002). A double incubation protocol was used, as described in previous studies (Smetters et al., 1999; Peterlin et al., 2000; Kozloski et al., 2001): (i) 2 min incubation, with 2 µl concentrated indicator solution applied directly to the hippocampal slice surface, with no stirring or gassing in the chamber

during this time. (ii) 60 min incubation with the remainder of the concentrated indicator solution added to the chamber to give a final concentration of 20 µM, with gentle gassing with 95% O_2 / 5% CO_2 and continuous stirring to ensure circulation of the indicator solution. Previous studies have suggested that the brief DMSO incubation does not have a deleterious effect upon the health of the neurons, since normal resting potentials and synaptic effects may be routinely recorded for some hours following the procedure (Smetters et al., 1999; Peterlin et al., 2000; Kozloski et al., 2001). Field potential recording and observation of neurons under DIC was carried out in control slices, in order to provide a reference point for assessment of the effect of the bulk-loading procedure upon the health of the neurons. In order to achieve an accurate comparison, control slices were taken from the same batch of slices at the same interval following slicing as those subjected to the bulk-loading procedure.

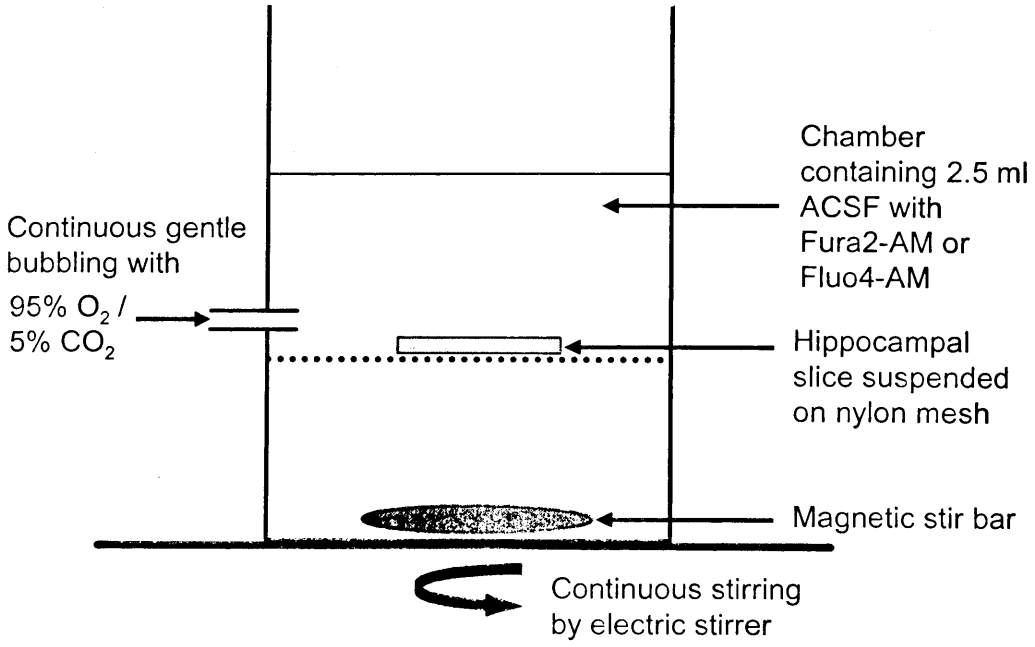

Figure 4.1 *Incubation chamber used for bulk-loading of Ca^{2+}-sensitive fluorescent indicators in hippocampal slices. The chamber contained 2.5 ml ACSF. Fura2-AM or Fluo4-AM were loaded into populations of neurons via a two-stage incubation protocol. Concentrated solutions (2 mM) of indicator in DMSO were applied directly to the slice surface for 2 min. Additional indicator was then added to give a final*

concentration of 20 µM. Continuous stirring via a magnetic stir bar and gentle bubbling with 95% O_2 / 5% CO_2 was carried out during the second stage.

4.2.3 Loading of fluorescent Ca^{2+} indicators – local pressure injection

Pressure injection of Ca^{2+}-sensitive fluorescent indicators to label localised populations of neurons was first described in a brain slice preparation by Regehr and Tank (1991). Three methods of local pressure injection of indicator solution into the hippocampal slice were tested in the present study. (i) Pressure injection via a borosilicate glass capillary with a tip diameter of ~20 µm. (ii) Nanoject device (Drummond), which could be set to pressure inject volumes between 4 and 76 nl of solution in single steps via a glass capillary. (iii) Injection via Hamilton syringes, with capacities of either 1 or 5 µl. Indicator solutions were prepared in DMSO at a concentration of 2 mM with 5% pluronic F-127. Injections were made directly into the slice at varying distances from the area to be stained. Following injection, slices were incubated in the dark for either 60 min or 120 min with continuous perfusion with ACSF (3ml/min), before transfer to the recording chamber.

4.2.4 Epifluorescence imaging of stimulus-evoked Ca^{2+} signals

After bulk-loading, slices were transferred to a submerged recording chamber on an upright microscope (Olympus BX50WI) equipped with both DIC optics and a Till Photonics wide-field fluorescence imaging system via a dual-port camera mounting system (Olympus WI-DPMC). A 60× immersion objective was combined with a 1-3× manual zoom for fluorescence imaging, and 0.35× and 1.0× lenses for DIC optics, maximising the number of neurons that could be viewed under fluorescence imaging. The recording chamber was perfused at 3 ml/min with ACSF. Slices were perfused for a minimum period of 15 min before epifluorescence imaging experiments were carried out, to allow for excess indicator to be washed out of the intercellular space. Epifluorescence images were acquired using a Till Photonics cooled charge-coupled device (CCD) camera. Camera acquisition was 40 ms per frame, and each pixel was

digitised at 12 bits. Image acquisition, storage and analysis were carried out using TillVision 4.0 software. Excitation light was delivered using a Till Photonics Polychrome II monochromator. Fura2-AM is a UV light-excitable ratiometric Ca^{2+} indicator. Upon binding of Ca^{2+}, Fura2 exhibits an absorption shift that can be observed by scanning the excitation spectrum between 300-400 nm, while monitoring the emission at 510 nm. Fluorescence-loaded cells were imaged with excitation light of two wavelengths: 340 nm (Ca^{2+}-bound) and 380 nm (Ca^{2+}-unbound). Emitted light was separated by a 400 nm dichroic mirror and filtered with a 420 nm long-pass filter. A ratiometric image sequence was then prepared by calculating F_{340}/F_{380} for each frame. Fluo4-AM is a non-ratiometric indicator, exhibiting a large increase in fluorescence intensity upon Ca^{2+} binding, with no accompanying spectral shift. A single excitation wavelength of 494 nm was used, together with a 500 nm dichroic mirror. Custom protocols designed using TillVision software were used for data acquisition. Images were acquired at 10Hz for a total of six seconds. Following a one second baseline period, a constant current isolated stimulator device under the control of the TillVision software was used to deliver an extracellular stimulus train, with intensities ranging from 100-500 μA. Various stimulation protocols were tested in order to achieve optimal activation of CA1 stratum radiatum interneurons and pyramidal cells, thereby maximising stimulus-induced spiking. Stimulus duration was 50 μs. Changes in intracellular Ca^{2+} concentration were then followed for the remaining five seconds of the image acquisition period. The relative change in fluorescence over time was defined as $\Delta F/F = (F_t - F_0) / F_0 + offset$, expressed as a percentage, where F_t is the fluorescence for each pixel at time t, and F_0 the fluorescence before the stimulus train. The addition of an offset was used for display purposes, in order to enhance image contrast. 60 frames each with an exposure time of 40 ms were taken at a frequency of 10 Hz. These sequences were analysed by generating a $\Delta F/F$ sequence, so that pixels showing an increase in fluorescence intensity appeared white over a dark background.

4.3 Results

4.3.1 Loading of individual CA1 neurons with Fluo4

In order to characterise the sensitivity of the Till Photonics epifluorescence imaging system, individual neurons were loaded with 50 μM Fluo4 via the patch pipette. This was a relatively low concentration of the indicator, so that comparisons of fluorescence changes within bulk-loaded neurons could be observed. The non-esterified polar form of Fluo4 was used, as the indicator was dialysed directly into the cell and did not diffuse across a membrane. This technique allowed precise control over the membrane potential of an individual neuron filled with a higher concentration of Fluo4 than could be achieved by bulk-loading of an entire slice. In whole-cell current clamp configuration, the neuron could be directly depolarised to induce spiking and concomitant opening of voltage-gated Ca^{2+} channels. In this way, the sensitivity of the Ca^{2+} fluorescence imaging system could be directly evaluated before more complex experiments utilising the bulk-loading procedure were carried out.

Recordings were made from CA1 stratum radiatum interneurons in whole-cell current clamp configuration. Once whole-cell recording was established, an interval of at least 10 min was allowed for the indicator to dialyse into the cell. Current was injected to maintain a membrane potential of -60mV. Following recording of a 1 second baseline in TillVision, current was injected to depolarise the cell to +20mV, thereby triggering a train of action potentials. A $\Delta F/F$ sequence was then prepared. A large elevation in Ca^{2+} fluorescence was detected when the interneurons were depolarised from -60 to +20mV, using brief current pulses to elicit single action potentials.. A total of 5 cells were recorded. Changes in fluorescence of 8 to 15% $\Delta F/F$ were detected. The mean overall fluorescence change in the soma was 12 ± 4% $\Delta F/F$. Increases in fluorescence intensity could clearly be observed in dendritic processes. These observations demonstrated that the experimental imaging setup was sufficiently sensitive for detection of changes in Ca^{2+} fluorescence intensity in individual dendrites in cells loaded with a high concentration of Fluo4.

4.3.2 Loading of fluorescent Ca^{2+} indicators - bulk-loading of entire slice

4.3.2.1 Extracellular stimulation of Schaffer collateral pathway

A steel bipolar extracellular stimulus electrode was positioned in CA1 stratum radiatum. This electrode was used to stimulate incoming Schaffer collaterals, thereby activating excitatory connections onto both CA1 pyramidal cells and interneurons. Stimulation of this pathway using sufficiently robust parameters would elicit spiking in CA1 pyramidal neurons and interneurons. Depolarisation of the postsynaptic neuron during an action potential is associated with a rapid influx of Ca^{2+} via voltage-gated Ca^{2+} channels (see Helmchen et al., 1996; Johnston et al., 1996). It was anticipated that this influx should be detectable under fluorescence imaging, as a proportion of the neurons would be stained with fluorescent Ca^{2+} indicator following bulk-loading of the entire slice. Various stimulus protocols were tested in order to determine parameters which would reliably elicit spike trains in CA1 neurons. Stimulus parameters used in these experiments were 20 pulses at 50 Hz. Stimulus intensity was 100-500 μA, with a 50 μs pulse duration. A field potential recording electrode was positioned within the imaging area in CA1 stratum radiatum or stratum pyramidale. Spike trains were recorded in response to extracellular stimulation of the Schaffer collateral pathway.

Field potential recordings were used as a criterion for assessing the health of the neurons within the hippocampal slice, since the staining procedure appeared to exert a deleterious effect upon the condition of the cells. If field potentials could not be elicited or had distorted kinetics, despite multiple re-positioning of recording and/or stimulus electrodes, this pointed towards a problem with synaptic transmission from Schaffer collaterals to CA1 pyramidal cells. One explanation may be poor condition of neurons within the slice. Detailed observation of neurons under DIC microscopy was also carried out, with the proportion of dead neurons used as an additional criterion for assessing slice condition. Dead neurons tended to have either a swollen, nucleated appearance, or had markedly shrunken soma. It is important to realise that there may be considerable variation in the health of neurons in slices from different batches. To

a lesser extent, there may also be some variation between slices from the same batch. This type of variation cannot be controlled for experimentally, and may result from a wide variety of factors within the slicing process. This underlines the fact that preparation of acute hippocampal slices which are suitably healthy for patch clamp electrophysiology and fluorescence imaging is a challenging experimental procedure. Even though all factors in the process were controlled as carefully and accurately as possible, considerable variation in slice condition between batches nonetheless occurred. Furthermore, neuronal condition deteriorated progressively with the age of the slice. The optimum time for imaging and electrophysiological recording was 1-3 hours following slicing. Slices older than 6-8 hours generally contained a high proportion of dead neurons and achieving successful experiments was difficult. In the present study, attempting to accurately quantify the relative proportion of dead neurons in each slice would have been extremely time-consuming. Instead, in each experiment a qualitative comparison of slice condition was made between control slices and slices subjected to the bulk-loading procedure. To ensure that the comparison was as accurate as possible, slices were taken from the same batch at the same time interval following slicing. The criteria used for this assessment were the appearance of pyramidal cells and interneurons under DIC observation, and analysis of field potential recordings.

A trial consisted of selecting a suitable imaging area and running the custom TillVision protocol. Images were acquired at 10Hz for 6 seconds, giving a total of 60 frames. The stimulus train was triggered via activation of the isolated stimulator device following a 1 second baseline, allowing 5 seconds for monitoring of stimulus-evoked Ca^{2+} transients. A $\Delta F/F$ sequence was prepared using a custom macro in TillVision. Between 3 and 20 trials were performed per slice, depending upon the condition of the neurons. Fewer trials were carried out in slices with poor or absent field potential recordings and widespread neuronal death observed under DIC microscopy. Trials were performed in different areas of the CA1 subfield in order to maximise the probability of detecting Ca^{2+} transients in CA1 pyramidal cells and interneurons

postsynaptically connected to incoming CA3 pyramidal cell axons. The imaging area and focal plane were systematically varied in order to achieve coverage of as much of the subfield as possible. A successful trial was defined as detection of significant elevations in fluorescence intensity in one or more neurons, which were time-locked to stimulation of presynaptic afferents (Fig 4.2). Following epifluorescence detection of stimulus-evoked somatic Ca^{2+} transients, attempts were made to identify the individual cell using DIC imaging. This was not always possible. The somata of individual interneurons in stratum radiatum are sometimes not clearly visible under DIC. The somata of pyramidal cells are densely packed within stratum pyramidale, leading to difficulties in correlating individual neurons detected under epifluorescence imaging with those observed under DIC. When a neuron displaying stimulus-evoked Ca^{2+} transients was successfully identified by correlation with the DIC image, a patch clamp recording could be made from the cell. There would be a greatly increased probability of evoking EPSCs via presynaptic stimulation, since the imaging technique revealed an excitatory synaptic connection between the afferent fibre bundle and the neuron being patch clamped. This illustrates that the technique could be usefully employed to investigate synaptic transmission in areas of low neuronal connectivity. Patch clamp recordings were not made during the present series of experiments, as the objective was to establish and optimise the epifluorescence imaging system for detection of excitatory synaptic connections.

A total of 94 slices were bulk-loaded with Fura2-AM for imaging of the CA1 subfield (Table 4.1). A total of 538 imaging trials were carried out. Of 214 trials in CA1 stratum pyramidale, 21 resulted in detection of one or more Ca^{2+} transients time-locked to triggering of the stimulus train by the custom TillVision protocol. This gave a success rate of 9.8%. These neurons were assumed to be pyramidal cells due to location. In some cases correlation under DIC observation of the somata of the neuron detected using epifluorescence imaging was possible. However, positively identifying under DIC individual pyramidal cells showing Ca^{2+} signals was always problematic due to dense packing of the somata in stratum pyramidale. In addition to

pyramidal cells, neurons detected close to stratum pyramidale may also be basket cells, a class of GABAergic interneuron with soma located around the border between stratum radiatum and stratum pyramidale (see Freund and Buzsaki, 1996). 4 of 324 trials were successful in stratum radiatum, giving a lower success rate of 1.2%. This may be explained in terms of the lower neuronal density of interneurons in stratum radiatum, in comparison with the numerous densely packed pyramidal cell soma in stratum pyramidale. It has been estimated that interneurons represent only around 10% of the neuronal population of the hippocampus (Amaral et al., 1990). There may, however, be many alternative explanations. Ca^{2+} transients in interneurons may be smaller in magnitude in comparison to those in pyramidal cells, leading to lower success rate in their detection. Alternatively, loading of fluorescent indicator into interneurons may occur more slowly or less efficiently in comparison to pyramidal cells. Finally, fewer stimulus-evoked action potentials may occur in interneurons, leading to lower Ca^{2+} influx in response to a given extracellular stimulus train.

Total number of slices bulk-loaded with Fura2-AM	Imaging area	Total number of imaging trials	Trials with neuronal Ca^{2+} signals detected	Percentage successful trials
94	CA1 stratum pyramidale	214	21	9.8%
	CA1 stratum radiatum	324	4	1.2%

Table 4.1 *Epifluorescence detection of action potential-associated somatic Ca^{2+} transients in CA1 subfield evoked by extracellular stimulation of Schaffer collaterals. Slices were bulk-loaded with Fura2-AM via two-stage incubation protocol. Successful trials were defined as detection of significant elevations in fluorescence intensity in one or more neurons, which were time-locked to stimulation of presynaptic afferents.*

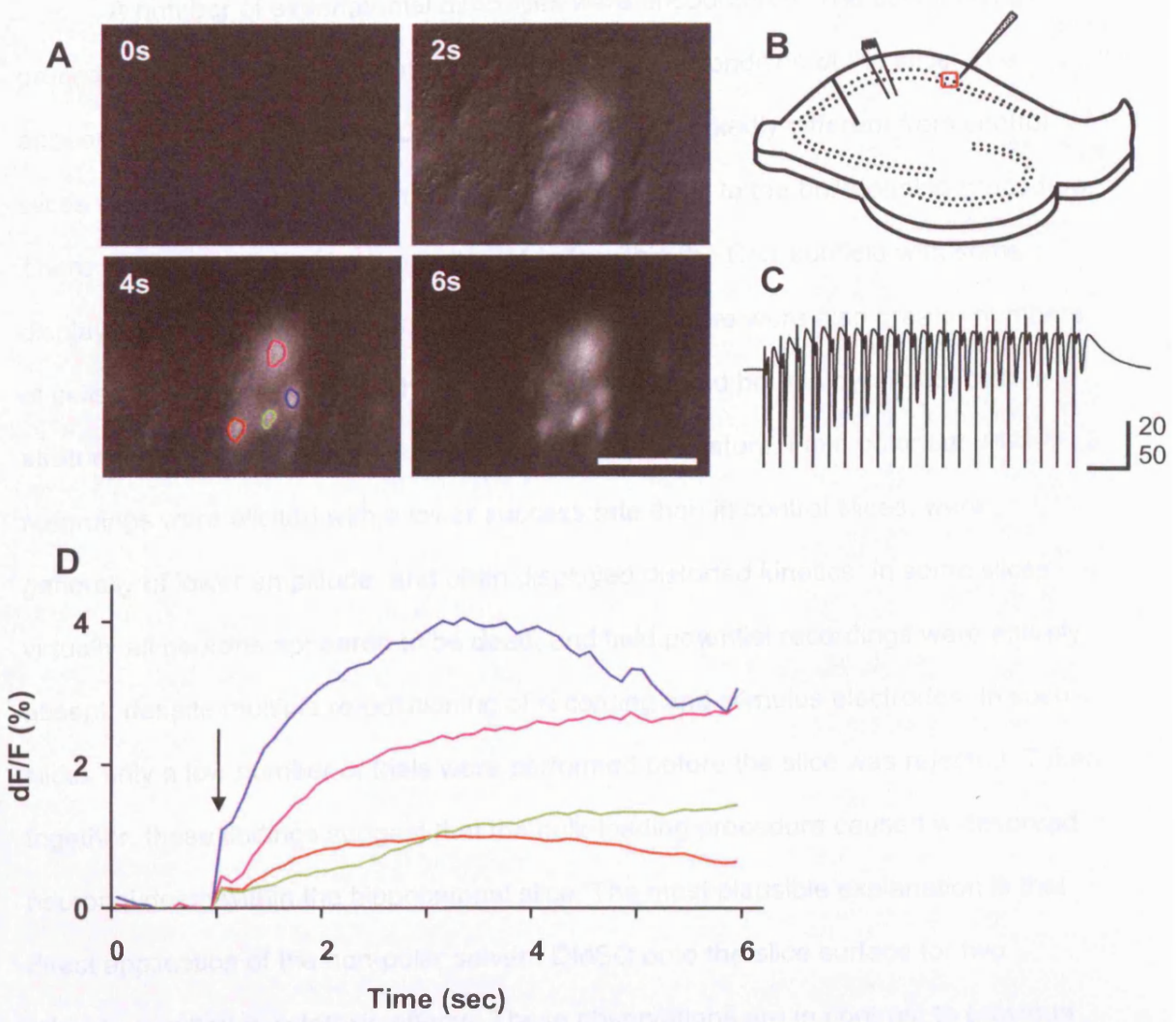

Figure 4.2 *Quantification of action potential-associated postsynaptic Ca^{2+} transients in individual CA1 pyramidal cell somata during a single successful imaging trial. The hippocampal slice was bulk-loaded with Fura2-AM in a two-stage incubation procedure. Schaffer collaterals inputs were activated via extracellular stimulation (20 pulses at 50 Hz).* ***A,*** *Still images from movie sequence at 0, 2, 4 and 6 seconds. 60 images were acquired at 10 Hz, giving a total sequence of 6 sec. The stimulus train was delivered following a 1 sec baseline. Somatic Ca^{2+} transients were detected in four cells. A region of interest (ROI) was drawn around each cell for analysis of change in fluorescence intensity (ΔF/F), using the TillVision software. Scale bar = 100 µm.* ***B,*** *Location of extracellular stimulus and field potential recording electrodes in hippocampal slice. Imaging area is shown by the red square. The area mainly covered stratum pyramidale.* ***C,*** *Field potential recording of population response to stimulus train obtained in CA1 stratum pyramidale.* ***D,*** *Time-course of ΔF/F for each putative pyramidal cell soma, surrounded by an ROI of the corresponding colour.. Arrow shows delivery of stimulus train following a 1 sec baseline.*

A number of experimental difficulties were encountered. The bulk-loading procedure had a markedly deleterious effect upon the condition of the slice. The appearance of neurons under DIC observation was markedly different from control slices from the same batch that had not been subjected to the bulk-loading procedure. There were a much greater proportion of cells within the CA1 subfield with soma displaying a highly swollen, nucleated appearance. There were also greater numbers of cells with shrunken soma. These observations applied both to pyramidal cells in stratum pyramidale, and to interneurons in stratum radiatum. Field potential recordings were elicited with a lower success rate than in control slices, were generally of lower amplitude, and often displayed distorted kinetics. In some slices virtually all neurons appeared to be dead, and field potential recordings were entirely absent, despite multiple re-positioning of recording and stimulus electrodes. In such slices only a low number of trials were performed before the slice was rejected. Taken together, these findings suggest that the bulk-loading procedure caused widespread neuronal death within the hippocampal slice. The most plausible explanation is that direct application of the non-polar solvent DMSO onto the slice surface for two minutes resulted in cytotoxic effects. These observations are in contrast to previous studies, which have reported that brief incubations in 100% DMSO do not adversely affect the condition of neurons within the slice (Smetters et al., 1999; Peterlin et al., 2000; Kozloski et al., 2001). Experiments were carried out in which the incubation involving pure DMSO was omitted, leaving a single 60 min incubation in 20 μM Fura2-AM. A total of 5 slices were tested. Field potential recordings and appearance of neurons under DIC were similar to control slices. A total of 48 imaging trials were performed in 5 slices. None resulted in detection of Ca^{2+} transients. These experiments confirmed that the incubation in pure DMSO was very likely to be responsible for the widespread deleterious effects upon neuronal health observed in slices subjected to the bulk-loading procedure. Furthermore, these findings suggest that the two-stage incubation was necessary to achieve a sufficient intracellular concentration of Fura2 for detection of stimulus-evoked Ca^{2+} signals. It is probable

that the brief application of concentrated indicator solution in pure DMSO to the slice surface greatly facilitates uptake of indicator across the hydrophobic cell membrane (Smetters et al., 1999; Peterlin et al., 2000; Kozloski et al., 2001; Billups et al., 2002). The success rate in detecting stimulus-evoked Ca^{2+} transients was low even when this step was included. Despite the widespread neuronal damage resulting from incubation in pure DMSO, omission of this step is clearly not possible if an acceptable level of staining is to be achieved.

4.3.2.2 Extracellular stimulation in CA3 subfield

The sensitivity of the Ca^{2+} imaging technique was further investigated by carrying out experiments the CA3 subfield, which contains a network of recurrent excitatory connections among the pyramidal neurons (e.g. Ishizuka et al., 1990). This area therefore exhibits an unusually high level of network excitability, and is susceptible to epileptiform discharges. In order to further evaluate the technique of combining bulk-loading of fluorescent Ca^{2+} indicators with extracellular stimulation, the objective of this series of experiments was to image Fura2-AM Ca^{2+} signals associated with widespread spiking of CA3 pyramidal neurons. It was anticipated that due to the highly excitable nature of the CA3 pyramidal cell network, more rapid and sustained firing of neurons could be achieved in comparison with activation of CA1 neurons via stimulation of a defined input pathway. Activation of widespread firing within the CA3 network may thus give rise to larger influxes of Ca^{2+} into a greater number of cells, thereby increasing the probability of detecting Ca^{2+} transients using epifluorescence imaging. The network of CA3 pyramidal cells was activated by positioning a steel bipolar extracellular stimulus electrode in the hilus or CA3 stratum lucidum to activate incoming mossy fibres (dentate granule cell axons), or in CA3 stratum pyramidale to directly activate CA3 pyramidal cells. Network excitability was increased by blockade of $GABA_A$ receptors using picrotoxin (100 μM) and $GABA_B$ receptors using CGP52432 (5 μM).

A lower success rate in eliciting stimulus-evoked Ca^{2+} signals was achieved in CA3 in comparison to CA1. A total of 36 slices were bulk-loaded with Fura2-AM for imaging of the CA3 subfield (Table 10.2). A total of 181 imaging trials were carried out. Of 92 trials in CA3 stratum pyramidale, 8 resulted in detection of one or more Ca^{2+} transients time-locked to presynaptic stimulation, giving a success rate of 8.7%. Of 89 trials in stratum radiatum, none were successful. Observation of the CA3 subfield under DIC indicated extremely widespread neuronal death following the bulk-loading procedure in comparison to control slices taken from the same batch. The majority of cells in both stratum pyramidale and radiatum displayed a swollen, nucleated appearance. Field potential recordings were obtained in the CA3 subfield in only in a low number of slices, confirming that the bulk-loading procedure has a markedly deleterious effect upon the neuronal population. Ca^{2+} signals were unlikely to be observed in the absence of detectable population spikes in postsynaptic neurons, since widespread activation of voltage-gated Ca^{2+} channels would not occur. The low success rate in eliciting Ca^{2+} signals in area CA3 may therefore be explained by extensive neuronal damage resulting from the bulk-loading procedure.

Total number of slices bulk-loaded with Fura2-AM	Imaging area	Total number of imaging trials	Total number of trials with Ca^{2+} signals detected	Percentage successful trials
36	CA3 stratum pyramidale	92	8	8.7%
	CA3 stratum radiatum	89	0	0

Table 4.2 *Epifluorescence detection of action potential-associated somatic Ca^{2+} transients in CA3 subfield following bulk-loading of slices with Fura2-AM via two-stage incubation protocol. Successful trials were defined as detection of significant elevations in fluorescence intensity in one or more putative neurons, which were time-locked to stimulation of presynaptic afferents.*

4.3.3 Loading of fluorescent Ca^{2+} indicators - local pressure injection

Local pressure injection of acetoxymethylester forms of fluorescent Ca^{2+} indicators into brain slices is an established experimental technique, which has been used to investigate many aspects of synaptic physiology (e.g. Regehr and Tank, 1991; 1994a; Wu and Saggau, 1994b; Kamiya and Ozawa, 1999). This technique was investigated as an alternative to the bulk-loading procedure, due to the difficulties associated with widespread neuronal death and low success rate in detecting action potential-associated somatic Ca^{2+} transients. The objective remained the same - to load a population of neurons with a membrane-permeant Ca^{2+}-sensitive fluorescent indicator, and use epifluorescence imaging of action potential-associated postsynaptic Ca^{2+} influxes to optically detect neurons postsynaptically connected to a specific afferent input pathway. It was anticipated that localised neuronal death would occur at the injection site due to pressure damage and cytotoxic effects of 100% DMSO in the indicator solution. Neurons were expected to survive and become loaded with indicator in a penumbra surrounding the injection site as the solution diffused through the slice.

Three methods of local pressure injection were tested. (i) borosilicate glass capillary with a tip diameter of ~20 µm, with pressure generated using a 1 ml syringe connected by silicon tubing; (ii) Nanoject device (Drummond, USA) which could be set to pressure inject volumes between 4 and 76 nl of solution in single steps via a glass capillary; (iii) Hamilton syringes (precisely gradated syringes with extremely fine steel needles), with capacities of either 1 or 5 µl. Pressure was generated manually by the experimenter when using the borosilicate glass capillary or Hamilton syringes, whereas the Nanoject device was electronically controlled. The three methods were evaluated extensively, the most important criteria being (i) optimum penetration of fluorescent indicator into the tissue, and (ii) minimal damage to the slice from the injection device.

2 µl of 2 mM Fura2-AM in DMSO with 5% pluronic F-127 was injected into two sites in each slice (Fig 4.3). (i) In CA1 stratum pyramidale or stratum radiatum towards

the subiculum, so that the indicator solution would diffuse through CA1 towards CA3. Injecting towards the subiculum ensured that CA3 pyramidal cell axons would remain intact. (ii) In CA3 stratum radiatum to load interneurons, or stratum pyramidale to load pyramidal cells. Physical damage to the slice and neuronal death resulting from injection were visually assessed using DIC microscopy. Penetration of Fura2-AM was assessed using epifluorescence imaging to examine background staining, and by running imaging trials combined with extracellular stimulation controlled by the TillVision software, as described above in previous experiments.

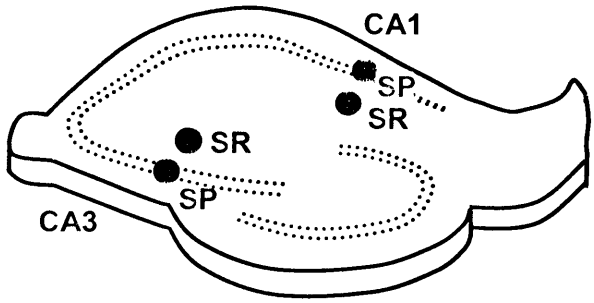

Figure 4.3 *Diagram of transverse hippocampal slice, showing position of sites for pressure injection of Fura2-AM to load localised neuronal populations in stratum pyramidale (SP) and stratum radiatum (SR) in CA1 and CA3 subfields. Three different pressure injection methods were tested, and ultimately the main set of experiments were performed using a Nanoject device.*

Borosilicate glass capillaries resulted in extensive damage to the tissue in the area surrounding the injection site. 10 slices were tested before the method was rejected. A total of 56 trials were recorded, with no detection of postsynaptic Ca^{2+} signals which were time-locked to presynaptic stimulation (n = 10 slices, 56 trials, 0% success rate). Hamilton syringes caused the least damage, but penetration of indicator into the tissue was poor due to the extremely fine diameter of the needle, which became blocked easily. 10 slices were tested before the method was rejected. A total of 38 trials were recorded, none of which were successful (n = 10 slices, 38 trials, 0% success rate). Subsequently, injections in the series of experiments

described in this section were performed using the Nanoject device. This was selected as the most suitable of the three methods, since it enabled a defined volume of indicator solution to be dispensed in precisely controlled steps via a finely extruded glass capillary. The Nanoject device provided the best balance between optimum indicator penetration and minimal tissue damage. 76nl of indicator solution was injected stepwise to give a total of 2 µl. Extensive neuronal damage was observed in the area immediately surrounding the injection site, due to the cytotoxic effect of DMSO and physical pressure damage. Damaged neurons with swollen somata were visible under DIC microscopy in a circular area, generally approximately 200-400 µm surrounding the injection site. Stained neurons were visible within a circular penumbra generally extending approximately 300-800 µm from the injection site. Imaging trials were carried out within this area, and also further outside the area of background staining containing visibly stained neurons, in case stained neurons were present with a baseline fluorescence too low to be detected in the absence of stimulus-evoked population spiking. 48 slices were injected with Fura2-AM, with a total of 506 imaging trials carried out (Table 4.3). The success rates in detecting stimulus-evoked postsynaptic somatic Ca^{2+} transients were similar to those achieved from bulk-loading of entire slices with Fura2-AM. 7.9% of trials (11 of 139) were successful in CA1 stratum pyramidale. 1.4% (3 of 202 of trials) were successful in CA1 stratum radiatum. 1.9% (2 of 103 trials) were successful in CA3 stratum radiatum. No Ca^{2+} transients were detected in CA3 stratum pyramidale (0 of 62 trials; 0% success rate).

Total number of slices injected with Fura2-AM	Imaging area	Total number of imaging trials	Total number of trials with Ca^{2+} signals detected	Percentage successful trials
48	CA1 s.pyramidale	139	11	7.9%
	CA1 s.radiatum	202	3	1.4%
	CA3 s.pyramidale	62	0	0
	CA3 s.radiatum	103	2	1.9%

Table 4.3 *Epifluorescence detection of action potential-associated somatic Ca^{2+} transients in CA1 and CA3 subfields following local pressure injection of Fura2-AM.*

4.4 Discussion

Following bulk-loading of entire hippocampal slices with membrane permeant Fura2-AM using a double incubation protocol (Smetters et al., 1999; Peterlin et al., 2000; Kozloski et al., 2001), Ca^{2+} signals elicited by trains of extracellular stimuli to the Schaffer collateral pathway could be detected with a success rate of approximately 10% in CA1 pyramidal cells, and 1% in CA1 stratum radiatum interneurons. In successful trials, Ca^{2+} signals corresponded to the soma of single neurons. dF/F values were quantified for individual cells, and were within the range 0.30-4.12%. Ca^{2+} signals were detected in a lower proportion of trials in CA3 compared to CA1. This difference may be explained by the significantly greater neuronal damage in area CA3 following the bulk-loading procedure. The major obstacle in eliciting Ca^{2+} signals in interneurons appeared to be widespread neuronal death in the superficial layers of the slice following the bulk-loading procedure. Similar success rates were achieved through pressure injection of indicator into specific areas of the slice, but Ca^{2+} signals were detected only within a localised area surrounding the injection site, making this method unsuitable for widespread probing of neuronal connectivity.

It is important to note that there are a number of differences between detecting Ca^{2+} transients by filling an individual neuron with fluorescent indicator via a patch pipette, and bulk-loading an entire slice. When loading an individual cell via the patch pipette, the intracellular concentration of fluorescent indicator is fixed. It is likely to be much higher than could be achieved through bulk-loading of an entire slice, as the indicator does not diffuse across a membrane. Ca^{2+} fluorescence signals are therefore likely to be weaker and more difficult to detect in neurons from a bulk-loaded slice. In addition, an individually stained cell is positively identified and can be viewed at the centre of the imaging field at the optimum focal plane. In a bulk-loaded slice, Ca^{2+} transients are detected only in stained cells which by chance are within the field of view and at the correct focal plane. Patch clamp recording from a single neuron provides far greater control over the membrane potential of the cell being imaged than extracellular stimulation of an afferent fibre bundle. Spike trains were recorded from a single cell, and triggered by depolarising the cell in current clamp mode. By contrast, triggering of spike trains via extracellular stimulation is less reliable, and it is impossible to determine whether an individual cell is spiking from field potential recordings, which show only population activity. These factors may explain the disparity between the clear Ca^{2+} signals obtained when filling individual neurons with Fluo4 via the patch pipette, and the failure to detect Ca^{2+} signals when carrying out extracellular stimulation of defined pathways in slices bulk-stained with Fura2-AM.

Stimulus-evoked Ca^{2+} transients were detected in a low proportion of trials. The success rate was especially low when imaging interneurons in stratum radiatum (< 2%, in comparison with 8-9% in stratum pyramidale). This may largely be explained in terms of the considerably greater neuronal density within stratum pyramidale in comparison to stratum radiatum. Interneurons have been estimated to make up only approximately 10% of the hippocampal neuronal population (Amaral et al., 1990). Other factors may also contribute towards the disparity between interneurons and pyramidal cells in terms of detecting stimulus-evoked Ca^{2+} transients. Specific subsets of interneurons in the hippocampus have been shown to display a selective

vulnerability in comparison to principal cells to many types of insult, including ischaemia (Hsu and Buzsaki, 1993) and models of temporal lobe epilepsy (Obenaus et al., 1993; Houser and Esclapez, 1996; Dinocourt et al., 2003). It is possible that hippocampal interneurons display a selective vulnerability to the deleterious effects of the bulk-loading procedure. Another factor potentially involved may be differences in efficacy of indicator uptake between pyramidal neurons and interneurons. Since the primary objective of the project was to establish the technique for identification of functional excitatory connections to interneurons, it is essential to significantly improve the success rate in eliciting and detecting stimulus-evoked Ca^{2+} signals.

Several factors may account for the low number of trials in which Ca^{2+} signals were observed in response to extracellular stimulation of defined input pathways. Despite continuous attempts to enhance the staining procedure and improve the survival rate of the neuronal population within the slice, bulk-loading invariably had a markedly deleterious effect upon slice condition. Clear differences in field potential recordings and the proportion of swollen, nucleated cells could be observed between stained and unstained slices from the same batch. Thus in contrast to previously reported findings (Smetters et al., 1999; Peterlin et al., 2000; Kozloski et al., 2001), a clear deterioration in slice quality following the two-stage bulk-loading procedure was consistently observed in the present study. This is likely to be primarily due to the cytotoxic effects of pure DMSO applied directly to the slice surface during the first stage of the bulk-loading procedure. DMSO affects membrane stability through its nature as a nonpolar hydrophobic solvent. In addition, application of DMSO to the slice surface would cause significant cell damage through osmotic effects, as the molarity of pure DMSO is approximately 14 M. Since the exposure to pure DMSO is relatively brief, it is likely that the majority of neuronal death would occur in the more superficial layers of the slice. However, as imaging is carried out using an epifluorescence system, only the superficial layers can be utilised for fluorescence imaging experiments. When searching for stained neurons under fluorescence imaging, it was apparent that the focal depth which could be observed was

considerably less than that under DIC imaging. Experiments in which the first stage of the incubation procedure was omitted (application of indicator in 100% DMSO directly to the slice surface) confirmed that this step was responsible for the widespread neuronal death resulting from the bulk-loading procedure. However, these experiments also demonstrated that this step was necessary in order to achieve a sufficient intracellular concentration of Fura2-AM for stimulus-evoked somatic Ca^{2+} transients to be detected.

Although local pressure injection of indicator solution had a less deleterious effect upon overall slice quality, the disadvantage of using the method for probing neuronal connectivity was that Ca^{2+} signals could only be detected within a localised area surrounding the injection site. When bulk-loading the entire slice with indicator, imaging trials were carried out over the entire subfield of interest and Ca^{2+} transients were often detected at some distance from the stimulus site. Making multiple injections within the same subfield to stain an entire area gave rise to a greater number of damaged areas surrounding the injection sites. Every effort was made to avoid tissue damage when injecting indicator solution. Injection capillaries were made as fine as possible, but a tip diameter ≥15 μm was necessary to avoid becoming blocked when inserted into the tissue, preventing further dye injection. Damaged areas may contain axons from the pathway being stimulated, adversely affecting detection of postsynaptic targets. It is important to note that previous studies utilising localised pressure injection of fluorescent indicators have involved injection into axon bundles to quantify presynaptic Ca^{2+} dynamics within a highly localised area (e.g. Regehr and Tank, 1991; 1994a; Wu and Saggau, 1994b; Kamiya and Ozawa, 1999). In contrast, the objective of the present study was imaging of postsynaptic Ca^{2+} signals in order to identify functional synaptic connections within a large area.

The efficacy of the bulk-loading procedure and the survival rate of the neuronal population could potentially be enhanced by using younger animals. Previous studies have reported that bulk-loading of fluorescent indicators into neurons is more effective in the developing neocortex, and used rats or mice aged P10-P23 (Smetters et al.,

1999; Peterlin et al., 2000; Kozloski et al., 2001). In contrast, the rats used in the present study were aged P21 to P25. There are clear developmental differences in the efficiency of bulk-loading between these age groups (Peterlin et al., 2000). However, it is important to note that there are also widespread developmental variations in expression of neurotransmitter receptors and voltage-gated ion channels. This factor must be considered if using younger animals when employing the epifluorescence imaging technique as an experimental tool to facilitate subsequent electrophysiological and pharmacological studies. Developmental differences in receptor expression, for example mGluR subtypes, may give rise to significant variations in results of pharmacological studies between juvenile and adult rats.

An inherent difficulty in using the Ca^{2+} epifluorescence imaging system to probe neuronal connectivity was reliably reconciling neurons displaying Ca^{2+} signals under epifluorescence imaging with individual cells under DIC observation. Often the Ca^{2+} signals detected were indistinct and could not be reliably correlated with individual neurons under DIC. Indeed, the strength of the epifluorescence imaging system is its temporal rather than spatial resolution. This problem was particularly apparent when attempting to identify individual pyramidal neurons in stratum pyramidale, due to the high neuronal density within this area. This issue could be addressed in two ways. Firstly, the strength of the Ca^{2+} signals could be improved, giving rise to a clearer fluorescence image and aiding identification of individual cells. Secondly, the number of neurons within the imaging field displaying Ca^{2+} signals could be increased, thereby enhancing the probability of detecting Ca^{2+} signals in neurons which could be clearly identified under DIC. Both of these objectives could be achieved if the deleterious effect of the bulk-loading procedure upon the neuronal population within the slice could be further reduced, and if the spatial sensitivity and reliability of the technique could be enhanced.

The original objective was to use minimal extracellular stimulation (e.g. single or paired stimuli) of afferent inputs to evoke action potentials in postsynaptically-connected cells. The associated Ca^{2+} transients could then be detected using

epifluorescence imaging. However, experimental evidence demonstrated that more robust presynaptic stimulation was necessary to elicit detectable postsynaptic Ca^{2+} signals. The robust extracellular stimulation of defined pathways necessary to elicit Ca^{2+} signals (e.g. 20 pulses at 50Hz) may cause accumulation of K^+ within the extracellular space through population spiking. Sufficient K^+ accumulation could result in depolarisation of neurons in the vicinity of the stimulus site, thereby activating voltage-gated Ca^{2+} channels. This may give rise to Ca^{2+} signals if such neurons were located within the imaging field. Although these Ca^{2+} signals may be temporally correlated with delivery of the extracellular stimulus to the input pathway, it does not follow that the Ca^{2+} signals indicate the presence of a monosynaptic excitatory connection. Indeed, previous studies have demonstrated step-like elevations in Ca^{2+} fluorescence intensity which can be correlated with individual presynaptic action potentials (Smetters et al., 1999; Peterlin et al., 2000; Kozloski et al., 2001). In contrast, some of the Ca^{2+} signals detected in this study increased as a bi-exponential curve. These factors could affect the reliability of detection of postsynaptically connected neurons using extracellular stimulation.

In conclusion, wide-field epifluorescence imaging and bulk-loading of neuronal populations with fluorescent indicators to detect postsynaptic action potential-associated Ca^{2+} transients, combined with extracellular stimulation of specific presynaptic afferent inputs, represents a potentially powerful and useful means of identifying excitatory connections in areas with low connectivity. However, the present study demonstrated that a number of major experimental difficulties would have to be overcome for the technique to be used successfully in this way.

Chapter 5. Glutamatergic synaptic transmission to CA1 stratum radiatum interneurons is modulated by group I mGluRs

5.1 Introduction

The remainder of the results chapters in this thesis (Chapters 5-9) describe detailed investigation of modulation of glutamatergic synaptic transmission from CA3 pyramidal axons to CA1 stratum radiatum interneurons by group I metabotropic glutamate receptors. Group I mGluRs comprise mGluR1 and mGluR5 subtypes. (S)-3,5-dihydroxyphenylglycine (DHPG) is a potent agonist which is highly selective for group I mGluRs (Schoepp et al., 1994; 1999). Expression of these receptors in transfected cell lines has demonstrated that group I mGluR activation is coupled via the G protein G_q to phosphoinositide (PI) hydrolysis, resulting in generation of the intracellular messengers diacylglycerol (DAG) and inositol trisphosphate (IP3). This in turn leads to activation of protein kinase C (PKC) and mobilisation of calcium from intracellular stores (Pin and Duvoisin, 1995; Hermans and Challiss, 2001). Group I mGluR activation directly affects excitability of hippocampal neurons in a variety of ways, the majority of which have been demonstrated in CA1 pyramidal cells (see Chapter 1, Section 1.2.4). The principal effects are depolarisation and increased firing of action potentials (e.g. Mannaioni et al., 2001). The underlying mechanisms involve modulation of ion channel function, and include inhibition of at least four distinct K^+ currents – the AHP current (Charpak et al., 1990; Desai and Conn, 1991; Ireland and Abraham, 2002), the M current (Charpak et al., 1990), a leak current (Guerineau et al., 1994) and a voltage-dependent slow-inactivating current (Luthi et al., 1996). There is also activation of Ca^{2+}-activated and Ca^{2+}-independent cationic conductances (Crepel et al., 1994; Guerineau et al., 1995; Congar et al., 1997; Heuss et al., 1999; Chuang et al., 2000; Chuang et al., 2002; Gee et al., 2003). Systematic investigation of these mechanisms in GABAergic interneurons has not yet been carried out. Group I mGluR activation further increases CA1 pyramidal cell excitability by decreasing

GABAergic inhibition (Desai and Conn, 1991; Gereau and Conn, 1995; Fitzsimonds and Dichter, 1996).

In addition to these mechanisms which directly affect neuronal excitability, group I mGluRs have been shown to powerfully modulate synaptic transmission in the hippocampus. Initial studies demonstrated that selective activation of group I mGluRs by DHPG in hippocampal slices caused a short-term, reversible depression of excitatory synaptic transmission from Schaffer collaterals to CA1 pyramidal cells. This effect was demonstrated using both field potential recording (Manzoni and Bockaert, 1995) and whole-cell patch clamp (Gereau and Conn, 1995; Rodriguez-Moreno et al., 1998; Mannaioni et al., 2001). Changes in paired-pulse ratio suggested that the mechanism involved a presynaptic action. This acute depression has been shown to be dependent upon the mGluR1 subtype in CA1 pyramidal cells (Mannaioni et al., 2001). In addition to this acute depression of synaptic transmission, group I mGluRs mediate a specific type of long-term depression (LTD) in the CA1 subfield, known as 'mGluR-LTD' (Palmer et al., 1997; Overstreet et al., 1997; Fitzjohn et al., 2001; Faas et al., 2002; Huang and Hsu, 2005). This type of LTD is discussed in detail in General Introduction, Section 1.4.5.3. Previous studies investigating mGluR-LTD have been carried out in CA1 pyramidal cells. It is currently unknown whether group I mGluR-dependent LTD occurs in CA1 interneurons, and if so, whether the phenomenon is interneuron subtype-specific. Group I mGluRs are required for induction of a form of stimulus-induced long-term potentiation in CA1 stratum oriens interneurons, which are innervated by axon collaterals of local CA1 pyramidal cells. However, this does not occur in CA1 stratum radiatum interneurons, many of which receive Schaffer collateral excitation and project to local pyramidal cells (Perez et al., 2001; Lapointe et al., 2004). It is important to realise that long-term synaptic plasticity is considerably less well characterised in GABAergic interneurons than in pyramidal cells, and remains a complex and controversial issue, due in part to the heterogeneity of the interneuron population. It should be noted that detailed investigation of long-term synaptic plasticity (mGluR-LTD) at Schaffer collateral connections onto CA1 interneurons was

not the primary objective of the projects described within this thesis. However, the experiments carried out raised a number of questions regarding this phenomenon, which warrant further investigation in future studies.

There are a number of interesting questions regarding modulation of excitatory synaptic transmission by group I mGluRs in the CA1 subfield. An important issue is whether the group I mGluR-mediated acute depression observed in pyramidal cells (Gereau and Conn, 1995; Manzoni and Bockaert, 1995; Rodriguez-Moreno et al., 1998; Mannaioni et al., 2001) also operates at excitatory connections onto GABAergic interneurons, and if so whether there are differences in the nature of the effect between pyramidal cells and interneurons. Furthermore, the mechanisms via which this depression is induced and expressed are currently unknown. Group I mGluR-dependent LTD has not been systematically investigated in interneurons, though as stated above, characterising this phenomenon is not within the objectives of this thesis. Given the heterogeneous nature of the hippocampal interneuron population, it may be expected that variations may occur in response to group I mGluR activation. A study by van Hooft et al. (2000) correlated immunocytochemical identification of CA1 oriens-alveus interneurons with the effect of mGluR agonists on inward current. However, no attempt has yet been made to correlate distinct subtypes of interneuron with the effects of group I mGluR activation upon synaptic transmission. It is important to address these questions, since modulatory mechanisms operating at excitatory connections onto interneurons can powerfully affect the recruitment of inhibitory drive within the hippocampus.

The objective of the experiments described in the present chapter was to determine whether the group I mGluR-dependent acute depression of excitatory synaptic transmission described at Schaffer collateral connections onto CA1 pyramidal cells (Gereau and Conn, 1995; Manzoni and Bockaert, 1995; Rodriguez-Moreno et al., 1998; Mannaioni et al., 2001) occurs in CA1 stratum radiatum interneurons. Given the extensive differences between glutamatergic synapses onto pyramidal cells and interneurons, quantitative comparisons of the acute depression

between the two cell types were carried out. A variety of pharmacological approaches were employed in order to confirm that the effect was mediated by group I mGluRs, with no involvement of group II and III receptors. Subsequent experiments aimed to identify the individual group I mGluR subtypes responsible for mediating depression of synaptic transmission in CA1 interneurons.

5.2 Methods

5.2.1 Whole-cell patch clamp recording of pharmacologically-isolated EPSCs

Whole-cell patch clamp recordings were made from CA1 pyramidal cells and stratum radiatum interneurons in 350 µm thick transverse hippocampal slices prepared from P21-28 Sprague-Dawley rats. Slices were continuously perfused with ACSF at a rate of 3 ml per minute. A cut was made in the slice between CA3 and CA1 to prevent the spread of stimulus-induced epileptiform discharges due to the network of recurrent excitatory collaterals in CA3. Patch clamp recording was visually guided by infra-red DIC microscopy. Neurons were voltage-clamped at -60 mV using a caesium gluconate-based intracellular solution containing QX314-Br (5 mM) to prevent spiking. Interneurons were identified initially by their location within stratum radiatum of the CA1 subfield, by their high input resistance, and subsequently by post-hoc morphological analysis. Neurons were loaded with biocytin (0.4% w/v) via the patch pipette to facilitate post hoc staining and subsequent visualisation by confocal microscopy. To record pharmacologically-isolated AMPA-kainate EPSCs, the following drugs were always present in the perfusion ACSF: DL-APV (50 µM) to block NMDA receptors, and picrotoxin (100 µM) to block $GABA_A$ receptors. Upon completion of the experiment, NBQX (10 µM) was bath applied to verify that EPSCs were mediated by AMPA/kainate receptors. A stainless steel bipolar stimulus electrode was positioned in stratum radiatum in the CA1 subfield, close to the cut between CA3 and CA1. Once stable whole-cell access had been achieved, monosynaptic EPSCs were elicited by single test pulses from a constant current

isolated stimulator. Stimulus intensity was progressively increased until maximal EPSC amplitude was determined, then reduced until EPSCs were around 250-300 pA in magnitude. The rationale behind this is discussed in Chapter 2, Section 2.4.2. Stimulus intensities ranged from 10 - 500 μA, though were usually < 200 μA, with a duration of 50 μs. If necessary the bipolar stimulus electrode was re-positioned within stratum radiatum once whole-cell access had been achieved, in order to optimally evoke clean monosynaptic EPSCs via Schaffer collateral stimulation, thereby removing any potential contamination resulting from polysynaptic responses. In order to test for presynaptic effects, paired pulse stimulation was delivered in each recording cycle. Alterations in PPR indicate a change in the release probability of neurotransmitter, suggesting involvement of a presynaptic mechanism (for review see Zucker and Regehr, 2002). Paired pulses were delivered at a frequency of 20 Hz, giving an inter-pulse interval of 50 ms. The recording duty cycle consisted of a single pulse, paired pulse, and calibration pulse to monitor the integrity of the whole-cell recording by measuring I_{hold}, R_S and R_A. The inter-trial interval was 10 s, giving a 30 s duty cycle. During whole-cell patch clamp recording it is essential to maintain stable access to the cell interior. Changes in parameters such as I_{hold} and R_S may affect other factors in the recording, such as EPSC amplitude. R_S was < 40 MΩ and I_{hold} was < 200 pA. Recordings were rejected if either of these parameters varied by > 20% over the course of the experiment. EPSC time courses were plotted using values calculated from the maximum amplitude of EPSCs elicited by single pulses every 30 s. Data were binned by three points, such that each point represents a 90 s interval, or the average of three data points.

5.2.2 Investigation of pharmacological effects

Unless otherwise stated, drugs were applied via the perfusion ACSF. Drugs were prepared in aliquots and frozen, then diluted 1:1000 in ACSF. Drugs were dissolved in the following solvents when preparing aliquots (final concentration in ACSF shown in brackets): DL-APV (50 μM) in 50 mM NaOH, picrotoxin (100 μM) in

DMSO, DHPG (30 μM) in water and ACPD (50 μM) in 50 mM NaOH. CHPG was used at a final concentration of 500 μM, but due to difficulties in dissolving the drug, aliquots were prepared at 100 mM in 100 mM NaOH and diluted 1:200. LY367385 (100 μM) was used to selectively block mGluR1, and MPEP (10 μM) was used to selectively block mGluR5. Following a 10 min baseline, slices were pre-exposed to one of the group I mGluR-selective antagonists for 10 min, allowing the drug to penetrate the tissue and reach its target receptors. This was followed by 20 min DHPG application to activate the remaining group I mGluR subtype, with 20 min washout. The selective antagonist remained in the perfusion solution throughout the exposure to DHPG and washout. In addition to demonstrating the contribution of individual group I mGluR subtypes to DHPG-induced effects, this experimental design also allowed the effect of blocking individual receptor subtypes upon baseline synaptic transmission to be investigated.

A 10 min baseline (20 data points) was recorded prior to drug application. This gave a stable reference for baseline EPSC amplitude, and ensured that the whole-cell recording remained stable according to the parameters I_{hold} and R_S measured using the calibration pulse in each duty cycle. Slices were continuously exposed to the drugs for a period of 20 min, followed by a 20 min washout in ACSF containing the same drugs present during baseline recording (usually DL-APV and picrotoxin). In certain experiments, slices were exposed to multiple drugs at different time points. Pharmacological effects on EPSC amplitudes were calculated from an average of 10 recording cycles (5 min), unless otherwise stated. Paired pulse ratios (PPR) were calculated from averages of 20 cycles and normalized to the baseline value obtained prior to the addition of DHPG.

Unless otherwise stated, interneurons were treated as a single population when analysing data. EPSCs were fully abolished by the addition of NBQX (10 μM) at the end of each experiment, confirming that they were mediated entirely by AMPA/kainate ionotropic glutamate receptors.

5.3 Results

5.3.1 DHPG depresses monosynaptic EPSCs in CA1 pyramidal cells

The initial objective of the investigation was to confirm that selective activation of group I mGluRs via DHPG application depresses monosynaptic Schaffer collateral-evoked EPSCs in CA1 pyramidal cells. This phenomenon has been demonstrated in a number of previous studies (Gereau and Conn, 1995; Manzoni and Bockaert, 1995; Rodriguez-Moreno et al., 1998; Mannaioni et al., 2001).

Single EPSCs were evoked every 30 s. Once a stable 10 min baseline (20 cycles) had been recorded, DHPG (30 μM) was bath applied for 20 min, followed by a 20 min washout. EPSCs were reduced to 30 ± 5% (mean ± SEM) of baseline amplitude ($p << 0.0001$, paired t test, $n = 5$; Fig. 5.1A). The onset of depression began within 6 minutes of DHPG application, accounting for the time taken for the drug to wash in to the slice, penetrate through the tissue, and bind to and activate receptors. Group I mGluR activation has been shown to depolarise pyramidal cells (see Chapter 1, Section 1.2.4). Recordings in the present study were carried out in voltage clamp configuration, so any depolarisation would be observed as a change in I_{hold}. However, depolarisation occurs primarily due to inhibition of various K^+ conductances (Charpak et al., 1990; Desai and Conn, 1991; Guerineau et al., 1994; Luthi et al., 1996). A caesium-based intracellular solution was used in the present study. This would prevent flux of K^+ ions through K^+ channels. Furthermore, QX314 was present in the intracellular solution, which blocks GIRK (G protein-coupled inward-rectifier)-class K^+ channels (Nathan et al., 1990). These factors would thus mask any postsynaptic DHPG-induced depolarisation. Indeed, no significant change in I_{hold} was detected. EPSC amplitude began to return towards baseline within 5 minutes of washout of DHPG. It is interesting to note that EPSC amplitude returned almost to baseline upon washout of DHPG, indicating that robust group I mGluR-dependent LTD did not occur. DHPG-induced LTD was apparent in 3 of the 5 cells recorded. However, this did not reach significance once the data were averaged. Since the objective of this series of experiments was not to investigate long-term synaptic plasticity, the duration of

recordings was limited to 50 minutes. This included a 20 min washout period. A longer washout, e.g. 60 or 120 min, would be required in order to quantify any long-term plastic effects induced by group I mGluR activation. EPSC amplitude did not reach a steady state, and was still returning towards baseline at the end of the 20 min washout period (Fig 5.1A). Nonetheless, it appeared that no significant long-term depression of EPSCs occurred following the initial acute depression when averaged across all 5 cells recorded. This finding is in contrast to a number of previous studies in CA1 pyramidal cells (e.g. Palmer et al., 1997; Overstreet et al., 1997; Fitzjohn et al., 2001; Faas et al., 2002; Huang and Hsu, 2005; reviewed in General Introduction, Section 1.4.5.3), which reported a large acute depression followed by a modest but significant prolonged depression of EPSCs, which persisted for > 60 min following washout of DHPG. It should be noted that in the present study, DHPG-induced LTD was apparent in 3 of the 5 cells recorded, and in any case only a limited number of data points were available for analysis of LTD. A greater number of longer-duration recordings from CA1 pyramidal cells would be necessary in order to draw definitive conclusions regarding this issue.

5.3.2 DHPG depresses monosynaptic EPSCs in CA1 stratum radiatum interneurons

The next series of experiments aimed to determine the effect of group I mGluR activation by DHPG in CA1 interneurons. DHPG (30 μM) evoked a depression of excitatory transmission in stratum radiatum interneurons to 56 ± 6% of baseline ($p << 0.0001$, paired t test, $n = 20$; Fig. 5.1B). No significant change in I_{hold} was detected. An important finding is that DHPG-induced depression in interneurons was significantly smaller than that observed in pyramidal cells ($p < 0.01$, unpaired t test). As discussed previously, hippocampal interneurons are a highly heterogeneous population, even within a restricted area such as the stratum radiatum layer of the CA1 subfield (Freund and Buzsaki, 1996; Parra et al., 1998; McBain and Fisahn, 2001; Freund, 2003). A large sample population of 20 interneurons was investigated, in order to provide an accurate overall representation of the effects of group I mGluR activation.

Scatter of results was much greater among interneurons than pyramidal cells, even with a much larger sample population of interneurons. The standard deviation (SD) of the maximal effect of DHPG application upon EPSC amplitude was ± 10% (n = 6) among pyramidal cells, and ± 25% (n = 20) among interneurons (Fig 5.1C). DHPG-evoked depression exhibited marked heterogeneity among interneurons, ranging between 0% and 92% depression relative to baseline (Figs 5.1C & 5.2). 25% of neurons (5 of 20 cells) were entirely unresponsive to group I mGluR activation via DHPG. EPSC amplitude following DHPG application was not significantly different from baseline in these cells. All interneurons were grouped together, including cells unresponsive to DHPG application. DHPG-evoked depression in interneurons was reversible - EPSC amplitude was not significantly different from baseline 20 minutes after washout. This observation indicates that group I mGluR-dependent LTD does not occur in the majority of CA1 stratum radiatum interneurons. However, it should be noted that in a small proportion of cells (10%, 2 of 20 cells), DHPG evoked a significant persistent depression which did not return to baseline upon washout. The magnitude of depression was not significantly different 20 minutes after washout. This is noticeably distinct from previously-reported mGluR-LTD in CA1 pyramidal cells, in which there was some return of EPSC amplitude towards baseline followed by a smaller persistent depression (e.g. Palmer et al., 1997; Fitzjohn et al., 2001).

The findings of the present study demonstrate that, in contrast to previous reports in pyramidal cells, group I mGluR activation via DHPG failed to induce LTD in the majority (90%) of CA1 stratum radiatum interneurons tested. Of the cells that did exhibit a persistent depression, there was no return at all of EPSC amplitude to baseline upon washout of DHPG. Without further experimentation, it is impossible to ascertain whether this due to underlying physiological mechanisms operating in certain subtypes of CA1 interneuron, or experimental issues, e.g. slower washout of DHPG due to recordings being made from cells deeper within the hippocampal slice.

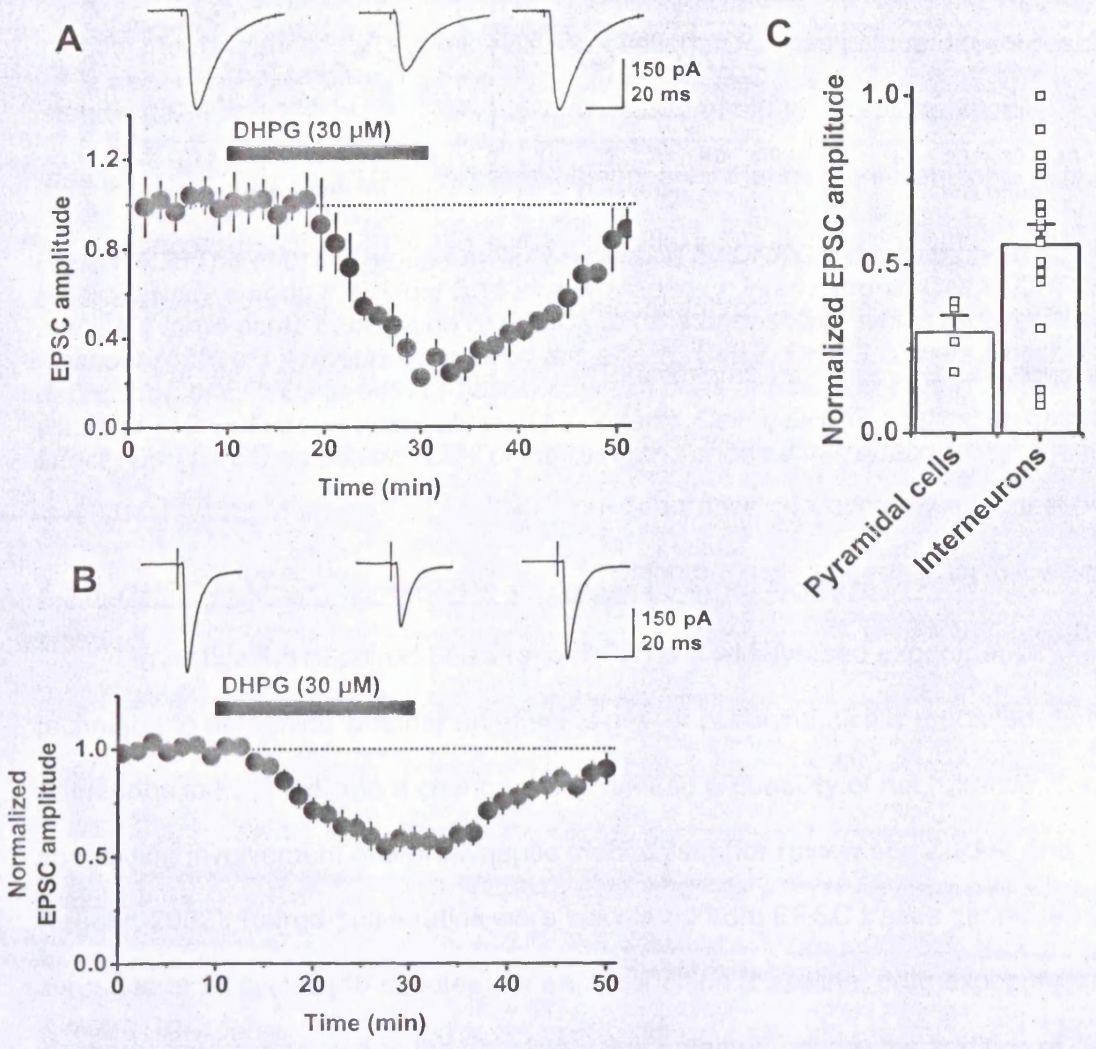

Figure 5.1 *The selective group I metabotropic glutamate receptor agonist DHPG depresses monosynaptic EPSCs in both CA1 pyramidal cells and CA1 stratum radiatum interneurons.* ***A,*** *EPSC amplitude (mean ± SEM) normalized to average baseline amplitude prior to addition of DHPG in CA1 pyramidal cells (n = 5). Representative sample traces from a single neuron before, during and after DHPG application (averages of 20 cycles) are shown above.* ***B,*** *Effect of DHPG on EPSCs recorded in stratum radiatum interneurons (n = 20). Single EPSCs were elicited every 30 sec. Data were binned such that each point represents a 90 sec interval, or the average of three data points.* ***C,*** *Summary of magnitude of DHPG-induced depression in CA1 pyramidal cells and interneurons. Group I mGluR-mediated depression was significantly greater in pyramidal cells than in interneurons. Open squares show values for individual cells, demonstrating that scatter of results was considerably greater among interneurons than pyramidal cells.*

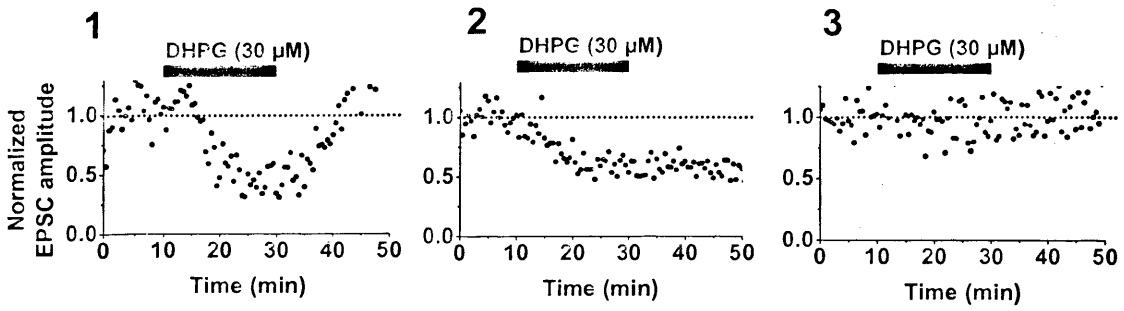

Figure 5.2 *The effect of group I mGluR activation by DHPG exhibits marked heterogeneity among individual CA1 stratum radiatum interneurons. Cell 1, DHPG causes a large acute depression of EPSCs to 36% of baseline, which recovers upon washout (65% of interneurons showed this effect). Cell 2, DHPG causes a persistent depression of EPSCs to 54% of baseline, which does not recover during 20 min washout (10% of interneurons showed this effect). Cell 3, DHPG application has no effect upon EPSC amplitude (25% of interneurons showed this effect).*

5.3.3 DHPG-induced depression is accompanied by an increase in PPR

Investigation of paired-pulse ratio (PPR) is a widely-used experimental technique to determine whether an effect is pre- or postsynaptically mediated. Alterations in PPR indicate a change in the release probability of neurotransmitter, suggesting involvement of a presynaptic mechanism (for review see Zucker and Regehr, 2002). Paired-pulse ratios were calculated from EPSC traces generated from averages of 20 cycles (10 minutes) for each condition (baseline, drug exposure, washout), and normalized to the baseline value obtained prior to the addition of DHPG. A reversible increase in paired-pulse ratio accompanied DHPG-evoked depression in both pyramidal cells and interneurons (Fig 5.3), implying a presynaptic mechanism of expression. In pyramidal cells, PPR increased to 138 ± 13% of baseline (paired t test, $p < 0.001$, $n = 5$) upon DHPG application, returning to 120 ± 7% of baseline upon washout. In interneurons, PPR increased to 135 ± 8% of baseline ($p < 0.001$, $n = 20$), returning to 108 ± 6% of baseline upon washout. In all analyses of paired-pulse ratios, statistical tests were performed on raw, as opposed to normalised, values.

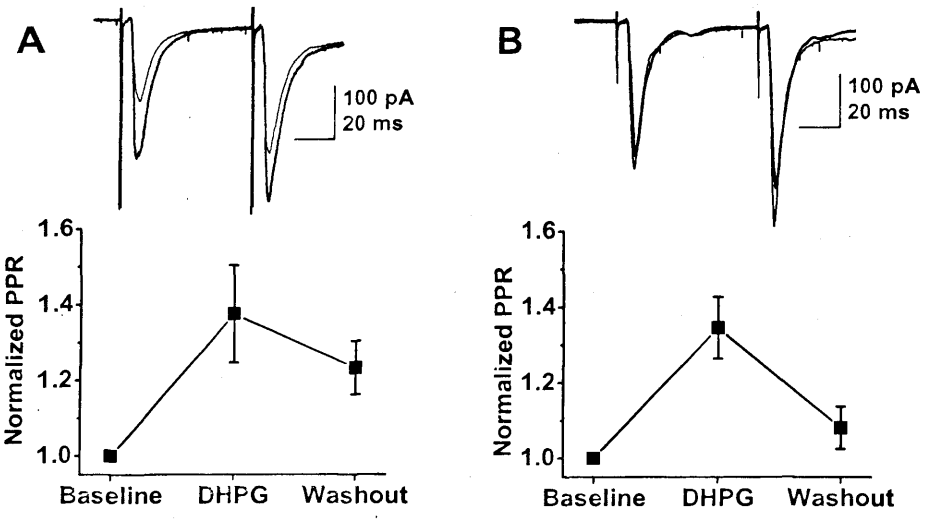

Figure 5.3 *DHPG-induced depression was accompanied by a reversible increase in paired pulse ratio in both pyramidal cells (**A**) and interneurons (**B**), implying a presynaptic action (mean PPR normalised to baseline). Representative sample traces from single neurons are shown above (average of 20 cycles for each condition. Thick lines: control and washout superimposed; thin lines: DHPG).*

5.3.4 The mGluR5 agonist CHPG does not significantly depress EPSCs in interneurons

An important experimental procedure before investigating the phenomenon further was to confirm that DHPG-induced depression was mediated exclusively by group I mGluRs. A number of alternative agonists were therefore tested. It was essential that any agonist used was exclusively selective for group I receptors, to avoid possible contamination of the response by other mGluRs. There are currently very few alternative agonists to DHPG which fit this role. CHPG is a potent mGluR agonist which is highly selective for the mGluR5 subtype (Doherty et al., 1997). No selective agonist is currently available for the mGluR1 subtype. However, activation of mGluR5 would confirm that DHPG-induced depression was group I mGluR-mediated, and may also reveal information regarding the subtypes involved. Alternatively, failure of CHPG to depress EPSC amplitude would suggest either that the phenomenon was mediated exclusively by the mGluR1 subtype; or that DHPG application induced depression by some mechanism other than selective group I mGluR activation. The required concentration of CHPG reported to achieve group I mGluR activation in

hippocampal slices is considerably higher than that of DHPG. Previous studies have indicated concentrations of CHPG of 500 μM (Nakamura et al., 2000) or 1 mM (Palmer et al., 1997; Doherty et al., 1997) are required to achieve maximal mGluR5 activation in hippocampal slices, as compared to the much lower concentration of 30 μM DHPG widely used to achieve maximal group I mGluR activation. Difficulties were encountered in preparing CHPG at such high concentrations. Even when prepared at a lower concentration of 100 mM, the drug did not dissolve readily in equimolar NaOH, the solvent recommended by the manufacturer (Tocris Cookson, UK). CHPG was subjected to prolonged stirring for one hour at high speed with a magnetic stir bar. The solution was then placed in a water bath in a sonicator for 10 minutes. CHPG appeared to be fully dissolved in the resultant dark brown solution. However, concerns were raised due to the high concentration of CHPG required and the difficulties encountered in preparing a solution of the drug.

CHPG (500 μM) was bath applied for 20 min, followed by 20 min washout. CHPG reduced EPSC amplitude to 91 ± 4 % of baseline. This effect was not significant (paired t test, $p = 0.60$, $n = 7$, Fig 5.4A_1). There was virtually no change in PPR, with CHPG application resulting in PPR of 103 ± 2% of baseline (paired t test, $p = 0.71$, $n = 7$, Fig 5.4A_2). In 5 of 7 cells (71% of cells), CHPG application did not significantly affect EPSC amplitude. However, CHPG depressed EPSCs in 2 of 7 cells, to 74% and 85% of baseline. This depression was not significant when the average was taken from the entire sample population of 7 cells. In a further 4 cells not included in the analysis, CHPG application clearly coincided with a large jump in I_{hold}, resulting in loss of the recording. The jump in I_{hold} occurred between 3 and 6 minutes following CHPG application. These cells were entirely stable prior to CHPG application.

In order to eliminate the possibility that CHPG failed to cause depression in 5 of 7 interneurons because these cells were entirely unresponsive to mGluR5 activation, experiments were carried out in which two agonists were applied to the same cell. Following a 10 min baseline, CHPG (500 μM) was applied for 20 min, then

DHPG (30 μM) for 20 min. With the inclusion of a 30 min washout period, this gave a total recording time of 80 minutes. Long duration whole-cell patch clamp recordings such as these present a difficult challenge, due to the increased probability of the integrity of the voltage-clamp being lost. Cells were rejected if I_{hold} or R_S varied by > 20% over the course of the experiment, since changes in these parameters could affect voltage-clamp recording of EPSCs. The probability of a cell being rejected as the result of these factors increased markedly beyond 45 min, and maintaining recordings longer than 60 min proved particularly challenging. Fig 5.4B shows two cells in which two distinct group I mGluR agonists were applied to the same CA1 interneuron. In both cells, 20 min application of CHPG had no effect upon EPSC amplitude or PPR, whereas subsequent 20 min exposure to DHPG caused significant depression. In cell 1, DHPG depressed EPSCs to 64% of baseline. This was a persistent depression which did not begin to return to baseline during a 30 min washout of DHPG, and was accompanied by an increase in PPR to 132%, decreasing to 122% upon washout. In cell 2, DHPG depressed EPSCs to 62% of baseline. This was an acute depression which returned fully to baseline during washout, and was accompanied by an increase in PPR to 141%, returning to 112% upon washout. These experiments clearly demonstrate that activation of group I mGluRs by DHPG causes significant depression of EPSCs even when CHPG application had no effect. This eliminates the possibility that CHPG failed to evoke depression in 5 of 7 cells (Fig 5.4A_1) because those interneurons were entirely insensitive to group I mGluR activation. Instead, these findings point towards a failure of CHPG to effectively activate mGluR5 at 500 μM concentration with 20 min exposure to the drug. An alternative explanation is that only 2 of the 7 interneurons expressed the mGluR5 subtype. It has previously been shown that, while most CA1 interneurons express both group I mGluR subtypes, some interneurons exclusively mGluR1 or mGluR5 (van Hooft et al., 2000).

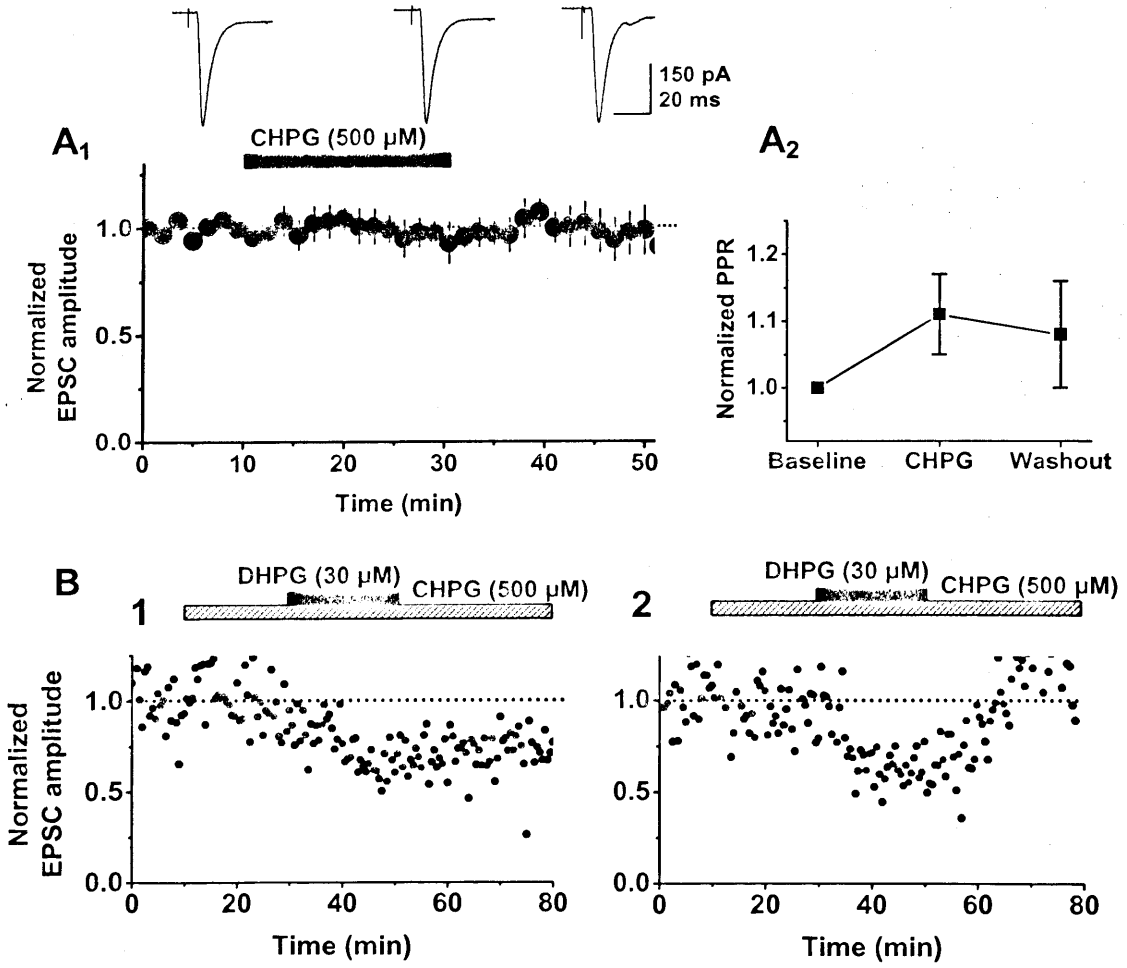

Figure 5.4 *The selective group I mGluR agonist DHPG causes acute synaptic depression, whereas the mGluR5 subtype-selective agonist CHPG does not.* ***A_1,*** *CHPG does not cause significant depression of EPSCs (mean ± SEM). Representative sample traces from a single interneuron before, during and after DHPG application (averages of 20 cycles) are shown above.* ***A_2,*** *CHPG does not significantly affect PPR.* ***C,*** *Whole-cell voltage clamp recordings from two individual CA1 interneurons, which were subjected to 20 min exposures to CHPG (500 µM) and subsequently DHPG (30 µM). Cell 1 – CHPG has no effect upon EPSC amplitude, whereas DHPG causes a depression which does not recover upon washout. Cell 2 – CHPG has no effect upon EPSC amplitude, while DHPG causes an acute depression which returns fully upon washout.*

5.3.5 The broad spectrum mGluR agonist ACPD causes acute depression in interneurons

DHPG is a potent and highly selective agonist of group I mGluRs (Schoepp et al., 1994; Pin and Duvoisin, 1995; Schoepp et al., 1999). The two group I mGluR subtypes mGluR1 and mGluR5 can be selectively blocked using the antagonists LY367385 and MPEP respectively (Schoepp et al., 1999). However, at the present time, only the mGluR5 subtype can be selectively activated, by the agonist CHPG. Experiments carried out in this thesis (see Section 5.3.4) indicated problems using this drug in hippocampal slices. In order to confirm that the DHPG-induced depression observed in previous experiments was mediated exclusively by mGluRs, and to further investigate the pharmacological profile of the effect, the broad-spectrum mGluR agonist 1*S*, 3*R*-ACPD was used. 1*S*, 3*R*-ACPD is relatively non-selective, acting on both group I mGluR subtypes (mGluR 1 and 5), both group II subtypes (mGluR 2 and 3) and most group III subtypes (mGluR 4, 6 and 8). However, ACPD is active at much lower concentrations at the group I mGluRs. Furthermore, it does not affect the widely-expressed presynaptic group III receptor mGluR7 even at high concentrations (Schoepp et al., 1999).

1*S*, 3*R*-ACPD (50 μM) was applied for 20 min. EPSCs recorded in interneurons were decreased to 58 ± 14% of baseline (paired t test, $p < 0.001$, $n = 5$, Fig 5.5A), returning close to baseline upon washout. This depression was accompanied by a reversible increase in PPR to 138 ± 10 % of baseline (paired t test, $p < 0.001$, $n = 5$, Fig 5.5B), returning to 116 ± 6% of baseline upon washout. The magnitude of ACPD-induced depression was not significantly different from the magnitude of DHPG-induced depression (paired t test, $p = 0.58$). 25% of neurons (1 of 5 cells) were entirely unresponsive to mGluR activation by ACPD, with the remaining 4 cells exhibiting significant depression. This is similar to the proportion of neurons which were unresponsive to group I mGluR activation via DHPG application (25%, 5 of 20 cells).

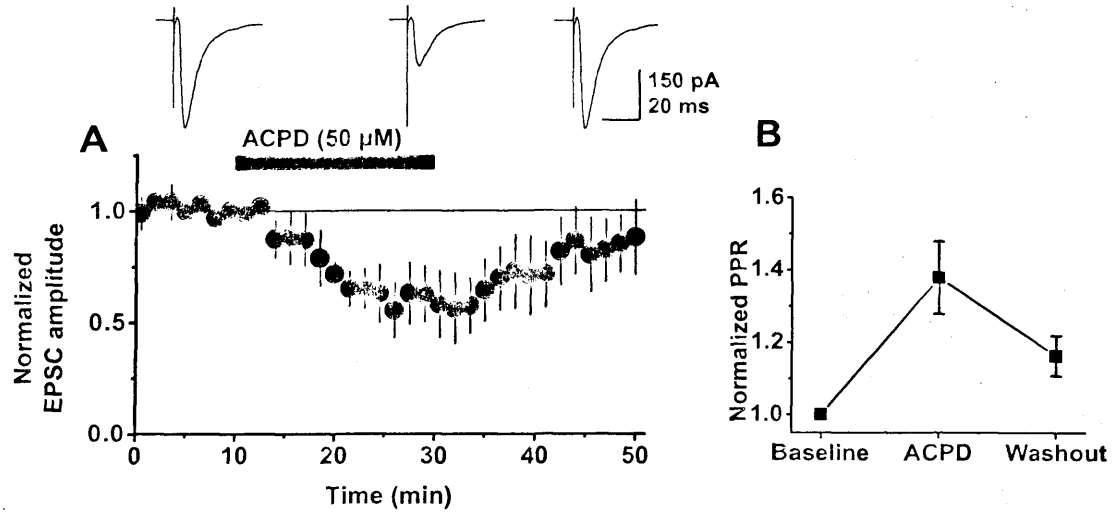

Figure 5.5 *The broad-spectrum metabotropic glutamate receptor agonist 1S, 3R-ACPD (50 µM) depresses monosynaptic EPSCs at glutamatergic Schaffer collateral inputs onto CA1 interneurons* ***A****. EPSC amplitude (mean ± SEM) normalised to average baseline amplitude (n = 5). Representative sample traces from single neurons are shown above, indicating EPSCs before, during and after ACPD application (averages of 20 cycles).* ***B****. ACPD-induced depression was accompanied by a reversible increase in PPR, suggesting that the mechanism involves a presynaptic action (mean PPR normalised by baseline amplitude, n = 5).*

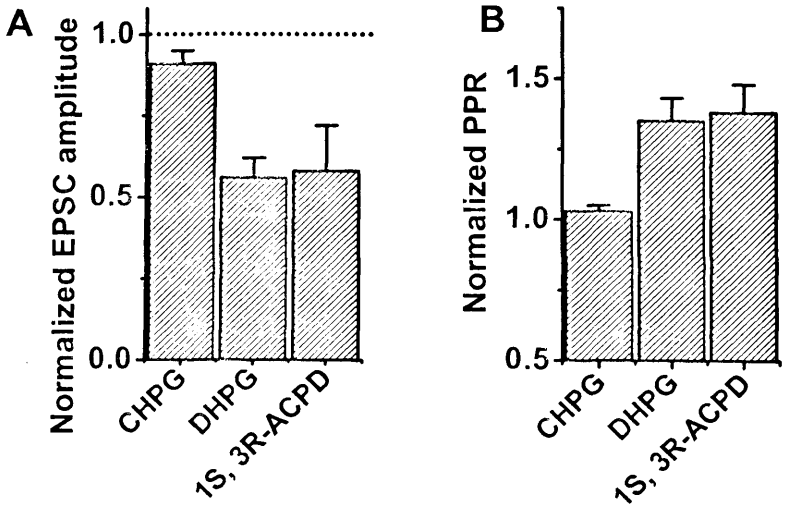

Figure 5.6 *Summary of effects of metabotropic glutamate receptor agonists on glutamatergic synaptic transmission from Schaffer collaterals to CA1 stratum radiatum interneurons. CHPG (500 µM) is a subtype-selective mGluR5 agonist; DHPG (30 µM) is a group I mGluR-selective agonist; 1S, 3R-ACPD (50 µM) is a broad spectrum mGluR agonist.* ***A,*** *Effect upon EPSC amplitude (normalized EPSC amplitude ± SEM).* ***B,*** *Effect upon PPR.*

5.3.6 mGluR1 and mGluR5 subtypes contribute differentially to short and long-term effects of DHPG

It is important to identify which group I mGluR subtypes are involved in mediating depression of excitatory synaptic transmission to CA1 interneurons, and determine whether different subtypes have distinct roles in the underlying mechanism. Although a variety of pharmacological tools are available to distinguish between groups of mGluRs, distinguishing between individual members within a group is much more problematic. Recent research has lead to increased availability of highly selective agonists and antagonists which act upon specific mGluR subtypes. At present a selective agonist is available for only one group I mGluR, the mGluR5-selective drug CHPG (Doherty et al., 1997). Experiments described in this chapter revealed technical difficulties when using CHPG in hippocampal slices due to the high concentrations necessary to achieve maximal mGlR5 activation (see Section 5.3.4). Antagonists are available which act with a high degree of specificity at individual group I mGluR subtypes. The highly mGluR1-selective nature of the 4-carboxyphenylgycine (4CPG) analogue LY367385 was first definitively reported by Clark et al. (1997). 2-methyl-6-(phenylethynyl)-pyridine (MPEP) was first described as strongly mGluR5-selective by Gasparini et al. (1999). By blocking one or other group I mGluR subtype using a selective antagonist, then activating the remaining subtype using DHPG, it is possible to investigate the contribution of individual subtypes to the phenomenon of DHPG-induced depression. The mGluR1-specific antagonist LY367385 has previously been shown to completely block the DHPG-evoked acute depression of EPSCs in CA1 pyramidal cells, indicating that there is no contribution to this short-term effect from mGluR5 in this cell type (Mannaioni et al., 2001). However, there are numerous differences in functional properties and modulatory mechanisms between excitatory connections onto pyramidal cells and interneurons. One important way in which this may be manifested is in differential expression of distinct mGluR subtypes at distinct classes of synapse, and the involvement of these receptors in modulatory effects.

The objective of the experiments described in this section was to determine which group I mGluR subtypes mediate DHPG-induced acute depression of EPSCs in CA1 stratum radiatum interneurons. Furthermore, by selectively blocking group I mGluR subtypes, it is possible to investigate effects mediated by persistent activation of these receptors. Previous research has shown that blockade of mGluRs leads to an enhancement of excitatory synaptic transmission to specific subsets of hippocampal interneurons, suggesting that glutamate release is subject to tonic inhibition by these receptors under normal physiological conditions (Losonczy et al., 2003). However, these experiments were not carried out in CA1 stratum radiatum interneurons, and the mGluR subtypes involved were not comprehensively investigated using a range of subtype-selective drugs. A further aim of the experiments described in this section was thus to investigate whether glutamate release at connections onto CA1 stratum radiatum interneurons is subject to modulation by persistently active group I mGluR subtypes.

Experiments were carried out to test the effect of pre-applying either the mGluR1-selective antagonist LY367385 (100 μM) or the mGluR5-selective antagonist MPEP (10 μM) on the acute effect of DHPG in interneurons. Neither drug had any significant effect on baseline transmission, arguing against tonic activation of these receptors by ambient glutamate (Fig 5.7 A_1 & B_1). In the continued presence of LY367385, bath application of DHPG (30 μM) depressed EPSCs to 70 ± 5% of baseline (paired t test, $p < 0.001$, $n = 10$; Fig 5.7A_1). This depression was significantly smaller than that observed in the absence of group I mGluR antagonists (unpaired t test, $p < 0.01$). Interestingly, the EPSC amplitude did not return to baseline upon DHPG washout. This persistent depression was highly consistent across all cells, as evidenced by the small standard deviation (± 15%) during the final 10 minutes of washout. None of the 10 cells showed any return of EPSCs towards baseline during 20 min washout. The depression was accompanied by a small but significant increase in PPR to 110 ± 4% of baseline (paired t test, $p < 0.05$, $n = 10$; Fig 5.7A_2), returning to 106 ± 3% upon washout. It is notable that there is considerably less variability in the

effect of DHPG in this subset of interneurons (standard deviation ± 15%, n = 10; Fig 5.7A_1) than in those in which DHPG was applied in the absence of any mGluR antagonists (standard deviation ± 25%, n = 20; Fig 5.1B), despite the smaller population size. In the continued presence of the mGluR5 blocker MPEP, DHPG again depressed EPSCs to 76 ± 8% of baseline ($p < 0.05$, n = 7; Fig. 5.7B_1). This depression was also smaller than that seen without group I mGluR blockers ($p < 0.01$). However, in this case the depression was fully reversible. It was accompanied by a non-significant increase in PPR to 106 ± 6% ($p = 0.37$), decreasing to 103 ± 3% upon washout (Fig 5.7B_2). The magnitude of DHPG-induced depression was not significantly different in the presence of LY367385 and MPEP (unpaired t test, $p < 0.001$), suggesting an approximately equal contribution of mGluR1 and mGluR5 to the depression. These results are summarised in Figure 5.8.

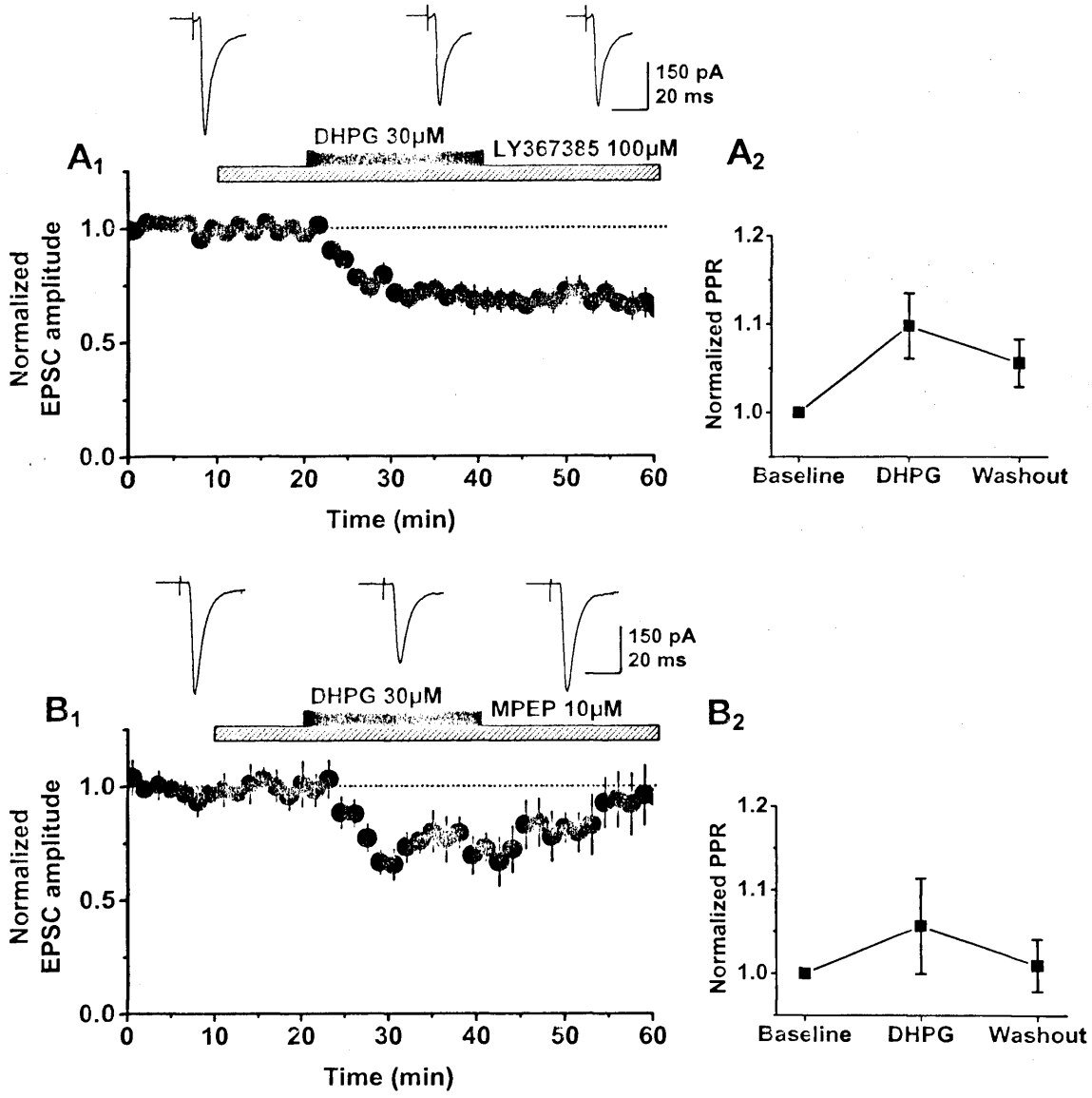

Figure 5.7 *mGluR1 and mGluR5 subtypes contribute differentially to short and long-term effects of DHPG.* ***A_1,*** *EPSC amplitude (± SEM) normalized to baseline, showing the effect of DHPG applied following a 10 min exposure to the selective mGluR1 antagonist LY367385 (n= 10).* ***B_1,*** *DHPG effect in the presence of the selective mGluR5 antagonist MPEP (n = 7). Representative sample traces from single neurons are shown above (averages of 20 cycles). DHPG caused a small but significant elevation in PPR presence of LY367385 (**A_2**), but had no effect upon PPR in the presence of MPEP (**B_2**).*

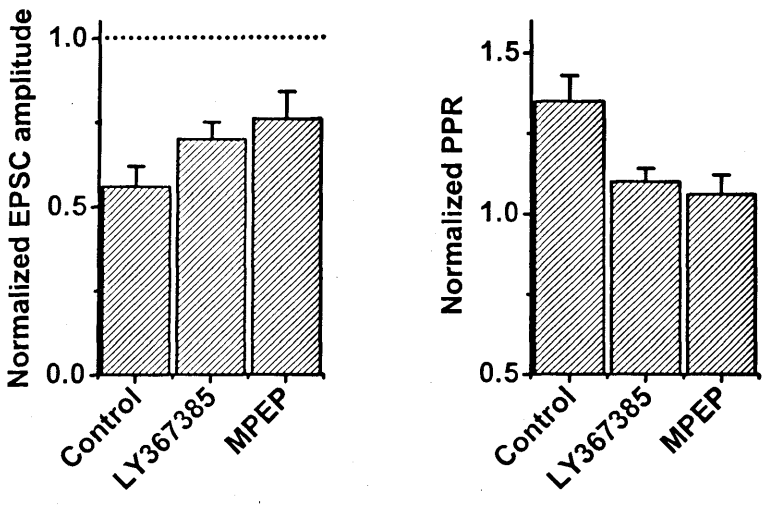

Figure 5.8 *Summary of effects of subtype-selective group I mGluR antagonists upon EPSC amplitude and PPR. The mGluR1-selective LY367385 and mGluR5-selective MPEP reduce the magnitude both of DHPG-induced depression of EPSCs and DHPG-induced increases in PPR. However, significant DHPG-induced depression occurs in the presence of either antagonist, indicating that both mGluR1 and mGluR5 subtypes are involved. Control, DHPG only.*

5.4 Discussion

The experiments described in this chapter have uncovered a number of novel findings regarding modulation of excitatory synaptic transmission to hippocampal interneurons by metabotropic glutamate receptors. Patch clamp electrophysiological recording in whole-cell voltage-clamp configuration was used to demonstrate that glutamatergic Schaffer collateral synapses onto CA1 stratum radiatum interneurons were robustly depressed by activation of group I mGluRs by the selective agonist (*S*)-3,5-DHPG. This agonist was also found to depress excitatory synaptic transmission at Schaffer collateral connections onto CA1 pyramidal cells, accompanied by significant elevations in PPR. This is in agreement with previously reported findings (Gereau and Conn, 1995; Manzoni and Bockaert, 1995; Rodriguez-Moreno et al., 1998; Mannaioni et al., 2001). A significant DHPG-induced LTD was not observed in CA1 pyramidal cells. This finding is puzzling, since it contrasts with numerous previous studies (e.g. Palmer et al., 1997; Overstreet et al., 1997; Fitzjohn et al., 2001; Faas et al., 2002; Huang and Hsu, 2005; reviewed in General Introduction, Section 1.4.5.3). DHPG-

induced LTD was apparent in 3 of the 5 cells recorded. However, this did not reach significance once the data were averaged. No clear explanation can be provided at present for the lack of LTD in the remaining 2 pyramidal cells. It should be noted that only a limited number of data points were available for analysis of LTD. The washout period was limited to 20 min, as investigation of long-term synaptic plasticity was not the goal of this series of experiments. A clearer picture would emerge if recordings of longer duration (minimum washout period 60 min) were made from a greater number of CA1 pyramidal cells. In this case, it is entirely possible that a significant LTD would be observed. It is difficult to speculate further on this issue without additional experimentation and more data.

The present study demonstrates that glutamatergic connections onto both CA1 pyramidal cells and CA1 stratum radiatum interneurons are subject to powerful inhibitory modulation by group I mGluRs. There are important differences in the effect between the two cell types. Firstly, the magnitude of DHPG-induced depression was significantly greater in pyramidal cells than in interneurons. This may have implications for the role of group I mGluR-mediated acute depression in network function within the hippocampus. For example, an elevation in ambient glutamate concentration during periods of high excitatory traffic may cause a large depression at connections onto pyramidal cells, reducing transmission from CA3 to CA1. The overall effect at excitatory connections onto interneurons would be smaller, ensuring that the recruitment of inhibitory drive was less pronounced. It is difficult to speculate in detail on the physiological role of this effect without further experimentation. Secondly, there was extensive heterogeneity in the response of CA1 stratum radiatum interneurons to DHPG, CHPG and ACPD, whereas the response of CA1 pyramidal cells to DHPG exhibited much less variation. It was necessary to use a large sample population of 20 interneurons to achieve the same SEM as a sample population of five pyramidal cells. Some interneurons exhibited an almost total attenuation of AMPA/kainate EPSCs (maximum depression 92%), whereas others were entirely unresponsive to DHPG. The extensive heterogeneity of the hippocampal interneuron population is well

documented (Freund and Buzsaki, 1996; Parra et al., 1998; McBain and Fisahn, 2001; Freund, 2003; Somogyi and Klausberger, 2005). Parra et al. (1998) categorised CA1 interneurons according to morphology, firing properties and response to various neurotransmitter receptor agonists. The study found that 39% of the sample population was responsive to mGluR activation by the broad spectrum agonist ACPD. The present study demonstrated that 75% of interneurons were responsive to group I mGluR activation by the selective agonist DHPG, with extensive variation in the magnitude of the response. A similar proportion (75%) were responsive to ACPD, though it should be noted that different measures of response were used between the two studies (changes in holding current in the study of Parra et al. (1998) versus alterations in synaptic transmission in the present study). Distinct subtypes of inhibitory interneuron may mediate specific computational functions within the hippocampus and other cortical networks (Buhl et al., 1994; Cobb et al., 1995; Freund and Buzsaki, 1996; Miles et al., 1996; Freund, 2003; Klausberger et al., 2003; 2005). The variation in response to DHPG among stratum radiatum interneurons may correlate with other factors such as patterns of axonal and dendritic projection, firing properties and expression of modulatory neurotransmitter receptors. The properties of group I mGluR-mediated acute depression in individual GABAergic interneurons may relate to the specific inhibitory role of the cell in the hippocampal network. One method by which this possibility could be investigated experimentally is by combining patch clamp electrophysiology with immunohistochemistry to facilitate morphological and neurochemical analysis of individual interneurons.

While DHPG is highly selective for group I mGluRs, 1*S*, 3*R*-ACPD is a broad-spectrum agonist which activates all known mGluRs except the group III receptor mGluR7 (Schoepp et al., 1999). A very similar magnitude of depression was induced by both DHPG (56 ± 6%, n = 20; Fig 5.1B) and ACPD (58 ± 14%, n = 5; Fig 5.5A). Provided that the agonists maximally activate their target receptors at the concentrations used in these experiments, these findings suggest that only group I mGluRs are involved in mediating the acute depression, with mGluR7 also causing

depression at this class of synapse (see below). Activation of non-group I mGluRs affected by ACPD (mGluR 2, 3, 4, 6 and 8) would be expected to produce a change in the magnitude of depression induced by DHPG if these receptors were involved in modulating acute depression at glutamatergic Schaffer collateral synapses onto CA1 stratum radiatum interneurons. The depression may be enhanced by additional contribution from non-group I mGluRs, or reduced in magnitude if those receptors potentiated transmission. However, the finding that the magnitude of depression remained essentially the same as that induced by DHPG implies that the non-group I mGluR receptors activated by ACPD are not directly involved in this phenomenon. Another possibility is that maximal activation of one or more mGluR subtypes was not achieved by either DHPG or ACPD. Finally, other mGluRs activated by ACPD may be involved, but may induce depression through the same mechanism as group I mGluRs. The concentrations of agonists were chosen based upon previous work in hippocampal slices which demonstrated maximal activation of receptors. The only mGluR subtype unaffected by ACPD is mGluR7. High-resolution immunohistochemical studies have demonstrated that mGluR7 is expressed presynaptically at glutamatergic and GABAergic synapses onto hippocampal interneurons but not pyramidal cells (Shigemoto et al., 1996; 1997; Kogo et al., 2004). Group III mGluRs, including predominantly mGluR7, have been shown to powerfully modulate transmission at both excitatory and inhibitory connections onto hippocampal interneurons. The selective group III mGluR agonist L-AP4 induces depression of both glutamatergic (Scanziani et al., 1998; Semyanov and Kullmann, 2000) and GABAergic (Semyanov and Kullmann, 2000; Kogo et al., 2004) inputs to CA1 interneurons but not pyramidal cells in a target-dependent manner. It is therefore possible that activation of group III mGluRs using the selective agonist L-AP4 may increase the magnitude of DHPG-induced depression.

The group I mGluR agonist CHPG is highly selective for mGluR5, having no effect at the mGluR1 subtype (Doherty et al., 1997). CHPG did not significantly depress EPSCs in CA1 stratum radiatum interneurons, causing a small depression in

only 2 of 7 cells. There are a number of possible explanations for this finding. Firstly, the depression induced by DHPG may not have been mediated by group I mGluRs. This is extremely unlikely, given the wealth of previous data on the potent and highly selective nature of this agonist, together with the finding that a similar depression was induced by ACPD. Alternatively, these findings may be explained by the fact that, while most CA1 interneurons express both group I mGluRs, certain types of interneuron express only the mGluR1 or the mGluR5 subtype (van Hooft et al., 2000). mGluR5 expression by only 2 of the 7 cells would account for the smaller overall depression of EPSCs observed when the mGluR5-selective agonist CHPG was used, as compared to DHPG which activates both mGluR subtypes. The remaining 5 cells may have exclusively expressed only the mGluR1 subtype, which is unaffected by CHPG. This is a plausible explanation, since expression of mGluRs is highly specific at distinct classes of hippocampal synapse. It is possible that DHPG-induced depression may be mediated by both group I mGluR subtypes or exclusively by one single subtype in distinct classes of stratum radiatum interneuron (van Hooft et al., 2000). It is important to note that technical issues within the experiment may have resulted in a failure of CHPG to reach its target receptors at a sufficient concentration to achieve maximal activation. Previous studies in brain slice preparations used CHPG at a concentration of 500 μM (Nakamura et al., 2000; White et al., 2003) or 1 mM (Palmer et al., 1997; Doherty et al., 1997) to achieve maximal activation of mGluR5. A concentration of 500 μM was used in the present study. It is possible that a higher concentration of CHPG of 1 mM was required to maximally activate mGluR5 in the hippocampal slice preparation used in this study. CHPG was used at a high concentration, and difficulties were encountered dissolving the drug when preparing aliquots. When bath applying drugs to the slice, aliquots of most of the drugs used were generally diluted 1:1000 in ACSF. Preparing CHPG aliquots at 500 mM proved impossible, as the drug did not readily dissolve in equimolar NaOH (the solvent recommended by the manufacturer, Tocris Cookson, UK). Even when aliquots were prepared at 100 mM for 1:200 dilution, CHPG required prolonged stirring and

sonication to dissolve. The drug appeared to be fully dissolved, but concerns were raised due to the thick, brown appearance of the resulting solution. It is possible that a considerable proportion of the CHPG was not fully dissolved, and thus did not penetrate through the tissue of the hippocampal slice and access the target receptors. Additionally, a longer exposure time may have been required for the drug to fully reach its target receptors. With a higher concentration of CHPG and a longer exposure time, it is possible that depression of EPSCs may have been of greater magnitude in interneurons expressing mGluR5, and that a greater proportion of CHPG-responsive interneurons may have been revealed. However, given the experimental difficulties involved in using CHPG at such high concentrations, it was not possible to perform these experiments in the time available. Investigating the effects of 1 mM CHPG on a sample population of five or more interneurons would be worthwhile in future studies. One conclusion which may be drawn from these experiments is that CHPG is a problematic drug to work with in brain slice preparations. It may be better suited to cell culture systems, where lower concentrations may be used and issues of perfusion and penetration through tissue to reach target receptors present less of a technical challenge. It was not necessary to carry out further experiments involving CHPG, since DHPG-induced depression was confirmed to be mediated by mGluRs by ACPD application and the other experiments described in this thesis.

A number of interesting discoveries were made when investigating the contribution of individual group I mGluR subtypes to DHPG-induced depression in interneurons. When mGluR1 was blocked using LY367385, the magnitude of depression of EPSCs by DHPG was remarkably consistent across all cells, with an overall range from 58 to 80 % of baseline (n = 10, Fig 5.7A_1). However, in 8 of the 10 cells the depression was highly consistent, ranging from 63% to 75%. This would suggest that mGluR5 was universally expressed in all of the interneurons studied, and the magnitude of depression of EPSCs caused by mGluR5 activation was highly consistent. As discussed above, although more sophisticated classification of

interneurons was necessary, it is probable that more than one, and possibly several, interneuron subtypes were included in the 10 cells recorded. mGluR5 thus appears to play an important role in modulating excitatory transmission to multiple subtypes of CA1 interneurons, being universally expressed in the sample population tested, and exerting a highly consistent effect upon depression of EPSCs.

The role of mGluR1 in modulating excitatory synaptic transmission appears to vary more widely than that of mGluR5 across the interneuron population tested in this study. The magnitude of depression of EPSCs by DHPG when mGluR5 was selectively blocked by MPEP, leaving only mGluR1 intact, ranged from 0% to 66% of baseline (n = 7). Thus one interneuron was entirely unaffected by selective mGluR1 activation. In 4 of the 7 cells, however, the effect of DHPG was consistent, with depression ranging from 70 to 85% of baseline. As discussed above, it is impossible to correlate these electrophysiological data with identified interneuron subtypes without the use of additional techniques to achieve a detailed classification of the interneurons being studied. Nevertheless, the relative importance of mGluR1 in modulation of excitatory synaptic transmission is clearly subject to greater variability among CA1 stratum radiatum interneurons than that of mGluR5.

The sum of the depression evoked in the presence of each of the blockers of mGluR1 and mGluR5 applied separately was approximately 54%, only slightly more than the depression observed when neither receptor was blocked (44%). It should be noted that conclusions drawn from these experiments should be interpreted with some degree of caution, since it is impossible to be certain that either receptor subtype was fully blocked by the selective antagonists. This issue could be addressed by repeating the experiment and applying DHPG in the simultaneous presence of both LY367385 and MPEP. Under these conditions, no depression of EPSC amplitude in response to DHPG application would be expected. This is an important experiment which was not included in the present study, and should be performed in future investigations.

Intriguingly, a persistent DHPG-evoked depression was uncovered when mGluR1 was blocked. This effect was highly consistent across all 10 cells tested. It

remains unclear why the persistent depression was not observed in the absence of the mGluR1 blocker LY367385. One possibility is that mGluR1 activation has an additional effect that contributes to recovery of transmitter release. Furthermore, in contrast to previously-reported group I mGluR-dependent LTD, there was no return of EPSC amplitude towards baseline upon washout of DHPG. The magnitude of depression remained the same during washout as during the acute phase. This type of persistent depression thus exhibits marked differences with mGluR-LTD reported in pyramidal cells in previous studies (e.g. Palmer et al., 1997; Fitzjohn et al., 2001; Tan et al., 2003). One potential strategy which could be used to further investigate mGluR5-dependent long-term depression in CA1 stratum radiatum interneurons is use of the mGluR agonist CHPG, which is highly selective for the mGluR5 subtype (Doherty et al., 1997). CHPG would activate mGluR5 while leaving mGluR1 unaffected, and could thus be used to confirm the existence of an mGluR5-mediated persistent depression in CA1 interneurons. This type of experimental design is less robust than the use of selective antagonists, since at present no mGluR1-selective agonist is available. Selective activation of both group I mGluR subtypes would be necessary to confirm that the persistent phase of the depression is mediated exclusively by mGluR5. Furthermore, serious technical difficulties were encountered during previous experimental work using CHPG in hippocampal slices, due to the high concentrations necessary to achieve maximal mGluR5 activation (see Chapter 5, Section 5.3.4). Given the extensive ongoing research into developing novel, highly selective pharmacological agents acting at individual metabotropic glutamate receptor subtypes, it is only a matter of time before an mGluR1-selective agonist and a superior mGluR5-selective agonist are discovered. The individual receptor subtypes involved in mediating group I mGluR-dependent LTD could then be investigated in distinct cell types using experimental strategies involving both selective agonists and antagonists. The research could be further improved by including techniques to achieve detailed classification of interneurons, such as immunohistochemical staining

for neurochemical markers, analysis of firing patterns etc., to achieve a more detailed picture of this apparently novel form of persistent depression.

The persistent DHPG-evoked depression revealed with mGluR1 blocked by LY367385 is consistent with selective coupling of mGluR5 to a cascade that leads to group I mGluR-mediated long-term depression, as has been reported in pyramidal cells (Palmer et al., 1997; Huber et al., 2001; Faas et al., 2002; Huang and Hsu, 2005). Taken together, these results are consistent with two relatively independent induction cascades, as has been proposed in pyramidal cells, with mGluR1 coupled to an acute depression and mGluR5 coupled to a more long-lasting depression of transmission. In the present experiments, both phenomena were associated with increases in PPR (though this did not reach significance in the presence of MPEP), implying presynaptic expression. The issue of whether DHPG-induced depression is mediated by pre- or postsynaptic group I mGluRs is addressed in detail the subsequent chapter. It should be noted that the primary objective of the projects described in this thesis was not a detailed characterisation of LTD mediated by metabotropic glutamate receptors. The main aims were to investigate modulation of excitatory synaptic transmission to hippocampal interneurons by group I mGluRs, to characterise in detail the mechanisms by which this occurs, and to explore the physiological significance of the effect. The apparent mGluR5-mediated LTD uncovered in these experiments is an interesting phenomenon and represents an important area of future research. Essential initial experiments would involve long-duration recordings (≥ 120 min) combined with more detailed characterisation of interneurons, according to morphological, neurochemical and physiological criteria. Such long duration recordings are feasible in brain slices when pyramidal cells are being investigated, since a field-potential recording electrode may be positioned around stratum pyramidale and used to record stable EPSPs (excitatory postsynaptic potentials) from localised populations of pyramidal cells for long-durations. Field potential recording from interneurons is not possible, since they are fewer in number and much more sparsely distributed, meaning that clear recordings of population

activity cannot be generated. It is instead necessary to use techniques for recording activity of individual neurons, such as sharp electrode recording or the various configurations of the patch clamp technique (whole-cell, perforated-patch, cell-attached etc.). Such techniques are inherently more challenging than field potential recording. Establishing recordings from individual neurons is more technically demanding. Maintaining long duration recordings, particularly beyond 45-60 minutes, is particularly difficult since the recording must remain fully stable according to strictly-defined predetermined criteria, and changes in experimental parameters (e.g. drifts in I_{hold} and R_S) are more likely to occur when making patch clamp recordings in individual neurons. Of course, it is nonetheless possible to investigate long-term synaptic plasticity by making long-duration recordings from single cells, but experiments have a higher failure rate and thus provide a lower data yield. However, due to the greatly increased resolution, information gained in this way is very valuable and has the potential to provide great insights. Furthermore, the greater flexibility of the patch clamp technique has many other advantages when working with interneurons, including the ability to overcome the problem of extensive heterogeneity of the interneuron population by correlating electrophysiological recording with analysis and classification of the individual cell, using criteria such as morphology, presence of neurochemical markers and analysis of physiological parameters, e.g. firing pattern. Detailed study of long term synaptic plasticity in GABAergic interneurons was not the objective of the projects discussed in this thesis, but this clearly remains an area of ongoing research with the potential to reveal valuable information regarding functional properties of inhibitory neuronal networks.

The findings described in this chapter raise a number of interesting questions. What is the mechanism via which group I mGluR activation causes depression of synaptic transmission? Although a number of previous studies have described DHPG-induced depression of excitatory synaptic transmission to CA1 pyramidal cells (Gereau and Conn, 1995; Manzoni and Bockaert, 1995; Rodriguez-Moreno et al., 1998; Mannaioni et al., 2001), none have attempted to address the issue of the

mechanisms via which the depression is induced and expressed. The consistent increase in PPR which accompanies DHPG-induced depression strongly implies that the mechanism involves a presynaptic action. However, high-resolution immunohistochemical studies have revealed predominantly postsynaptic expression of group I mGluRs (Martin et al., 1992; Baude et al., 1993; Lujan et al., 1996; Shigemoto et al., 1997; Lujan et al., 1997; Lopez-Bendito et al., 2002). It is thus important to uncover the underlying physiological basis of group I mGluR-mediated depression. Which receptors are responsible for mediating group I mGluR depression? Previous work has shown that only the mGluR1 subtype is involved in CA1 pyramidal cells (Mannaioni et al., 2001), but it is important to determine whether different subtypes, and therefore potentially different signalling cascades and other downstream effects, are involved in interneurons. How can the heterogeneity in the response of CA1 interneurons to DHPG be explained? Unlike pyramidal cells, CA1 interneurons exhibit wide variation in the magnitude of group I mGluR-mediated depression. Morphological, physiological and neurochemical analysis of interneurons may reveal correlations between interneuron subtype and response to group I mGluR agonists. What is the physiological importance of group I mGluR-mediated depression of glutamatergic synaptic transmission to CA1 interneurons? This is the most complex question, and the most difficult to address. Further experimentation is necessary to uncover the role of this effect in hippocampal network function. Elucidating the underlying mechanism may provide important clues. Further information may be provided by attempting to activate group I mGluRs by physiologically-released glutamate as opposed to an exogenous agonist. These questions are addressed in the following chapters.

The experiments discussed in the latter part of this chapter (Section 5.3.6) describe the existence of an apparently novel form of mGluR5-mediated persistent depression of excitatory synaptic transmission to CA1 stratum radiatum interneurons. Furthermore, although expression of both mGluR1 and mGluR5 in hippocampal interneurons has previously been shown using RT-PCR (van Hooft et al., 2000; see

Chapter 1, Section 1.2.6), the present study represents the first demonstration that these receptors play an active role in modulation of glutamatergic synaptic transmission from Schaffer collaterals to CA1 interneurons. This finding is in contrast to the mechanism operating at Schaffer collateral connections onto CA1 pyramidal cells, in which only the mGluR1 subtype is involved (Mannaioni et al., 2001), and is thus a further example of different modulatory mechanisms operating at specific types of synaptic connection.

Chapter 6: Pre- versus postsynaptic induction and expression of group I mGluR-mediated depression

6.1 Introduction

Activation of group I mGluRs using the selective agonist DHPG leads to an acute depression of glutamatergic synaptic transmission, which is accompanied by a robust increase in paired pulse ratio (PPR) in both CA1 stratum radiatum interneurons (demonstrated in present study) and CA1 pyramidal cells (Gereau and Conn, 1995; Manzoni and Bockaert, 1995; Rodriguez-Moreno et al., 1998; Mannaioni et al., 2001; also shown in present study). The consistent elevation in PPR suggests that the mechanism of group I mGluR-mediated acute depression involves a presynaptic action. However, high-resolution immunohistochemical studies have reported a predominantly postsynaptic location for group I mGluRs (Martin et al., 1992; Baude et al., 1993; Lujan et al., 1996; Shigemoto et al., 1997; Lujan et al., 1997; Petralia et al., 1997; Lopez-Bendito et al., 2002). It is of central importance in investigating modulation of synaptic transmission by mGluRs to determine the mechanisms via which mGluRs exert their effects. One possible explanation for the apparent presynaptic expression of DHPG-evoked depression is that activation of postsynaptic group I mGluRs results in the release of a factor which acts upon presynaptic receptors. This type of phenomenon is known as retrograde signalling, and is a mechanism via which information can be relayed by neurons back to the cells which innervate them. This can be important for a variety of reasons, for example homeostatic maintenance of the level of network excitability.

A potential candidate for the factor released by postsynaptic group I mGluR activation is GABA. Group I mGluRs depolarize hippocampal neurons by inhibiting at least four distinct K^+ currents – the AHP current (Charpak et al., 1990; Desai and Conn, 1991), the M current (Charpak et al., 1990), a leak current (Guerineau et al., 1994) and a voltage-dependent slow-inactivating current (Luthi et al., 1996). There is also activation of Ca^{2+}-activated and Ca^{2+}-independent cationic conductances (Crepel

et al., 1994; Guerineau et al., 1995). Depolarisation of interneurons in this way leads to increased spiking and release of GABA. Although the postsynaptic neuron was voltage clamped, thereby preventing any change in membrane potential, firing of surrounding neurons may have led to GABA accumulation in the extracellular space, with activation of presynaptic $GABA_B$ receptors leading to depression of glutamate release. A similar mechanism has been proposed for part of the action of kainate on GABAergic transmission in the hippocampus (Frerking et al., 1999). $GABA_B$ receptors are heptahelical G protein-coupled receptors (GPCRs). Unlike the ionotropic $GABA_A$ receptors, which directly gate an ion channel, $GABA_B$ receptors are coupled via G proteins (predominantly $G_{i\alpha}$- and $G_{o\alpha}$-type) to intracellular signal transduction cascades. Downstream targets of $GABA_B$ receptor activation include adenylate cyclase, inwardly rectifying K^+ channels and voltage-gated Ca^{2+} channels. $GABA_B$ receptor-mediated activation of K^+ channels produces postsynaptic hyperpolarisation and inhibits neuronal excitability (for review see Bettler et al., 2004). Activation of $GABA_B$ receptors on presynaptic terminals causes an inhibition of neurotransmitter release via inhibition of N-type and P/Q-type Ca^{2+} channels (Doze et al., 1995; Lei and McBain, 2003). Of particular relevance to the present study are reports that presynaptic $GABA_B$ receptors depress both glutamatergic and GABAergic synaptic connections onto CA3 stratum radiatum interneurons, via inhibition of N-type and P/Q-type Ca^{2+} channels (Lei and McBain, 2003). This indicates that excitatory synaptic connections onto hippocampal interneurons are an important target for $GABA_B$ receptor modulation, lending support to the idea that these receptors may be involved in the mechanism of DHPG-induced acute depression.

Another potential mechanism to account for the presynaptic depression is the release of endocannabinoids acting as retrograde messengers. Endocannabinoid signalling is reviewed in detail in Chapter 1, Section 1.4.5.2. These molecules have been shown to be released in response to postsynaptic group I mGluR activation, and to subsequently inhibit neurotransmitter release by acting as retrograde messengers upon presynaptic CB1 receptors. Recent high-resolution immunohistochemical and

electrophysiological evidence have demonstrated that functional CB1 receptors are expressed at Schaffer collateral terminals, and act to inhibit glutamatergic synaptic transmission to CA1 pyramidal cells (Katona et al., 2006; Kawamura et al., 2006; Takahashi and Castillo, 2006). This makes endocannabinoids strong candidates for a potential retrograde signal mediating acute depression in CA1 interneurons.

If a short-range physical or chemical retrograde signal is involved in mediating the apparent presynaptic expression of DHPG-evoked depression, it is important to determine whether the signal is released from the recorded interneuron itself. This was tested by interfering with the signalling cascade downstream from postsynaptic group I mGluRs in the recorded cell, leaving surrounding interneurons intact. Target-dependent expression of mGluRs has been demonstrated in previous studies. For example, electron microscopy combined with immunocytochemistry has been used to show that the group III receptor mGluR7a is strongly expressed at presynaptic terminals contacting interneurons but not pyramidal cells. This high level of target-dependent segregation has been shown at both glutamatergic (Shigemoto et al., 1996; 1997) and GABAergic (Somogyi et al., 2003) terminals in area CA1 of the hippocampus. It is thus possible that there is close pairing between pre- and postsynaptic neurons, such that a retrograde factor released from a postsynaptic cell acts only upon directly opposed presynaptic axon terminals. However, there is extensive evidence for 'spillover' of glutamate to neighbouring synapses (Kullmann et al., 1996; Asztely et al., 1997; Rusakov and Kullmann, 1998; Scimemi et al., 2004), and it is possible that this may occur with other types of neurotransmitter. At the concentration used in the experiments described in this thesis, the selective agonist DHPG would be expected to maximally activate a large proportion of group I mGluRs in the hippocampal slice. If group I mGluR activation via DHPG causes release of a retrograde factor, interfering with this mechanism in the recorded neuron may not fully abolish DHPG-induced effects if the retrograde factor can spill over from nearby synapses. The signalling cascade downstream from postsynaptic group I mGluR activation was abolished in the recorded cell by applying two compounds

intracellularly via the patch pipette. Firstly, the non-hydrolysable G protein analogue GDPßS was used to prevent signalling through the group I mGluR-associated G protein $G_{q/11}$, and thus inhibit downstream effects such as phospholipase C activation (for review see Pin and Duvoisin, 1995; Hermans and Challiss, 2001). An important downstream signalling effect of group I mGluR activation is release of Ca^{2+} from intracellular stores (triggered primarily by the G protein-dependent activation of the phosphatidyl inositide/PLC signalling pathway), which has a variety of downstream effects within the cell (see Pin and Duvoisin, 1995). Intracellular Ca^{2+} signalling was therefore inhibited by applying a high concentration of the rapid Ca^{2+} chelator BAPTA.

The objective of the experiments described in the present chapter was to determine whether DHPG-induced acute depression in CA1 interneurons is pre- or postsynaptically mediated, and whether an additional factor is released as the result of group I mGluR activation.

6.2 Methods

Whole-cell voltage-clamp recordings of pharmacologically-isolated AMPA EPSCs were obtained from CA1 stratum radiatum interneurons as described previously (Chapter 2; also Chapter 5, Section 5.2). $GABA_B$ receptors were blocked via a 10 min pre-exposure to the selective antagonist CGP52342 (5 µM), which has been shown to fully block $GABA_B$ receptor-mediated presynaptic depression at other synapses (e.g. Chandler et al., 2003). CB1 endocannabinoid receptors were blocked by pre-incubation of slices in the selective CB1 receptor antagonist AM251 (2 µM). Slices were exposed to the drug for at least 25 minutes to ensure penetration (Wilson and Nicoll, 2001). AM251 is a hydrophobic molecule which penetrates slowly through the slice, hence the extended pre-incubation period. A combination of antagonists were used to block a number of neurotransmitter receptors involved in modulation of synaptic transmission. $GABA_B$ receptors were inhibited using CPG52432 (5 µM). A_1 adenosine receptors were blocked using DPCPX (200 nM). All mGluR subtypes were

blocked using LY341495 (1 μM), which acts primarily on groups I and II, and MSOP (100 μM), which acts on group III receptors (Schoepp et al., 1999). Subsequent detailed review of previously unfamiliar papers revealed that this selection of drugs was sub-optimal, and is likely to have not provided complete blockade of group I mGluRs (M. Capogna, personal communication). LY341495 is a highly potent group II mGluR antagonist (Fitzjohn et al., 1998; Kingston et al., 1998), but is less effective at group I mGluRs and would not have provided a complete blockade at 1 μM concentration (Fitzjohn et al., 1998). A better solution would have been to block group I mGluRs by including either CPCCOEt, or selectively blocking both receptors using LY367385 (for mGluR1) and MPEP (for mGluR5). Although an effective group III mGluR antagonist, MSOP is not the best compound available for this purpose. Alternative antagonists should have been used, either CPPG, or an increased concentration of LY341495 (20 μM; Fitzjohn et al., 1998).

Downstream group I mGluR signalling was inhibited by applying two compounds intracellularly via the patch pipette. G protein signalling was inhibited by replacing the standard 0.3 mM Na_3GTP in the pipette solution with 1 mM GDPβS, a non-hydrolysable GTP analogue. In addition, 0.2 mM EGTA in the intracellular solution was replaced with 10 mM BAPTA, in order to prevent an mGluR-mediated elevation in cytoplasmic Ca^{2+} concentration, secondary to release of intracellular Ca^{2+} or Ca^{2+} channel activation. An interval of at least 15 min was allowed between obtaining whole-cell access and the start of the recording, to ensure penetration of GDPβS and BAPTA into the neuron.

6.3 Results

6.3.1 DHPG-induced depression is not mediated by $GABA_B$ receptors

Following a 10 min pre-exposure to the selective $GABA_B$ receptor antagonist CGP52432 (5 μM), DHPG evoked a depression of EPSCs to 53 ± 11 % of baseline ($p < 0.001$, $n = 8$; Fig 6.1A). This was accompanied by a reversible increase in PPR to 128 ± 8 % of baseline ($p < 0.01$; Fig 6.1B). The magnitude of this depression was not significantly different from that of control experiments carried out in the absence of CGP52432 (paired t test, $p < 0.001$). Since 5 μM CGP52432 fully blocks $GABA_B$ receptor-mediated presynaptic depression at other synapses (e.g. Chandler et al., 2003), this finding argues that the action of DHPG on EPSCs does not involve $GABA_B$ receptors. The results could have been made yet more definitive by testing CGP52432 against a $GABA_B$-mediated synaptic response, or against a $GABA_B$ receptor agonist, in order to provide a positive control.

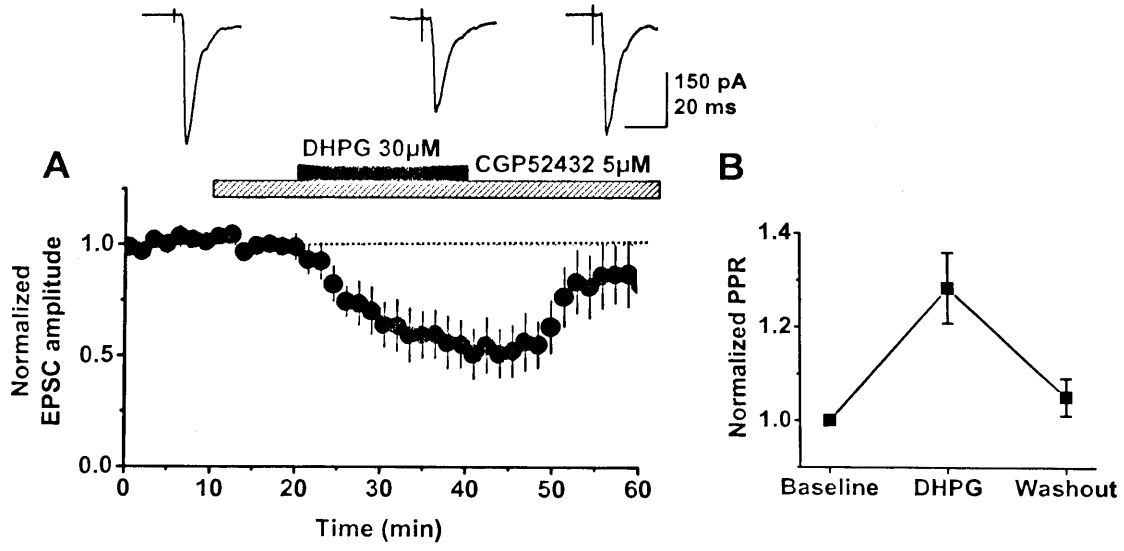

Figure 6.1 *$GABA_B$ receptors are not involved in group I mGluR-mediated acute depression of synaptic transmission.* ***A,*** *Effect of DHPG on EPSC amplitude (mean ± SEM), applied following 10 min exposure to the $GABA_B$ receptor antagonist CGP52432, on EPSC amplitudes (n= 9).* ***B,*** *DHPG causes a reversible elevation in PPR.*

6.3.2 DHPG-induced depression is not mediated by CB1 endocannabinoid receptors

Following a 10 min baseline, slices were pre-exposed for 25 min to the selective CB1 endocannabinoid receptor antagonist AM251 (2 μM). This aim of this prolonged exposure was to ensure that the hydrophobic molecule penetrated into the tissue so that maximal blockade of the target receptors was achieved. A 20 min exposure to DHPG subsequently evoked an acute depression of EPSCs to 51 ± 6% of baseline ($p < 0.001$, $n = 5$; Fig 6.2A), accompanied by a reversible increase in PPR to 145 ± 15 % of baseline ($p < 0.001$; Fig 6.2B). EPSC amplitude returned to baseline upon washout, while PPR decreased to 110 ± 8%. The magnitude of depression was not significantly different from control experiments (paired t test, $p < 0.005$) , arguing against a role for CB1 receptors in group I mGluR-mediated acute depression of excitatory synapses onto CA1 interneurons.

To further test for involvement of CB1 endocannabinoid receptors, a long-duration recording was made from a CA1 stratum radiatum interneuron (Fig 6.2C). Following a 10 min baseline, DHPG (30 μM) was applied for 20 min, resulting in a depression of EPSCs to 60% of baseline. DHPG was then washed out for 20 min. EPSCs returned to 95% of baseline. AM251 (2 μM) was applied for 25 min to ensure penetration of the hydrophobic molecule into the slice. A second exposure to DHPG resulted in a depression of EPSCs to 52% of baseline. The magnitude of DHPG induced depression was very similar following washout and pre-exposure to AM251 (60% and 52%), further suggesting that CB1 receptors are not involved in the mechanism. In contrast to the first washout, there was only a small return of EPSCs towards baseline during the second washout when CB1 receptors were blocked by AM251, suggesting a possible role for CB1 receptors in group I mGluR-mediated LTD. A greater number of recordings (minimum $n = 5$) is required for statistical analysis of this design of experiment, using a paired t test for the magnitude of DHPG-induced depression before and after pre-exposure to AM251. However, long-duration patch clamp recordings of 120 min are technically difficult to obtain, with a high failure rate

resulting from loss of recordings due to changes in I_{hold} and R_S which are beyond predetermined experimental limits (> 20%).

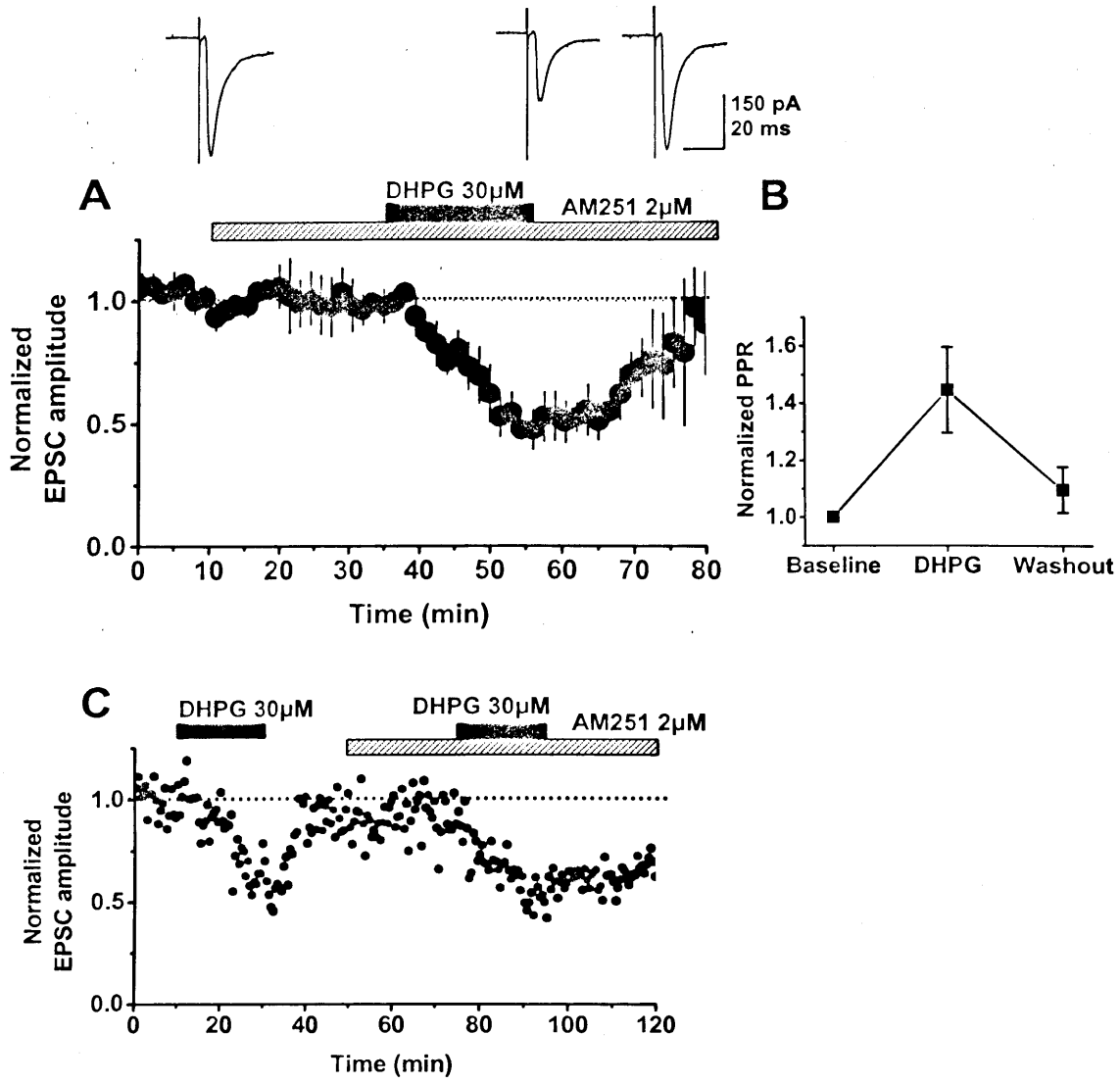

Figure 6.2 *CB1 endocannabinoid receptors are not involved in the group I mGluR-mediated acute depression.* ***A,*** *Effect of DHPG on EPSC amplitude (± SEM) following a 25 min exposure to the selective CB1 receptor antagonist AM251 (n = 5).* ***B,*** *DHPG causes a reversible elevation in PPR.* ***C,*** *Recording from a single neuron showing that the magnitude DHPG-induced depression is very similar before and after pre-exposure to AM251.*

In 2 of 7 cells, 25 min exposure to AM251 caused a significant increase in EPSC amplitude (cell 1, 162% of baseline; cell 2, 159% of baseline; Fig 6.3), suggesting that excitatory synaptic connections onto certain subtypes of CA1 stratum

radiatum interneuron may be subject to tonic inhibition by CB1 endocannabinoid receptors. EPSC amplitude appeared to reach a steady state prior to DHPG application, but this cannot be definitively confirmed since insufficient recording time was allowed to determine whether a plateau had been reached. It is possible that EPSC amplitude may have continued to increase if DHPG had not been applied. Following pre-exposure to AM251, DHPG caused a significant depression of EPSCs in both cells (cell 1, DHPG depressed EPSCs from 162% to 123% of baseline, a total depression of 39%; cell 2, DHPG depressed EPSCs from 159% to 127% of baseline, a total depression of 32%). These findings further confirm that the mechanism of DHPG-induced depression does not directly involve CB1 endocannabinoid receptors. These two cells were not included in the analysis shown in Fig 6.2A & B, which comprises 5 of the 7 cells recorded which did not show an increase in EPSC amplitude in response to AM251.

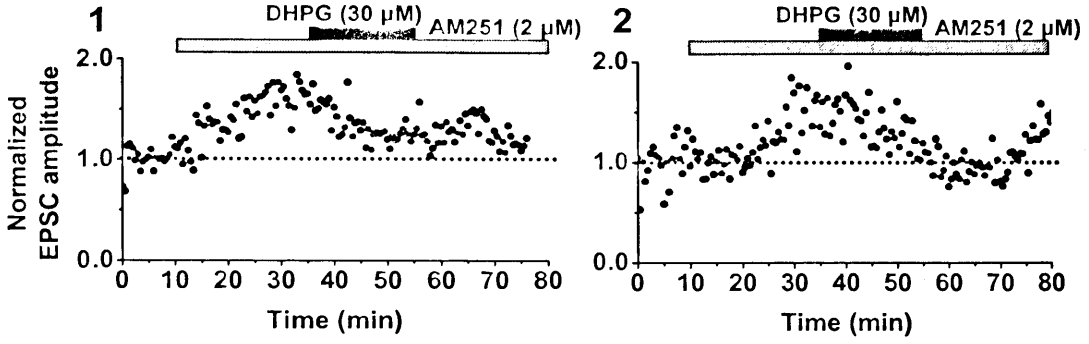

Figure 6.3 *The selective CB1 receptor antagonist causes an increase in EPSC amplitude in 2 of 7 cells, suggesting possible tonic endocannabinoid inhibition at certain excitatory synaptic connections onto interneurons. Subsequent exposure to DHPG causes depression of EPSCs, confirming that group I mGluR-mediated depression is not dependent upon CB1 endocannabinoid receptors.*

6.3.3 DHPG-induced depression is attenuated by antagonists of mGluRs, $GABA_B$ receptors and A_1 adenosine receptors

Several antagonists were applied simultaneously to block various neurotransmitter receptors which may be involved in mediating modulatory effects at excitatory connections onto CA1 interneurons. All mGluR subtypes were blocked using LY341495, which acts primarily on groups I and II, and MSOP, which acts on group III receptors (Schoepp et al., 1999); $GABA_B$ receptors were inhibited using CPG52432; and A_1 adenosine receptors were blocked using DPCPX. Following 20 min pre-exposure to the antagonists LY341495 (1 μM), MSOP (100 μM), CGP52432 (5 μM) and DPCPX (200 nM), DHPG was applied for 20 min, with 20 min washout. The cocktail of antagonists had no significant effect upon EPSC amplitude (paired t test, $p < 0.001$), implying that glutamatergic synaptic connections onto CA1 stratum radiatum interneurons are not subject to tonic inhibition from group I, II or III mGluRs, $GABA_B$ receptors or A_1 adenosine receptors. Following pre-exposure to these drugs, DHPG induced a significant depression to 78 ± 3% of baseline, which returned almost to baseline upon washout ($p < 0.001$, $n = 6$, Fig 6.4A). This depression was significantly smaller than that observed in control experiments in which DHPG alone was applied (paired t test, $p < 0.01$). DHPG-induced depression was accompanied by a significant elevation in PPR to 123 ± 9% of baseline ($p < 0.05$, $n = 6$), which returned to 107 ± 6% upon washout (Fig 6.4B). An unexpected result from this series of experiments was that a significant DHPG-induced depression persisted in the presence of antagonists of group I, II and III mGluRs. This finding may be explained in two ways. Either DHPG affects receptors other than mGluRs in hippocampal slices at the concentration used in this study; or one or more mGluR subtypes was incompletely blocked by the concentrations of LY341495 and MSOP used in these experiments. There is extensive evidence for the highly group I mGluR-selective action of DHPG (for review see Schoepp et al., 1999), and it is thus unlikely that other neurotransmitter systems were affected by this drug. A more plausible explanation is that mGluRs were incompletely blocked, thereby reducing, but not fully attenuating,

DHPG-induced acute depression. MSOP is a highly selective group III mGluR antagonist (Schoepp et al., 1999), and is very commonly used at 100 μM concentration in brain slice preparations (e.g. Semyanov and Kullmann, 2000; Rusakov et al., 2004). However, LY341495 is less well characterised. It is a broad-spectrum mGluR antagonist which appears to be primarily selective for group I and II mGluRs (Fitzjohn et al., 1998; Schoepp et al., 1999). Concentrations of LY341495 used to block mGluRs in hippocampal slices have varied widely in previous studies. Some studies have used 1 μM concentration (e.g. Losonczy et al., 2003), whereas others have used higher concentrations of 20 μM (e.g. Fitzjohn et al., 1998; Kemp and Bashir, 1999; Watabe et al., 2002) or 100 μM (Fitzjohn et al., 1998). A probable explanation for the small DHPG-induced depression observed in the present series of experiments is therefore incomplete blockade of group I and/or group II mGluRs, due to a concentration of LY341495 (1 μM) which was too low. The experiments should therefore be repeated using a higher concentration of LY341495, such as 20 μM or 100 μM (Fitzjohn et al., 1998).

In order to clarify the role of adenosine receptors in DHPG-induced depression in CA1 interneurons, experiments should be carried out in which slices are pre-exposed only to the A_1 adenosine receptor antagonist DPCPX, followed by DHPG application. In the absence of the other antagonists, the role of A_1 adenosine receptors could be interpreted more definitively.

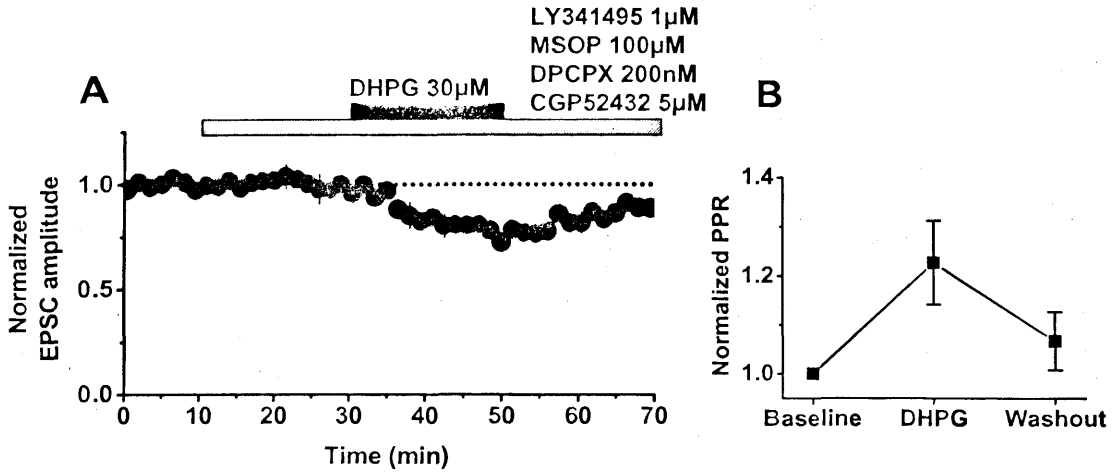

Figure 6.4 *DHPG-induced depression of EPSCs is significantly attenuated in the presence of antagonists of group I, II and III mGluRs, $GABA_B$ receptors and A_1 adenosine receptors. However, a significant depression persists, and is accompanied by an increase in PPR which returns to baseline upon washout (n = 6).*

6.3.4 Blockade of Ca^{2+} and G protein signalling in single neurons attenuates DHPG-induced depression

Downstream targets of mGluR activation were inhibited in the postsynaptic neuron from which the whole-cell recording was made. G protein signalling was blocked using the non-hydrolysable GTP analogue GDPβS (1 mM), while Ca^{2+} signalling was attenuated using the rapid Ca^{2+} chelator BAPTA (10 mM). Both drugs were applied intracellularly via the patch pipette. DHPG-evoked depression of EPSCs was markedly attenuated: a non-significant reduction of amplitude to 84 ± 9 % of baseline was observed (paired t test; p = 0.07; n = 7; Fig 6.5A), with no significant change in PPR (103 ± 6 %; paired t test; p = 0.76; Fig 6.5B).

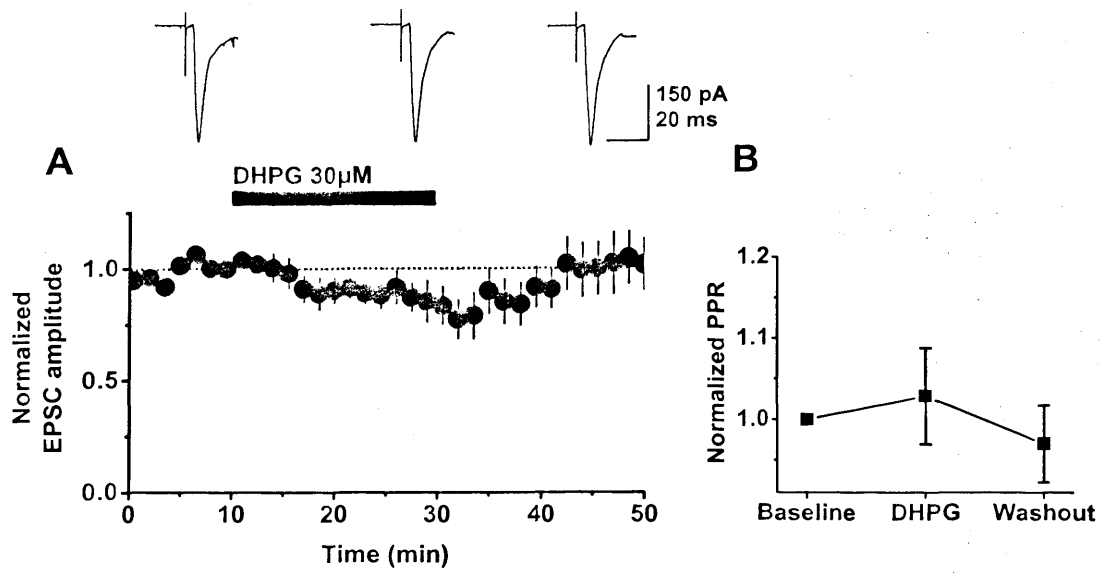

Figure 6.5 *DHPG-induced depression is attenuated by blockade of postsynaptic G protein and Ca^{2+} signalling.* ***A,*** *Effect of DHPG on EPSC amplitude (mean ± SEM), obtained in interneurons recorded with a pipette solution containing the non-hydrolysable GTP analogue GDPβS, and the Ca^{2+} chelator BAPTA (n = 7).* ***B,*** *DHPG application evoked no significant change in PPR.*

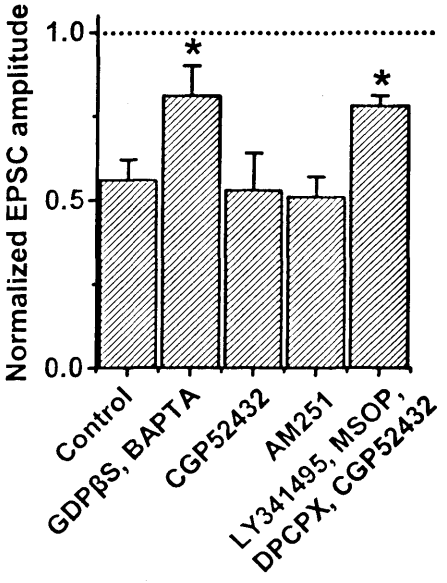

Figure 6.6 *Summary of pharmacological manipulations designed to determine whether group I mGluR depression in CA1 interneurons is pre- or postsynaptically mediated. The magnitude of DHPG-induced depression is significantly reduced by (i) blockade of intracellular G protein and Ca^{2+} signalling; and (ii) blockade of mGluR, A_1 adenosine and $GABA_B$ receptors.*

6.4 Discussion

The objective of the experiments described in the present chapter was to investigate the mechanism via which group I mGluR activation by DHPG results in an acute depression of excitatory synaptic transmission to CA1 interneurons. In particular, the aim of these experiments was to determine whether pre- or postsynaptic mechanisms mediate induction and expression of DHPG-induced depression. One issue which raised a number of question was the robust increase in PPR associated with DHPG-induced depression, suggesting that the mechanism involves a presynaptic action. However, high-resolution immunohistochemical studies have consistently reported a predominantly postsynaptic location for group I mGluRs. Both mGluR1 and mGluR5 have been detected in a peri-synaptic annulus at glutamatergic synapses both in the hippocampus and in the cerebellar cortex (Martin et al., 1992; Baude et al., 1993; Lujan et al., 1996; Shigemoto et al., 1997; Lujan et al., 1997; Petralia et al., 1997; Lopez-Bendito et al., 2002). The simplest explanation for these observations is that DHPG-induced acute depression results from a decrease in glutamate release from Schaffer collateral terminals, triggered by activation of presynaptic group I mGluRs which had not been previously detected by high-resolution immunohistochemical studies. One possible reason may be a low level of receptor expression at axon terminals in comparison to the postsynaptic membrane. Thus the weak signal resulting from antibody binding to presynaptic receptors would be masked by the much stronger signal resulting from antibody binding to postsynaptic receptors. Another possibility may be a lower level of antibody binding to presynaptic receptors due to the morphology of the synaptic cleft. However, an alternative hypothesis to explain the apparent presynaptic expression of DHPG-evoked depression is that activation of postsynaptic group I mGluRs by DHPG results in the release of a factor which acts upon presynaptic receptors. This explanation is consistent both with the abundant postsynaptic expression of mGluR1 and mGluR5 revealed by high-resolution immunohistochemical studies (Martin et al., 1992; Baude et al., 1993; Lujan et al., 1996; Shigemoto et al., 1997; Lujan et al., 1997; Petralia et

al., 1997; Lopez-Bendito et al., 2002); and with the apparent presynaptic expression of DHPG-induced depression demonstrated in both CA1 interneurons and pyramidal cells by the experiments carried out in this thesis, and in CA1 pyramidal cells by previously reported studies (Gereau and Conn, 1995; Manzoni and Bockaert, 1995; Rodriguez-Moreno et al., 1998; Mannaioni et al., 2001). Numerous pharmacological manipulations were carried out in the experiments described in this chapter in an attempt to identify the potential retrograde signal that couples postsynaptic group I mGluR-mediated signalling to presynaptic modulation of glutamate release at excitatory synaptic connections onto CA1 interneurons.

Group I mGluR activation has been shown to depolarize interneurons, causing increased spiking and release of GABA. This occurs via inhibition of various K^+ conductances (Charpak et al., 1990; Desai and Conn, 1991; Guerineau et al., 1994; Luthi et al., 1996), and activation of Ca^{2+}-activated and Ca^{2+}-independent cationic conductances (Crepel et al., 1994; Guerineau et al., 1995). In interneurons, this depolarisation leads to increased spiking and release of GABA. Accumulation of GABA in the extracellular space could conceivably result in depression of EPSCs in CA1 stratum radiatum interneurons via increased activation of presynaptic metabotropic $GABA_B$ receptors, which would in turn inhibit glutamate release from Schaffer collateral terminals by acting upon N-type and P/Q-type Ca^{2+} channels (see Doze et al., 1995; Lei and McBain, 2003). Two lines of evidence from the present study argue against this hypothesis. Firstly and most importantly, the magnitude of DHPG-induced depression of EPSCs was unaffected by the specific $GABA_B$ antagonist CGP52432. Previous work has shown that this is a highly selective and potent antagonist of the $GABA_B$ receptor (e.g. Chandler et al., 2003). Secondly, manipulation of G protein and Ca^{2+} signalling only within the recorded neuron using drugs applied via the patch pipette was sufficient to reduce the magnitude of DHPG-induced depression below significance. If DHPG-induced depression resulted from widespread depolarisation of interneurons and increased release of GABA acting upon presynaptic $GABA_B$ receptors, intracellular blockade of downstream effects of

group I mGluR activation in the recorded neuron would be unlikely to have a large effect upon the magnitude of depression. The surrounding interneurons would be unaffected, becoming depolarised and releasing GABA in response to DHPG application. This would cause increased activation of presynaptic $GABA_B$ receptors, inhibiting glutamate release from Schaffer collateral terminals onto CA1 stratum radiatum interneurons. However, blockade of postsynaptic group I mGluR signalling in only the recorded interneuron was sufficient to prevent DHPG-induced depression, further ruling out a direct involvement of presynaptic $GABA_B$ receptors.

Endocannabinoids are potentially a better candidate for a factor released postsynaptically in response to group I mGluR activation, because they have been shown to act as a local retrograde signal affecting GABA and glutamate release (Wilson and Nicoll, 2001; Kreitzer and Regehr, 2001b). Indeed, group I mGluR activation has been shown to trigger endocannabinoid release leading to presynaptic inhibition of GABA and glutamate release in the cerebellum (Maejima et al., 2001), brainstem (Kushmerick et al., 2004), hippocampus (Varma et al., 2001; Rouach and Nicoll, 2003), ventral tegmental area (Bellone and Luscher, 2005), and nucleus accumbens (Robbe et al., 2002). Earlier immunohistochemical studies failed to detect CB1 receptors on hippocampal glutamatergic terminals (Tsou et al., 1999; Katona et al., 1999b; Hajos et al., 2000; Nyiri et al., 2005). However, very recent studies have demonstrated CB1 receptor expression at glutamatergic Schaffer collateral terminals, although at lower levels than at GABAergic axon terminals (Katona et al., 2006; Kawamura et al., 2006). Some actions of endocannabinoids have been proposed to be mediated by an as yet uncharacterized receptor (Hajos et al., 2001; Hoffman et al., 2005). Glutamatergic synaptic transmission in the hippocampus has been shown to be modulated by the endocannabinoid signalling system (Misner and Sullivan, 1999; Ohno-Shosaku et al., 2002), and recent studies have shown definitively that excitatory synaptic transmission from Schaffer collaterals to CA1 pyramidal cells is depressed by CB1 receptors (Kawamura et al., 2006; Takahashi and Castillo, 2006). There is thus considerable evidence, particularly from recent studies, to suggest that

endocannabinoids may be the retrograde factor involved in DHPG-evoked depression in CA1 stratum radiatum interneurons. However, pre-exposure to the selective CB1 antagonist AM251 did not affect the magnitude of DHPG-induced depression of EPSCs in CA1 stratum radiatum interneurons in the present study, indicating that endocannabinoids are not the retrograde messenger in this system (Fig 6.2A & B).

To examine in more detail the involvement of CB1 receptors, a long-duration recording was made from a CA1 stratum radiatum interneuron. DHPG was applied, washed out, and then re-applied following pre-exposure to AM251. The magnitude of DHPG induced depression was very similar with and without pre-exposure to AM251, further suggesting that CB1 receptors are not involved in the mechanism (Fig 6.2C). It should be noted that these data were obtained from a single interneuron. Further long-duration recordings would be required in order to increase the number of cells and facilitate statistical analysis (paired t test for magnitude of DHPG-induced depression before and after pre-exposure to AM251). However, this experimental design requires a whole-cell voltage-clamp recording of 120 min duration. Attempting to make such long recordings inevitably leads to a greatly increased number of failures due to sudden loss of the patch clamp recording, and rejection of cells due to changes in I_{hold} and R_S which are beyond acceptable predetermined experimental parameters. Such experiments were not carried out since the data shown in Fig 6.2 clearly indicate that CB1 endocannabinoid receptors are not directly involved in group I mGluR-mediated acute depression at excitatory connections onto CA1 stratum radiatum interneurons. Interestingly, in contrast to the first washout, EPSCs returned only very slightly towards baseline during the second washout when CB1 receptors were blocked by AM251. This suggests a possible role for CB1 receptors in group I mGluR-mediated LTD in CA1 interneurons, since blockade of these receptors caused DHPG to bring about a persistent depression of EPSCs which follows the initial acute phase. These findings may initially appear to contrast with those of Rouach and Nicoll (2003), who demonstrated that endocannabinoids contribute to the acute phase but not the persistent phase of group I mGluR-mediated depression. However, their study

was carried out in CA1 pyramidal cells as opposed to interneurons. Furthermore, they conclude that the effects observed in their study were mediated by a non-CB1 endocannabinoid receptor, since the DHPG-induced acute depression was unaffected in the CB1 knockout mouse and by the CB1-selective antagonist AM251. Alternatively, it is possible that re-activating group I mGluRs within a certain temporal window following the first activation is responsible for induction of this persistent depression of EPSCs. In other words, the first activation of group I mGluRs may act as a 'switch', which causes the second activation to bring about LTD following the acute depression. It is impossible to speculate further on this issue without a greater number of recordings. Nevertheless, the findings from the interneuron recording shown in Fig 6.2C raise a number of interesting questions. If future studies were carried out in order to systematically investigate group I mGluR-mediated LTD in CA1 interneurons, experiments should be included which examine the involvement of the endocannabinoid system.

In 2 of 7 cells, 25 min exposure to AM251 caused a significant increase in EPSC amplitude (Fig 6.3), suggesting that excitatory synaptic connections onto certain subtypes of CA1 stratum radiatum interneuron may be subject to tonic inhibition by CB1 endocannabinoid receptors. This phenomenon was not explored in detail due to time constraints, but merits further investigation in future studies. It is impossible to draw further conclusions regarding endocannabinoid-mediated tonic inhibition from the available data. Subsequent experiments to investigate this phenomenon would involve recording from a larger sample population of interneurons, so that the proportion of cells displaying this effect could be accurately determined. The experiments would be carried out in the same way, but without DHPG application, thereby allowing EPSC amplitude to reach a steady state following AM251 application. This potential tonic inhibition of glutamatergic connections onto CA1 stratum radiatum interneurons by CB1 endocannabinoid receptors represents an interesting area of future research.

Signalling cascades downstream from postsynaptic mGluR activation were inhibited only in the recorded neuron by applying compounds via the patch pipette. Group I mGluRs are closely associated with the G proteins $G_{q/11}$, which in turn are coupled to activation of the enzyme phospholipase C and subsequent activation of the phosphatidyl inositide signalling cascade (reviewed in Chapter 1, Section 1.2.3; see also Hermans and Challiss, 2001 for review). G proteins are composed of α, β and γ subunits. Activation via ligand binding results in a conformational change in G protein-coupled receptors (GPCRs) such as mGluRs, causing them to catalyse exchange of GDP for GTP in their associated G proteins. This results in dissociation of the heteromeric G protein, generating α-GTP and βγ subunits, both of which then interact with their downstream targets. The GTPase activity of the G protein α subunit mediates hydrolysis of GTP to GDP, with concomitant conversion of the G protein back to the inactive state. The non-hydrolysable GTP analogue GDPβS was used to block G protein signalling by inhibiting the GTPase activity of the G protein α subunit. GTP hydrolysis is an essential step in the G protein signalling cascade. By replacing 0.3 mM Na_3GTP in the patch pipette with 1 mM GDPβS, GTP hydrolysis was prevented, locking G proteins in the inactive state and thus inhibiting all downstream effects. The second intracellular manipulation was blockade of Ca^{2+} signalling by a high concentration (10 mM) of the rapid Ca^{2+} chelator BAPTA. Group I mGluR activation has been shown to result in release of Ca^{2+} from intracellular stores, an important downstream effect of the phosphoinositide signalling cascade (Pin and Duvoisin, 1995; Hermans and Challiss, 2001). The possibility of Ca^{2+} channel activation can also not be ruled out. Combining these two strategies for blocking downstream effects of group I mGluR activation in the recorded neuron resulted in a reduction of the magnitude of DHPG-induced depression from 56 ± 6% to a non-significant 84 ± 9%. Although this does not exclude an additional presynaptic location of some group I receptors, the finding that postsynaptic manipulation of G protein and Ca^{2+} signalling almost abolished DHPG-evoked depression argues that such receptors do not play a large role. The residual non-significant depression observed in

these experiments could be explained by a small contribution of mGluR-mediated signalling in neighboring neurons. The finding that interfering with the cascade triggered by group I mGluRs in the postsynaptic cell alone prevented the effect of DHPG sets constraints on the signal that can travel to the presynaptic elements of glutamatergic synapses: it makes a long-range signal (such as a peptide transmitter) a poor candidate because this should still be released from neighboring interneurons where G protein signalling and/or Ca^{2+} elevation were intact. Instead, it argues for a short-range physical or chemical signal that gives the postsynaptic neuron privileged access to regulatory mechanisms in the presynaptic glutamatergic varicosities in direct synaptic contact.

Chapter 7. Modulation of presynaptic Ca^{2+} channels by group I mGluRs

7.1 Introduction

Activation of group I mGluRs causes an acute depression of excitatory synaptic transmission to CA1 stratum radiatum interneurons. Although anatomical studies have suggested that group I mGluRs are expressed predominantly postsynaptically in the hippocampus (Martin et al., 1992; Baude et al., 1993; Lujan et al., 1996; Shigemoto et al., 1997; Lujan et al., 1997; Petralia et al., 1997; Lopez-Bendito et al., 2002), electrophysiological evidence reported in previous studies (Gereau and Conn, 1995; Manzoni and Bockaert, 1995; Rodriguez-Moreno et al., 1998; Mannaioni et al., 2001) and this thesis indicates that the mechanism of depression involves a presynaptic action. One hypothesis is that activation of postsynaptic group I mGluRs results in the release of an as-yet unidentified retrograde signal, which acts upon presynaptic receptors to bring about an inhibition of glutamate release. Many modulatory influences that act upon neurotransmitter release are mediated by G protein-coupled receptors, which act in large part via inhibition of presynaptic Ca^{2+} channels. Ca^{2+} influx into the presynaptic terminal via voltage-gated channels is the trigger for release of neurotransmitter vesicles. A detailed review of the highly complex process of synaptic vesicle exocytosis is beyond the scope of this thesis. Such a review is not directly relevant to the present discussion, since the focus of this chapter is the involvement of presynaptic Ca^{2+} channels in group I mGluR-mediated synaptic depression. To summarise the process briefly, incoming action potentials depolarise the axon terminal, causing activation of voltage-gated Ca^{2+} channels. There is a large and rapid increase in Ca^{2+} concentration, which is restricted within local microdomains in the presynaptic terminal. Clusters of Ca^{2+} channels are localised near docked synaptic vesicles in active zones. Within microdomains, Ca^{2+} acts rapidly ($\leq$ 200 µs) over short distances (tens of nanometres), at very high local

concentrations (≥ 10 μM, compared with the resting intracellular Ca^{2+} concentration of ~100 nM) to trigger synaptic vesicle release. Fusion of docked and primed vesicles in the active zone with the presynaptic membrane is mediated by a number of proteins known as the SNARE complex. The fusion process remains incompletely understood, but the most widely accepted view is that vesicle-associated proteins (v-SNAREs) such as VAMP interact with proteins on the target membrane (t-SNAREs) such as SNAP-25 and syntaxin to overcome the energy barrier involved in fusion of the vesicle membrane with the membrane of the presynaptic terminal. The SNARE complex brings the vesicle and plasma membranes into close proximity, representing one of the final steps in the exocytosis process. The Ca^{2+} influx triggers vesicle fusion by binding to an integral synaptic vesicle membrane protein known as synaptotagmin. The large cytoplasmic portion of synaptotagmin contains two Ca^{2+} binding C2 domains (C2A and C2B), which interact with SNARE complex proteins and phospholipids in a Ca^{2+}-dependent manner. One or more of these interactions is thought to be the triggering event for vesicle fusion. As stated above, the mechanism of synaptic vesicle fusion is highly complex, and many steps in the process remain incompletely understood.

The resting intracellular [Ca^{2+}] is ~100 nM, with an extracellular [Ca^{2+}] of ~1.5 mM. The Nernst potential for Ca^{2+} ions (E_{Ca}) is extremely positive, estimated at approximately 120-130 mV in most types of neuron (Hille, 2001). Upon opening of voltage-gated Ca^{2+} channels, there is thus a large and rapid influx of Ca^{2+} ions into the neuron due to the strong electrochemical driving force. There are numerous distinct Ca^{2+} channels, which may be classified according to a variety of criteria, including structural nomenclature, Snutch gene class and sensitivity to various pharmacological agents (for review see Hille, 2001). The Ca^{2+} channels which are concentrated in presynaptic terminals and are responsible for mediating the influx of Ca^{2+} that triggers vesicle exocytosis are the high voltage-activated (HVA) N-type and P/Q-type channels, with also in some cases a much smaller residual contribution from R-type

channels (Wu and Saggau, 1997; Reid et al., 2003). Presynaptic Ca^{2+} channels involved in mediating vesicle release have been shown by many studies to be important targets for modulation by GPCRs (for review see Wu and Saggau, 1997). N-type Ca^{2+} channels show a higher sensitivity to G proteins than P/Q type channels (Zhang et al., 1996; Currie and Fox, 1997). In keeping with this concept, blockade of N-type Ca^{2+} channels has been shown to occlude the effect of presynaptic CB1 receptor activation on GABA release (Wilson et al., 2001). N-type Ca^{2+} channels have been strongly implicated as the main targets in group III mGluR modulation of synaptic transmission (Millan and Sanchez-Prieto, 2002; 2002a; Millan et al., 2002b; 2003) Moreover, Ca^{2+} imaging has revealed a direct of effect of group III mGluRs on N-type channel-mediated Ca^{2+} influx in individual axonal varicosities (Rusakov et al., 2004).

Although the putative retrograde signal released following postsynaptic group I mGluR activation could not yet be definitively identified (see Chapter 6), experiments were also carried out in order to investigate presynaptic effects occurring during DHPG-induced acute depression of glutamatergic synaptic transmission to CA1 interneurons. One possibility was that a retrograde signal acted presynaptically to inhibit Ca^{2+} influx via N-type and/or P/Q-type Ca^{2+} channels, thereby reducing glutamate release from Schaffer collateral terminals and depressing EPSCs in CA1 stratum radiatum interneurons. The objectives of the experiments described in this chapter were as follows. Firstly, to confirm that N-type and P/Q-type Ca^{2+} channels could be specifically blocked in a subtype-selective manner in hippocampal slices, using highly specific peptide toxins. Secondly, to determine whether DHPG-induced acute depression of EPSCs in CA1 interneurons was affected by blockade of these Ca^{2+} channel subtypes. Investigation of the presynaptic expression of the effect in this manner would reveal further information regarding the mechanism of DHPG-induced depression in interneurons.

7.2 Methods

Whole-cell voltage-clamp recordings of pharmacologically-isolated AMPA EPSCs were obtained from CA1 stratum radiatum interneurons as described previously (Chapter 2; also Chapter 5, Section 5.2). Presynaptic Ca^{2+} channels involved in neurotransmitter release were blocked using selective peptide antagonists. N-type channels were blocked using ω-conotoxin GVIA (CgTx, 250 nM, obtained from AnaSpec Inc., USA), and P/Q-type channels were blocked using ω-agatoxin IVA (AgTx, 100 nM, obtained from Alexis Biochemicals, USA). These antagonists are highly purified peptide toxins. Technical difficulties were encountered when using these molecules in hippocampal slices, since they are large molecules and appeared to penetrate poorly through the tissue, reaching a low proportion of their target Ca^{2+} channels. The selective Ca^{2+} channel antagonists had high molecular weights (CgTx 3039 Da; AgTx 5202 Da). The antagonists were prepared on ice from lyophilised powder into concentrated aliquots in purified water, and subsequently diluted 1:500 in ACSF. The perfusion system was set up to re-circulate ACSF containing the Ca^{2+} channel antagonists, since they were highly expensive. Care was taken to avoid cross-contamination of ACSF containing different drugs, and the re-circulation did not appear to adversely affect the experiments in any way. As the project progressed, experimental evidence appeared to reveal that CgTx and AgTx were not exerting maximal effects upon their target Ca^{2+} channels. The most likely cause was poor penetration of the large peptide molecules through the tissue of the hippocampal slice. Some experiments aimed to attempt to overcome the problem of peptide Ca^{2+} channel antagonists penetrating only into the superficial layers of the slice. In addition to continuous exposure to the selective Ca^{2+} channel antagonists during the experiment via the perfusion ACSF whilst in the recording chamber, hippocampal slices were pre-exposed to the antagonists for two hours in a custom-built submersion chamber (see Chapter 4, Fig 4.1). The chamber contained 5 ml ACSF, which was bubbled continuously with 95% O_2 / 5% CO_2 via a fine tube. Slices were submerged on a mesh gauze. The chamber was placed on an electric stirrer, which was used to gently rotate

a small magnetic stirring bar in the bottom of the chamber, ensuring that ACSF was circulated continuously around the slice. Submerging slices in this way also ensured that toxins could penetrate both sides of the slice.

7.3 Results

The objective of the first series of experiments was to test the efficacy of the selective Ca^{2+} channel blockers. Both CgTx (250 nM) and AgTx (100 nM) were bath applied in the ACSF perfusing the hippocampal slices in the recording chamber. An incubation period of 25 min for each drug was used in order to allow the high molecular weight peptide molecules to penetrate through the tissue and reach their target Ca^{2+} channels. The concentrations of Ca^{2+} antagonists used were relatively low, partly due to their extremely high cost, and partly due to successful blockade of the relevant channels in previous studies carried out in this laboratory (e.g. Rusakov et al., 2004). This factor may have contributed towards the long-term equilibration of the antagonists. If more time had been available, experiments would have been repeated using concentrations at least twice as high, and concentrations up to 10 times higher could have been used without loss of specificity.

Once a 10 min baseline had been recorded, CgTx was applied for 25 min followed by AgTx for 25 min. Unless otherwise stated, drugs applied earlier in the experiment remained in the perfusion solution while additional drugs were added, i.e. CgTx remained present while AgTx was applied. CgTx significantly depressed EPSCs to 81 ± 7 of baseline ($p < 0.05$, $n = 8$, Fig 7.1A_1), with AgTx causing a further depression to 58 ± 7% of baseline ($p < 0.01$, $n = 8$). The depression caused was 19 ± 7% by CgTx and 23 ± 7% by AgTx. These findings clearly suggested an incomplete blockade of N-type and P/Q-type Ca^{2+} channels. Previous studies have demonstrated that N-type and P/Q-type Ca^{2+} channels are almost entirely responsible for mediating the influx of Ca^{2+} into the presynaptic terminal that triggers release of

neurotransmitter, with a low level of contribution from R-type Ca^{2+} channels in some cases (Wu and Saggau, 1997; Reid et al., 2003). The peptide toxins CgTx and AgTx are large molecules (3039 Da and 5202 Da respectively). A plausible explanation for these observations was thus that the toxins penetrated poorly through the dense tissue of the slice, and reached a relatively small proportion of their target Ca^{2+} channels during the 25 min exposure. It should be noted that in these and subsequent control experiments, the effect of the first drug had often not reached a steady state before the second drug was added. Thus over a longer time period CgTx may have caused a depression larger than 19 ± 7%, but this effect was masked by the addition of AgTx. The magnitude of depression induced by AgTx is in fact the combined effect of AgTx and CgTx. These issues result from the slow onset of effects of the peptide toxins and delayed time to reach steady state. This is again likely to be due to poor penetration of the peptide molecules through the slice tissue. The values determined for the effects of the drugs on EPSC amplitude may therefore not be fully accurate. The problem could be overcome by allowing prolonged exposure to each toxin until steady state was reached, e.g. one hour in CgTx followed by one hour in AgTx. However, this raises the technical difficulty of maintaining stable long-duration whole cell patch clamp recordings. The high failure rate would make this experimental approach time-consuming.

Subsequent experiments aimed to attempt to overcome the problem of peptide Ca^{2+} channel antagonists penetrating only into the superficial layers of the slice. Hippocampal slices were pre-exposed to the selective Ca^{2+} channel antagonists for two hours in a custom-built submersion chamber. A major disadvantage of this experimental approach is that it is was impossible to quantify the effects of the Ca^{2+} channel antagonists when applied in this way, since parameters such as EPSC amplitude cannot be compared in the same neuron before, during and after drug application. In the first series of experiments, slices were pre-exposed to CgTx for two hours in the submersion chamber. Once a 15 min baseline had been recorded, AgTx

(100 nM) was applied for 25 min, followed by NiCl (100 μM) for 25 min. The aim of applying NiCl was to test for involvement of R-type Ca^{2+} channels. AgTx depressed EPSCs to 69 ± 8% of baseline ($p < 0.01$, $n = 6$, Fig $7.1B_1$), with NiCl causing a further depression to 41 ± 9% of baseline ($p << 0.0001$, $n = 6$). The depression caused was 31 ± 8% by AgTx and 28 ± 9% by NiCl. This suggests a possible contribution of up to 30% by R-type Ca^{2+} channels to AMPA-kainate EPSCs at Schaffer collateral connections onto CA1 stratum radiatum interneurons. However, a more plausible explanation is that the effects of AgTx had not reached steady state at the point when NiCl was applied. Thus if an exposure longer than 25 min had been used, a larger depression may have been elicited by AgTx, with less effect upon EPSC amplitude subsequently exerted by NiCl. A large EPSC component was present following pre-exposure to CgTx and application of AgTx, indicating that blockade of N-type and P/Q-type Ca^{2+} channels was incomplete under these experimental conditions. In an attempt to achieve a total blockade of N-type and P/Q-type Ca^{2+} channels, slices were incubated for two hours in both CgTx and AgTx. EPSCs were virtually abolished in slices subjected to this procedure. Whole cell voltage-clamp recordings were made from CA1 stratum radiatum interneurons. Large amplitude EPSCs could not be elicited. Stimulus electrodes were re-positioned multiple times during recoding in order to verify that only low amplitude EPSCs could be elicited ($n = 6$ cells in 6 separate slices. Fig $7.1C_{1\&2}$). Accurate representations of stimulus and recording electrode positions were recorded. Even at high stimulus intensities (> 300 μA) with two bipolar stimulus electrodes placed close to the cell, maximal EPSC amplitude was generally ≤ 50 pA, as compared to ≤ 400-500 pA in control slices taken from the same batch at the same time, incubated in the submersion chamber in the absence of the Ca^{2+} channel antagonists. Fig $7.1C_2$ shows typical EPSC traces recorded in control slices and in slices following 2 hrs pre-exposure to both CgTx and AgTx. Only very low amplitude EPSCs could be elicited following incubation in both toxins, suggesting extensive blockade of both N-type and P/Q-type Ca^{2+} channels, with a consequent large reduction in glutamate release elicited via extracellular stimulation of Schaffer

collaterals. Fig 7.1C_1 shows the time course of EPSCs recorded following 2 hrs pre-exposure to CgTx and AgTx. EPSCs generally ≤ 50 pA were recorded. The figure shows raw EPSC amplitudes in pA, since normalisation of such low values would produce widely scattered points. Addition of NiCl to block R-type Ca^{2+} channels caused a further reduction in EPSC amplitude, indicating that R-type channels make a small contribution to glutamate release at Schaffer collateral synapses onto CA1 stratum radiatum interneurons.

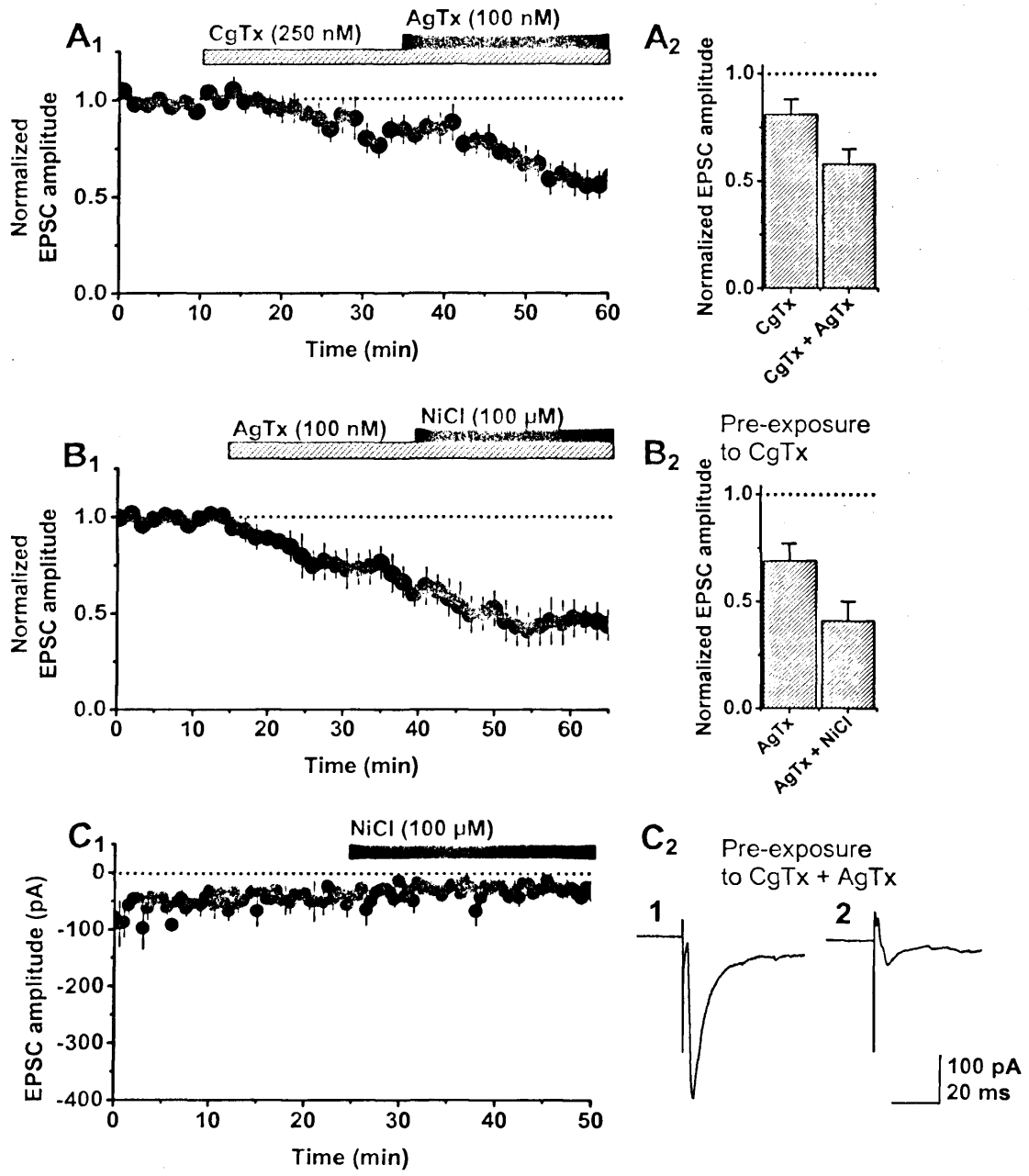

Figure 7.1 *Three series of control experiments were carried out in order to test the efficacy of selective Ca^{2+} blockers. The peptide toxins ω-Conotoxin GVIA (250 nM) and ω-Agatoxin IVA (100 nM) were used to block N-type channels and P/Q-type channels respectively.* ***$A_{1\&2}$.*** *CgTx and AgTx both induce depression of EPSCs. However, the substantial remaining EPSC component suggests an incomplete blockade of N-type and P/Q-type channels.* ***$B_{1\&2}$.*** *EPSCs are depressed by AgTx following two hour pre-exposure to CgTx. Once again the magnitude of the remaining EPSC component points towards an incomplete blockade of N-type and P/Q-type channels. A further depression of EPSCs is induced by NiCl, indicating a contribution of R-type Ca^{2+} channels to glutamate release.* ***C_1.*** *EPSCs are virtually abolished following two hour pre-exposure to both CgTx and AgTx. NiCl causes a slight further depression.* ***C_2.*** *EPSCs recorded in control slice (1) and following two hour pre-exposure to both CgTx and AgTx (2).*

Control experiments demonstrated that N-type and/or P/Q-type Ca^{2+} channels could be selectively blocked by a prolonged (≥ 2 hr) incubation in the peptide antagonist in a custom submersion chamber with constant gentle stirring. The objective of the subsequent series of experiments was to determine whether group I mGluR-mediated acute depression in CA1 interneurons involved a reduction in glutamate release from Schaffer collateral terminals via an action on presynaptic Ca^{2+} channels involved in vesicle exocytosis. DHPG was applied following selective blockade of N-type or P/Q-type Ca^{2+} channels. When N-type channels were blocked by 2 hrs pre-exposure to CgTx, DHPG evoked a depression of EPSCs to 63 ± 9 % of baseline ($p < 0.01$, $n = 6$; Fig 7.2A_1). This was not significantly different from the depression observed in control experiments (paired t test, $p < 0.01$). In contrast, when P/Q-type channels were blocked by 2 hrs pre-exposure to AgTx, the effect of DHPG was abolished: a non-significant depression to 92 ± 6% of baseline was observed ($p = 0.88$, $n = 7$; Fig 7.2B_1). Following pre-exposure to CgTx, DHPG caused an increase in PPR to 105 ± 7%, which did not reach significance (paired t test, $p = 0.10$; Fig 7.2A_2). This result is surprising, since an elevation in PPR would be expected to accompany the DHPG-induced depression of EPSC amplitude, based upon all other findings within this study. The probable explanation is that an increase in PPR occurred, but fell short of reaching statistical significance due to the relatively large standard deviation. Following pre-exposure to AgTx, DHPG did not produce any significant effect upon PPR (97 ± 5%, $p = 0.28$; Fig 7.2B_2).

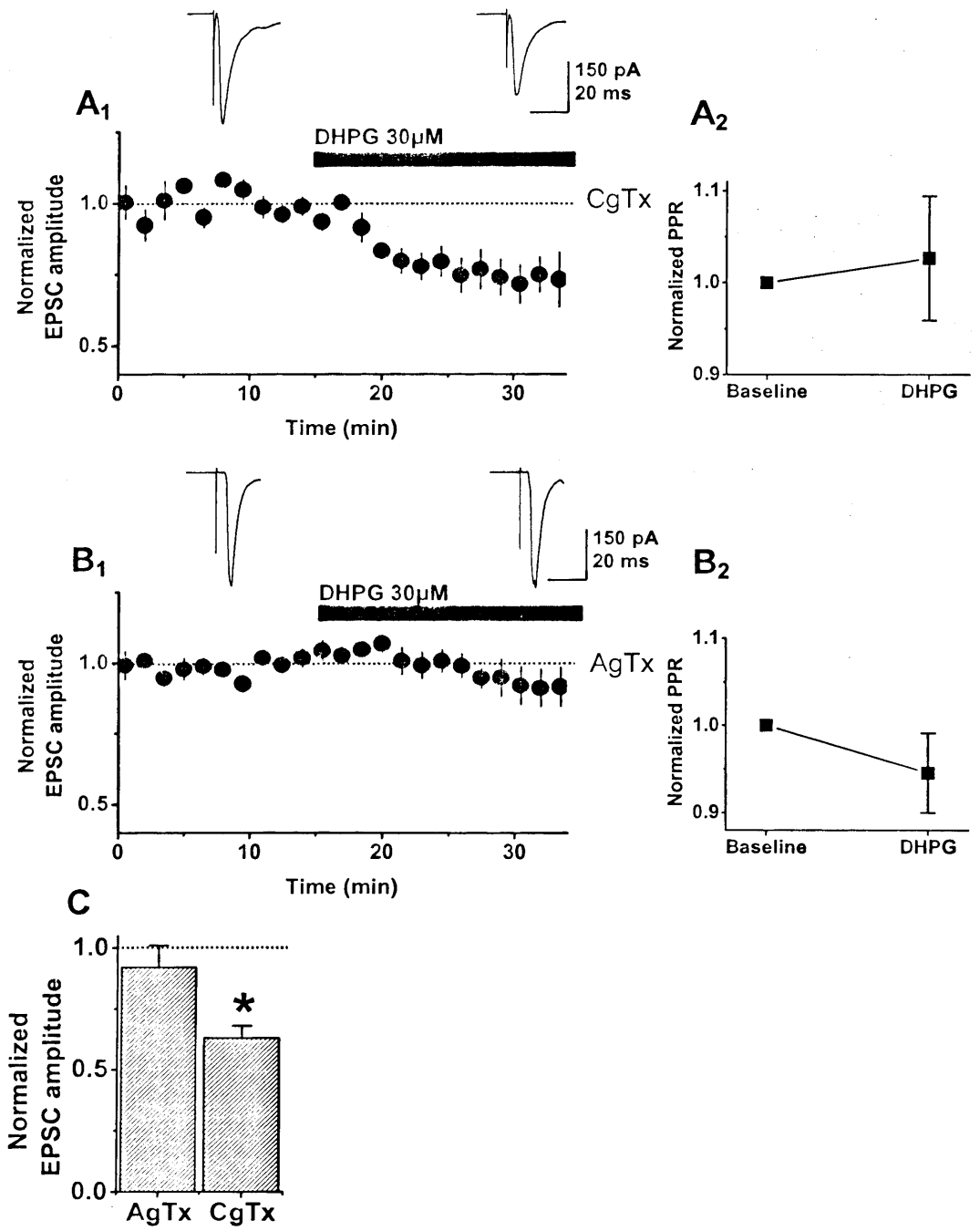

Figure 7.2 *Group I mGluR-mediated acute depression of synaptic transmission is occluded by blockade of P/Q-type but not N-type Ca^{2+} channels.* ***A,*** *Effect of DHPG on EPSC amplitude (± SEM) when applied following a two hour pre-incubation in the selective N-type Ca^{2+} channel blocker ω-conotoxin GVIA (CgTx) (n = 6).* ***B,*** *Effect of DHPG when applied following incubation in the selective P/Q-type Ca^{2+} channel blocker ω-agatoxin IVA (AgTx) (n= 7).* ***C,*** *Summary of results, showing mean EPSC amplitude in the presence of DHPG, normalized to baseline.*

7.4 Discussion

Initial control experiments demonstrated that application of CgTx followed by AgTx via the perfusion system did not result in a complete blockade of N-type and P/Q-type Ca^{2+} channels. The maximum total depression elicited by the combined effect of these two selective antagonists was 42 ± 7%. Previous studies have suggested that N-type and P/Q-type Ca^{2+} channels are almost entirely responsible for mediating the influx of Ca^{2+} into the presynaptic terminal that triggers release of neurotransmitter, with some residual contribution from R-type Ca^{2+} channels (see Wu and Saggau, 1997; Reid et al., 2003). Thus the maximum total depression expected if CgTx and AgTx fully blocked their target Ca^{2+} channels would be closer to 90%. Previous studies by Poncer et al. (1997; 2000) using paired recordings combined with selective peptide Ca^{2+} channel antagonists have shown that, at GABAergic synapses in the hippocampus, transmitter release is triggered entirely by either N-type or P/Q-type channels, depending upon the identity of the interneuron. IPSPs (inhibitory postsynaptic potentials) generated by interneurons located in stratum radiatum were fully abolished by the N-type Ca^{2+} channel antagonist ω-conotoxin MVIIA, while IPSPs generated by interneurons in stratum lucidum and stratum oriens were entirely blocked by the P/Q-type Ca^{2+} channel antagonist ω-agatoxin IVA. As discussed previously, excitatory synaptic connections onto hippocampal interneurons are a poorly described class of synapse, and the presynaptic Ca^{2+} channels involved in mediating glutamate release have not yet been characterised. If similar mechanisms operate at both glutamatergic and GABAergic synapses, it may be expected that glutamate release would be triggered entirely by either N-type or P/Q-type channels, and that N-type channels would be responsible in stratum radiatum interneurons (Poncer et al., 1997; 2000). If this were the case, only one of the selective Ca^{2+} channel antagonists would have been effective, and would have suppressed EPSCs almost to baseline. On the other hand, studies on excitatory synapses in autaptic cultures prepared from hippocampal pyramidal cells have demonstrated non-uniform

distribution of N-type and P/Q-type channels, even at terminals originating from the same afferent (Reid et al., 1997). However, these experiments were carried out in autaptic cultures, and no studies have been performed at excitatory connections onto interneurons in hippocampal slices. The composition of the population of presynaptic Ca^{2+} channels involved in mediating glutamate release, and their distribution at presynaptic terminals, are therefore unknown. In the present study, both CgTx and AgTx elicited some depression of EPSCs. There is extensive evidence for widespread variation in both morphological and functional properties between glutamatergic and GABAergic synapses. It is therefore entirely possible that both N-type and P/Q-type channels are responsible for triggering glutamate release at excitatory connections onto CA1 stratum radiatum interneurons. A bimodal distribution of results was not observed, lending no support to the hypothesis that only one type of channel is responsible for mediating glutamate release at connections onto distinct interneuron subtypes. The combined effect of both toxins did not depress EPSCs to baseline following a 50 min exposure to CgTx and 25 min exposure to AgTx. It is possible that an increased depression would have been observed with longer exposure to the antagonist, potentially reaching ≥ 90% if sufficient recording time were allowed (e.g. one hour in each toxin). However, this raises the technical difficulty of making extremely long-duration patch clamp recordings, especially given that further experimentation with mGluR-selective drugs was necessary once blockade of presynaptic Ca^{2+} channels had been successfully established. The relatively low total depression elicited by the two toxins suggests an incomplete blockade of presynaptic N-type and P/Q-type Ca^{2+} channels (see Wu and Saggau, 1997; Reid et al., 2003). This was likely to be due to poor penetration of the high molecular weight peptide toxins into the slice tissue. This problem was compounded by variation in the depth of the recorded neuron within the slice. All neurons from which patch clamp recordings were made are in the relatively superficial layers of the slice, due to limitations of visualisation of neurons under DIC microscopy, and penetration of the patch pipette through the tissue. However, there was still considerable variation in the depth of the

soma of the recorded cell within the slice. If there are limitations upon how far the peptide toxins can penetrate into the tissue, there is likely to be some correlation between the magnitude of depression of transmitter release, and the depth of the neuron within the slice. This represented a clear source of error, and an improved experimental design which allowed for maximal blockade of target Ca^{2+} channels by CgTx and AgTx was required. Pre-incubating slices for a prolonged period (2 hours) in a submersion chamber with a small volume of ACSF containing peptide selective Ca^{2+} channel antagonists overcame the difficulty of long exposures being required in order to achieve blockade of Ca^{2+} channels, by allowing increased time for the toxins to penetrate through the tissue and access their target Ca^{2+} channels. Constant stirring of the ACSF within the chamber also assisted in circulation of the toxins within the tissue. However, since electrophysiological recordings were not being made during application of the antagonists, it was impossible to follow and quantify blockade of the Ca^{2+} channels. Following exposure to only one antagonist (either CgTx or AgTx), the extent of the blockade could not be confirmed, since Ca^{2+} influx occurred through the remaining channel type, and EPSCs could still be evoked via extracellular stimulation. It is impossible to determine the degree to which one subtype may compensate for blockade of the other. When slices were pre-exposed for 2 hrs to both CgTx and AgTx, EPSCs were virtually abolished, and could not be evoked when recording from several cells across numerous slices, even when the stimulus electrode was re-positioned multiple times within CA1 stratum radiatum (see Fig $7.1C_2$). These observations would suggest that application of CgTx and AgTx via prolonged exposure in the submersion chamber resulted in successful blockade of target N-type and P/Q-type Ca^{2+} channels. However, this type of control experiment is considerably less direct and robust than monitoring blockade of Ca^{2+} channels via continuous electrophysiological recording. When blocking only one type of channel via pre-exposure to the selective peptide antagonist in the submersion chamber, it was impossible to confirm that the channel had been fully blocked, since EPSCs would still be evoked due to glutamate release elicited via entry of Ca^{2+} via the other type of

channel. Nevertheless, given the technical constraints encountered, this experimental design was selected as the best available under the circumstances. To enhance reliability of the data, use of knockout mice for either N-type or P/Q-type Ca^{2+} channels would provide a substrate for testing efficacy of subtype-selective antagonists.

The control experiments carried out using prolonged pre-incubations in either CgTx or AgTx in the submersion chamber suggested that either N-type or P/Q-type channels (or both types) could be entirely blocked by a two hour pre-exposure in one of the peptide toxins. Slices in which one population of presynaptic Ca^{2+} channels had been entirely blocked in this way were subsequently transferred to the recording chamber, with continued application of the specific peptide Ca^{2+} channel antagonist via the perfusion system throughout the experiment. Following recording of a stable EPSC baseline, DHPG was applied for 20 min in order to determine whether the magnitude of group I mGluR-mediated acute depression was affected by blockade of N-type or P/Q-type Ca^{2+} channels. Blockade of N-type Ca^{2+} channels by 2 hr pre-exposure to CgTx resulted in a large depression of EPSCs in response to DHPG, which was not significantly different in magnitude from control experiments (Fig 7.2A_1). In contrast, blockade of P/Q-type Ca^{2+} channels by 2 hr pre-exposure to AgTx fully abolished DHPG-induced depression of EPSCs (Fig 7.2B_1; data summarized in Fig 7.2C). The results presented in this study argue that N-type Ca^{2+} channels are not the target of the cascade leading from group I mGluR activation. Instead they are consistent with the hypothesis that postsynaptic group I mGluR activation in CA1 stratum radiatum interneurons leads to inhibition of presynaptic P/Q-type Ca^{2+} channels at Schaffer collateral axon terminals via a retrograde signal, resulting in a decrease in glutamate release and hence a reduction in EPSC amplitude. However, these findings should be interpreted with caution, because an effect on transmitter release independent of any modulation of Ca^{2+} channels could give the same result if P/Q-type channels co-localized with a sub-population of release sites that were

sensitive to group I mGluRs – see Rusakov et al., (2004). One interesting aspect of these findings is that DHPG-induced depression of EPSCs was not significantly greater than in control studies when N-type Ca^{2+} channels were blocked by pre-incubation in CgTx. If the effects of group I mGluR activation were mediated by depression of glutamate release via inhibition of exclusively P/Q-type Ca^{2+} channels, then an almost total attenuation of EPSC amplitude would be expected in response to DHPG application when only P/Q-type channels were left intact due to blockade of N-type channels by CgTx. This result remains unexplained, but suggests that presynaptic boutons do not simply fall into two classes, i.e. those that use N-type Ca^{2+} channels and are insensitive to DHPG and those that use P/Q-type channels and are sensitive.

Despite the uncertainty surrounding the retrograde factor, the present study implies that DHPG-induced depression in CA1 interneurons is expressed through a presynaptic mechanism. It persisted when N-type channels were blocked, but was occluded when P/Q-type channels were blocked. The preferential involvement of P/Q-type channels is unexpected because N-type Ca^{2+} channels are more usually implicated as downstream targets in cascades involving modulation of synaptic transmission. CB1 receptor agonists have been argued to act on N-type channels at GABAergic terminals (Wilson et al., 2001). Previous studies have also demonstrated that N-type Ca^{2+} channels are considerably more sensitive to G protein modulation than P/Q-type channels (Zhang et al., 1996; Currie and Fox, 1997). Furthermore, N-type channels, rather than P/Q-type channels, have been identified as major targets in group III mGluR modulation of synaptic transmission (Millan and Sanchez-Prieto, 2002; 2002a; Millan et al., 2002b; 2003; Rusakov et al., 2004). However, the previous evidence that endocannabinoids act on N-type channels in hippocampal interneurons is based on occlusion experiments, which are open to alternative interpretation, and direct evidence that Ca^{2+} influx is reduced has not been reported (Rusakov et al., 2004). Furthermore, although N-type Ca^{2+} channels have been strongly implicated as

the main targets in group III mGluR modulation of synaptic transmission (Millan and Sanchez-Prieto, 2002; 2002a; Millan et al., 2002b; 2003; Rusakov et al., 2004), functional coupling between group I mGluRs and presynaptic Ca^{2+} channels is less well understood. Group I mGluR activation has been shown to inhibit presynaptic Ca^{2+} currents in the neocortex (Choi and Lovinger, 1996) and basal ganglia (Stefani et al., 1998). Studies in *Xenopus* oocytes have shown that N-type Ca^{2+} channels are sensitive to modulation by mGluR5a (Sanchez-Prieto et al., 2004). An important recent study by Kitano et al. (2003) demonstrated that mGluR1a and the pore forming $Ca_v2.1$ subunit of P/Q-type Ca^{2+} channels are strongly co-localised in cultured rat brain cerebellar Purkinje neurons, and when co-expressed in heterologous expression systems (COS-7 cells). This association occurred via direct interaction between the C-terminal intracellular domains of the two proteins. Activation of mGluR1a via DHPG application resulted in a strong inhibition of Ca^{2+} influx via P/Q-type channels, as demonstrated by fluorescent Ca^{2+} imaging and whole-cell electrophysiological recordings. The study of Kitano et al. (2003) therefore provides strong evidence for functional coupling between group I mGluR activation and inhibition of Ca^{2+} influx specifically via P/Q-type channels. Although such mechanisms have not yet been demonstrated in the hippocampus, it remains entirely possible that at glutamatergic synaptic connections onto CA1 stratum radiatum interneurons, group I mGluRs couple preferentially to P/Q-type, rather than N-type, Ca^{2+} channels in order to bring about a reduction of Ca^{2+} influx into the presynaptic terminal, with consequent inhibition of neurotransmitter release. However, this functional coupling may not necessarily involve a direct physical interaction, since anatomical evidence strongly supports predominantly postsynaptic expression of group I mGluRs in the hippocampus (Martin et al., 1992; Baude et al., 1993; Lujan et al., 1996; Shigemoto et al., 1997; Lujan et al., 1997; Petralia et al., 1997; Lopez-Bendito et al., 2002).

Chapter 8. Group I mGluR-mediated heterosynaptic depression in CA1 interneurons

8.1 Introduction

Group I mGluRs are involved in mediating both short- and long-term synaptic plasticity. Group I mGluR-mediated LTD has been characterised in CA1 pyramidal cells (e.g. Palmer et al., 1997; Overstreet et al., 1997; Fitzjohn et al., 2001; Huang and Hsu, 2005; see Chapter 1, Section 1.4.5.3). Despite their possible role in LTD, previous studies have suggested that group I mGluRs do not contribute to long-term potentiation in stratum radiatum interneurons (Perez et al., 2001; Lapointe et al., 2004). In the present study, robust group I mGluR-evoked LTD was not observed in CA1 stratum radiatum interneurons, except when mGluR1 was blocked using LY367385, allowing mGluR5 to be selectively activated by DHPG application (Chapter 5, Section 5.3.6). Synaptic stimulation protocols such as prolonged low-frequency activity that might induce a form of use-dependent mGluR-mediated LTD were therefore not pursued exhaustively. Instead, evidence was sought that glutamate release in a separate afferent pathway could mimic the effect of exogenous agonist application. Within this thesis, a more relevant issue than long-term synaptic plasticity is whether group I mGluR-mediated acute depression contributes to short-term heterosynaptic interactions. An important question regarding the physiological role of group I mGluR-mediated acute depression of excitatory synaptic transmission to CA1 interneurons is whether the effect of DHPG can be mimicked by synaptic release of the endogenous ligand glutamate. If so, it is necessary to determine whether glutamate released from one Schaffer collateral terminal can activate group I mGluRs at other, nearby independent synaptic connections onto CA1 interneurons, causing depression of excitatory transmission.

The classical view of fast chemical synaptic transmission was that neurotransmitter molecules act locally upon postsynaptic receptors and are cleared rapidly from the synaptic cleft within a few milliseconds, both by diffusion and specific

re-uptake mechanisms. Many ionotropic receptors have relatively low affinities for their endogenous agonist, and together with the fact that rapid clearance by specific transporters restricts the spread of neurotransmitter, synaptic transmission was thought to occur in a simple point-to-point fashion. However, there is now extensive evidence that diffusion of glutamate from the synaptic cleft can activate receptors at other nearby synapses. This phenomenon is known as spillover, and is responsible for cross-talk between neighboring synapses (Asztely et al., 1997; Rusakov and Kullmann, 1998; Semyanov and Kullmann, 2000; Arnth-Jensen et al., 2002; Scimemi et al., 2004). Glutamate spillover has been shown to lead to activation of inhibitory presynaptic mGluRs at other synapses located close to the original release site. This phenomenon has been demonstrated at glutamatergic mossy fibre synapses in the hippocampus (Scanziani et al., 1997; Vogt and Nicoll, 1999); at GABAergic synapses in the cerebellum (Mitchell and Silver, 2000); and among interneuron networks in the CA1 subfield of the hippocampus (Semyanov and Kullmann, 2000). Given that different classes of synapse vary widely in functional properties and expression of pre- and postsynaptic neurotransmitter receptors, it is important to determine whether group I mGluR-mediated depression of EPSCs at excitatory connections onto CA1 interneurons could be evoked by spillover of glutamate from nearby synapses. This would shed further light upon the physiological role of group I mGluRs within the hippocampal network.

The aim of the projects discussed in this chapter was to determine whether the effects of the exogenous selective group I mGluR agonist DHPG upon excitatory transmission to CA1 interneurons could be reproduced by endogenously released glutamate. A number of experimental protocols were tested, which were designed to activate group I mGluRs using stimulus-evoked glutamate release at Schaffer collateral connections onto CA1 stratum radiatum interneurons. The main objective was to examine heterosynaptic effects; that is, to attempt to activate group I mGluRs via spillover of glutamate released from an independent Schaffer collateral pathway. This would determine whether the powerful modulatory effect upon excitatory synaptic

transmission to CA1 interneurons revealed using the potent exogenous agonist DHPG could be reproduced by release of the endogenous ligand glutamate; and demonstrate whether there were any differences in the properties of the modulatory effect when elicited in this way.

8.2 Methods

Whole-cell voltage-clamp recordings of pharmacologically-isolated AMPA EPSCs were obtained from CA1 stratum radiatum interneurons as described previously (Chapter 2; also Chapter 5, Section 5.2). CGP52432 (5 μM) was included in order to block $GABA_B$ receptors, which have been shown to mediate long-range heterosynaptic actions in the hippocampus (Isaacson et al., 1993), and could thus potentially lead to complications in interpretation of results. A two-pathway experimental design was used (Fig 8.1C). Both stimulus electrodes were positioned within CA1 stratum radiatum to activate Schaffer collaterals. Stimulus intensity was adjusted so that evoked EPSC amplitude was the same from both pathways. EPSC amplitude was 250-300 pA in most experiments. One stimulating electrode (the test pathway, A) was positioned to generate single EPSCs in interneurons, followed by paired EPSCs so that PPR could be determined, followed by a calibration pulse in each recording cycle. The second stimulus electrode was used to deliver trains of stimuli to an alternate, independent pathway (the conditioning pathway, B). The aim was to elicit substantial glutamate release from the independent conditioning pathway, and determine whether spillover would activate group I mGluRs in the test pathway.

Two experimental designs were tested. The first involved brief trains of stimuli (5 pulses at 50 Hz) delivered to the conditioning pathway within each duty cycle, in order to determine whether spillover of glutamate from this pathway affected the amplitude of single EPSCs and PPR in the test pathway. The second experimental design involved recording a long baseline of 20 minutes, with single and paired stimuli

delivered to the test pathway in each duty cycle. Single stimuli were also delivered to the conditioning pathway in each duty cycle to confirm that EPSCs of consistently the same amplitude were elicited. Following a 20 min baseline, a single tetanic stimulation of 100 pulses at 100 Hz was delivered to the conditioning pathway, in order to evoke a large release of glutamate from presynaptic Schaffer collateral terminals, thereby raising ambient glutamate concentration within the extracellular space. This single dramatic elevation in glutamate concentration may thus increase activation of modulatory receptors at connections within the test pathway. A further 20 min was then recorded, in order to determine whether tetanic stimulation of the conditioning pathway altered EPSC amplitude in the test pathway.

Cross paired-pulse analysis was used to verify that both pathways were fully independent. The degree to which test and conditioning pathways were independent was assessed by looking for paired-pulse cross-facilitation. In each recording, prior to running the main experimental protocol, a separate protocol was used to assess cross-paired pulse facilitation. Results were determined from the average of 30 cycles (25 sec per cycle, total 12.5 minutes). Each duty cycle comprised paired pulses at 20 Hz delivered to the test pathway (A) and conditioning pathway (B) in the following order: AA, BB, AB, BA. If test and conditioning pathways were fully independent, paired-pulse facilitation should be observed within each pathway, but not when a pulse was delivered following a stimulus to the other pathway (Fig 8.1E). Cells were rejected if cross-paired pulse analysis did not demonstrate that test and conditioning pathways were fully independent.

8.3 Results

8.3.1 Heterosynaptic depression of glutamatergic transmission to CA1 interneurons is not induced by short conditioning bursts to an independent Schaffer collateral pathway

In investigating whether heterosynaptic depression could be evoked at excitatory connections onto CA1 interneurons, the first experimental design tested was an adaptation of a protocol previously shown to elicit heterosynaptic depression of IPSCs in CA1 interneurons by group III mGluRs via glutamate spillover (Semyanov and Kullmann, 2000). The objective of this set of experiments was to determine whether relatively small amounts of glutamate released by a brief stimulus train to an independent Schaffer collateral pathway would activate group I mGluRs within a short time interval. Single and paired EPSCs were elicited in the test pathway by the first stimulus electrode. The second stimulus electrode was used to deliver a short burst of 5 stimuli at 50 Hz to the conditioning pathway. This was followed by a single stimulus to the test pathway after a short delay to elicit a single EPSC (Fig 8.1A & B). Control trials and trials with conditioning stimuli were interleaved within in each duty cycle. The delay between conditioning train and test stimulus was 100 ms. The duty cycle was as follows: (i) single stimulus to test pathway; (ii) paired stimuli at 20 Hz to test pathway to examine PPR; (iii) single stimulus to test pathway, preceded by 5 pulses at 50 Hz to conditioning pathway with 100 ms interval; (iv) no stimuli; (v) calibration pulse. Inter-trial interval was 5 s, giving a 25 s duty cycle. Evoked EPSC amplitude varied between cycles in all experiments carried out in this project. In other words, there was a small variation in EPSC amplitude in response each stimulus, even though stimulus intensity remained fixed. This variability results mainly from probabilistic quantal glutamate release. However, comparing amplitudes of control EPSCs with EPSCs following the conditioning train within each individual cycle would not yield accurate results, since any heterosynaptic effects may be obscured by this natural variation. The time course showing EPSC amplitude throughout the experiment is therefore not shown. Instead, it was necessary to record as many data points as possible and compare mean values for test EPSC amplitude in control and

conditioning trials over the entire experiment. The mean amplitude of the single EPSC in the test pathway was compared with and without prior delivery of the conditioning burst, in order to determine whether the stimulus burst to the conditioning pathway altered EPSC amplitude in the test pathway. A 30 min baseline (25 sec per cycle, total 72 cycles) was recorded in the presence of DL-APV (50 μM), picrotoxin (100 μM) and GCP52432 (5 μM) to record isolated AMPA currents in the usual manner, in order to determine whether any heterosynaptic effects occurred in the absence of pharmacological agents acting upon neurotransmitter systems involved in modulation of synaptic transmission. Following the 30 min baseline, all mGluRs were blocked using the selective group III mGluR antagonist MSOP (100 μM) together with MCPG (500 μM), which acts as an antagonist at group I and II mGluRs (Schoepp et al., 1999). A further 30 min (72 cycles) was recorded in the presence of the mGluR antagonists. Blocking all mGluRs would indicate whether there was any effect upon heterosynaptic depression mediated by this class of modulatory receptor. If any change in heterosynaptic depression was observed, the individual mGluR subtypes involved could be identified in subsequent experiments using more selective pharmacological agents.

$EPSC_{Test}$ refers to cycles in which the EPSC in the test pathway (A) was preceded by a stimulus burst in the conditioning pathway (B); $EPSC_{Control}$ refers to cycles in which no stimuli were delivered to the conditioning pathway. With a 100 ms interval between conditioning burst and test stimulus, the mean ratio of $EPSC_{Test}/EPSC_{Control}$ was 90 ± 9%. This depression of test EPSCs relative to control was non-significant (paired t test, $p = 0.15$, $n = 5$, Fig 8.1D). This result fell only just short of reaching statistical significance, suggesting that a small heterosynaptic depression may be induced by activation of mGluRs by relatively small amounts of glutamate released by a brief stimulus train to an independent Schaffer collateral pathway. Subsequently, experiments were carried out in the presence of the mGluR antagonists MCPG (500 μM) and MSOP (100 μM). During the subsequent 30 min of

the recording, the mean ratio of $EPSC_{Test}/EPSC_{Control}$ was 95 ± 7%. This effect was not significant (p = 0.49, n = 5, Fig 8.1D). The effect of mGluR antagonists on the ratio of $EPSC_{Test}/EPSC_{Control}$ was not significant (paired t test, p = 0.15, n = 5).

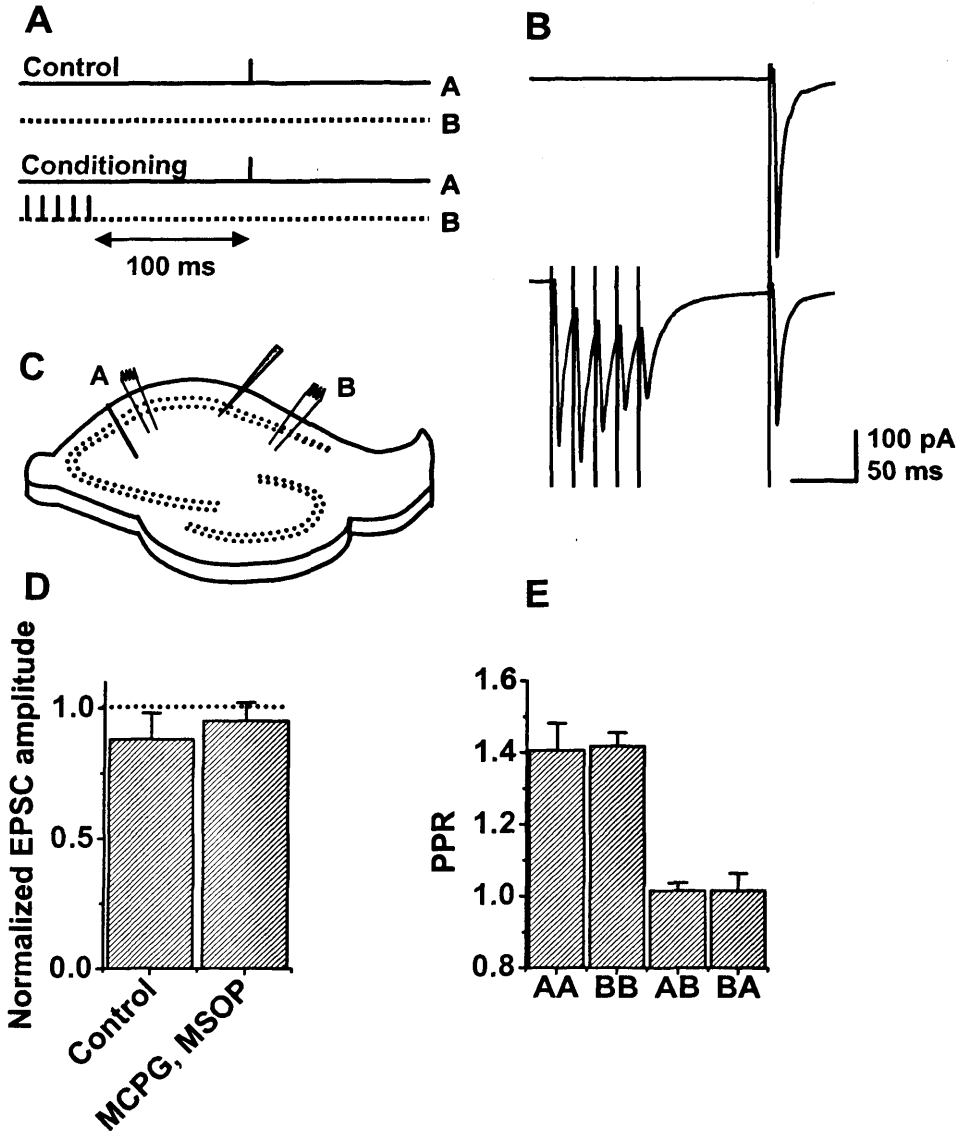

Figure 8.1. *Glutamate release elicited by five conditioning pulses in each recording cycle did not elicit heterosynaptic depression.* ***A,*** *In control trials, a single EPSC was evoked in the test pathway (A) only. In conditioning trials, the test EPSC was preceded by a burst of 5 stimuli at 50 Hz to evoke EPSCs in the independent conditioning pathway (B), thereby raising the ambient glutamate concentration within the extracellular space. The interval between conditioning burst (pathway B) and test EPSC (pathway A) was 100 ms (represented by arrow). Control and conditioning trials were delivered within each duty cycle (total 144 cycles per experiment).* ***B,*** *Representative sample traces from a single neuron, showing control and conditioning trials (averages of 20 cycles).* ***C,*** *Schematic representation of transverse hippocampal*

slice, showing position of recording and stimulus electrodes. ***D,*** *Mean values (± SEM) for EPSC amplitude in test pathway (A) following conditioning burst, normalised by mean value of control trials. A small heterosynaptic depression of EPSCs was detected in the test pathway, but did not reach significance. The magnitude was reduced very slightly when all 8 mGluR subtypes were blocked using MCPG (500 μM) and MSOP (100 μM), but the difference was not significant.* ***E,*** *Mean values (± SEM) for PPR. Cross paired-pulse analysis was used as a criterion to confirm that test and conditioning pathways were independent. Paired-pulse facilitation (PPF) occurred within each pathway (AA, BB), but paired-pulse stimulation across pathways (AB, BA) did not affect paired-pulse ratio (PPR ≈ 1), confirming that test and conditioning pathways were independent. Cells were rejected if stimulation of one pathway significantly affected PPR in the other.*

8.3.2 The excitatory amino acid transporter antagonist TBOA caused experimental difficulties, and did not enhance heterosynaptic effects

Experiments described in the previous section indicated that no apparent heterosynaptic effects were evoked by a short burst of stimuli to the conditioning pathway, followed after a 100 ms interval by a single EPSC to the test pathway. One possible explanation is that the increased level of glutamate released in response to the conditioning stimulus was rapidly cleared from the extracellular space by uptake via excitatory amino acid transporters (EAATs), before diffusion of glutamate to nearby synapses and activation of mGluRs in the test pathway could take place. There is substantial evidence that increasing glutamate availability in the extracellular space through inhibition of EAATs enhances spillover and consequent mGluR-mediated heterosynaptic effects (Semyanov and Kullmann, 2000; Brasnjo and Otis, 2001; Zhang and Sulzer, 2003; Marcaggi et al., 2003; see Discussion). The aim of the experiments described in this section was therefore to block EAATs, prolonging the availability of glutamate released in response to the conditioning burst within the extracellular space. It was proposed that inhibition of glutamate re-uptake may lead to enhanced diffusion of neurotransmitter to nearby synapses (spillover), and thus an increased probability of detecting mGluR-mediated heterosynaptic effects in the independent test pathway.

Five subtypes of EAATs (EAAT1-5) have been cloned from mammalian tissues. EAAT1 and EAAT2 have the greatest impact on clearance of glutamate released during neurotransmission, and are abundantly expressed in the plasma membranes of glial cells at excitatory synaptic connections (Seal and Amara, 1999; Amara and Fontana, 2002; Shigeri et al., 2004; see Discussion). TBOA is a competitive, non-transportable blocker which is highly selective for the EAAT1 and EAAT2 transporter subtypes (Shimamoto et al., 1998; Shigeri et al., 2004). TBOA was bath applied at a concentration of 50 μM. The duty cycle was identical to that used in the previous series of experiments (Section 8.3.1) - (i) single stimulus to test pathway; (ii) paired stimuli at 20 Hz to test pathway to examine PPR; (iii) single stimulus to test pathway, preceded by 5 pulses at 50 Hz to conditioning pathway; (iv) no stimuli; (v) calibration pulse. Inter-trial interval was 5 s, giving a 25 s duty cycle. The delay between conditioning train and test stimulus was 100 ms. Experiments had a total recording duration of 60 min, and were carried out as follows: (i) 20 min baseline; (ii) 20 min in the presence of TBOA, to determine whether blockade of EAAT1 and EAAT2 affected the magnitude of heterosynaptic effects induced by the 5 pulse conditioning train; (iii) 20 min in the presence of TBOA, MCPG and MSOP, to determine whether blockade of all 8 mGluR subtypes affected heterosynaptic effects.

TBOA application caused a number of experimental difficulties. Whole-cell voltage clamp recordings were made from a total of 7 CA1 stratum radiatum interneurons in this set of experiments. Recordings were entirely stable in terms of I_{hold}, R_S and EPSC amplitude during the baseline period. Bath application of TBOA (50 μM) appeared to be responsible for loss of recording in 4 of 7 cells (57% of cells overall). Within 2 to 6 min of TBOA application, dramatic elevations in EPSC amplitude were observed, together with alterations in EPSC kinetics. EPSC amplitude became larger and highly variable between stimuli. EPSC kinetics were also markedly altered, changing from smooth curves with rapid return to baseline, indicating clean monosynaptic EPSCs; to slower currents with jagged decay (suggesting polysynaptic

effects) and much slower return to baseline. These alterations to stimulus-evoked EPSCs were shortly followed within 1 to 4 min by a large increase in I_{hold}, resulting in loss of the whole-cell recording (n = 4 of 7 cells). These effects were clearly attributable to the effects of TBOA, given that the cells were entirely stable for over 20 min prior to application of the drug, and recordings were lost within 2 to 6 min of TBOA application. In 3 of 7 cells, these effects did not occur, and the 60 min experiment was completed. However, TBOA application nonetheless caused a serious problem which prevented meaningful interpretation of the results. In the absence of TBOA, EPSC amplitude returned to baseline following the conditioning burst of 5 stimuli to pathway B, such that the amplitude of the subsequent single EPSC to the test pathway (A) which followed after 100 ms was measured from baseline (Fig 8.2A_1). In the presence of TBOA, EPSC amplitude was markedly altered, even in cells which did not experience a large jump in I_{hold} with consequent loss of the recording. Blockade of EAAT1 and EAAT2 increased the ambient glutamate concentration in the extracellular space, blocking uptake by these transporters in the plasma membrane of astrocytes close to the excitatory synapse. This resulted in dramatically increased short-term potentiation during the conditioning burst, and a slowing of the return of EPSC amplitude towards baseline (Fig 8.2A_2). With a 100 ms interval between conditioning burst and test EPSC, the amplitude had not returned to baseline. The single EPSC evoked in the test pathway (A) therefore occurred during the decay of the 5 pulse conditioning train evoked in the conditioning pathway (B). It was impossible to accurately determine the amplitude of the test EPSC and compare with control, since it was not measured from baseline. Control and conditioning trials were delivered during each duty cycle. The single test EPSC to pathway A was measured from baseline during control trials, since it was not preceded by a conditioning stimulus burst to pathway B. However, during conditioning trials, the test EPSC to pathway A occurred during decay of the conditioning burst EPSCs from pathway B. This decay was greatly lengthened by blockade of EAAT1 and EAAT2 by TBOA. Since the amplitude of the single test EPSC to pathway A was

thus not measured from baseline in conditioning trials, interpretation of the results from experiments in the presence of TBOA was impossible. Test EPSC amplitude could not be accurately compared between control and conditioning trials. It was therefore impossible to detect any heterosynaptic effects induced by the 5 pulse conditioning burst when glutamate uptake was blocked using TBOA. The interval between conditioning burst and test EPSC was increased from 100 ms to 250 ms, in order to determine whether EPSC amplitude would return to baseline following the conditioning burst with this longer interval. Following a 20 min baseline, CA1 stratum radiatum interneurons were exposed to TBOA for 30 min, using the 250 ms interval throughout the experiment (n = 3). In all 3 cells, EPSC amplitude did not return to baseline during the 250 ms following the 5 pulse conditioning burst to pathway B (Fig $8.2B_{1\&2}$). Even with this extended interval, analysis of heterosynaptic effects induced by the 5 pulse burst to the independent conditioning pathway therefore remained impossible.

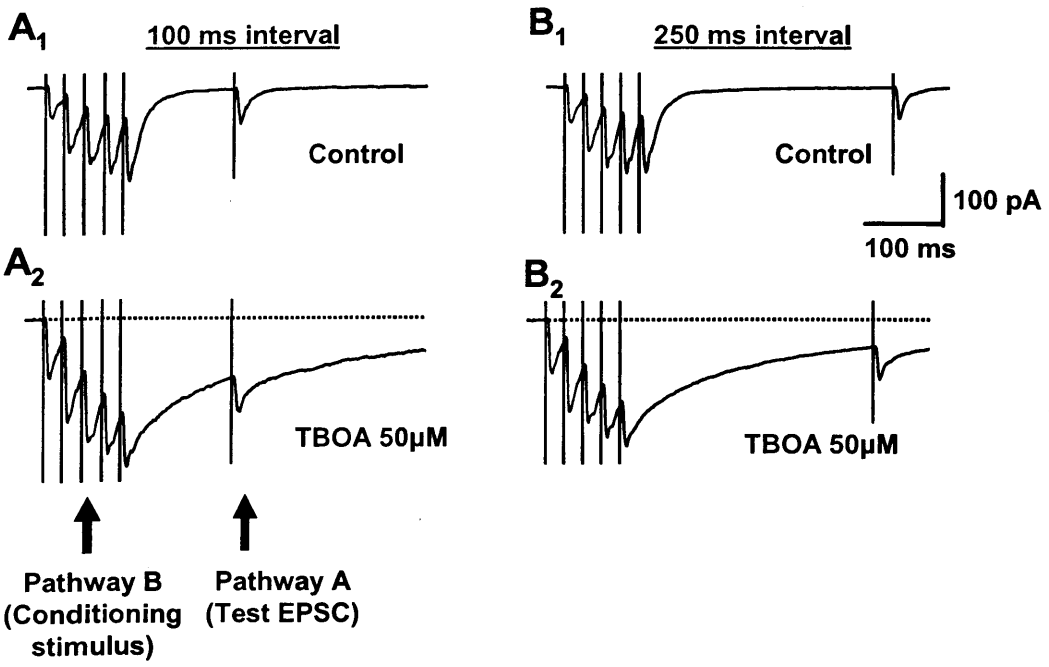

Figure 8.2 *Traces from experiments which aimed to induce heterosynaptic depression of glutamatergic transmission to CA1 interneurons in a test pathway (A) by delivering conditioning trains of five stimuli to an independent conditioning pathway (B).* ***A_1,*** *EPSC amplitude returned to baseline during the 100 ms interval between conditioning burst (pathway B) and single test EPSC (pathway A).* ***A_2,*** *When glutamate concentration in the extracellular space was raised by blocking uptake using the selective EAAT1 and EAAT2 antagonist TBOA (50 µM), short-term potentiation of EPSCs during the conditioning train was much greater, and EPSC amplitude did not return to baseline during the 100 ms interval (dotted line shows baseline). The single test EPSC (pathway A) was delivered during return of EPSCs towards baseline, making interpretation of the results impossible.* ***$B_{1\&2}$,*** *A similar difficulty was encountered even when the interval between conditioning burst and test EPSC was increased to 250 ms.*

8.3.3 Heterosynaptic depression was induced in the test pathway by a single tetanic stimulus to the independent conditioning pathway

A second experimental design was tested in order to determine whether heterosynaptic depression could be induced at excitatory synaptic connections onto CA1 stratum radiatum interneurons. An alternative strategy was employed in order to evoke a large release of glutamate from the conditioning pathway (B), which may then activate mGluRs in the independent test pathway (A). Rather than delivering a short burst of 5 stimuli in each cycle, a single large tetanic conditioning stimulus of 100 pulses at 100 Hz was delivered to pathway B once during the experiment, and the

effect upon EPSC amplitude in pathway A monitored. Following a 20 min baseline, the conditioning tetanus was delivered in a single cycle and the subsequent 20 min were recorded. The duty cycle was as follows: (i) single stimulus to test pathway (A); (ii) paired stimuli at 20 Hz to test pathway (A) to examine PPR; (iii) single stimulus to conditioning pathway (B); (iv) no stimuli; (v) calibration pulse. Inter-trial interval was 5 s, giving a 25 s duty cycle. Although the aim of the experiment was not to investigate the effect of the conditioning tetanus on pathway B, it was nonetheless important to ensure stability of the conditioning pathway during the baseline period by delivering a single stimulus in each duty cycle, in order to confirm that monosynaptic EPSCs of consistent amplitude were evoked. A stable baseline in both pathway A and B was thus one of the criteria for a successful experiment. Homosynaptic depression was not investigated because in the conditioning pathway, the stimulus protocol would inevitably evoke a number of phenomena which would preclude accurate analysis of the data. These include use-dependent forms of synaptic plasticity such as post-tetanic potentiation and synaptic depression, and effects mediated by release of endocannabinoids and/or adenosine.

Tetanic stimulation of the conditioning pathway evoked a small but significant heterosynaptic depression, which persisted for approximately 5-6 minutes. This was preceded by a larger, non-specific depression, which was evoked as a result of the powerful tetanic stimulation of the conditioning pathway. The non-specific depression subsided within 2 minutes following the tetanus. For this reason, the period of +20 to +22 minutes overall during the experiment (4 cycles) was not included in the analysis of the magnitude of the specific heterosynaptic depression (the tetanus was delivered at +20 minutes). The magnitude of heterosynaptic depression in each interneuron was determined by taking the mean EPSC amplitude for a 5 minute period (12 cycles) from 3 to 8 minutes following the tetanus (i.e. +23 to +28 minutes). The mean of this value across all cells was then calculated to determine the overall magnitude of depression. The EPSC amplitude following tetanus was 85 ± 4% of baseline ($p <$

0.05, n = 6; Fig 8.3A_1). This is consistent with group I mGluR-mediated heterosynaptic depression. However, an alternative interpretation of this result is that glutamate acts on group III, as opposed to group I, mGluRs. These receptors have been shown to modulate Schaffer collateral inputs to CA1 interneurons (Scanziani et al., 1998), and to mediate a short-lasting heterosynaptic depression of GABAergic transmission to CA1 interneurons lasting < 200 ms (Semyanov and Kullmann, 2000). The contribution of group III mGluRs was tested by performing the experiment in the continued presence of the selective antagonist MSOP (100 μM). A 100 Hz tetanus delivered to the conditioning pathway in the presence of MSOP evoked a depression of EPSCs to 81 ± 7 of baseline, which again persisted for approximately 6 minutes ($p < 0.05$, n = 5, Fig 8.3B_1). This demonstrated that group III mGluRs do not contribute to the tetanus-evoked heterosynaptic depression of EPSCs. Selective antagonists were used in order to determine whether group I mGluRs are involved. mGluR1 and mGluR5 were blocked using LY367385 (100 μM) and MPEP (10 μM) respectively. Both mGluR1 and mGluR5 were blocked in initial experiments. If an effect upon the magnitude of tetanus-induced heterosynaptic depression were found to occur, one or other antagonist could be omitted in subsequent experiments, in order to determine whether the depression is mediated by mGluR1, mGluR5, or both subtypes. The contribution of each subtype could be directly quantified. The greater degree of specificity given by using this pharmacological approach thus provided a clear advantage over using a broad-spectrum group I mGluR antagonist such a ACPD. The first set of experiments was carried out in the continued presence of both selective group I mGluR antagonists, together with MSOP to block group III mGluRs as in the previous set of experiments. The 100 Hz tetanus evoked only a non-significant depression (to 95 ± 5% of baseline, n = 6; $p = 0.11$; Fig 8.3C_1) with shorter recovery (full return to baseline within 4 minutes). These results argue for a new role of group I mGluRs in mediating heterosynaptic depression of EPSCs in interneurons.

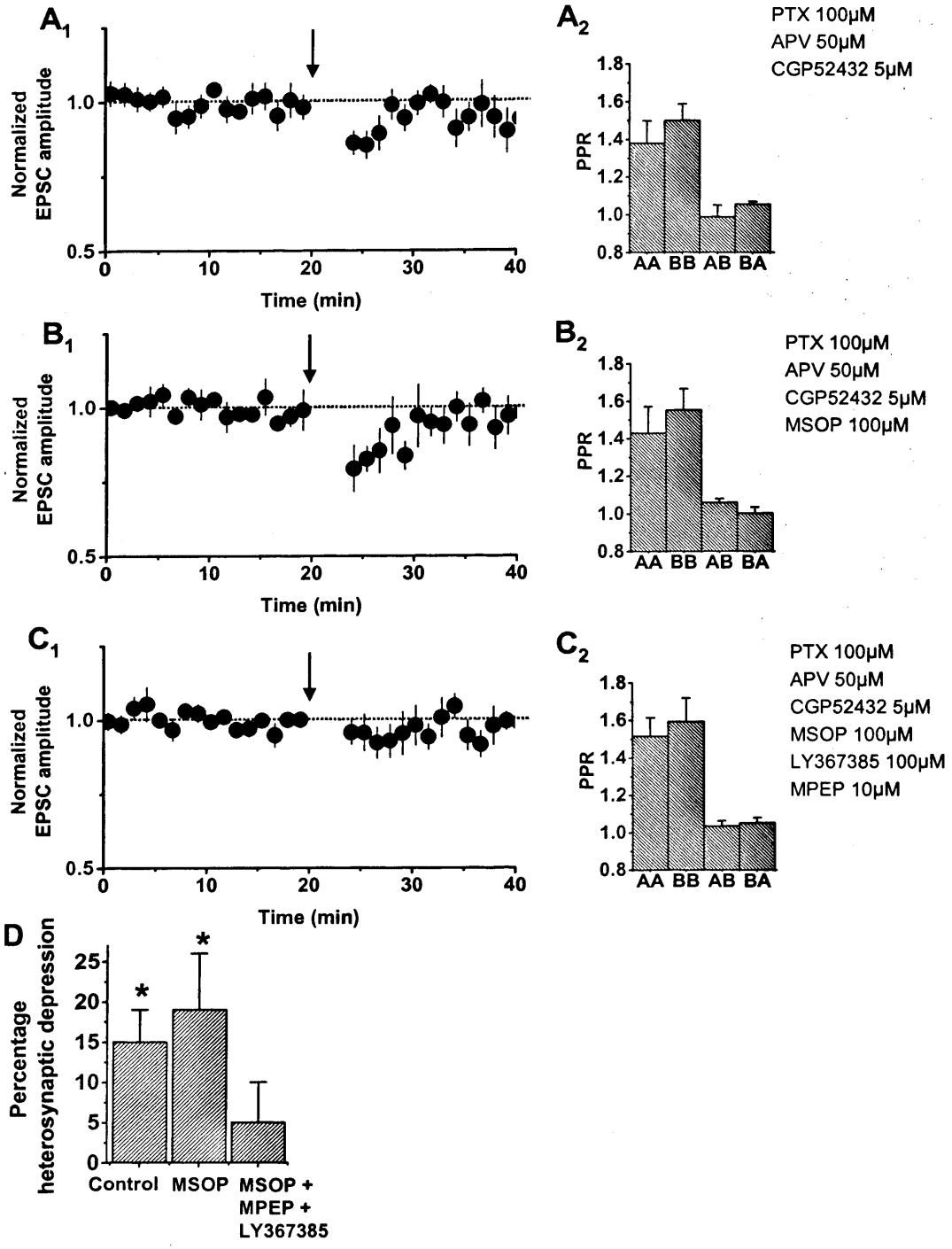

Figure 8.3 *A single tetanic stimulation delivered to an independent Schaffer collateral input evoked group I mGluR-mediated heterosynaptic depression.* ***A,*** *Effect of tetanizing an independent population of afferents on EPSC amplitude (± SEM;* ***A_1****) normalised to baseline amplitude in control experiments. The tetanus was delivered to an independent conditioning pathway at the time indicated by the arrow, and was followed by heterosynaptic depression lasting several minutes.* ***A_2,*** *Cross-facilitation results for the same dataset. Absence of cross facilitation (PPR ≈ 1) was used as a criterion for independence of test (A) and conditioning (B) pathways (average of 30 cycles for each condition: AA, BB: each pathway stimulated twice, AB, BA: one pathway stimulated after the other; data expressed as a ratio of the EPSC evoked alone).* ***B,*** *Heterosynaptic depression of similar magnitude to control was induced in*

the presence of MSOP to selectively block group III mGluRs. ***C,*** *Data obtained in the additional presence of LY367385 and MPEP to block mGluR1 and mGluR5, respectively, showing complete blockade of heterosynaptic depression.* ***D,*** *Summary of results, showing the EPSC amplitude, measured 3-8 minutes following tetanisation and normalized by baseline, for each condition.*

8.4 Discussion

The present study reveals a novel role for group I mGluRs in modulating glutamate release from Schaffer collaterals at excitatory synapses on CA1 stratum radiatum interneurons. A single tetanic stimulation of 100 pulses at 100 Hz delivered to a conditioning pathway resulted in a small but significant heterosynaptic depression of an independent test pathway, which persisted for several minutes. This depression was unaffected by blockade of group III mGluRs, but was abolished by group I mGluR antagonists (Fig 8.3). Although the effect of synaptic glutamate release from a neighboring pathway was small, it underestimates the full dynamic range of the phenomenon (DHPG application caused a roughly 50 % decrease in glutamatergic drive to interneurons). A possible reason for the small heterosynaptic depression is that only a minority of Schaffer collaterals innervating the interneuron were activated by the tetanus. This is in contrast to maximal activation of all group I mGluRs by bath application of the highly selective exogenous agonist DHPG.

Interleaving a brief train of five stimuli in a separate conditioning pathway with a single stimulus in the test pathway within each duty cycle failed to elicit significant heterosynaptic depression of excitatory inputs onto CA1 interneurons (Fig 8.1). Interestingly, this type of experimental design has previously been used to reveal a small but robust group III mGluR-mediated heterosynaptic depression of GABA release among CA1 interneurons (Semyanov and Kullmann, 2000). However, a small heterosynaptic depression which did not reach significance was seen at glutamatergic Schaffer collateral connections onto CA1 interneurons in the present study. The magnitude of this depression was 10 ± 9%, while that observed in the study of Semyanov and Kullmann (2000) was 14 ± 1%. The latter study had a greater number

of recorded cells. It would be worthwhile to continue these experiments, in order to determine whether increasing the n number, and thereby reducing standard deviation (SD), would cause the results to reach significance. This experimental design could be altered in a number of ways in order to improve the possibility of evoking heterosynaptic depression. Firstly, the interval between conditioning burst and test EPSC could be altered. This approach is problematic, however. Increasing the 100 ms interval (e.g. to 250 ms) is unlikely to enhance heterosynaptic depression. During the longer interval, increased clearance of glutamate released in response to the conditioning burst would occur, due both to uptake by EAATs and diffusional processes. Less glutamate would therefore be available within the extracellular space to activate mGluRs when the test EPSC was evoked, thus reducing rather than enhancing heterosynaptic depression. Shortening the interval between conditioning burst and test EPSC may prove equally problematic, since sufficient time must be allowed for return to baseline following the conditioning burst before delivery of the test EPSC (see Fig 8.2). However, reducing the duration of the interval would increase availability of glutamate within the extracellular space when the test EPSC was evoked. Determining whether heterosynaptic effects could be induced using a 50 ms or 75 ms interval represents a worthwhile experimental approach for future studies.

Secondly, the number of stimuli in each conditioning burst could be increased, e.g. from 5 to 10, thereby raising the amount of glutamate released from the conditioning pathway in response to each burst. This would elevate glutamate concentration within the extracellular space, potentially enhancing spillover and activation of mGluRs in the test pathway. This represents an experimental approach with the potential to successfully increase the probability of inducing heterosynaptic effects using this type of protocol. In the present study, it was instead decided to explore the effect of a single tetanus to the conditioning pathway. However, increasing the number of stimuli in the conditioning burst is a potentially successful approach for future experiments. It is important to realise that the number of stimuli in the

conditioning burst may not directly correlate with the magnitude of any evoked heterosynaptic effects. The effect of the conditioning burst of 5 stimuli at 50 Hz upon EPSCs in the conditioning pathway was not systematically analysed, since stimulus-induced short-term synaptic plasticity is not the focus of this thesis. There was some variation in response of EPSC amplitude to this stimulus protocol. However, in the majority of experiments carried out, there was an initial enhancement of EPSC amplitude – the second EPSC was larger than the first, an example of paired pulse facilitation. However, subsequent EPSCs became progressively smaller, indicating stimulus-induced short-term depression (Fig 8.1B). These effects are likely to result primarily from depletion of glutamate vesicles within the presynaptic terminals, which in turn affects activation of postsynaptic AMPA receptors. The increase in amplitude of the second EPSC (i.e. PPF) is likely to be due to increased Ca^{2+} accumulation within the presynaptic terminal, resulting in enhancement of glutamate release. However, subsequent stimuli delivered within a short time window may deplete glutamate vesicles within the presynaptic terminal, inhibiting transmitter release and thus resulting in a progressive depression of EPSC amplitude. It is important to realise that increasing the number of stimuli in the conditioning burst (e.g. from 5 to 10) may result in diminishing glutamate release with each stimulus. While this approach may potentially enhance heterosynaptic effects in the test pathway, it is complicated by short-term plasticity within the conditioning pathway.

Thirdly, heterosynaptic effects could be enhanced by inhibiting uptake of glutamate from the extracellular space, potentially leading to increased spillover and activation of mGluRs in the test pathway in response to the conditioning burst. In addition to diffusional processes, the termination of glutamatergic neurotransmission is mediated by transmembrane high-affinity Na^+-dependent glutamate/aspartate transporters. Five subtypes of EAATs (EAAT1-5) have been cloned from mammalian tissues. These transporters couple the electrochemical gradient of three co-transported Na^+ ions and one proton, together with one counter-transported K^+ ion, to that of glutamate. EAAT1 and EAAT2 have the greatest impact on clearance of

glutamate released during neurotransmission, and are abundantly expressed in the plasma membranes of glial cells at excitatory synaptic connections. EAAT3, EAAT4 and EAAT5 are expressed by forebrain neurons, Purkinje cells and photoreceptor cells respectively. These three subtypes appear to have far more subtle roles in regulating neuronal excitability and signalling (for detailed review see Seal and Amara, 1999; Amara and Fontana, 2002; Shigeri et al., 2004). Group I mGluRs have a high affinity for glutamate (Conn and Pin, 1997). In Purkinje and striatal cells a cationic conductance activated by mGluR1 has been shown to be highly sensitive to manipulations of extracellular glutamate, with mGluR1 activation enhanced when EAATs are selectively blocked (Brasnjo and Otis, 2001; Zhang and Sulzer, 2003). Indeed, extracellular pooling of glutamate, achieved by recruitment of multiple afferents leads to activation of mGluR1 (Marcaggi et al., 2003). This may also explain the finding that mGluR-activated currents are preferentially evoked by high-frequency presynaptic activity (Batchelor and Garthwaite, 1997). In the hippocampus, group III mGluR-mediated heterosynaptic depression at GABAergic connections between CA1 interneurons is enhanced by blocking glutamate uptake (Semyanov and Kullmann, 2000). There is thus substantial evidence that increasing glutamate availability in the extracellular space through inhibition of EAATs enhances spillover and consequent mGluR-mediated heterosynaptic effects. In the present study, blockade of EAAT1 and EAAT2 was carried out using the highly selective, competitive, non-transportable antagonist TBOA (Shimamoto et al., 1998; Shigeri et al., 2004). However, this resulted in experimental complications which made meaningful interpretation of the results impossible. TBOA application caused a dramatic enhancement in summation of EPSCs during the conditioning burst, together with slowing of return of EPSC amplitude to baseline. These effects may be attributed to increased glutamate concentration within the extracellular space, due to blockade of EEAT1 and EAAT2, the primary mechanism responsible for rapid glutamate clearance. In control trials, test EPSC amplitude (pathway A) was measured from baseline, whereas in conditioning trials the test EPSC was evoked during decay of the conditioning EPSCs

towards baseline (Fig 8.2). Test EPSC amplitude could therefore not be accurately compared between control and conditioning trials, preventing detection of any potential heterosynaptic effects. Attempting to overcome this difficulty by increasing the interval between conditioning burst and test EPSC from 100 ms to 250 ms proved unsuccessful, as EPSC amplitude still did not return to baseline during this period. Furthermore, in a high proportion of recordings (n = 4 of 7 cells), TBOA application appeared to be directly responsible for loss of the whole-cell voltage-clamp recording, due to a large increase in I_{hold}. One possible explanation may be that these observations are consistent with persistent ionotropic glutamate receptor activation causing an osmotic load upon the neuron. Blocking glutamate uptake using TBOA was therefore an unsuccessful experimental approach. A potential way to overcome these difficulties would be to use a lower concentration of TBOA, blocking a sufficient proportion of EAATs to enhance spillover, without evoking the issues discussed above. However, such a strategy is imprecise, due to variations between slices. When attempting to elicit heterosynaptic effects by using brief bursts of conditioning stimuli, it appears that some means of enhancing glutamate concentration within the extracellular space is required. However, blockade of EAAT1 and EAAT2 using TBOA is not a successful means of achieving this aim. As discussed, a number of experimental strategies may potentially be used in order to improve the possibility of evoking heterosynaptic depression at Schaffer collateral inputs to CA1 stratum radiatum interneurons using short bursts of conditioning stimuli. These ideas could be explored further in future experiments. However, in the present study, an alternate experimental design was found to successfully elicit heterosynaptic depression.

A robust, albeit small and reversible, heterosynaptic depression was observed, following a single high-frequency tetanus delivered to the conditioning pathway. This was insensitive to blockade of group III mGluRs, but was abolished by blocking group I mGluRs. An important step in future investigations in to identify whether mGluR1, mGluR5 or both receptors are responsible for mediating the effect. This could be

achieved by repeating experiments but omitting one or other of the selective group I mGluR antagonists.

What is the potential physiological role of the group I mGluR-mediated depression of excitation of interneurons? The different time-course and glutamate release requirements of the group I and group III mGluR-mediated forms of heterosynaptic depression may reflect distinct signalling cascades: in the case of group III mGluR-mediated heterosynaptic depression, spillover of glutamate directly affects presynaptic terminals. In the case of group I mGluR-mediated heterosynaptic interaction, in contrast, the induction of a postsynaptic cascade may well explain the more prolonged, albeit reversible, depression. The earlier finding that blocking postsynaptic G protein and Ca^{2+} signalling in the recorded cell abolished the effect of DHPG makes unlikely (although does not preclude) diffusion of a retrograde messenger from neighboring neurons to the glutamatergic axons mediating the test EPSC. A more plausible explanation for group I mGluR-mediated heterosynaptic depression is that glutamate released from other Schaffer collateral inputs onto the same interneuron is responsible for triggering the induction cascade.

Chapter 9. Morphological classification of CA1 interneuron subtypes and correlation with group I mGluR-mediated effects

9.1 Introduction

In contrast to pyramidal cells, which are relatively homogeneous, GABAergic interneurons in the hippocampus are a highly heterogeneous population. This issue is discussed in detail in the General Introduction (Chapter 1, Section 1.3). The distinctive characteristics displayed by specific interneuron subtypes are thought to reflect their specialised roles in mediating specific functions within the hippocampus and other cortical networks (Miles et al., 1996; Freund, 2003). GABAergic interneurons may be classified according to somatodendritic morphology, physiological factors such as firing pattern, presence of specific neurochemical markers, and other criteria (Freund and Buzsaki, 1996; Parra et al., 1998; McBain and Fisahn, 2001; Maccaferri and Lacaille, 2003; see Chapter 1, Section 1.3). However, no unified classification system currently exists (Maccaferri and Lacaille, 2003). This is due to the complexity in variation of these numerous criteria. For example, Parra et al. (1998) identified subsets of hippocampal interneurons which could be grouped together in terms of morphology. However, within these groups interneurons exhibited widespread variations in other criteria such as firing pattern and expression of specific neurotransmitter receptors. Providing a single definitive classification of a given interneuron is therefore highly problematic.

In the experiments described in this thesis, widespread heterogeneity in the response of CA1 stratum radiatum interneurons to various pharmacological manipulations was observed. The effect of group I mGluR activation via application of the selective agonist DHPG varied widely, from 0-92% depression of EPSC amplitude (n = 20; Figs 5.1C & 5.2). The overall magnitude of EPSC depression was 56 ± 6% of baseline ($p << 0.0001$, paired t test, n = 20; Fig 5.1B). The standard deviation (SD) of the maximal effect of DHPG application upon EPSC amplitude was ± 10% (n = 6) among pyramidal cells, and ± 25% (n = 20) among interneurons (Fig 5.1C). DHPG-

evoked depression thus exhibited much greater variation among interneurons than pyramidal cells, with a greater standard deviation despite the larger sample population. There was thus considerably greater variation in the response of interneurons to group I mGluR activation than pyramidal cells, reflecting the heterogeneity of the hippocampal interneuron population. This variation among interneurons was also apparent throughout the other pharmacological studies described within this thesis.

In the present study, results could be interpreted much more clearly if interneurons from which patch clamp recordings were made were accurately classified, and correlated with pharmacological effects. However, this presented a number of difficulties. mGluR1 is abundantly expressed in several neurochemically-defined classes of hippocampal interneuron within the CA1 subfield (van Hooft et al., 2000; Ferraguti et al., 2004). Analysis of neurochemical markers within individual neurons requires detailed immunohistochemical work combined with confocal imaging. There are numerous markers which must be tested for in order to accurately classify GABAergic interneurons, including peptides (e.g. somatostatin (SS), cholecystokinin (CCK), vasointestinal peptide (VIP) and substance P); and Ca^{2+}-binding proteins (e.g. calbindin, parvalbumin and calretinin) (Freund and Buzsaki, 1996; McBain and Fisahn, 2001). Every single experiment described in this thesis was performed solely by the author. Carrying out a detailed immunohistochemical and confocal imaging analysis of every neuron recorded would have dramatically reduced the time available for electrophysiological studies. In the present study, because a caesium-based pipette solution containing QX314-Br was used to optimize voltage clamp, interneuron firing patterns and detailed effects of DHPG on postsynaptic cation conductances could not be analysed (van Hooft et al., 2000). In the absence of detailed neurochemical and physiological analysis of interneurons, attempts were made to relate the heterogeneity in DHPG effect to the somatodendritic morphology and location within stratum radiatum of the cell. Neurons were filled with biocytin via the patch pipette during whole-cell electrophysiological recording, and subsequently

fixed and stained using streptavidin conjugated to Alexa488. Detailed morphological images were then obtained using confocal microscopy.

The objective of this chapter is to describe the morphological subtypes of CA1 interneuron observed during the experiments described in this thesis, and to determine whether any correlation existed between interneuron morphology and effects observed during combined electrophysiological and pharmacological studies.

9.2 Methods

9.2.1 Confocal imaging of neuronal morphology

During whole-cell patch clamp electrophysiological recording, neurons were routinely filled with biocytin (0.4% w/v), which was applied via inclusion in the patch pipette filling solution. Subsequent immunostaining of the recorded cell was carried out using streptavidin conjugated to Alexa488. Following recording, slices were fixed in 4% PFA in 1 ml PBS overnight at 4°C. PBS was used to rinse PFA from the slice. Membranes were permeabilised using Triton X-100, and immunostaining was carried out using streptavidin conjugated to Alexa488. A three-dimensional image of the neuron, together with its location within the hippocampal slice, was then obtained using confocal imaging. This process is described in detail in General Methods, Chapter 2, Section 2.5.

9.3 Results

9.3.1 Confocal imaging of neuronal morphology

The different morphological subtypes of CA1 stratum radiatum interneuron from which whole-cell patch clamp recordings were made are described in this section. A number of morphologically-distinct interneuron subtypes were identified through post-hoc staining and confocal imaging. Pyramidal cells were also visually

identified, in order to confirm that recordings were made from the correct cell type. Interneuron classification was attempted according to a number of criteria.

1. Somatodendritic morphology (i.e. uni-, bi-, or multipolar interneurons).
2. Position of soma within CA1 stratum radiatum (i.e. closer to stratum pyramidale (proximal), or stratum lacunosum-moleculare (distal).
3. Dendritic projection pattern (layers of CA1 to which dendritic projections could be visually identified).

It is important to realise that neurons were fixed within a 350 µm thick transverse hippocampal slice. Dendrites projecting upwards or downwards beyond the limit of the slice would be severed during the slicing process. This could lead to incorrect interpretation of dendritic projection patterns, since dendrites may be cut before reaching their final target area. This problem is impossible to overcome when working with a thin brain slice preparation, though it should be noted that this severing of dendrites did not appear to occur in every cell imaged. The most important criteria for morphological classification of interneurons are thus (i) axonal projections, since this defines the target outputs of the interneuron; (ii) pattern of dendritic projections, since this defines the layer(s) in which the cell receives afferent input; (iii) location of the soma with stratum radiatum.

It should be noted that not every neuron included in the electrophysiological studies described in this thesis was subjected to immunostaining and confocal imaging. This is because morphological analysis of interneurons was introduced as an additional experimental procedure during the course of the series of experiments carried out in this thesis. Electrophysiological studies in which morphological analysis of interneurons was not carried out were: (i) Effect of $GABA_B$ receptor blockade upon group I mGluR activation (Chapter 6, Section 6.3.1); (ii) Effect of mGluR blockade using ACPD upon group I mGluR activation (Chapter 5, Section 5.3.5); (iii) Blockade of intracellular signal transduction cascades downstream from group I mGluR activation in the recorded neuron, using GDPβS and BAPTA (Chapter 6, Section

6.3.4); (iv) Heterosynaptic depression experiments with conditioning burst delivered in each duty cycle (Chapter 8, Section 8.3.1). In addition there was a failure rate of 6.3% (n = 6 of 95 slices), in which no neurons were visible under confocal fluorescence imaging in an immunostained slice. This may result from a number of possible factors within the immunohistochemistry procedure, for example unsuccessful membrane permeabilisation or poor penetration of the streptavidin-Alexa488 conjugate.

A total of 84 interneurons and 5 pyramidal cells were visualised. In a small proportion of neurons, axons were clearly visible in the confocal image (6.0%; n = 5 of 84 interneurons). Axons were identified as distinct from dendrites since they: (i) were of a smaller diameter; (ii) extended for some distance from the soma before branching; (iii) branched far more extensively than dendrites; (iv) showed larger, more intricate patterns of ramification at the end of collaterals. In contrast, dendrites were thicker and followed a straighter, more ordered profile than axons. They began branching close to the soma, and were stereotypical in terms of branching patterns, with clear-cut, angular branches that occurred less frequently than those of axonal processes. In the majority of neurons, axons were visualised poorly or not at all. The reasons for this are unclear, but may involve the following factor (J. Heeroma, personal communication). Axons are smaller in diameter than dendrites, potentially resulting in slower diffusion of biocytin, especially in extremely finely-branched structures. This issue may be overcome to some extent by replacing biocytin with neurobiotin. It is important to realise that accurate visualisation of axonal projections is extremely important in defining interneuron classes, since this defines the target outputs of the interneuron. This highlights a major weakness in the present study.

. The majority of interneurons were multipolar (90.5%; n = 76 of 84 cells), with numerous trunk-like dendritic projections emanating from the soma. A smaller number of interneurons were bipolar (9.5%; n = 8 of 84 cells), with two large dendritic branches at the soma. No unipolar interneurons were imaged. Classification of interneurons according to horizontal / vertical orientation of dendritic projections was more problematic. This is not a widely-used means of interneuron classification. Pre-

existing systems are focused upon defining interneuron subtypes according to axonal as opposed to dendritic projection patterns, for example oriens-lacunosum moleculare, 'O-LM cells', and pyramidale-lacunosum moleculare, 'P-LM cells' (Freund and Buzsaki, 1996; McBain and Fisahn, 2001; Maccaferri and Lacaille, 2003; see Chapter 1, Section 1.3). Dendritic projections often appeared to terminate within multiple layers of the CA1 subfield. This complication was compounded by the issue of severing of dendritic projections before reaching their final target location due to working with a thin slice preparation. Since the majority of interneurons were identified as multipolar cells, with numerous dendritic projections emanating from the soma, definitive classification of neurons according to horizontal / vertical orientation of dendritic projections could frequently not be carried out with complete certainty. A small number of interneurons displayed an orientation of dendrites which was obviously horizontal (i.e. dendrites aligned along the length of CA1 stratum radiatum) or vertical (i.e. dendrites running across stratum radiatum, from stratum pyramidale to stratum lacunosum-moleculare). However, in most cases the pattern of dendritic projections was too complex for a single descriptive term to be applied with total confidence. In the present study it was therefore clear that classification of interneurons according to dendritic projection pattern (i.e. horizontal / vertical projection; or target layers of CA1 to which dendritic projections could be visually identified) were not ideal criteria. Nonetheless, they were selected as the most suitable given the relatively limited data available, highlighting the requirement for more detailed interneuron classification based upon not only morphology, but also neurochemical and physiological analysis.

9.3.2 Chi squared statistical analysis of data

Although classification of interneurons into discrete categories was problematic, as described above, statistical analysis was attempted on one subset of data, in order to demonstrate more conclusively that no correlation could be found between morphology and pharmacological effects. This highlights further the

requirement for more comprehensive means of interneuron classification, i.e. inclusion of neurochemical analysis using immunohistochemistry to detect markers such as CCK, SS, parvalbumin, calretinin, calbindin etc.; and physiological analysis, for example categorisation of interneuron action potential firing patterns. This would allow interneurons to be divided into discrete subsets with a greater degree of certainty (see Parra et al., 1998). The chi squared test was selected as the most appropriate method of statistical analysis. The Student's t-test and Analysis of Variance (ANOVA) are used to analyse measurement data which, in theory, are continuously variable. Between a measurement of, say, 1 µm and 2 µm there is a continuous range from 1.0001 to 1.9999 µm. However, in some types of experiment, it is necessary to record how many individuals fall into a particular category, e.g. horizontally- or vertically-orientated interneurons, bi- or multi-polar interneurons, etc. These counts, or enumeration data, are discontinuous (e.g. 1, 2, 3 etc.), and must therefore be treated differently from continuous data. Often the appropriate test is chi-squared (χ^2), which is used to test whether the number of individuals in different categories fit a null hypothesis, known as an expectation (E) value.

Due to the difficulty in classifying interneurons into discrete categories based upon morphology alone, together with the fact that a large sample population is required to perform a chi squared analysis in order to satisfy the underlying mathematical assumptions, namely that each category should contain no less than 5 cells, this statistical analysis was attempted on one set of data only. This was the data set for the control experiments, in which the magnitude of EPSC depression caused by 20 min DHPG application in CA1 interneurons was measured. The total sample population was 20 cells (Chapter 5, Fig 5.1 B & C). This was the largest sample population of any data set in the thesis. Given the size of the sample population, and the requirement for at least 5 cells in each category, only a relatively simple chi squared analysis with a low number of morphological categories could be carried out. I firstly construct a table, containing the actual observed (O) values, followed by the

expected (E) values if the null hypothesis is correct. Each E value is then subtracted from the corresponding O value (O – E). The O-E values are squared, and divided by the relevant E value, to give $(O-E)^2/E$. The sum of all of the $(O-E)^2/E$ values is then calculated, to give the total, which is termed X^2. Now I compare my X^2 value with a χ^2 (chi squared) value in a table of X^2. It may appear that there are 3 degrees of freedom (because there are 4 categories; df = n - 1). But there is actually one degree of freedom. The reason is that I lose one degree of freedom because I had 4 categories (df = n – 1); and I lose a further 2 degrees of freedom because I used two pieces of information to construct my null hypothesis - I used a column total and a row total. Once I had used these I would have needed only one data entry in order to fill in the rest of the values (therefore I have one degree of freedom). With one degree of freedom, the Yates correction must be used (subtract 0.5 from each O-E value). It is important to note that when there are only two categories (e.g. proximal and distal) or, more correctly, when there is only one degree of freedom, the chi squared test should not strictly be applied. There have been various attempts to correct this deficiency, but the simplest is to apply the Yates correction to the data. To do this, I simply subtract 0.5 from each calculated value of O-E. Then I continue as usual but with these new (corrected) O-E values: I calculate (with the corrected values) $(O-E)^2$, $(O-E)^2/E$ and then sum the $(O-E)^2/E$ values to get X^2. The Yates correction is only applied when there are two categories (one degree of freedom).The table is thus generated as follows.

Category	Calculated values	**Proximal to stratum pyramidale**	**Distal from stratum pyramidale**	Row totals
EPSC depression ≤ 22%	Observed (O)	7	3	10
	Expected (E)	5	5	10
	O-E	2	-2	0
Yates correction	|O-E| - 0.5	1.5	-1.5	0
	$(O-E_{corrected})^2/E$	**0.45**	**0.45**	
EPSC depression > 22%	Observed (O)	4	6	10
	Expected (E)	5	5	10
	O-E	-1	1	0
Yates correction	|O-E| - 0.5	0.5	0.5	0
	$(O-E_{corrected})^2/E$	**0.05**	**0.05**	**$X^2 = 1.00$**
	Column totals	10	10	**n = 20** (total sample population)

Table 9.1 *Chi squared analysis comparing magnitude of EPSC depression induced by group I mGluR activation via DHPG application against location of interneuron somata in stratum radiatum layer. Total EPSC depression was 44 ± 6%. This was therefore split in half to give ≤ 22% and > 22% EPSC depression. Stratum radiatum was arbitrarily divided in half, and two values for soma position in were selected – proximal to stratum pyramidale and distal from stratum pyramidale (i.e. closer to stratum lacunosum moleculare). Total sample population size was 20 interneurons. This relatively simplistic analysis was necessary due to the size of the sample population and the requirement of the chi squared test to have a minimum of 5 cells in each category.*

I now compare the calculated value for X^2 against a χ^2 value in a chi squared table, using n – 1 degrees of freedom (where n represents the number of categories, in this case two; because I used two pieces of information to construct my null hypothesis - I used a column total and a row total) and a probability value of p = 0.05. If the calculated X^2 value does not exceed the tabulated χ^2 (chi squared) value, then there is no significant difference from the expected (E) value, and thus no reason to

reject the null hypothesis - i.e. there is only a 5% probability that the calculated X^2 value does not correlate with the null hypothesis. In this case, the calculated X^2 value was 1.00, and the tabulated value for χ^2 for 1 degrees of freedom is 3.84 at p = 0.05; 6.64 at p = 0.01; and 10.83 at p = 0.001. Thus the calculated X^2 value does not exceed the tabulated χ^2 value for 1 degrees of freedom even at the p = 0.001 probability level. There is thus only a 0.1% probability that the data do not correlate with the expected (E) value, i.e. a null hypothesis. In other words, the chi squared analysis demonstrates that, in this case, there is very unlikely to be any correlation between the magnitude of DHPG-induced EPSC depression and the position of the interneuron somata within the stratum radiatum layer.

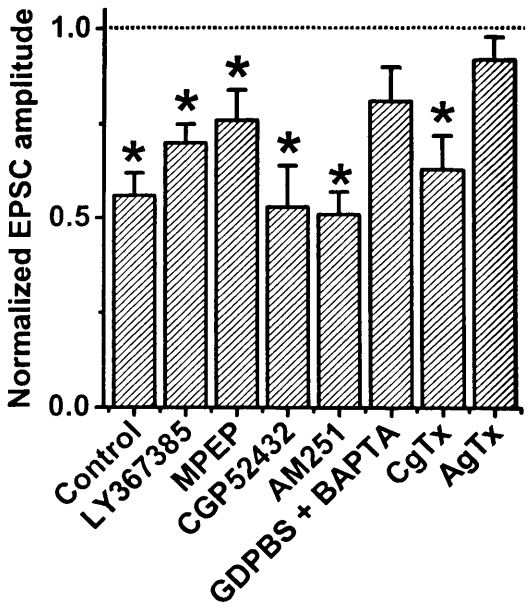

Figure 9.1 *Summary of the effects of pharmacological manipulations on the magnitude of the DHPG-induced acute depression. DHPG was applied following pre-exposure to the antagonists listed on the x axis. Control, DHPG alone.*

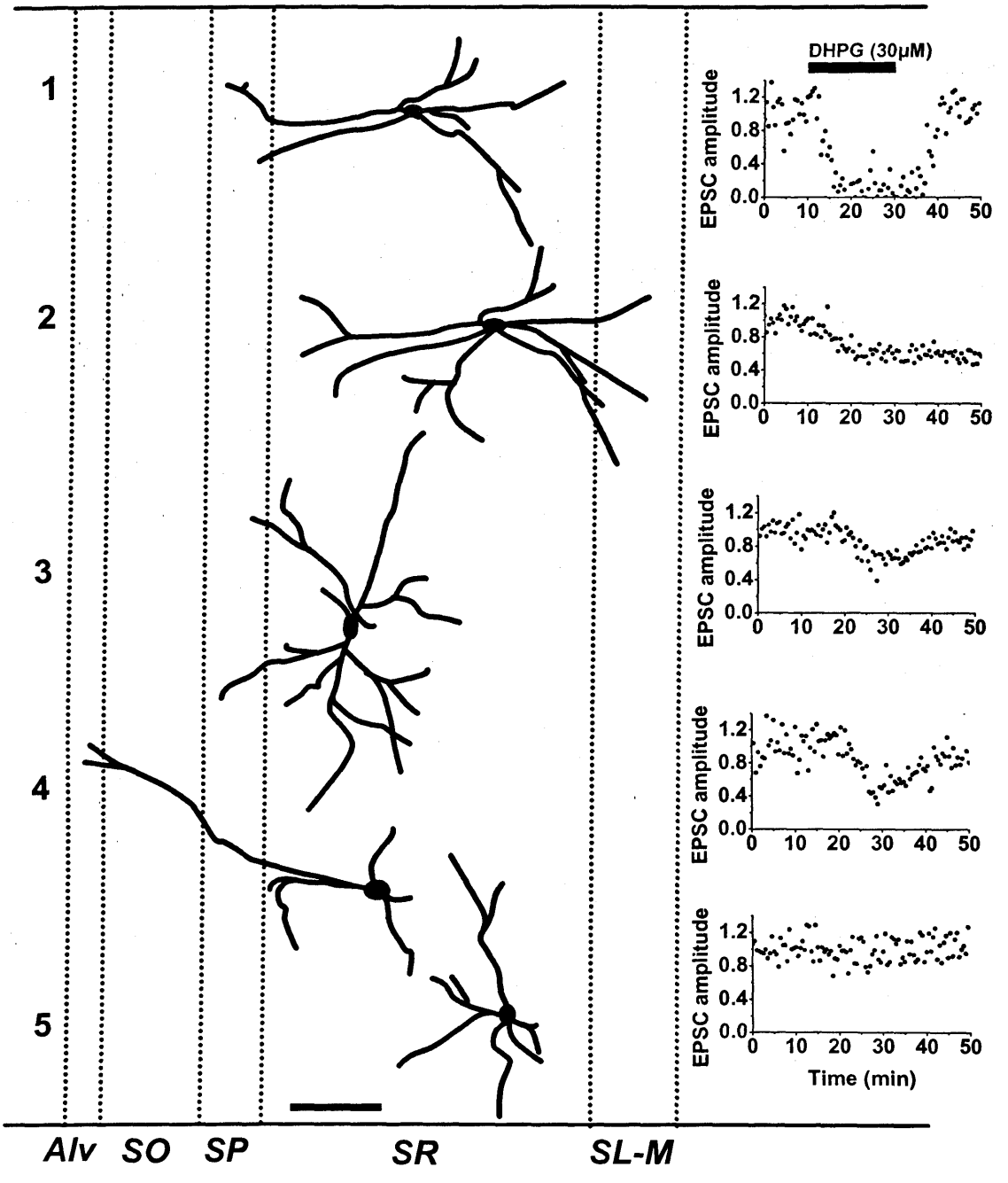

Figure 9.2 *Somatodendritic patterns obtained from confocal imaging of five representative stratum radiatum interneurons, together with the effect of DHPG application upon EPSC amplitude in each cell. No consistent differences in the effect of DHPG were observed in 84 interneurons, when related to the position of the soma within stratum radiatum or dendritic orientation. This purpose of this figure is not to show correlations between somatodendritic patterns of interneurons and effects of DHPG, since no such relationships were identified; instead, it simply shows representative examples of five interneurons. Alv, alveus; SO, stratum oriens; SP, stratum pyramidale; SR, stratum radiatum; SL-M, stratum lacunosum-moleculare. Scale bar = 100 μm.*

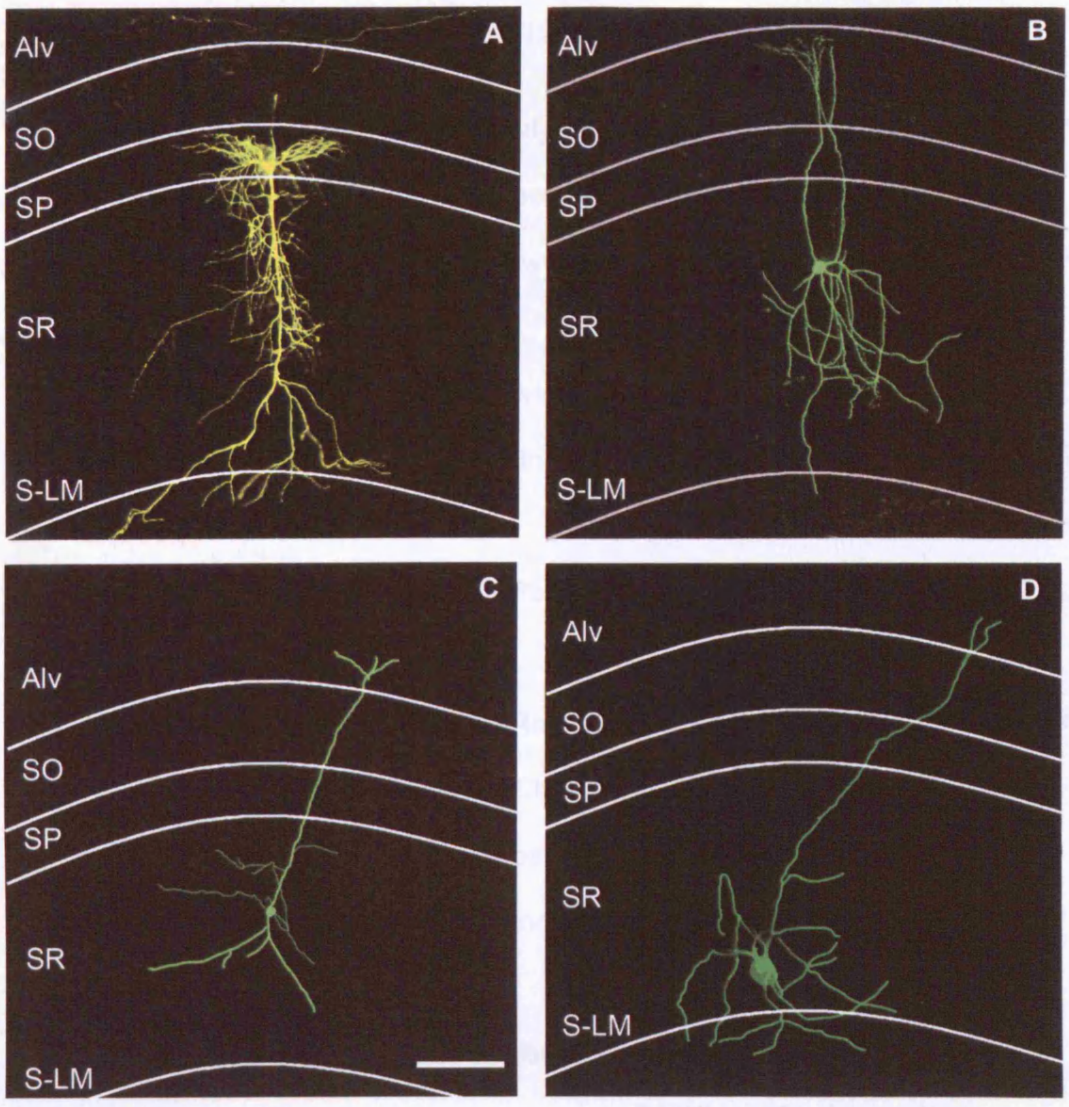

Figure 10.3 *Confocal images of CA1 neurons showing patterns of dendritic projections. Alv, alveus; SO, stratum oriens; SP, stratum pyramidale; SR, stratum radiatum; S-LM, stratum lacunosum-moleculare.* ***A****, pyramidal cell. Axons are visible extending through SO and running along the alveus in both directions, towards the subiculum and fimbria/fornix.* ***B****, stratum radiatum interneuron, with soma in upper SR. Extensive dendritic ramifications are visible within SR. Dendrites project through SP and SO, terminating at the alveus.* ***C****, stratum radiatum interneuron, with soma in mid-SR. Dendrites project within a confined area in SR. There is a single large-diameter dendritic projection extending through SP and SO, terminating in the alveus.* ***D****, Stratum radiatum interneuron, with soma in lower SR. Dendrites ramify within SR, extending downwards into S-LM. There is a single large-diameter dendritic projection extending through SP and SO, terminating in the alveus. Scale bar = 100* µm

9.3.2 Correlation of pharmacological effects with confocal imaging of neuronal morphology

As noted above, morphological analysis of interneurons was not carried out in all sets of experiments. Correlations between morphology of CA1 stratum radiatum interneurons and pharmacological effects were investigated in the following series of experiments.

1. Effect of group I mGluR activation via DHPG and CHPG (Chapter 5).
2. Group I mGluR subtypes involved in mediating DHPG-induced depression of EPSCs (Chapter 5).
3. Interaction between group I mGluRs and CB1 endocannabinoid receptors (Chapter 6).
4. Interaction between group I mGluRs and N-type and P/Q-type Ca^{2+} channels, including all control experiments (Chapter 7).
5. Some experiments in which heterosynaptic depression was induced by a single tetanic stimulation of the conditioning pathway (Chapter 8).

Somatodendritic morphology and position of the soma within stratum radiatum were correlated with the magnitude of changes in EPSC amplitude due to pharmacological manipulations reflecting the objective of the experiment. No distinct correlations were found between interneuron morphology and pharmacological effects in any of the series of experiments analysed in this thesis. The results of the present study thus indicate that additional means of classification are required to achieve a detailed analysis of interneuron subtypes, which could then be correlated with electrophysiological data.

9.4 Discussion

In the present study, no distinct correlations were found between interneuron morphology (as defined by somatodendritic pattern and location of soma within CA1 stratum radiatum) and response of CA1 stratum radiatum interneurons to various pharmacological manipulations, in a number of studies investigating modulation of excitatory synaptic transmission by group I mGluRs. Hippocampal interneurons are a highly heterogeneous population (Freund and Buzsaki, 1996; Parra et al., 1998; McBain and Fisahn, 2001; Maccaferri and Lacaille, 2003), and it is certain that the results of electrophysiological studies described in this thesis were obtained from a number of distinct subtypes of CA1 stratum radiatum interneurons. Nonetheless, CA1 interneurons were treated as a single population in analysis of electrophysiological experiments. Insufficiently large sample populations were used in each experiment to ensure that statistical analysis (chi squared) could be used to give a definitive overall result. It is clear that a great deal more information regarding modulation of glutamatergic synaptic transmission to CA1 interneurons by group I mGluRs could be obtained if the results of electrophysiological studies were combined with detailed and accurate classification of interneurons into specific subtypes. For example, there was widespread variation in the effect of group I mGluR activation via application of the selective agonist DHPG, with depression of EPSCs varying from 0-92% ($n = 20$; Chapter 5, section 5.3.2). A large sample population was used, and the overall effect of group I mGluR activation in CA1 interneurons was highly significant (depression of EPSCs to $56 \pm 6\%$ of baseline, $p << 0.0001$, paired t test, $n = 20$; Fig. 5.1B). However, it is important to consider the interneurons which displayed a response to DHPG that varied widely from the mean value, i.e. those which showed an unusually large depression (maximum 92%) and those which were unresponsive. Could such cells be correlated with specific subtypes of CA1 interneuron, with distinct functional roles within the hippocampal network? One of the main conclusions of this thesis is that correlation of electrophysiological data with accurate, detailed classification of interneurons into distinct subtypes is required in order to fully understand the role

played by group I mGluRs in modulation of excitatory synaptic transmission to CA1 interneurons, and the overall implications of this modulatory mechanism in the function of the hippocampal network. Additional means of identification, including physiological and neurochemical analysis, are required to achieve more definitive classification of interneurons into distinct subtypes, which could then be correlated with electrophysiological data.

The present study has shown that anatomical identification alone clearly does not yield sufficient information for detailed classification of interneurons into distinct subtypes. However, high-resolution three-dimensional confocal imaging of patterns of axonal and dendritic projections can provide important information regarding the role of an interneuron within neuronal circuits, and represents one major criterion by which classification can be achieved. Clear, detailed confocal images of both CA1 pyramidal cells and interneurons were obtained in the present study, using an experimental procedure involving loading neurons with biocytin and immunostaining using a streptavidin-Alexa488 conjugate. The success rate of clearly imaging somatodendritic pattern of individual recorded interneurons was high, with no neurons visible in only a small proportion of immunostained slices (6.3%; n = 6 of 95 slices). Patterns of dendritic projections could be consistently identified both at high resolution and over long distances, though using relatively thin hippocampal slices (350 μm) raises the issue of severing of axonal and dendritic processes before the final target location is reached.

However, a major shortcoming was that axonal processes were visualised in only a low proportion of interneurons (6.0% of cells; n = 5 of 84). The difficulty in identifying axons lead to serious problems in interneuron classification. Accurate imaging of axonal projections is essential in classifying interneuron subtypes, since this allows the target outputs of the cell to be identified. Although many strategies for classification exist, one system involves identifying interneurons according to the two specific layers containing the soma and axonal processes, e.g. oriens-lacunosum moleculare, 'O-LM cells', pyramidale-lacunosum moleculare, 'P-LM cells', oriens-

oriens and radiatum 'O-bistratified cells', etc. (Freund and Buzsaki, 1996; Maccaferri and Lacaille, 2003; see Chapter 1, Section 1.3). However, due to the low proportion of interneurons in which axons were clearly identified under confocal microscopy in the present study, classification using this type of system was not possible. The effectiveness of this technique in aiding identification of distinct interneuron subtypes would be greatly enhanced by increasing the proportion of cells in which axons could be clearly identified. Similar problems had been experienced by another lab member. However, by re-imaging the same neurons under confocal microscopy in a different laboratory, a much greater success rate in accurately defining patterns of axonal projections was achieved (J. Heeroma, personal communication). Axonal projection patterns may thus potentially be accurately identified by imaging the present data set under these different conditions. This would considerably enhance the value of the data described in the present chapter in correlating interneuron morphology with mGluR-related pharmacological effects.

The fact that no clear correlations were found between CA1 interneuron morphology and results from electrophysiological studies reflects the limitations of using a single criterion for interneuron classification. Morphological characterisation of interneurons is a useful and important descriptive criterion. However, as the results of this study clearly demonstrate, the role of an interneuron within an active brain network is also strongly defined by its physiological properties, which must also be characterised. In addition, detailed neurochemical analysis is required to achieve an accurate classification of a given interneuron subtype. As discussed previously, complications still exist because it is becoming increasingly clear that multiple criteria must be used to accurately identify an interneuron, and no unified classification system is currently available (Maccaferri and Lacaille, 2003; Somogyi and Klausberger, 2005; see Chapter 1, Section 1.3.1).

Chapter 10. General discussion

10.1 Summary of experimental findings

The following novel experimental findings have been described in this thesis.

1. Group I metabotropic glutamate receptors mediate an acute depression of glutamatergic synaptic transmission from Schaffer collaterals to CA1 stratum radiatum interneurons. This modulatory phenomenon displays the following characteristics.
   - It is reversible upon washout of the selective agonist DHPG, implying the existence of an acute depression only, with no involvement of the persistent long-term depression (LTD) that is seen in CA1 pyramidal cells (e.g. Palmer et al., 1997; Oliet et al., 1997; Faas et al., 2002; Huang and Hsu, 2005). The exception is when the mGluR5 subtype alone is selectively activated, when an unusual form of persistent synaptic depression is observed (Chapter 5, Fig 5.7)
   - It is sensitive to postsynaptic manipulations, including inhibition of G protein signalling and changes in intracellular Ca^{2+} levels (Chapter 6).
   - The inhibition of excitatory synaptic transmission is expressed at least partially as a presynaptic reduction of glutamate release.
   - The presynaptic depression is occluded by blocking P/Q-type, but not N-type, Ca^{2+} channels (Chapter 7, Fig 7.2).
   - Together with the fact that group I mGluR-mediated acute depression is sensitive to postsynaptic manipulations, and is expressed as a presynaptic reduction of glutamate release, this implies the existence of some kind of retrograde signal from the postsynaptic to the presynaptic terminal. However, neither CB1 endocannabinoid receptors, A_1 adenosine receptors nor $GABA_B$ receptors appear to be required for the decrease in glutamate release, suggesting the existence of a retrograde signal of currently

unknown molecular origin (Chapter 6). One potential candidate yet to be investigated is nitric oxide (NO), which has been shown to act as a synaptic retrograde messenger in the neocortex (e.g. Hardingham and Fox, 2006). For review of NO signalling, see Boehning and Snyder (2003).

2. Both mGluR1 and mGluR5 subtypes contribute to the acute depression, in contrast to previous reports in CA1 pyramidal cells, in which the acute depression appears to be mediated entirely by the mGluR1 subtype (Mannaioni et al., 2001).

3. The present study demonstrated for the first time that group I mGluRs mediate heterosynaptic depression evoked by intense activity in neighboring axons (Chapter 8, Fig 8.3).

4. Extensive heterogeneity in response to numerous pharmacological manipulations was detected among CA1 stratum radiatum interneurons. For example, DHPG-evoked depression of EPSCs exhibited much greater variation among interneurons than CA1 pyramidal cells, with a greater standard deviation despite a considerably larger sample population.

5. Morphological analysis of neurons from which electrophysiological recordings were obtained was carried out using immunohistochemistry combined with confocal microscopy. No clear correlations were detected between pharmacological effects and neuronal morphology, highlighting the requirement for additional means of interneuron classification (e.g. neurochemical and physiological analysis) in future research.

10.2 Quantitative comparison of two distinct classes of glutamatergic afferent input to CA1 interneurons for modulation by group III mGluRs

In the General Discussion, I first consider the two projects that did not involve group I mGluR modulation of excitatory synaptic connections onto CA1 interneurons, before discussing and drawing conclusions from the group I mGluR projects which form the main part of this thesis. The central objective of this thesis has been investigation of the functional properties and modulation of excitatory synaptic connections onto GABAergic interneurons in the CA1 subfield of the hippocampus. This research is important for a number of reasons, which are discussed in detail in the General Introduction (Chapter 1, Sections 2, 3 and 4). Briefly, GABAergic interneurons are critically involved in a wide variety of network functions, yet the functional and modulatory properties of the excitatory synapses through which they sense the activity of the principal cell population are at present relatively poorly characterised. An important questions is whether all classes of excitatory input to a given interneuron are subject to the same modulatory mechanisms; and whether there may be quantitative differences in the strength of modulatory effects, and susceptibility to activation by glutamate spillover, at different classes of input. This would provide additional levels of control in activation of the GABAergic system within the hippocampal network. Such differences in functional properties and modulatory effects at distinct classes of input to the same inhibitory interneuron have not yet been extensively investigated in the hippocampus and elsewhere in the neocortex. Group III mGluRs were chosen as a suitable candidate receptor for this study, since they have been widely shown to be expressed presynaptically in highly specific patterns, and to inhibit release of both glutamate and GABA at various classes of synapse (for review see Pin and Duvoisin, 1995; Conn and Pin, 1997; Anwyl, 1999).

This preliminary study was carried out at the start of the Ph.D. during familiarisation with the patch clamp technique. Serious technical difficulties were encountered in reliably evoking monosynaptic EPSCs in the same interneuron via extracellular stimulation of two distinct input classes. This low success rate (Chapter

3, Tables 3.1 and 3.2) made quantitative comparison of the two inputs for modulation by group III mGluRs impossible without recording from large numbers of cells, which would have proved extremely time-consuming, given the constraints of the Ph.D. The decision was taken to move on to alternative projects, returning to this investigation if the remaining time within the Ph.D. permitted. Thus only limited conclusions can be drawn from the data obtained in this project. Firstly, The principal experimental difficulty appeared to be evoking EPSCs in stratum oriens interneurons through activation of CA1 pyramidal cell axons via extracellular stimulation of the alveus pathway. This suggested a low level of connectivity between CA1 pyramidal cell axon collaterals and stratum oriens interneurons. These electrophysiological findings support previously-reported anatomical data, which have demonstrated that local CA1 pyramidal cell axon collaterals are very thin relative to the parent branch, display few varicosities, and rarely extend more than 100 μm into stratum oriens (Knowles and Schwartzkroin, 1981). Secondly, careful re-positioning of stimulus electrodes within the hippocampal slice once the whole-cell configuration had been established often improved the success rate in evoking monosynaptic EPSCs, presumably by activating different axon bundles which were directly connected to the cell being recorded. This was thus found to be a valuable experimental approach, which was frequently employed in subsequent experiments during the course of the Ph.D. Placing the stimulus electrode close to the recording electrode raises the complication of direct depolarisation of interneuron dendrites and soma by extracellular stimulus current, as opposed to activation of glutamatergic synaptic inputs by stimulation of presynaptic afferents. An alternative explanation is that different subtypes of CA1 stratum oriens interneuron may be more strongly connected to CA1 pyramidal cell axons, reflecting their relative importance in feed-back inhibitory circuits. This issue could be addressed by post-hoc morphological analysis of recorded interneurons, which would also be important for definitive classification if future studies were carried out in CA1 basket cells. These experiments were carried out at the beginning of the PhD, during familiarisation with the patch clamp technique, between November 2002 and February

2003. A subsequent study achieved success in evoking excitatory synaptic responses in single CA1 interneurons via stimulation of both alveus and Schaffer collateral pathways, indicating that this experimental approach is indeed possible with further optimisation. There were distinct differences in synaptic dynamics between these two inputs, underlining that distinct classes of excitatory input to the same neuron may display different functional properties (Wierenga and Wadman, 2003). It may therefore be reasonably proposed that they may also exhibit differences in modulatory mechanisms, particularly by mGluRs which display highly specific expression patterns. Unfortunately, due to technical difficulties and the time constraints of the project, it was not possible to investigate the effects of group III mGluR activation upon EPSC amplitude by applying the selective agonist L-AP4, nor to examine tonic activation of these receptors using the selective antagonist MSOP. These represent important areas of future research.

10.3 Optical probing of glutamatergic synaptic connections in hippocampal slices using Ca^{2+} epifluorescence imaging

I now consider the conclusions that can be drawn from the project involving optical probing of glutamatergic synaptic connections in hippocampal slices using Ca^{2+} epifluorescence imaging. The initial objective of the project was to adapt the optical probing technique (Smetters et al., 1999; Peterlin et al., 2000; Kozloski et al., 2001; Billups et al., 2002) so that action potential-associated Ca^{2+} signals could be detected in postsynaptic targets of axon bundles in defined afferent input pathways activated by extracellular stimulation, as opposed to activation of single presynaptic 'trigger' cells. This method could be used, for example, to detect neurons postsynaptically-connected to axon collaterals in specific input pathways in areas with low levels of connectivity, for example CA1 pyramidal cell axons and stratum oriens interneurons (see Chapter 3). By visualising stimulus-evoked Ca^{2+} signals and then patch-clamping synaptically-connected neurons, the success rate in evoking

monosynaptic EPSCs from two distinct input classes in the same interneuron could be dramatically enhanced, thereby facilitating complex electrophysiological experiments such as those described in Chapter 3. Once successfully established, the optical probing technique could also be used for detection of postsynaptic targets of single presynaptic neurons which had been patch clamped and stimulated to fire trains of action potentials, as in the original design of the method (Smetters et al., 1999).

However, the present study highlighted a number of technical challenges which would have to be overcome in order to successfully apply the optical probing technique to detection of glutamatergic synaptic connections onto interneurons. A detailed discussion of these issues is provided in Chapter 4, Section 4.4. Firstly, the success rate in detecting stimulus-evoked Ca^{2+} transients associated with action potentials in postsynaptic neurons would have to be dramatically increased (Chapter 4, Tables 4.1 and 4.2). The primary reason for the low success rates observed in the present study was widespread neuronal death within the hippocampal slice following the two-stage bulk-loading procedure. The fewer healthy neurons within a slice, the lower the probability of detecting action potential-associated Ca^{2+} transients. Success rate would also be improved if the staining procedure were further optimised, such that following staining, a greater proportion of neurons contained a higher concentration of indicator. Attention would have to be focused particularly on interneurons, since investigation of excitatory synaptic connections to this cell type is the overall objective of this thesis. A particularly low success rate in detecting action potential-associated Ca^{2+} transients was apparent in stratum radiatum interneurons in CA1 and CA3 subfields. This was mainly due to the fact that interneurons are more sparsely distributed than pyramidal cells and comprise only around 10% of the hippocampal neuronal population (Amaral et al., 1990); and also possibly due to a selective vulnerability of this cell type to the cytotoxic effects of the staining procedure. Further issues must be considered if the technique were to be used for identifying excitatory synaptic connections in order to facilitate combined electrophysiological and pharmacological studies. Robust stimulus protocols were found to be necessary for

detection of Ca^{2+} signals. Such protocols may induce long-term synaptic plasticity (LTP), which would affect the results of electrophysiological studies of synaptic transmission. This problem could potentially be overcome by improving the staining and imaging procedures, so that Ca^{2+} signals could be detected with greater sensitivity, meaning that less robust presynaptic stimulation was required. A further difficulty in performing electrophysiological studies following the imaging procedure is the continued presence within the neurons of an unknown concentration of fluorescent indicator. These molecules are powerful Ca^{2+} buffers and may therefore affect the results of many types of pharmacological study by interfering with intracellular signalling cascades. Wide-field epifluorescence imaging and bulk-loading of neuronal populations with fluorescent indicators to detect postsynaptic action potential-associated Ca^{2+} transients has previously been shown as a powerful means of probing neuronal connectivity within networks. Furthermore, the technique may readily be used to facilitate establishing paired recordings between individual monosynaptically-connected cell pairs (Smetters et al., 1999; Peterlin et al., 2000; Kozloski et al., 2001). The present study has shown that in certain cases the method may also be useful in detecting excitatory synaptic connections in areas with low connectivity in order to facilitate combined electrophysiological and pharmacological studies. However, the technique is not always suitable for this purpose, and a number of major experimental difficulties must be overcome in order to improve its effectiveness.

10.4 Modulation of excitatory synaptic transmission to CA1 interneurons by group I mGluRs

I now discuss the implications of the experimental findings from the five chapters (Chapters 5 to 9) describing modulation of synaptic transmission from glutamatergic Schaffer collateral inputs onto CA1 interneurons by group I mGluRs. This study shows that group I mGluRs mediate depression of excitatory transmission

in stratum radiatum interneurons, which is sensitive to postsynaptic manipulations and is expressed at least partially as a presynaptic reduction of glutamate release. Both mGluR1 and mGluR5 contribute to the acute depression, and neither CB1 nor $GABA_B$ receptors appear to be required for the decrease in glutamate release. The presynaptic depression is occluded by blocking P/Q-, but not N-type Ca^{2+} channels. Finally, this study has shown for the first time that group I mGluRs mediate heterosynaptic depression evoked by intense activity in neighboring axons.

The group I mGluR-mediated depression in interneurons differs in several respects from what has been reported in pyramidal neurons. First, the acute depression was not followed by a robust persistent depression (LTD). Although group I mGluR-mediated LTD was also not detected in pyramidal cells in the present study, it has been widely reported in previous investigations (e.g. Palmer et al., 1997; Overstreet et al., 1997; Fitzjohn et al., 2001; Faas et al., 2002; Huang and Hsu, 2005; reviewed in General Introduction, Section 1.4.5.3). The lack of detection of this phenomenon in CA1 pyramidal cells in this study may be explained in terms of a relatively subtle effect failing to reach statistical significance due to an insufficiently large sample population. LTD was observed in 3 of 6 pyramidal cells, and only a limited number of data points were available for analysis since the objective of the experiments was not to investigate long-term synaptic plasticity (Chapter 5, Fig 5.1). Second, both mGluR1 and mGluR5 contribute to the acute depression. The sum of the depression evoked in the presence of each of the blockers of mGluR1 and mGluR5 applied separately was approximately 54%, only slightly more than the depression observed when neither receptor was blocked (44%) (Chapter 5). Intriguingly, a modest persistent DHPG-evoked depression was uncovered when mGluR1 was blocked (Chapter 5, Fig $5.7A_1$). Taken together, these results are consistent with two relatively independent induction cascades, as has been proposed in pyramidal cells, with mGluR1 coupled to an acute depression and mGluR5 coupled to a more long-lasting depression of transmission (e.g. Huber et al., 2001). In the

present experiments, both phenomena were associated with a robust increase in PPR, implying presynaptic expression. It remains unclear why a persistent depression was not observed in the absence of the mGluR1 blocker. One possibility is that mGluR1 activation has an additional effect that contributes to recovery of transmitter release.

Both mGluR1 and mGluR5 have been detected in a peri-synaptic annulus at glutamatergic synapses both in the hippocampus and in the cerebellar cortex (Martin et al., 1992; Baude et al., 1993; Lujan et al., 1996; Shigemoto et al., 1997; Lujan et al., 1997; Petralia et al., 1997; van Hooft et al., 2000; Lopez-Bendito et al., 2002). Although this does not exclude an additional presynaptic location of some group I receptors, the finding that postsynaptic manipulation of G protein and Ca^{2+} signalling almost abolished DHPG-evoked depression (Chapter 6) argues that such receptors do not play a large role. The residual non-significant depression observed in this experiment could be explained by a small contribution of mGluR-mediated signalling in neighboring neurons. Group I mGluRs have a high affinity for glutamate (Conn and Pin, 1997). In Purkinje and striatal cells a cationic conductance activated by mGluR1 has been shown to be highly sensitive to manipulations of extracellular glutamate (Brasnjo and Otis, 2001; Zhang and Sulzer, 2003). Indeed, extracellular pooling of glutamate, achieved by recruitment of multiple afferents leads to activation of mGluR1 (Marcaggi et al., 2003). This may also explain the finding that mGluR-activated currents are preferentially evoked by high-frequency presynaptic activity (Batchelor and Garthwaite, 1997).

The postsynaptic induction and presynaptic expression of DHPG-evoked depression implies that a retrograde signal links the two. Group I mGluRs depolarize neurons by inhibiting several K^+ conductances (Charpak et al., 1990; Desai and Conn, 1991; Guerineau et al., 1994; Luthi et al., 1996) and activating Ca^{2+}-activated and Ca^{2+}-independent cationic conductances (Crepel et al., 1994; Guerineau et al., 1995), leading to increased spiking and release of GABA. This could conceivably

result in depression of EPSCs via increased activation of presynaptic metabotropic $GABA_B$ receptors. However, this would not explain why manipulation of G protein and Ca^{2+} signalling in one cell is sufficient to prevent the depression. Moreover, the depression was unaffected by the selective $GABA_B$ antagonist CGP52432. DHPG application did not result in depolarisation in the recorded neuron (see Chapter 5, Section 5.3.1). However, this was because a caesium-based intracellular solution containing QX314 was used, thereby blocking K^+ flux through the channels primarily responsible for mediating the depolarisation. However, other interneurons in the slice were not affected in this manner, and would thus be expected to exhibit increased spiking and release of GABA, thereby raising the ambient GABA concentration.

Endocannabinoids are potentially a better candidate, because they have been shown to act as a local retrograde signal affecting GABA and glutamate release (Wilson and Nicoll, 2001; Kreitzer and Regehr, 2001b). Indeed, group I mGluR activation has been shown to trigger endocannabinoid release leading to presynaptic inhibition of GABA and glutamate release in the cerebellum (Maejima et al., 2001), brainstem (Kushmerick et al., 2004), hippocampus (Varma et al., 2001; Rouach and Nicoll, 2003), ventral tegmental area (Bellone and Luscher, 2005), and nucleus accumbens (Robbe et al., 2002). Until recently, CB1 receptors had not been detected on hippocampal glutamatergic terminals in immunohistochemical studies (Katona et al., 1999b). Nevertheless, because some actions of endocannabinoids have been proposed to be mediated by an as yet uncharacterized receptor (Hajos et al., 2001) this class of molecules cannot be fully ruled out as the retrograde factor involved in DHPG-evoked depression. In the present study, pre-exposure to the selective CB1 antagonist AM251 did not affect the magnitude of DHPG-induced depression of EPSCs in interneurons. This lends no support to the hypothesis that endocannabinoids are the retrograde messenger in this system.

Notwithstanding the uncertainty surrounding the retrograde factor, the present study implies that the DHPG-induced depression is expressed through a presynaptic

mechanism. It persisted when N-type channels were blocked, but was fully occluded when P/Q-type channels were blocked (Chapter 7).

What is the physiological role of the group I mGluR-mediated depression of excitation of interneurons? Evidence was sought that glutamate release in a separate afferent pathway could mimic the effect of exogenous agonist application (Chapter 8). Interleaving a brief train of stimuli in a separate conditioning pathway with a single stimulus in the test pathway has previously been used to reveal a group III mGluR-mediated heterosynaptic depression of GABA release onto interneurons (Semyanov and Kullmann, 2000). When applied to EPSCs in the present study, with group III mGluRs blocked, a possible heterosynaptic interaction was seen, but fell just short of reaching statistical significance (Chapter 8, Fig 8.1). It is possible that a group I mGluR-mediated heterosynaptic depression may have reached significance using this protocol, simply by increasing the sample size in this experiment. Instead, however, a robust, albeit small and reversible, heterosynaptic depression was observed following a single high-frequency tetanus delivered to the conditioning pathway (Chapter 8, Fig 8.3). This was insensitive to blockade of group III mGluRs, but was abolished by blocking group I mGluRs.

The different time-course and glutamate release requirements of the group I and group III mGluR-mediated forms of heterosynaptic depression may reflect distinct signalling cascades: in the case of group III mGluR-mediated heterosynaptic depression, spillover of glutamate directly affects presynaptic terminals. In the case of group I mGluR-mediated heterosynaptic interaction, in contrast, the induction of a postsynaptic cascade may well explain the more prolonged, albeit reversible, depression. The earlier finding that blocking postsynaptic G protein and Ca^{2+} signalling in the recorded cell abolished the effect of DHPG makes unlikely (although does not preclude) diffusion of a retrograde messenger from neighboring neurons to the glutamatergic axons mediating the test EPSC. Instead, the simplest explanation for group I mGluR-mediated heterosynaptic depression is that glutamate itself is

responsible for triggering the induction cascade in the recorded cell, leading indirectly to presynaptic inhibition of glutamate release.

The present study reveals a novel role for group I mGluRs in modulating glutamate release from Schaffer collaterals at synapses on interneurons. Although the effect of synaptic glutamate release from a neighboring pathway was small, it underestimates the full dynamic range of the phenomenon (DHPG application caused a roughly 50 % decrease in glutamatergic drive to interneurons; Chapter 5, Fig 5.1). A possible reason for the small heterosynaptic depression is that only a minority of Schaffer collaterals innervating the interneuron were activated by the tetanus. This heterosynaptic depression potentially leads to disinhibition of pyramidal cells. Although its adaptive significance is unclear, it must be put into the context of other synaptic, heterosynaptic, and extrasynaptic actions of glutamate and GABA, which are likely to alter interneuron depolarization under conditions of intense network activity. Interestingly, in contrast to the group I mGluR-mediated depression, lasting a few minutes, exhibited by stratum radiatum interneurons, the same receptors mediate a long-lasting tetanus-induced potentiation of EPSCs in stratum oriens interneurons (Perez et al., 2001; Lapointe et al., 2004). Given the distinct innervation and projection patterns of stratum radiatum and stratum oriens interneurons, it is tempting to speculate that group I mGluR activation may simultaneously depress feed-forward inhibition and facilitate feed-back inhibition.

References

Acsady,L., Kamondi,A., Sik,A., Freund,T., and Buzsaki,G. (1998). GABAergic cells are the major postsynaptic targets of mossy fibers in the rat hippocampus. J. Neurosci. *18*, 3386-3403.

Ali,A.B., Deuchars,J., Pawelzik,H., and Thomson,A.M. (1998). CA1 pyramidal to basket and bistratified cell EPSPs: dual intracellular recordings in rat hippocampal slices. J. Physiol *507 (Pt 1)*, 201-217.

Ali,A.B., and Thomson,A.M. (1998). Facilitating pyramid to horizontal oriens-alveus interneurone inputs: dual intracellular recordings in slices of rat hippocampus. J. Physiol *507 (Pt 1)*, 185-199.

Amara,S.G., and Fontana,A.C. (2002). Excitatory amino acid transporters: keeping up with glutamate. Neurochem. Int. *41*, 313-318.

Amaral,D.G., Ishizuka,N., and Claiborne,B. (1990). Neurons, numbers and the hippocampal network. Prog. Brain Res. *83*, 1-11.

Anderson,P., Bliss,T.V., and Skrede,K.K. (1971). Lamellar organization of hippocampal pathways. Exp. Brain Res. *13*, 222-238.

Angulo,M.C., Lambolez,B., Audinat,E., Hestrin,S., and Rossier,J. (1997). Subunit composition, kinetic, and permeation properties of AMPA receptors in single neocortical nonpyramidal cells. J. Neurosci. *17*, 6685-6696.

Anwyl,R. (1999). Metabotropic glutamate receptors: electrophysiological properties and role in plasticity. Brain Res. Brain Res. Rev. *29*, 83-120.

Arnth-Jensen,N., Jabaudon,D., and Scanziani,M. (2002). Cooperation between independent hippocampal synapses is controlled by glutamate uptake. Nat. Neurosci. *5*, 325-331.

Asztely,F., Erdemli,G., and Kullmann,D.M. (1997). Extrasynaptic glutamate spillover in the hippocampus: dependence on temperature and the role of active glutamate uptake. Neuron *18*, 281-293.

Atzori,M., Lau,D., Tansey,E.P., Chow,A., Ozaita,A., Rudy,B., and McBain,C.J. (2000). H2 histamine receptor-phosphorylation of Kv3.2 modulates interneuron fast spiking. Nat. Neurosci. *3*, 791-798.

Bahn,S., Volk,B., and Wisden,W. (1994). Kainate receptor gene expression in the developing rat brain. J. Neurosci. *14*, 5525-5547.

Baskys,A., and Malenka,R.C. (1991). Agonists at metabotropic glutamate receptors presynaptically inhibit EPSCs in neonatal rat hippocampus. J. Physiol *444*, 687-701.

Batchelor,A.M., and Garthwaite,J. (1997). Frequency detection and temporally dispersed synaptic signal association through a metabotropic glutamate receptor pathway. Nature *385*, 74-77.

Batchelor,A.M., Madge,D.J., and Garthwaite,J. (1994). Synaptic activation of metabotropic glutamate receptors in the parallel fibre-Purkinje cell pathway in rat cerebellar slices. Neuroscience *63*, 911-915.

Baude,A., Bleasdale,C., Dalezios,Y., Somogyi,P., and Klausberger,T. (2006). Immunoreactivity for the GABAA Receptor {alpha}1 Subunit, Somatostatin and Connexin36 Distinguishes Axoaxonic, Basket, and Bistratified Interneurons of the Rat Hippocampus. Cereb. Cortex.

Baude,A., Nusser,Z., Molnar,E., McIlhinney,R.A., and Somogyi,P. (1995). High-resolution immunogold localization of AMPA type glutamate receptor subunits at synaptic and non-synaptic sites in rat hippocampus. Neuroscience *69*, 1031-1055.

Baude,A., Nusser,Z., Roberts,J.D., Mulvihill,E., McIlhinney,R.A., and Somogyi,P. (1993). The metabotropic glutamate receptor (mGluR1 alpha) is concentrated at perisynaptic membrane of neuronal subpopulations as detected by immunogold reaction. Neuron *11*, 771-787.

Begg,M., Pacher,P., Batkai,S., Osei-Hyiaman,D., Offertaler,L., Mo,F.M., Liu,J., and Kunos,G. (2005). Evidence for novel cannabinoid receptors. Pharmacol. Ther. *106*, 133-145.

Bellone,C., and Luscher,C. (2005). mGluRs induce a long-term depression in the ventral tegmental area that involves a switch of the subunit composition of AMPA receptors. Eur. J. Neurosci. *21*, 1280-1288.

Ben-Ari,Y., and Cossart,R. (2000). Kainate, a double agent that generates seizures: two decades of progress. Trends Neurosci. *23*, 580-587.

Bettler,B., Kaupmann,K., Mosbacher,J., and Gassmann,M. (2004). Molecular structure and physiological functions of GABA(B) receptors. Physiol Rev. *84*, 835-867.

Billups,B., Wong,A.Y., and Forsythe,I.D. (2002). Detecting synaptic connections in the medial nucleus of the trapezoid body using calcium imaging. Pflugers Arch. *444*, 663-669.

Blackstad,T.W., Brink,K., Hem,J., and Jeune,B. (1970). Distribution of hippocampal mossy fibers in the rat. An experimental study with silver impregnation methods. J. Comp Neurol. *138*, 433-449.

Blasco-Ibanez,J.M., and Freund,T.F. (1995). Synaptic input of horizontal interneurons in stratum oriens of the hippocampal CA1 subfield: structural basis of feed-back activation. Eur. J. Neurosci. *7*, 2170-2180.

Boehning,D., and Snyder,S.H. (2003). Novel neural modulators. Annu. Rev. Neurosci. *26*, 105-131.

Brasnjo,G., and Otis,T.S. (2001). Neuronal glutamate transporters control activation of postsynaptic metabotropic glutamate receptors and influence cerebellar long-term depression. Neuron *31*, 607-616.

Buhl,E.H., Halasy,K., and Somogyi,P. (1994). Diverse sources of hippocampal unitary inhibitory postsynaptic potentials and the number of synaptic release sites. Nature *368*, 823-828.

Bureau,I., Bischoff,S., Heinemann,S.F., and Mulle,C. (1999). Kainate receptor-mediated responses in the CA1 field of wild-type and GluR6-deficient mice. J. Neurosci. *19*, 653-663.

Buzsaki,G. (1984). Feed-forward inhibition in the hippocampal formation. Prog. Neurobiol. *22*, 131-153.

Capogna,M. (2004). Distinct properties of presynaptic group II and III metabotropic glutamate receptor-mediated inhibition of perforant pathway-CA1 EPSCs. Eur. J. Neurosci. *19*, 2847-2858.

Carmant,L., Woodhall,G., Ouardouz,M., Robitaille,R., and Lacaille,J.C. (1997). Interneuron-specific Ca2+ responses linked to metabotropic and ionotropic glutamate receptors in rat hippocampal slices. Eur. J. Neurosci. *9*, 1625-1635.

Chandler,K.E., Princivalle,A.P., Fabian-Fine,R., Bowery,N.G., Kullmann,D.M., and Walker,M.C. (2003). Plasticity of GABA(B) receptor-mediated heterosynaptic interactions at mossy fibers after status epilepticus. J. Neurosci. *23*, 11382-11391.

Charpak,S., Gahwiler,B.H., Do,K.Q., and Knopfel,T. (1990). Potassium conductances in hippocampal neurons blocked by excitatory amino-acid transmitters. Nature *347*, 765-767.

Chicurel,M.E., and Harris,K.M. (1992). Three-dimensional analysis of the structure and composition of CA3 branched dendritic spines and their synaptic relationships with mossy fiber boutons in the rat hippocampus. J. Comp Neurol. *325*, 169-182.

Choi,S., and Lovinger,D.M. (1996). Metabotropic glutamate receptor modulation of voltage-gated Ca2+ channels involves multiple receptor subtypes in cortical neurons. J. Neurosci. *16*, 36-45.

Chow,A., Erisir,A., Farb,C., Nadal,M.S., Ozaita,A., Lau,D., Welker,E., and Rudy,B. (1999). K(+) channel expression distinguishes subpopulations of parvalbumin- and somatostatin-containing neocortical interneurons. J. Neurosci. *19*, 9332-9345.

Christensen,J.K., Paternain,A.V., Selak,S., Ahring,P.K., and Lerma,J. (2004). A mosaic of functional kainate receptors in hippocampal interneurons. J. Neurosci. *24*, 8986-8993.

Chuang,S.C., Bianchi,R., and Wong,R.K. (2000). Group I mGluR activation turns on a voltage-gated inward current in hippocampal pyramidal cells. J. Neurophysiol. *83*, 2844-2853.

Chuang,S.C., Zhao,W., Young,S.R., Conquet,F., Bianchi,R., and Wong,R.K. (2002). Activation of group I mGluRs elicits different responses in murine CA1 and CA3 pyramidal cells. J. Physiol *541*, 113-121.

Claiborne,B.J., Amaral,D.G., and Cowan,W.M. (1986). A light and electron microscopic analysis of the mossy fibers of the rat dentate gyrus. J. Comp Neurol. *246*, 435-458.

Cobb,S.R., Buhl,E.H., Halasy,K., Paulsen,O., and Somogyi,P. (1995). Synchronization of neuronal activity in hippocampus by individual GABAergic interneurons. Nature *378*, 75-78.

Congar,P., Leinekugel,X., Ben-Ari,Y., and Crepel,V. (1997). A long-lasting calcium-activated nonselective cationic current is generated by synaptic stimulation or exogenous activation of group I metabotropic glutamate receptors in CA1 pyramidal neurons. J. Neurosci. *17*, 5366-5379.

Conn,P.J., and Pin,J.P. (1997). Pharmacology and functions of metabotropic glutamate receptors. Annu. Rev. Pharmacol. Toxicol. *37*, 205-237.

Connors,B.W., and Gutnick,M.J. (1990). Intrinsic firing patterns of diverse neocortical neurons. Trends Neurosci. *13*, 99-104.

Cossart,R., Epsztein,J., Tyzio,R., Becq,H., Hirsch,J., Ben-Ari,Y., and Crepel,V. (2002). Quantal release of glutamate generates pure kainate and mixed AMPA/kainate EPSCs in hippocampal neurons. Neuron *35*, 147-159.

Cossart,R., Esclapez,M., Hirsch,J.C., Bernard,C., and Ben-Ari,Y. (1998). GluR5 kainate receptor activation in interneurons increases tonic inhibition of pyramidal cells. Nat. Neurosci. *1*, 470-478.

Crepel,V., Aniksztejn,L., Ben-Ari,Y., and Hammond,C. (1994). Glutamate metabotropic receptors increase a Ca(2+)-activated nonspecific cationic current in CA1 hippocampal neurons. J. Neurophysiol. *72*, 1561-1569.

Csicsvari,J., Hirase,H., Czurko,A., and Buzsaki,G. (1998). Reliability and state dependence of pyramidal cell-interneuron synapses in the hippocampus: an ensemble approach in the behaving rat. Neuron *21*, 179-189.

Cui,C., and Mayer,M.L. (1999). Heteromeric kainate receptors formed by the coassembly of GluR5, GluR6, and GluR7. J. Neurosci. *19*, 8281-8291.

Currie,K.P., and Fox,A.P. (1997). Comparison of N- and P/Q-type voltage-gated calcium channel current inhibition. J. Neurosci. *17*, 4570-4579.

Darstein,M., Petralia,R.S., Swanson,G.T., Wenthold,R.J., and Heinemann,S.F. (2003). Distribution of kainate receptor subunits at hippocampal mossy fiber synapses. J. Neurosci. *23*, 8013-8019.

De,P.L., Cascio,M.G., and Di,M., V (2004). The endocannabinoid system: a general view and latest additions. Br. J. Pharmacol. *141*, 765-774.

Desai,M.A., and Conn,P.J. (1991). Excitatory effects of ACPD receptor activation in the hippocampus are mediated by direct effects on pyramidal cells and blockade of synaptic inhibition. J. Neurophysiol. *66*, 40-52.

Desai,M.A., McBain,C.J., Kauer,J.A., and Conn,P.J. (1994). Metabotropic glutamate receptor-induced disinhibition is mediated by reduced transmission at excitatory synapses onto interneurons and inhibitory synapses onto pyramidal cells. Neurosci. Lett. *181*, 78-82.

Deuchars,J., and Thomson,A.M. (1996). CA1 pyramid-pyramid connections in rat hippocampus in vitro: dual intracellular recordings with biocytin filling. Neuroscience *74*, 1009-1018.

Di,M., V, Fontana,A., Cadas,H., Schinelli,S., Cimino,G., Schwartz,J.C., and Piomelli,D. (1994). Formation and inactivation of endogenous cannabinoid anandamide in central neurons. Nature *372*, 686-691.

Dingledine,R., Borges,K., Bowie,D., and Traynelis,S.F. (1999). The glutamate receptor ion channels. Pharmacol. Rev. *51*, 7-61.

Dinocourt,C., Petanjek,Z., Freund,T.F., Ben-Ari,Y., and Esclapez,M. (2003). Loss of interneurons innervating pyramidal cell dendrites and axon initial segments in the CA1 region of the hippocampus following pilocarpine-induced seizures. J. Comp Neurol. *459*, 407-425.

Doherty,A.J., Palmer,M.J., Henley,J.M., Collingridge,G.L., and Jane,D.E. (1997). (RS)-2-chloro-5-hydroxyphenylglycine (CHPG) activates mGlu5, but no mGlu1, receptors expressed in CHO cells and potentiates NMDA responses in the hippocampus. Neuropharmacology *36*, 265-267.

Doherty,J., and Dingledine,R. (1997). Regulation of excitatory input to inhibitory interneurons of the dentate gyrus during hypoxia. J. Neurophysiol. *77*, 393-404.

Doherty,J., and Dingledine,R. (1998). Differential regulation of synaptic inputs to dentate hilar border interneurons by metabotropic glutamate receptors. J. Neurophysiol. *79*, 2903-2910.

Doherty,J.J., Alagarsamy,S., Bough,K.J., Conn,P.J., Dingledine,R., and Mott,D.D. (2004). Metabotropic glutamate receptors modulate feedback inhibition in a developmentally regulated manner in rat dentate gyrus. J. Physiol *561*, 395-401.

Doze,V.A., Cohen,G.A., and Madison,D.V. (1995). Calcium channel involvement in GABAB receptor-mediated inhibition of GABA release in area CA1 of the rat hippocampus. J. Neurophysiol. *74*, 43-53.

Du,J., Zhang,L., Weiser,M., Rudy,B., and McBain,C.J. (1996). Developmental expression and functional characterization of the potassium-channel subunit Kv3.1b in parvalbumin-containing interneurons of the rat hippocampus. J. Neurosci. *16*, 506-518.

Edwards,F.A., Konnerth,A., Sakmann,B., and Takahashi,T. (1989). A thin slice preparation for patch clamp recordings from neurones of the mammalian central nervous system. Pflugers Arch. *414*, 600-612.

Erisir,A., Lau,D., Rudy,B., and Leonard,C.S. (1999). Function of specific K(+) channels in sustained high-frequency firing of fast-spiking neocortical interneurons. J. Neurophysiol. *82*, 2476-2489.

Faas,G.C., Adwanikar,H., Gereau,R.W., and Saggau,P. (2002). Modulation of presynaptic calcium transients by metabotropic glutamate receptor activation: a differential role in acute depression of synaptic transmission and long-term depression. J. Neurosci. *22*, 6885-6890.

Ferraguti,F., Cobden,P., Pollard,M., Cope,D., Shigemoto,R., Watanabe,M., and Somogyi,P. (2004). Immunolocalization of metabotropic glutamate receptor 1alpha (mGluR1alpha) in distinct classes of interneuron in the CA1 region of the rat hippocampus. Hippocampus *14*, 193-215.

Fisahn,A., Pike,F.G., Buhl,E.H., and Paulsen,O. (1998). Cholinergic induction of network oscillations at 40 Hz in the hippocampus in vitro. Nature *394*, 186-189.

Fitzjohn,S.M., Bortolotto,Z.A., Palmer,M.J., Doherty,A.J., Ornstein,P.L., Schoepp,D.D., Kingston,A.E., Lodge,D., and Collingridge,G.L. (1998). The potent mGlu receptor antagonist LY341495 identifies roles for both cloned and novel mGlu receptors in hippocampal synaptic plasticity. Neuropharmacology *37*, 1445-1458.

Fitzjohn,S.M., Palmer,M.J., May,J.E., Neeson,A., Morris,S.A., and Collingridge,G.L. (2001). A characterisation of long-term depression induced by metabotropic glutamate receptor activation in the rat hippocampus in vitro. J. Physiol *537*, 421-430.

Fitzsimonds,R.M., and Dichter,M.A. (1996). Heterologous modulation of inhibitory synaptic transmission by metabotropic glutamate receptors in cultured hippocampal neurons. J. Neurophysiol. *75*, 885-893.

Fraser,D.D., and MacVicar,B.A. (1991). Low-threshold transient calcium current in rat hippocampal lacunosum-moleculare interneurons: kinetics and modulation by neurotransmitters. J. Neurosci. *11*, 2812-2820.

Frerking,M., Malenka,R.C., and Nicoll,R.A. (1998). Synaptic activation of kainate receptors on hippocampal interneurons. Nat. Neurosci. *1*, 479-486.

Frerking,M., Petersen,C.C., and Nicoll,R.A. (1999). Mechanisms underlying kainate receptor-mediated disinhibition in the hippocampus. Proc. Natl. Acad. Sci. U. S. A *96*, 12917-12922.

Freund,T.F. (2003). Interneuron Diversity series: Rhythm and mood in perisomatic inhibition. Trends Neurosci. *26*, 489-495.

Freund,T.F., and Buzsaki,G. (1996). Interneurons of the hippocampus. Hippocampus *6*, 347-470.

Freund,T.F., Katona,I., and Piomelli,D. (2003). Role of endogenous cannabinoids in synaptic signaling. Physiol Rev. *83*, 1017-1066.

Fricker,D., and Miles,R. (2000). EPSP amplification and the precision of spike timing in hippocampal neurons. Neuron *28*, 559-569.

Gasparini,F., Lingenhohl,K., Stoehr,N., Flor,P.J., Heinrich,M., Vranesic,I., Biollaz,M., Allgeier,H., Heckendorn,R., Urwyler,S., Varney,M.A., Johnson,E.C., Hess,S.D., Rao,S.P., Sacaan,A.I., Santori,E.M., Velicelebi,G., and Kuhn,R. (1999). 2-Methyl-6-(phenylethynyl)-pyridine (MPEP), a potent, selective and systemically active mGlu5 receptor antagonist. Neuropharmacology *38*, 1493-1503.

Gee,C.E., Benquet,P., and Gerber,U. (2003). Group I metabotropic glutamate receptors activate a calcium-sensitive transient receptor potential-like conductance in rat hippocampus. J. Physiol *546*, 655-664.

Gee,C.E., and Lacaille,J.C. (2004). Group I metabotropic glutamate receptor actions in oriens/alveus interneurons of rat hippocampal CA1 region. Brain Res. *1000*, 92-101.

Geiger,J.R., Lubke,J., Roth,A., Frotscher,M., and Jonas,P. (1997). Submillisecond AMPA receptor-mediated signaling at a principal neuron-interneuron synapse. Neuron *18*, 1009-1023.

Geiger,J.R., Melcher,T., Koh,D.S., Sakmann,B., Seeburg,P.H., Jonas,P., and Monyer,H. (1995). Relative abundance of subunit mRNAs determines gating and Ca2+ permeability of AMPA receptors in principal neurons and interneurons in rat CNS. Neuron *15*, 193-204.

Gereau,R.W., and Conn,P.J. (1995). Multiple presynaptic metabotropic glutamate receptors modulate excitatory and inhibitory synaptic transmission in hippocampal area CA1. J. Neurosci. *15*, 6879-6889.

Goldstein,S.A., Bockenhauer,D., O'Kelly,I., and Zilberberg,N. (2001). Potassium leak channels and the KCNK family of two-P-domain subunits. Nat. Rev. Neurosci. *2*, 175-184.

Guerineau,N.C., Bossu,J.L., Gahwiler,B.H., and Gerber,U. (1995). Activation of a nonselective cationic conductance by metabotropic glutamatergic and muscarinic agonists in CA3 pyramidal neurons of the rat hippocampus. J. Neurosci. *15*, 4395-4407.

Guerineau,N.C., Gahwiler,B.H., and Gerber,U. (1994). Reduction of resting K+ current by metabotropic glutamate and muscarinic receptors in rat CA3 cells: mediation by G-proteins. J. Physiol *474*, 27-33.

Gulyas,A.I., Megias,M., Emri,Z., and Freund,T.F. (1999). Total number and ratio of excitatory and inhibitory synapses converging onto single interneurons of different types in the CA1 area of the rat hippocampus. J. Neurosci. *19*, 10082-10097.

Gulyas,A.I., Miles,R., Hajos,N., and Freund,T.F. (1993a). Precision and variability in postsynaptic target selection of inhibitory cells in the hippocampal CA3 region. Eur. J. Neurosci. *5*, 1729-1751.

Gulyas,A.I., Miles,R., Sik,A., Toth,K., Tamamaki,N., and Freund,T.F. (1993b). Hippocampal pyramidal cells excite inhibitory neurons through a single release site. Nature *366*, 683-687.

Hajos,N., Katona,I., Naiem,S.S., Mackie,K., Ledent,C., Mody,I., and Freund,T.F. (2000). Cannabinoids inhibit hippocampal GABAergic transmission and network oscillations. Eur. J. Neurosci. *12*, 3239-3249.

Hajos,N., Ledent,C., and Freund,T.F. (2001). Novel cannabinoid-sensitive receptor mediates inhibition of glutamatergic synaptic transmission in the hippocampus. Neuroscience *106*, 1-4.

Hall,R.A., Premont,R.T., and Lefkowitz,R.J. (1999). Heptahelical receptor signaling: beyond the G protein paradigm. J. Cell Biol. *145*, 927-932.

Hardingham,N., and Fox,K. (2006). The role of nitric oxide and GluR1 in presynaptic and postsynaptic components of neocortical potentiation. J. Neurosci. *26*, 7395-7404.

Harris,K.M., and Stevens,J.K. (1989). Dendritic spines of CA 1 pyramidal cells in the rat hippocampus: serial electron microscopy with reference to their biophysical characteristics. J. Neurosci. *9*, 2982-2997.

He,Y., Janssen,W.G., and Morrison,J.H. (1998). Synaptic coexistence of AMPA and NMDA receptors in the rat hippocampus: a postembedding immunogold study. J. Neurosci. Res. *54*, 444-449.

Helmchen,F., Imoto,K., and Sakmann,B. (1996). Ca2+ buffering and action potential-evoked Ca2+ signaling in dendrites of pyramidal neurons. Biophys. J. *70*, 1069-1081.

Henze,D.A., Urban,N.N., and Barrionuevo,G. (2000). The multifarious hippocampal mossy fiber pathway: a review. Neuroscience *98*, 407-427.

Hermans,E., and Challiss,R.A. (2001). Structural, signalling and regulatory properties of the group I metabotropic glutamate receptors: prototypic family C G-protein-coupled receptors. Biochem. J. *359*, 465-484.

Heuss,C., Scanziani,M., Gahwiler,B.H., and Gerber,U. (1999). G-protein-independent signaling mediated by metabotropic glutamate receptors. Nat. Neurosci. *2*, 1070-1077.

Hille, B (2001) Ion Channels of Excitable Membranes. Sunderland, MA (USA). Sinauer Associates Inc.

Hoffman,A.F., Macgill,A.M., Smith,D., Oz,M., and Lupica,C.R. (2005). Species and strain differences in the expression of a novel glutamate-modulating cannabinoid receptor in the rodent hippocampus. Eur. J. Neurosci. *22*, 2387-2391.

Hollmann,M., Hartley,M., and Heinemann,S. (1991). Ca2+ permeability of KA-AMPA--gated glutamate receptor channels depends on subunit composition. Science *252*, 851-853.

Hollmann,M., and Heinemann,S. (1994). Cloned glutamate receptors. Annu. Rev. Neurosci. *17*, 31-108.

Houamed,K.M., Kuijper,J.L., Gilbert,T.L., Haldeman,B.A., O'Hara,P.J., Mulvihill,E.R., Almers,W., and Hagen,F.S. (1991). Cloning, expression, and gene structure of a G protein-coupled glutamate receptor from rat brain. Science *252*, 1318-1321.

Houser,C.R., and Esclapez,M. (1996). Vulnerability and plasticity of the GABA system in the pilocarpine model of spontaneous recurrent seizures. Epilepsy Res. *26*, 207-218.

Hsu,M., and Buzsaki,G. (1993). Vulnerability of mossy fiber targets in the rat hippocampus to forebrain ischemia. J. Neurosci. *13*, 3964-3979.

Huang,C.C., and Hsu,K.S. (2005). Sustained activation of metabotropic glutamate receptor 5 and protein tyrosine phosphatases mediate the expression of (S)-3,5-dihydroxyphenylglycine-induced long-term depression in the hippocampal CA1 region. J. Neurochem.

Huang,C.C., You,J.L., Wu,M.Y., and Hsu,K.S. (2004). Rap1-induced p38 mitogen-activated protein kinase activation facilitates AMPA receptor trafficking via the GDI.Rab5 complex. Potential role in (S)-3,5-dihydroxyphenylglycene-induced long term depression. J. Biol. Chem. *279*, 12286-12292.

Huber,K.M., Kayser,M.S., and Bear,M.F. (2000). Role for rapid dendritic protein synthesis in hippocampal mGluR-dependent long-term depression. Science *288*, 1254-1257.

Huber,K.M., Roder,J.C., and Bear,M.F. (2001). Chemical induction of mGluR5- and protein synthesis--dependent long-term depression in hippocampal area CA1. J. Neurophysiol. *86*, 321-325.

Huettner,J.E. (1990). Glutamate receptor channels in rat DRG neurons: activation by kainate and quisqualate and blockade of desensitization by Con A. Neuron *5*, 255-266.

Ireland,D.R., and Abraham,W.C. (2002). Group I mGluRs increase excitability of hippocampal CA1 pyramidal neurons by a PLC-independent mechanism. J. Neurophysiol. *88*, 107-116.

Isa,T., Itazawa,S., Iino,M., Tsuzuki,K., and Ozawa,S. (1996). Distribution of neurones expressing inwardly rectifying and Ca(2+)-permeable AMPA receptors in rat hippocampal slices. J. Physiol *491 (Pt 3)*, 719-733.

Isaacson,J.S., Solis,J.M., and Nicoll,R.A. (1993). Local and diffuse synaptic actions of GABA in the hippocampus. Neuron *10*, 165-175.

Ishizuka,N., Weber,J., and Amaral,D.G. (1990). Organization of intrahippocampal projections originating from CA3 pyramidal cells in the rat. J. Comp Neurol. *295*, 580-623.

Johnston,D., Magee,J.C., Colbert,C.M., and Cristie,B.R. (1996). Active properties of neuronal dendrites. Annu. Rev. Neurosci. *19*, 165-186.

Jonas,P., and Burnashev,N. (1995). Molecular mechanisms controlling calcium entry through AMPA-type glutamate receptor channels. Neuron *15*, 987-990.

Jonas,P., Racca,C., Sakmann,B., Seeburg,P.H., and Monyer,H. (1994). Differences in Ca2+ permeability of AMPA-type glutamate receptor channels in neocortical neurons caused by differential GluR-B subunit expression. Neuron *12*, 1281-1289.

Kamiya,H., and Ozawa,S. (1999). Dual mechanism for presynaptic modulation by axonal metabotropic glutamate receptor at the mouse mossy fibre-CA3 synapse. J. Physiol *518 (Pt 2)*, 497-506.

Katona,I., Acsady,L., and Freund,T.F. (1999a). Postsynaptic targets of somatostatin-immunoreactive interneurons in the rat hippocampus. Neuroscience *88*, 37-55.

Katona,I., Sperlagh,B., Sik,A., Kafalvi,A., Vizi,E.S., Mackie,K., and Freund,T.F. (1999b). Presynaptically located CB1 cannabinoid receptors regulate GABA release from axon terminals of specific hippocampal interneurons. J. Neurosci. *19*, 4544-4558.

Katona,I., Urban,G.M., Wallace,M., Ledent,C., Jung,K.M., Piomelli,D., Mackie,K., and Freund,T.F. (2006). Molecular composition of the endocannabinoid system at glutamatergic synapses. J. Neurosci. *26*, 5628-5637.

Kawaguchi,Y., and Hama,K. (1988). Physiological heterogeneity of nonpyramidal cells in rat hippocampal CA1 region. Exp. Brain Res. *72*, 494-502.

Kawamura,Y., Fukaya,M., Maejima,T., Yoshida,T., Miura,E., Watanabe,M., Ohno-Shosaku,T., and Kano,M. (2006). The CB1 cannabinoid receptor is the major cannabinoid receptor at excitatory presynaptic sites in the hippocampus and cerebellum. J. Neurosci. *26*, 2991-3001.

Kemp,N., and Bashir,Z.I. (1999). Induction of LTD in the adult hippocampus by the synaptic activation of AMPA/kainate and metabotropic glutamate receptors. Neuropharmacology *38*, 495-504.

Kew,J.N., Ducarre,J.M., Pflimlin,M.C., Mutel,V., and Kemp,J.A. (2001). Activity-dependent presynaptic autoinhibition by group II metabotropic glutamate receptors at the perforant path inputs to the dentate gyrus and CA1. Neuropharmacology *40*, 20-27.

Khakh,B.S., Gittermann,D., Cockayne,D.A., and Jones,A. (2003). ATP modulation of excitatory synapses onto interneurons. J. Neurosci. *23*, 7426-7437.

Kim,S.J., Kim,Y.S., Yuan,J.P., Petralia,R.S., Worley,P.F., and Linden,D.J. (2003). Activation of the TRPC1 cation channel by metabotropic glutamate receptor mGluR1. Nature *426*, 285-291.

Kingston,A.E., Ornstein,P.L., Wright,R.A., Johnson,B.G., Mayne,N.G., Burnett,J.P., Belagaje,R., Wu,S., and Schoepp,D.D. (1998). LY341495 is a nanomolar potent and selective antagonist of group II metabotropic glutamate receptors. Neuropharmacology *37*, 1-12.

Kitano,J., Nishida,M., Itsukaichi,Y., Minami,I., Ogawa,M., Hirano,T., Mori,Y., and Nakanishi,S. (2003). Direct interaction and functional coupling between metabotropic glutamate receptor subtype 1 and voltage-sensitive Cav2.1 Ca2+ channel. J. Biol. Chem. *278*, 25101-25108.

Klausberger,T., Magill,P.J., Marton,L.F., Roberts,J.D., Cobden,P.M., Buzsaki,G., and Somogyi,P. (2003). Brain-state- and cell-type-specific firing of hippocampal interneurons in vivo. Nature *421*, 844-848.

Klausberger,T., Marton,L.F., Baude,A., Roberts,J.D., Magill,P.J., and Somogyi,P. (2004). Spike timing of dendrite-targeting bistratified cells during hippocampal network oscillations in vivo. Nat. Neurosci. *7*, 41-47.

Klausberger,T., Marton,L.F., O'Neill,J., Huck,J.H., Dalezios,Y., Fuentealba,P., Suen,W.Y., Papp,E., Kaneko,T., Watanabe,M., Csicsvari,J., and Somogyi,P. (2005). Complementary roles of cholecystokinin- and parvalbumin-expressing GABAergic neurons in hippocampal network oscillations. J. Neurosci. *25*, 9782-9793.

Knowles,W.D., and Schwartzkroin,P.A. (1981). Axonal ramifications of hippocampal Ca1 pyramidal cells. J. Neurosci. *1*, 1236-1241.

Kobilka,B. (1992). Adrenergic receptors as models for G protein-coupled receptors. Annu. Rev. Neurosci. *15*, 87-114.

Kogo,N., Dalezios,Y., Capogna,M., Ferraguti,F., Shigemoto,R., and Somogyi,P. (2004). Depression of GABAergic input to identified hippocampal neurons by group III metabotropic glutamate receptors in the rat. Eur. J. Neurosci. *19*, 2727-2740.

Koh,D.S., Burnashev,N., and Jonas,P. (1995a). Block of native Ca(2+)-permeable AMPA receptors in rat brain by intracellular polyamines generates double rectification. J. Physiol *486 (Pt 2)*, 305-312.

Koh,D.S., Geiger,J.R., Jonas,P., and Sakmann,B. (1995b). Ca(2+)-permeable AMPA and NMDA receptor channels in basket cells of rat hippocampal dentate gyrus. J. Physiol *485 (Pt 2)*, 383-402.

Kozloski,J., Hamzei-Sichani,F., and Yuste,R. (2001). Stereotyped position of local synaptic targets in neocortex. Science *293*, 868-872.

Kreitzer,A.C., and Regehr,W.G. (2001a). Cerebellar depolarization-induced suppression of inhibition is mediated by endogenous cannabinoids. J. Neurosci. *21*, RC174.

Kreitzer,A.C., and Regehr,W.G. (2001b). Retrograde inhibition of presynaptic calcium influx by endogenous cannabinoids at excitatory synapses onto Purkinje cells. Neuron *29*, 717-727.

Kullmann,D.M. (2000). Spillover and synaptic cross talk mediated by glutamate and GABA in the mammalian brain. Prog. Brain Res. *125*, 339-351.

Kullmann,D.M. (2001). Presynaptic kainate receptors in the hippocampus: slowly emerging from obscurity. Neuron *32*, 561-564.

Kullmann,D.M., Erdemli,G., and Asztely,F. (1996). LTP of AMPA and NMDA receptor-mediated signals: evidence for presynaptic expression and extrasynaptic glutamate spill-over. Neuron *17*, 461-474.

Kunishima,N., Shimada,Y., Tsuji,Y., Sato,T., Yamamoto,M., Kumasaka,T., Nakanishi,S., Jingami,H., and Morikawa,K. (2000). Structural basis of glutamate recognition by a dimeric metabotropic glutamate receptor. Nature *407*, 971-977.

Kushmerick,C., Price,G.D., Taschenberger,H., Puente,N., Renden,R., Wadiche,J.I., Duvoisin,R.M., Grandes,P., and von,G.H. (2004). Retroinhibition of presynaptic Ca2+ currents by endocannabinoids released via postsynaptic mGluR activation at a calyx synapse. J. Neurosci. *24*, 5955-5965.

Lacaille,J.C., Mueller,A.L., Kunkel,D.D., and Schwartzkroin,P.A. (1987). Local circuit interactions between oriens/alveus interneurons and CA1 pyramidal cells in hippocampal slices: electrophysiology and morphology. J. Neurosci. *7*, 1979-1993.

Lamsa,K., Heeroma,J.H., and Kullmann,D.M. (2005). Hebbian LTP in feed-forward inhibitory interneurons and the temporal fidelity of input discrimination. Nat. Neurosci. *8*, 916-924.

Lapointe,V., Morin,F., Ratte,S., Croce,A., Conquet,F., and Lacaille,J.C. (2004). Synapse-specific mGluR1-dependent long-term potentiation in interneurones regulates mouse hippocampal inhibition. J. Physiol *555*, 125-135.

Lei,S., and McBain,C.J. (2003). GABA B receptor modulation of excitatory and inhibitory synaptic transmission onto rat CA3 hippocampal interneurons. J. Physiol *546*, 439-453.

Lei,S., and McBain,C.J. (2002). Distinct NMDA receptors provide differential modes of transmission at mossy fiber-interneuron synapses. Neuron *33*, 921-933.

Lei,S., and McBain,C.J. (2004). Two Loci of expression for long-term depression at hippocampal mossy fiber-interneuron synapses. J. Neurosci. *24*, 2112-2121.

Li,X.G., Somogyi,P., Ylinen,A., and Buzsaki,G. (1994). The hippocampal CA3 network: an in vivo intracellular labeling study. J. Comp Neurol. *339*, 181-208.

Lien,C.C., and Jonas,P. (2003). Kv3 potassium conductance is necessary and kinetically optimized for high-frequency action potential generation in hippocampal interneurons. J. Neurosci. *23*, 2058-2068.

Llano,I., Leresche,N., and Marty,A. (1991). Calcium entry increases the sensitivity of cerebellar Purkinje cells to applied GABA and decreases inhibitory synaptic currents. Neuron *6*, 565-574.

Lopez-Bendito,G., Shigemoto,R., Fairen,A., and Lujan,R. (2002). Differential distribution of group I metabotropic glutamate receptors during rat cortical development. Cereb. Cortex *12*, 625-638.

Lorento De No,R. (1934). J. Psychol. Neurol. *45*, 113−177.

Losonczy,A., Somogyi,P., and Nusser,Z. (2003). Reduction of excitatory postsynaptic responses by persistently active metabotropic glutamate receptors in the hippocampus. J. Neurophysiol. *89*, 1910-1919.

Losonczy,A., Zhang,L., Shigemoto,R., Somogyi,P., and Nusser,Z. (2002). Cell type dependence and variability in the short-term plasticity of EPSCs in identified mouse hippocampal interneurones. J. Physiol *542*, 193-210.

Lujan,R., Nusser,Z., Roberts,J.D., Shigemoto,R., and Somogyi,P. (1996). Perisynaptic location of metabotropic glutamate receptors mGluR1 and mGluR5 on dendrites and dendritic spines in the rat hippocampus. Eur. J. Neurosci. *8*, 1488-1500.

Lujan,R., Roberts,J.D., Shigemoto,R., Ohishi,H., and Somogyi,P. (1997). Differential plasma membrane distribution of metabotropic glutamate receptors mGluR1 alpha, mGluR2 and mGluR5, relative to neurotransmitter release sites. J. Chem. Neuroanat. *13*, 219-241.

Luthi,A., Gahwiler,B.H., and Gerber,U. (1996). A slowly inactivating potassium current in CA3 pyramidal cells of rat hippocampus in vitro. J. Neurosci. *16*, 586-594.

Maccaferri,G., and Dingledine,R. (2002). Control of feedforward dendritic inhibition by NMDA receptor-dependent spike timing in hippocampal interneurons. J. Neurosci. *22*, 5462-5472.

Maccaferri,G., and Lacaille,J.C. (2003). Interneuron Diversity series: Hippocampal interneuron classifications--making things as simple as possible, not simpler. Trends Neurosci. *26*, 564-571.

Maccaferri,G., Roberts,J.D., Szucs,P., Cottingham,C.A., and Somogyi,P. (2000). Cell surface domain specific postsynaptic currents evoked by identified GABAergic neurones in rat hippocampus in vitro. J. Physiol *524 Pt 1*, 91-116.

Maejima,T., Hashimoto,K., Yoshida,T., Aiba,A., and Kano,M. (2001). Presynaptic inhibition caused by retrograde signal from metabotropic glutamate to cannabinoid receptors. Neuron *31*, 463-475.

Mannaioni,G., Marino,M.J., Valenti,O., Traynelis,S.F., and Conn,P.J. (2001). Metabotropic glutamate receptors 1 and 5 differentially regulate CA1 pyramidal cell function. J. Neurosci. *21*, 5925-5934.

Manzoni,O., and Bockaert,J. (1995). Metabotropic glutamate receptors inhibiting excitatory synapses in the CA1 area of rat hippocampus. Eur. J. Neurosci. *7*, 2518-2523.

Marcaggi,P., Billups,D., and Attwell,D. (2003). The role of glial glutamate transporters in maintaining the independent operation of juvenile mouse cerebellar parallel fibre synapses. J. Physiol *552*, 89-107.

Martin,L.J., Blackstone,C.D., Huganir,R.L., and Price,D.L. (1992). Cellular localization of a metabotropic glutamate receptor in rat brain. Neuron *9*, 259-270.

Martina,M., and Jonas,P. (1997). Functional differences in Na+ channel gating between fast-spiking interneurones and principal neurones of rat hippocampus. J. Physiol *505 (Pt 3)*, 593-603.

Martina,M., Schultz,J.H., Ehmke,H., Monyer,H., and Jonas,P. (1998). Functional and molecular differences between voltage-gated K+ channels of fast-spiking interneurons and pyramidal neurons of rat hippocampus. J. Neurosci. *18*, 8111-8125.

Martina,M., Vida,I., and Jonas,P. (2000). Distal initiation and active propagation of action potentials in interneuron dendrites. Science *287*, 295-300.

Masu,M., Tanabe,Y., Tsuchida,K., Shigemoto,R., and Nakanishi,S. (1991). Sequence and expression of a metabotropic glutamate receptor. Nature *349*, 760-765.

Matyas,F., Freund,T.F., and Gulyas,A.I. (2004). Convergence of excitatory and inhibitory inputs onto CCK-containing basket cells in the CA1 area of the rat hippocampus. Eur. J. Neurosci. *19*, 1243-1256.

McBain,C.J., DiChiara,T.J., and Kauer,J.A. (1994). Activation of metabotropic glutamate receptors differentially affects two classes of hippocampal interneurons and potentiates excitatory synaptic transmission. J. Neurosci. *14*, 4433-4445.

McBain,C.J., and Dingledine,R. (1993). Heterogeneity of synaptic glutamate receptors on CA3 stratum radiatum interneurones of rat hippocampus. J. Physiol *462*, 373-392.

McBain,C.J., and Fisahn,A. (2001). Interneurons unbound. Nat. Rev. Neurosci. *2*, 11-23.

McBain,C.J., Freund,T.F., and Mody,I. (1999). Glutamatergic synapses onto hippocampal interneurons: precision timing without lasting plasticity. Trends Neurosci. *22*, 228-235.

Miles,R. (1990). Synaptic excitation of inhibitory cells by single CA3 hippocampal pyramidal cells of the guinea-pig in vitro. J. Physiol *428*, 61-77.

Miles,R., and Poncer,J.C. (1996). Paired recordings from neurones. Curr. Opin. Neurobiol. *6*, 387-394.

Miles,R., Toth,K., Gulyas,A.I., Hajos,N., and Freund,T.F. (1996). Differences between somatic and dendritic inhibition in the hippocampus. Neuron *16*, 815-823.

Miles,R., and Wong,R.K. (1986). Excitatory synaptic interactions between CA3 neurones in the guinea-pig hippocampus. J. Physiol *373*, 397-418.

Millan,C., Castro,E., Torres,M., Shigemoto,R., and Sanchez-Prieto,J. (2003). Co-expression of metabotropic glutamate receptor 7 and N-type Ca(2+) channels in single cerebrocortical nerve terminals of adult rats. J. Biol. Chem. *278*, 23955-23962.

Millan,C., Lujan,R., Shigemoto,R., and Sanchez-Prieto,J. (2002a). The inhibition of glutamate release by metabotropic glutamate receptor 7 affects both [Ca2+]c and cAMP: evidence for a strong reduction of Ca2+ entry in single nerve terminals. J. Biol. Chem. *277*, 14092-14101.

Millan,C., Lujan,R., Shigemoto,R., and Sanchez-Prieto,J. (2002b). Subtype-specific expression of group III metabotropic glutamate receptors and Ca2+ channels in single nerve terminals. J. Biol. Chem. *277*, 47796-47803.

Millan,C., and Sanchez-Prieto,J. (2002). Differential coupling of N- and P/Q-type calcium channels to glutamate exocytosis in the rat cerebral cortex. Neurosci. Lett. *330*, 29-32.

Mishina,M., Sakimura,K., Mori,H., Kushiya,E., Harabayashi,M., Uchino,S., and Nagahari,K. (1991). A single amino acid residue determines the Ca2+ permeability of AMPA-selective glutamate receptor channels. Biochem. Biophys. Res. Commun. *180*, 813-821.

Misner,D.L., and Sullivan,J.M. (1999). Mechanism of cannabinoid effects on long-term potentiation and depression in hippocampal CA1 neurons. J. Neurosci. *19*, 6795-6805.

Mitchell,S.J., and Silver,R.A. (2000). Glutamate spillover suppresses inhibition by activating presynaptic mGluRs. Nature *404*, 498-502.

Monory,K., Massa,F., Egertova,M., Eder,M., Blaudzun,H., Westenbroek,R., Kelsch,W., Jacob,W., Marsch,R., Ekker,M., Long,J., Rubenstein,J.L., Goebbels,S., Nave,K.A., During,M., Klugmann,M., Wolfel,B., Dodt,H.U., Zieglgansberger,W., Wotjak,C.T., Mackie,K., Elphick,M.R., Marsicano,G., and Lutz,B. (2006). The endocannabinoid system controls key epileptogenic circuits in the hippocampus. Neuron *51*, 455-466.

Nakamura,T., Nakamura,K., Lasser-Ross,N., Barbara,J.G., Sandler,V.M., and Ross,W.N. (2000). Inositol 1,4,5-trisphosphate (IP3)-mediated Ca2+ release evoked by metabotropic agonists and backpropagating action potentials in hippocampal CA1 pyramidal neurons. J. Neurosci. *20*, 8365-8376.

Nakanishi,S. (1992). Molecular diversity of glutamate receptors and implications for brain function. Science *258*, 597-603.

Nathan,T., Jensen,M.S., and Lambert,J.D. (1990). The slow inhibitory postsynaptic potential in rat hippocampal CA1 neurones is blocked by intracellular injection of QX-314. Neurosci. Lett. *110*, 309-313.

Nusser,Z., Lujan,R., Laube,G., Roberts,J.D., Molnar,E., and Somogyi,P. (1998). Cell type and pathway dependence of synaptic AMPA receptor number and variability in the hippocampus. Neuron *21*, 545-559.

Nusser,Z., Mulvihill,E., Streit,P., and Somogyi,P. (1994). Subsynaptic segregation of metabotropic and ionotropic glutamate receptors as revealed by immunogold localization. Neuroscience *61*, 421-427.

Nyiri,G., Cserep,C., Szabadits,E., Mackie,K., and Freund,T.F. (2005). CB1 cannabinoid receptors are enriched in the perisynaptic annulus and on preterminal segments of hippocampal GABAergic axons. Neuroscience *136*, 811-822.

Nyiri,G., Stephenson,F.A., Freund,T.F., and Somogyi,P. (2003). Large variability in synaptic N-methyl-D-aspartate receptor density on interneurons and a comparison with pyramidal-cell spines in the rat hippocampus. Neuroscience *119*, 347-363.

O'Hara,P.J., Sheppard,P.O., Thogersen,H., Venezia,D., Haldeman,B.A., McGrane,V., Houamed,K.M., Thomsen,C., Gilbert,T.L., and Mulvihill,E.R. (1993). The ligand-binding domain in metabotropic glutamate receptors is related to bacterial periplasmic binding proteins. Neuron *11*, 41-52.

Obenaus,A., Esclapez,M., and Houser,C.R. (1993). Loss of glutamate decarboxylase mRNA-containing neurons in the rat dentate gyrus following pilocarpine-induced seizures. J. Neurosci. *13*, 4470-4485.

Ohno-Shosaku,T., Maejima,T., and Kano,M. (2001). Endogenous cannabinoids mediate retrograde signals from depolarized postsynaptic neurons to presynaptic terminals. Neuron *29*, 729-738.

Ohno-Shosaku,T., Tsubokawa,H., Mizushima,I., Yoneda,N., Zimmer,A., and Kano,M. (2002). Presynaptic cannabinoid sensitivity is a major determinant of depolarization-induced retrograde suppression at hippocampal synapses. J. Neurosci. *22*, 3864-3872.

Okamoto,T., Sekiyama,N., Otsu,M., Shimada,Y., Sato,A., Nakanishi,S., and Jingami,H. (1998). Expression and purification of the extracellular ligand binding region of metabotropic glutamate receptor subtype 1. J. Biol. Chem. *273*, 13089-13096.

O'Keefe, J. (1978) The Hippocampus as a Cognitive Map. Oxford. Oxford University Press.

Oliet,S.H., Malenka,R.C., and Nicoll,R.A. (1997). Two distinct forms of long-term depression coexist in CA1 hippocampal pyramidal cells. Neuron *18*, 969-982.

Oliva,A.A., Jr., Jiang,M., Lam,T., Smith,K.L., and Swann,J.W. (2000). Novel hippocampal interneuronal subtypes identified using transgenic mice that express green fluorescent protein in GABAergic interneurons. J. Neurosci. *20*, 3354-3368.

Overstreet,L.S., Pasternak,J.F., Colley,P.A., Slater,N.T., and Trommer,B.L. (1997). Metabotropic glutamate receptor mediated long-term depression in developing hippocampus. Neuropharmacology *36*, 831-844.

Palczewski,K., Kumasaka,T., Hori,T., Behnke,C.A., Motoshima,H., Fox,B.A., Le,T., I, Teller,D.C., Okada,T., Stenkamp,R.E., Yamamoto,M., and Miyano,M. (2000). Crystal structure of rhodopsin: A G protein-coupled receptor. Science *289*, 739-745.

Palmer,M.J., Irving,A.J., Seabrook,G.R., Jane,D.E., and Collingridge,G.L. (1997). The group I mGlu receptor agonist DHPG induces a novel form of LTD in the CA1 region of the hippocampus. Neuropharmacology *36*, 1517-1532.

Parra,P., Gulyas,A.I., and Miles,R. (1998). How many subtypes of inhibitory cells in the hippocampus? Neuron *20*, 983-993.

Paternain,A.V., Herrera,M.T., Nieto,M.A., and Lerma,J. (2000). GluR5 and GluR6 kainate receptor subunits coexist in hippocampal neurons and coassemble to form functional receptors. J. Neurosci. *20*, 196-205.

Perez,Y., Morin,F., and Lacaille,J.C. (2001). A hebbian form of long-term potentiation dependent on mGluR1a in hippocampal inhibitory interneurons. Proc. Natl. Acad. Sci. U. S. A *98*, 9401-9406.

Perouansky,M., and Yaari,Y. (1993). Kinetic properties of NMDA receptor-mediated synaptic currents in rat hippocampal pyramidal cells versus interneurones. J. Physiol *465*, 223-244.

Peterlin,Z.A., Kozloski,J., Mao,B.Q., Tsiola,A., and Yuste,R. (2000). Optical probing of neuronal circuits with calcium indicators. Proc. Natl. Acad. Sci. U. S. A *97*, 3619-3624.

Petralia,R.S., Wang,Y.X., Singh,S., Wu,C., Shi,L., Wei,J., and Wenthold,R.J. (1997). A monoclonal antibody shows discrete cellular and subcellular localizations of mGluR1 alpha metabotropic glutamate receptors. J. Chem. Neuroanat. *13*, 77-93.

Pin,J.P., and Duvoisin,R. (1995). The metabotropic glutamate receptors: structure and functions. Neuropharmacology *34*, 1-26.

Pitler,T.A., and Alger,B.E. (1992). Postsynaptic spike firing reduces synaptic GABAA responses in hippocampal pyramidal cells. J. Neurosci. *12*, 4122-4132.

Pitler,T.A., and Alger,B.E. (1994). Depolarization-induced suppression of GABAergic inhibition in rat hippocampal pyramidal cells: G protein involvement in a presynaptic mechanism. Neuron *13*, 1447-1455.

Poncer,J.C., McKinney,R.A., Gahwiler,B.H., and Thompson,S.M. (2000). Differential control of GABA release at synapses from distinct interneurons in rat hippocampus. J. Physiol *528 Pt 1*, 123-130.

Poncer,J.C., McKinney,R.A., Gahwiler,B.H., and Thompson,S.M. (1997). Either N- or P-type calcium channels mediate GABA release at distinct hippocampal inhibitory synapses. Neuron *18*, 463-472.

Pouille,F., and Scanziani,M. (2001). Enforcement of temporal fidelity in pyramidal cells by somatic feed-forward inhibition. Science *293*, 1159-1163.

Pouille,F., and Scanziani,M. (2004). Routing of spike series by dynamic circuits in the hippocampus. Nature *429*, 717-723.

Price,C.J., Karayannis,T., Pal,B.Z., and Capogna,M. (2005). Group II and III mGluRs-mediated presynaptic inhibition of EPSCs recorded from hippocampal interneurons of CA1 stratum lacunosum moleculare. Neuropharmacology *49 Suppl 1*, 45-56.

Racca,C., Stephenson,F.A., Streit,P., Roberts,J.D., and Somogyi,P. (2000). NMDA receptor content of synapses in stratum radiatum of the hippocampal CA1 area. J. Neurosci. *20*, 2512-2522.

Rammes,G., Palmer,M., Eder,M., Dodt,H.U., Zieglgansberger,W., and Collingridge,G.L. (2003). Activation of mGlu receptors induces LTD without affecting postsynaptic sensitivity of CA1 neurons in rat hippocampal slices. J. Physiol *546*, 455-460.

Regehr,W.G., and Tank,D.W. (1991). Selective fura-2 loading of presynaptic terminals and nerve cell processes by local perfusion in mammalian brain slice. J. Neurosci. Methods *37*, 111-119.

Reid,C.A., Bekkers,J.M., and Clements,J.D. (2003). Presynaptic Ca2+ channels: a functional patchwork. Trends Neurosci. *26*, 683-687.

Reid,C.A., Clements,J.D., and Bekkers,J.M. (1997). Nonuniform distribution of Ca2+ channel subtypes on presynaptic terminals of excitatory synapses in hippocampal cultures. J. Neurosci. *17*, 2738-2745.

Reyes,A., Lujan,R., Rozov,A., Burnashev,N., Somogyi,P., and Sakmann,B. (1998). Target-cell-specific facilitation and depression in neocortical circuits. Nat. Neurosci. *1*, 279-285.

Ribak,C.E. (1978). Aspinous and sparsely-spinous stellate neurons in the visual cortex of rats contain glutamic acid decarboxylase. J. Neurocytol. *7*, 461-478.

Robbe,D., Kopf,M., Remaury,A., Bockaert,J., and Manzoni,O.J. (2002). Endogenous cannabinoids mediate long-term synaptic depression in the nucleus accumbens. Proc. Natl. Acad. Sci. U. S. A *99*, 8384-8388.

Robbins,M.J., Ciruela,F., Rhodes,A., and McIlhinney,R.A. (1999). Characterization of the dimerization of metabotropic glutamate receptors using an N-terminal truncation of mGluR1alpha. J. Neurochem. *72*, 2539-2547.

Rodriguez-Moreno,A., Sistiaga,A., Lerma,J., and Sanchez-Prieto,J. (1998). Switch from facilitation to inhibition of excitatory synaptic transmission by group I mGluR desensitization. Neuron *21*, 1477-1486.

Romano,C., Miller,J.K., Hyrc,K., Dikranian,S., Mennerick,S., Takeuchi,Y., Goldberg,M.P., and O'Malley,K.L. (2001). Covalent and noncovalent interactions mediate metabotropic glutamate receptor mGlu5 dimerization. Mol. Pharmacol. *59*, 46-53.

Romano,C., Sesma,M.A., McDonald,C.T., O'Malley,K., Van den Pol,A.N., and Olney,J.W. (1995). Distribution of metabotropic glutamate receptor mGluR5 immunoreactivity in rat brain. J. Comp Neurol. *355*, 455-469.

Romano,C., Yang,W.L., and O'Malley,K.L. (1996). Metabotropic glutamate receptor 5 is a disulfide-linked dimer. J. Biol. Chem. *271*, 28612-28616.

Rouach,N., and Nicoll,R.A. (2003). Endocannabinoids contribute to short-term but not long-term mGluR-induced depression in the hippocampus. Eur. J. Neurosci. *18*, 1017-1020.

Royer,S., Martina,M., and Pare,D. (1999). An inhibitory interface gates impulse traffic between the input and output stations of the amygdala. J. Neurosci. *19*, 10575-10583.

Rusakov,D.A., and Kullmann,D.M. (1998). Extrasynaptic glutamate diffusion in the hippocampus: ultrastructural constraints, uptake, and receptor activation. J. Neurosci. *18*, 3158-3170.

Rusakov,D.A., Kullmann,D.M., and Stewart,M.G. (1999). Hippocampal synapses: do they talk to their neighbours? Trends Neurosci. *22*, 382-388.

Rusakov,D.A., Wuerz,A., and Kullmann,D.M. (2004). Heterogeneity and specificity of presynaptic Ca2+ current modulation by mGluRs at individual hippocampal synapses. Cereb. Cortex *14*, 748-758.

Ruth,R.E., Collier,T.J., and Routtenberg,A. (1988). Topographical relationship between the entorhinal cortex and the septotemporal axis of the dentate gyrus in rats: II. Cells projecting from lateral entorhinal subdivisions. J. Comp Neurol. *270*, 506-516.

Ruth,R.E., Collier,T.J., and Routtenberg,A. (1982). Topography between the entorhinal cortex and the dentate septotemporal axis in rats: I. Medial and intermediate entorhinal projecting cells. J. Comp Neurol. *209*, 69-78.

Sanchez-Prieto,J., Paternain,A.V., and Lerma,J. (2004). Dual signaling by mGluR5a results in bi-directional modulation of N-type Ca2+ channels. FEBS Lett. *576*, 428-432.

Saugstad,J.A., Marino,M.J., Folk,J.A., Hepler,J.R., and Conn,P.J. (1998). RGS4 inhibits signaling by group I metabotropic glutamate receptors. J. Neurosci. *18*, 905-913.

Scanziani,M., Gahwiler,B.H., and Charpak,S. (1998). Target cell-specific modulation of transmitter release at terminals from a single axon. Proc. Natl. Acad. Sci. U. S. A *95*, 12004-12009.

Scanziani,M., Salin,P.A., Vogt,K.E., Malenka,R.C., and Nicoll,R.A. (1997). Use-dependent increases in glutamate concentration activate presynaptic metabotropic glutamate receptors. Nature *385*, 630-634.

Schoepp,D.D., Goldsworthy,J., Johnson,B.G., Salhoff,C.R., and Baker,S.R. (1994). 3,5-dihydroxyphenylglycine is a highly selective agonist for phosphoinositide-linked metabotropic glutamate receptors in the rat hippocampus. J. Neurochem. *63*, 769-772.

Schoepp,D.D., Jane,D.E., and Monn,J.A. (1999). Pharmacological agents acting at subtypes of metabotropic glutamate receptors. Neuropharmacology *38*, 1431-1476.

Scimemi,A., Fine,A., Kullmann,D.M., and Rusakov,D.A. (2004). NR2B-containing receptors mediate cross talk among hippocampal synapses. J. Neurosci. *24*, 4767-4777.

Seal,R.P., and Amara,S.G. (1999). Excitatory amino acid transporters: a family in flux. Annu. Rev. Pharmacol. Toxicol. *39*, 431-456.

Semyanov,A., and Kullmann,D.M. (2000). Modulation of GABAergic signaling among interneurons by metabotropic glutamate receptors. Neuron *25*, 663-672.

Semyanov,A., and Kullmann,D.M. (2001). Kainate receptor-dependent axonal depolarization and action potential initiation in interneurons. Nat. Neurosci. *4*, 718-723.

Shepherd,G.M., and Harris,K.M. (1998). Three-dimensional structure and composition of CA3-->CA1 axons in rat hippocampal slices: implications for presynaptic connectivity and compartmentalization. J. Neurosci. *18*, 8300-8310.

Shigemoto,R., Kinoshita,A., Wada,E., Nomura,S., Ohishi,H., Takada,M., Flor,P.J., Neki,A., Abe,T., Nakanishi,S., and Mizuno,N. (1997). Differential presynaptic localization of metabotropic glutamate receptor subtypes in the rat hippocampus. J. Neurosci. *17*, 7503-7522.

Shigemoto,R., Kulik,A., Roberts,J.D., Ohishi,H., Nusser,Z., Kaneko,T., and Somogyi,P. (1996). Target-cell-specific concentration of a metabotropic glutamate receptor in the presynaptic active zone. Nature *381*, 523-525.

Shigemoto,R., Nomura,S., Ohishi,H., Sugihara,H., Nakanishi,S., and Mizuno,N. (1993). Immunohistochemical localization of a metabotropic glutamate receptor, mGluR5, in the rat brain. Neurosci. Lett. *163*, 53-57.

Shigeri,Y., Seal,R.P., and Shimamoto,K. (2004). Molecular pharmacology of glutamate transporters, EAATs and VGLUTs. Brain Res. Brain Res. Rev. *45*, 250-265.

Shimamoto,K., Lebrun,B., Yasuda-Kamatani,Y., Sakaitani,M., Shigeri,Y., Yumoto,N., and Nakajima,T. (1998). DL-threo-beta-benzyloxyaspartate, a potent blocker of excitatory amino acid transporters. Mol. Pharmacol. *53*, 195-201.

Singer,W. (1999). Neuronal synchrony: a versatile code for the definition of relations? Neuron *24*, 49-25.

Singer,W. (1993). Synchronization of cortical activity and its putative role in information processing and learning. Annu. Rev. Physiol *55*, 349-374.

Smetters,D., Majewska,A., and Yuste,R. (1999). Detecting action potentials in neuronal populations with calcium imaging. Methods *18*, 215-221.

Snyder,E.M., Philpot,B.D., Huber,K.M., Dong,X., Fallon,J.R., and Bear,M.F. (2001). Internalization of ionotropic glutamate receptors in response to mGluR activation. Nat. Neurosci. *4*, 1079-1085.

Somogyi,P., Dalezios,Y., Lujan,R., Roberts,J.D., Watanabe,M., and Shigemoto,R. (2003). High level of mGluR7 in the presynaptic active zones of select populations of GABAergic terminals innervating interneurons in the rat hippocampus. Eur. J. Neurosci. *17*, 2503-2520.

Somogyi,P., and Klausberger,T. (2005). Defined types of cortical interneurone structure space and spike timing in the hippocampus. J. Physiol *562*, 9-26.

Sorra,K.E., and Harris,K.M. (1993). Occurrence and three-dimensional structure of multiple synapses between individual radiatum axons and their target pyramidal cells in hippocampal area CA1. J. Neurosci. *13*, 3736-3748.

Stefani,A., Spadoni,F., and Bernardi,G. (1998). Group I mGluRs modulate calcium currents in rat GP: functional implications. Synapse *30*, 424-432.

Stein,V., and Nicoll,R.A. (2003). GABA generates excitement. Neuron *37*, 375-378.

Stella,N., Schweitzer,P., and Piomelli,D. (1997). A second endogenous cannabinoid that modulates long-term potentiation. Nature *388*, 773-778.

Steward,O., and Scoville,S.A. (1976). Cells of origin of entorhinal cortical afferents to the hippocampus and fascia dentata of the rat. J. Comp Neurol. *169*, 347-370.

Storm-Mathisen,J., Leknes,A.K., Bore,A.T., Vaaland,J.L., Edminson,P., Haug,F.M., and Ottersen,O.P. (1983). First visualization of glutamate and GABA in neurones by immunocytochemistry. Nature *301*, 517-520.

Sugiyama,H., Ito,I., and Hirono,C. (1987). A new type of glutamate receptor linked to inositol phospholipid metabolism. Nature *325*, 531-533.

Svoboda,K.R., Adams,C.E., and Lupica,C.R. (1999). Opioid receptor subtype expression defines morphologically distinct classes of hippocampal interneurons. J. Neurosci. *19*, 85-95.

Swanson,G.T., and Heinemann,S.F. (1998). Heterogeneity of homomeric GluR5 kainate receptor desensitization expressed in HEK293 cells. J. Physiol *513 (Pt 3)*, 639-646.

Swanson,L.W., and Cowan,W.M. (1977). An autoradiographic study of the organization of the efferent connections of the hippocampal formation in the rat. J. Comp Neurol. *172*, 49-84.

Szabadics,J., Varga,C., Molnar,G., Olah,S., Barzo,P., and Tamas,G. (2006). Excitatory effect of GABAergic axo-axonic cells in cortical microcircuits. Science *311*, 233-235.

Takahashi,K.A., and Castillo,P.E. (2006). The CB1 cannabinoid receptor mediates glutamatergic synaptic suppression in the hippocampus. Neuroscience *139*, 795-802.

Takumi,Y., Ramirez-Leon,V., Laake,P., Rinvik,E., and Ottersen,O.P. (1999). Different modes of expression of AMPA and NMDA receptors in hippocampal synapses. Nat. Neurosci. *2*, 618-624.

Tamamaki,N., Watanabe,K., and Nojyo,Y. (1984). A whole image of the hippocampal pyramidal neuron revealed by intracellular pressure-injection of horseradish peroxidase. Brain Res. *307*, 336-340.

Tan,Y., Hori,N., and Carpenter,D.O. (2003). The mechanism of presynaptic long-term depression mediated by group I metabotropic glutamate receptors. Cell Mol. Neurobiol. *23*, 187-203.

Tanabe,Y., Masu,M., Ishii,T., Shigemoto,R., and Nakanishi,S. (1992). A family of metabotropic glutamate receptors. Neuron *8*, 169-179.

Thomson,A.M. (1997). Activity-dependent properties of synaptic transmission at two classes of connections made by rat neocortical pyramidal axons in vitro. J. Physiol *502 (Pt 1)*, 131-147.

Toth,K., and McBain,C.J. (1998). Afferent-specific innervation of two distinct AMPA receptor subtypes on single hippocampal interneurons. Nat. Neurosci. *1*, 572-578.

Toth,K., and McBain,C.J. (2000). Target-specific expression of pre- and postsynaptic mechanisms. J. Physiol *525 Pt 1*, 41-51.

Toth,K., Suares,G., Lawrence,J.J., Philips-Tansey,E., and McBain,C.J. (2000). Differential mechanisms of transmission at three types of mossy fiber synapse. J. Neurosci. *20*, 8279-8289.

Tsou,K., Mackie,K., Sanudo-Pena,M.C., and Walker,J.M. (1999). Cannabinoid CB1 receptors are localized primarily on cholecystokinin-containing GABAergic interneurons in the rat hippocampal formation. Neuroscience *93*, 969-975.

Tsuchiya,D., Kunishima,N., Kamiya,N., Jingami,H., and Morikawa,K. (2002). Structural views of the ligand-binding cores of a metabotropic glutamate receptor complexed with an antagonist and both glutamate and Gd3+. Proc. Natl. Acad. Sci. U. S. A *99*, 2660-2665.

Tsuji,Y., Shimada,Y., Takeshita,T., Kajimura,N., Nomura,S., Sekiyama,N., Otomo,J., Usukura,J., Nakanishi,S., and Jingami,H. (2000). Cryptic dimer interface and domain organization of the extracellular region of metabotropic glutamate receptor subtype 1. J. Biol. Chem. *275*, 28144-28151.

van Hooft,J.A., Giuffrida,R., Blatow,M., and Monyer,H. (2000). Differential expression of group I metabotropic glutamate receptors in functionally distinct hippocampal interneurons. J. Neurosci. *20*, 3544-3551.

Varma,N., Carlson,G.C., Ledent,C., and Alger,B.E. (2001). Metabotropic glutamate receptors drive the endocannabinoid system in hippocampus. J. Neurosci. *21*, RC188.

Vogt,K.E., and Nicoll,R.A. (1999). Glutamate and gamma-aminobutyric acid mediate a heterosynaptic depression at mossy fiber synapses in the hippocampus. Proc. Natl. Acad. Sci. U. S. A *96*, 1118-1122.

Washburn,M.S., Numberger,M., Zhang,S., and Dingledine,R. (1997). Differential dependence on GluR2 expression of three characteristic features of AMPA receptors. J. Neurosci. *17*, 9393-9406.

Watabe,A.M., Carlisle,H.J., and O'Dell,T.J. (2002). Postsynaptic induction and presynaptic expression of group 1 mGluR-dependent LTD in the hippocampal CA1 region. J. Neurophysiol. *87*, 1395-1403.

Watanabe,J., Rozov,A., and Wollmuth,L.P. (2005). Target-specific regulation of synaptic amplitudes in the neocortex. J. Neurosci. *25*, 1024-1033.

White,A.M., Kylanpaa,R.A., Christie,L.A., McIntosh,S.J., Irving,A.J., and Platt,B. (2003). Presynaptic group I metabotropic glutamate receptors modulate synaptic transmission in the rat superior colliculus via 4-AP sensitive K(+) channels. Br. J. Pharmacol. *140*, 1421-1433.

Whittington,M.A., Stanford,I.M., Colling,S.B., Jefferys,J.G., and Traub,R.D. (1997). Spatiotemporal patterns of gamma frequency oscillations tetanically induced in the rat hippocampal slice. J. Physiol *502 (Pt 3)*, 591-607.

Whittington,M.A., Traub,R.D., and Jefferys,J.G. (1995). Synchronized oscillations in interneuron networks driven by metabotropic glutamate receptor activation. Nature *373*, 612-615.

Wierenga,C.J., and Wadman,W.J. (2003). Excitatory inputs to CA1 interneurons show selective synaptic dynamics. J. Neurophysiol. *90*, 811-821.

Wilson,R.I., Kunos,G., and Nicoll,R.A. (2001). Presynaptic specificity of endocannabinoid signaling in the hippocampus. Neuron *31*, 453-462.

Wilson,R.I., and Nicoll,R.A. (2001). Endogenous cannabinoids mediate retrograde signalling at hippocampal synapses. Nature *410*, 588-592.

Woodhall,G., Gee,C.E., Robitaille,R., and Lacaille,J.C. (1999). Membrane potential and intracellular Ca2+ oscillations activated by mGluRs in hippocampal stratum oriens/alveus interneurons. J. Neurophysiol. *81*, 371-382.

Wu,L.G., and Saggau,P. (1994b). Adenosine inhibits evoked synaptic transmission primarily by reducing presynaptic calcium influx in area CA1 of hippocampus. Neuron *12*, 1139-1148.

Wu,L.G., and Saggau,P. (1994a). Presynaptic calcium is increased during normal synaptic transmission and paired-pulse facilitation, but not in long-term potentiation in area CA1 of hippocampus. J. Neurosci. *14*, 645-654.

Wu,L.G., and Saggau,P. (1997). Presynaptic inhibition of elicited neurotransmitter release. Trends Neurosci. *20*, 204-212.

Xiao,M.Y., Zhou,Q., and Nicoll,R.A. (2001). Metabotropic glutamate receptor activation causes a rapid redistribution of AMPA receptors. Neuropharmacology *41*, 664-671.

Zhang,H., and Sulzer,D. (2003). Glutamate spillover in the striatum depresses dopaminergic transmission by activating group I metabotropic glutamate receptors. J. Neurosci. *23*, 10585-10592.

Zhang,J.F., Ellinor,P.T., Aldrich,R.W., and Tsien,R.W. (1996). Multiple structural elements in voltage-dependent Ca2+ channels support their inhibition by G proteins. Neuron *17*, 991-1003.

Zucker,R.S., and Regehr,W.G. (2002). Short-term synaptic plasticity. Annu. Rev. Physiol *64*, 355-405.